Modification of Silicon Nitride and Silicon Carbide Surfaces for Food and Biosensor Applications

Promotoren:

Prof. dr. H. Zuilhof, Hoogleraar in de Organische Chemie, Wageningen Universiteit

Prof. dr. ir. R.M. Boom, Hoogleraar in de Levensmiddelenproceskunde, Wageningen Universiteit

Co-Promotor:

Dr. ir. C.G.P.H Schroën, Universitair docent, sectie Levensmiddelenproceskunde, Wageningen Universiteit

Promotiecomissie:

Dr. R. Boukherroub	(Université Lille 1, France)
Dr. R.G.H. Lammertink	(Universiteit Twente)
Prof. dr. E.J.R. Sudhölter	(Technische Universiteit Delft)
Prof. dr. ir. W. Norde	(Wageningen Universiteit)

Dit onderzoek is uitgevoerd binnen de onderzoekschool VLAG

Modification of Silicon Nitride and Silicon Carbide Surfaces for Food and Biosensor Applications

Michel Rosso

Proefschrift

Ter verkrijging van de graad van doctor

op gezag van de Rector Magnificus

van Wageningen Universiteit,

Prof. Dr. M. J. Kropff,

in het openbaar te verdedigen

op dinsdag 2 Juni 2009

des namiddags te 16.00 uur in de Aula

Michel Rosso (2009) - Modification of silicon nitride and silicon carbide surfaces for food and biosensor applications

PhD thesis submitted to Wageningen University – with summaries in English and in Dutch

ISBN: 978-90-8585-379-4

To my family and friends,

Contents

Chapter 1

General Introduction

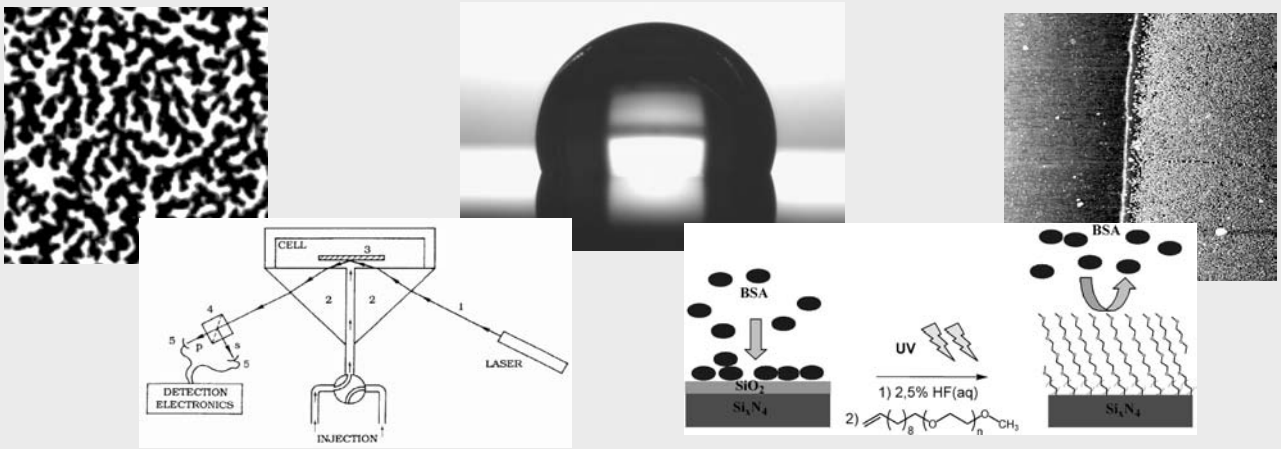

Surface science: a study at the boundaries

Surfaces and interfaces may represent only a tiny part of our world, when compared to the space occupied by bulk masses, but innumerable reaction, creation or destruction processes start on the shallow boundaries defining and separating materials, lands or seas, living cells or individuals. Taking the planet Earth as an example, the small boundary layer below about 5 km of altitude above its solid crust represents only a tiny fraction of its total radius (~ 6400 km), but all the intricate physical and chemical processes necessary for the emergence and subsistence of a complex life are gathered in that confined space.

Likewise, the first few nanometers at the surface of a material can entirely determine its interfacial properties (wetting, catalytic activity, etc.). In chemistry, surfaces are situated at the confluence of all disciplines: analytical, theoretical, physical, inorganic, organic and bioorganic chemists can find interesting developments for their work while studying surfaces. Lately, the highest award in the field of chemistry, the Nobel prize, was awarded to Gerhardt Ertl for his pioneering surface chemistry relating to the interaction of gases with metal surfaces, a field of research that has helped uncover the mechanisms at work in many gas-solid and liquid-solid catalyzed reactions.[1] Some of these heterogeneous reactions, such as the synthesis of ammonia developed by Haber and Mittasch (1905-1912), or refining of petroleum oil by catalytic cracking to produce gasoline, are indeed part of the foundations of our modern economies.[2,3]

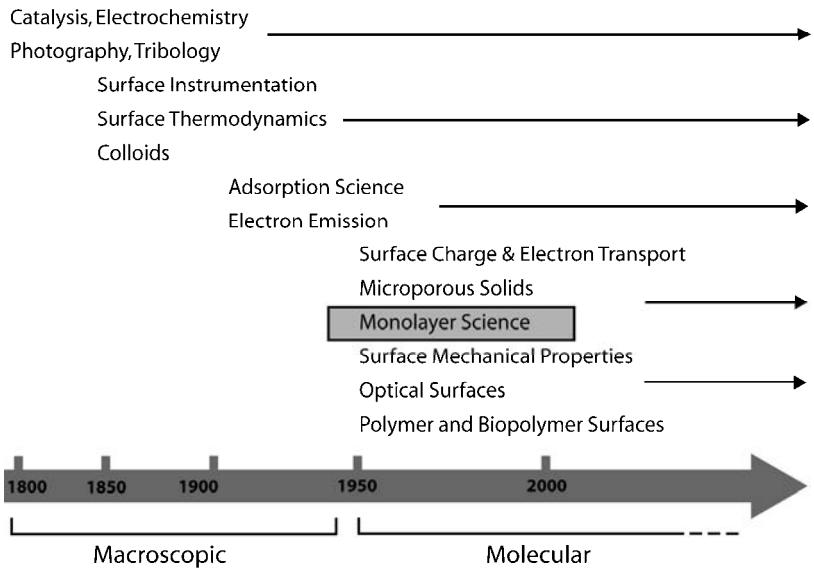

Figure 1. Time line of historical development in surface science (adapted from G.A. Somorjai[2]).

Other areas of surface science include colloids science, electrochemistry, surface spectroscopy and microscopy. Within the various fields of surface science, the preparation of covalently attached organic monolayers has been especially developed in the last 30 years (Figure 1). This technique for the surface modification of inorganic substrates involves the formation of organic monolayers of linear molecules, attached through a covalent bond between one of their end groups and the inorganic surface. These composite structures have allowed a precise control of the interfacial properties of solid materials, among which especially gold, glass and silicon surfaces have been studied in detail.[4]

Examples of organic monolayers

These three main classes of covalent organic monolayers differ in the nature of the covalent bonds linking the alkyl chains to the inorganic surface (Figure 2): thiol monolayers on gold rely on the interaction of sulfur with noble metals, like gold, silver, or copper. Alkylsilane monolayers can be formed by the reaction of an alkyl silane (usually chloro- or alkoxysilane) with the surface hydroxyl groups of oxygen-containing materials, like glass or silica. Alkene-based monolayers are in most cases formed by a hydrosilylation reaction between alkene molecules and hydrogen-terminated silicon surfaces.

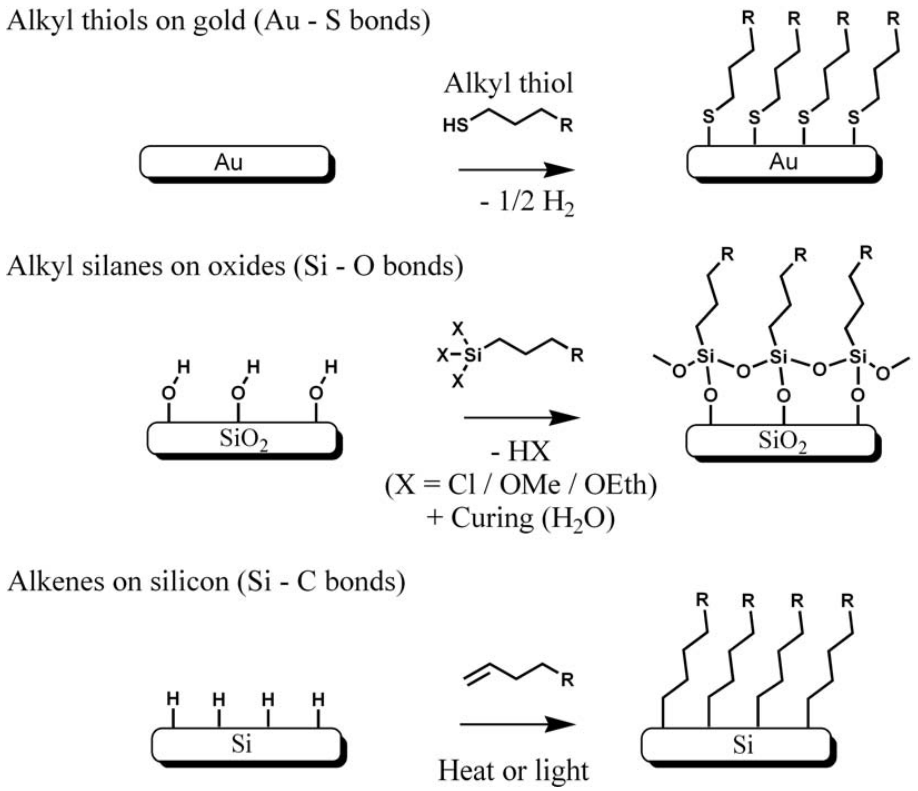

Figure 2. Three main classes of covalent organic monolayers.

Silicon-rich materials

This thesis is focused in particular on other surfaces, and discusses the preparation and study of alkene-based monolayers on robust silicon-rich materials, namely silicon-rich silicon nitride (Si_xN_4, $3.5 < x < 4.5$) and silicon carbide (SiC). In addition, it presents fundamental studies relating to their application in biofunctional and biorepellent surfaces. The exceptional mechanical and chemical robustness of Si_xN_4 and SiC makes these substrates attractive for applications where harsh conditions and / or prolonged exposure are applied. Moreover, Si_xN_4 and SiC have properties that differ from those of materials commonly used for the formation of organic monolayers (gold, glass, or silicon), and the chemistry presented in here thus provides the scientist or engineer with more choices in the selection of a suitable substrate (Table 1).

Table 1. Properties of inorganic substrates for the formation of organic monolayers*

Material (Formula)	Type**	Bandgap (eV)	Hardness ($kg.mm^{-2}$)	Refractive index
Silicon (Si)	SC	1.1	1150	3.87
Silicon carbide (SiC)	SC	2.3 – 3.3[5]	3720	2.6
Silicon nitride (Si_3N_4)	I	5.1	3400	2[6]
Si-rich silicon nitride (Si_xN_4, $3.5<x<4.5$)	I / SC	2 – 4	-	2 – 2.3[7]
Diamond (C)	I	5.5	> 6000	2.42
Silica (SiO_2)	I	~ 9	741	1.46

*All data from Weber, J.M. *Handbook of Optical Materials*,[8] unless stated otherwise.
** I: insulator, C: conductor, SC: semiconductor.

Stoichiometric silicon nitride (Si_3N_4) can form robust insulating coatings, but this material can develop a very high surface stress that negatively affects its mechanical properties.[9] In comparison, silicon-rich silicon nitride displays very low residual stress, and can form homogeneous coatings by chemical vapor deposition (CVD).[6] The composition of the material can be controlled by tuning the proportions of the compounds used as precursors in the CVD process (usually NH_3/SiH_2Cl_2). This material is indeed used commonly, for

example, for the coating of microfabricated membranes (microsieves, see Chapter 3 and 9) or microelectromechanical systems (MEMS). Silicon carbide had long been perceived as a potential replacement for silicon in electronic applications, but it was only in 1989, with the founding of CREE Inc., that SiC LED's (light emitting diodes) and high quality wafers became widely available due to the breakthrough of "step-controlled epitaxy".[5] Since then, the quality and availability of SiC materials have been steadily improved, and applications in high-power electronics and sensors are increasingly investigated.

Application of Si_xN_4 and SiC can even be enhanced if effective surface modification techniques are becoming available. Therefore, the aim of the research presented in this thesis was to develop versatile modification methods for Si_xN_4 and SiC and to investigate the functionalization of these surfaces with robust organic monolayers for various applications.

Outline of the thesis

This thesis focuses on the formation of organic monolayers, and Chapter 2 and 3 give an overview of their potential and actual applications: Chapter 2 gives a description of thiol, silane, and alkene-based monolayers, and their application in biocompatible coatings, surface nano- and micropatterning, and sensing. Chapter 3 describes the particular case of microfabricated silicon nitride filtration membranes (microsieves), and the possibility to increase their surface biocompatibility with oligomeric or polymeric protein-repellent coatings.

Chapter 4 gives a number of examples of chemical and biochemical functionalizations of Si_xN_4 surfaces, using a thermal grafting method combined with conventional surface organic reactions. Emphasis is put on the stability of the coatings, and on the possibility to produce tailor-made biofunctional silicon nitride surfaces. Chapter 5 describes the extension of this method to the modification of SiC surfaces and the formation of ester-terminated surfaces. Chapter 6 presents a mild modification technique – UV-induced grafting of alkenes onto Si_xN_4 and SiC surfaces – that also lead to a significant improvement of the monolayer quality. Besides easier reaction conditions and lower consumption of reactants, this reaction opens the way to surface patterning of the inorganic surfaces and the modification of sensitive microfabricated devices. In Chapter 4 to 6, the chemical functionalizations are studied using X-ray photoelectron spectroscopy (XPS), infrared reflection absorption spectroscopy (IRRAS), atomic force microscopy (AFM), time-of-flight secondary ion mass spectrometry

(ToF-SIMS) and static water contact angle, and compared to results obtained for unmodified surfaces in order to elucidate the mechanism of the attachment reactions.

In Chapter 7, the UV-induced functionalization method is used to graft ethylene glycol oligomers directly onto plain Si_xN_4 surfaces, to study the biorepellence of the obtained coatings. The adsorption of two proteins, BSA and fibrinogen, is studied *in situ* with reflectometry, and *ex situ* with AFM and static water contact angles, and the potential of these monolayers to prevent protein adsorption onto surfaces is evaluated.

Chapter 8 reports preliminary results regarding the formation of oligoethylene glycol coatings on the surface of silicon nitride microsieves, in order to improve their filtration performance. The characterization of the modified membranes with XPS and some initial filtration experiments is described in combination with the encountered experimental challenges.

Chapter 9 presents an alternative physical functionalization method of methyl-terminated alkyl monolayers on silicon and Si_xN_4 surfaces, using a controlled oxidation with a plasma. The fast (< 3 s) and reproducible reaction is studied with IRRAS and XPS, and reflectometry is carried out to demonstrate the potential of this functionalization method to produce biosensing surfaces.

Chapter 10 briefly discusses the main results of the research described in this thesis. In addition, it presents a critical evaluation of the main scientific future challenges that are relevant for the continuation of this highly exciting line of research.

References

(1) http://nobelprize.org/nobel_prizes/chemistry/laureates/2007/ertl-autobio.html.

(2) Somorjai, G. A. *Introduction to Surface Science and Catalysis*. Wiley & Sons: New York, 1994.

(3) Bond, G. C. *Metal-Catalysed Reactions of Hydrocarbons*. Springer: New York, 2005.

(4) Ulman, A. *Chem. Rev.* **1996,** *96*, 1533-1554.

(5) Saddow, S. E.; Agarwal, A. *Advances in Silicon Carbide: Processing and Applications*. Artech House Inc.: Boston, 2004.

(6) Andersen, K. N.; Svendsen, W. E.; Stimpel-Lindner, T.; Sulima, T.; Baumgartner, H. *Appl. Surf. Sci.* **2005,** *243*, 401-408.

(7) Dal Negro, L.; Yi, J. H.; Hiltunen, M.; Michel, J.; Kimerling, L. C.; Hamel, S.; Williamson, A. J.; Galli, G.; Chang, T.-W. F.; Sukhovatin, V.; Sargent, E. H. *J. Exp. Nanosci.* **2006,** *1*, 29-50.

(8) Weber, M. J. *Handbook of Optical Materials*. CRC Press: New York, 2003.

(9) French, P. J.; Sarro, P. M.; Mallee, R.; Fakkeldij, E. J. M.; Wolffenbuttel, R. F. *Sens. Actuators, A* **1997,** *58*, 149-157.

Chapter 2

Covalent Organic Monolayers for Bionanotechnology

This chapter is a review of some applications of covalent organic monolayers related to bionanotechnology. An introduction to the formation of alkylthiol, alkylsilane and alkene-based monolayers is given, followed by examples of their implementation in three fields of research: the formation of biorepellent surfaces, the micro- and nanopatterning of surfaces and the production of optical and electrical biosensors.

A modified version of this chapter will be published as:
"*Covalent Organic Monolayers for Bionanotechnology*", Rosso, M.; Schroën, C.G.P.H.; Zuilhof H., manuscript in preparation

Introduction

Within the wealth of applications of surface science (catalysis, coating, colloids science, etc), the preparation of covalently bound organic monolayers has been especially developed in the last 20 years.[1-8] This technique for the surface modification of inorganic substrates involves the formation of organic monolayers of (linear) molecules, attached by one of their end groups to the surfaces by a covalent bond. These composite structures allow a precise control over the interfacial properties of solid materials, among which especially gold, glass and silicon have been studied in detail.

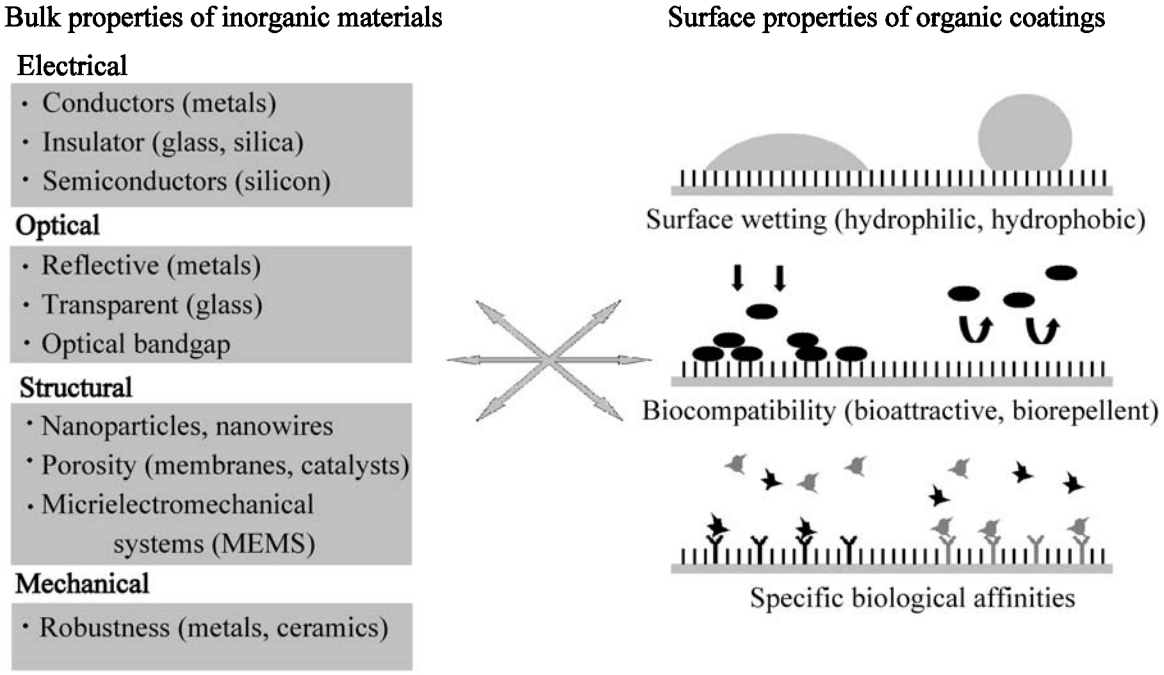

Figure 1. Examples of potential combinations obtainable by the formation of organic monolayers on the surfaces of inorganic materials.

The main advantage of organic monolayers is to add functionality to inorganic materials via the versatile tuning of surface properties (Figure 1): the bulk features of the material (electrical, optical, magnetic, mechanical, structural) are largely maintained, while their surface behavior (wetting, passivation, bioresistance, biochemical affinity, etc) can be tuned through a nanometer-sized coating.

In the first part of this chapter, an overview is given of the preparation of three of the most used categories of monolayers: alkyl thiol monolayers on gold surfaces, alkyl silane monolayers on glass and alkene monolayers on silicon surfaces.

In a second part, illustrative examples are presented of applications of these covalently attached organic monolayers. Three areas of research are discussed in relation to biotechnology: the formation of bioresistant surfaces, the use of monolayers to from micro- and nanopatterns onto surfaces, and finally the use of organic monolayers in biosensors, where several optical and electrical detection techniques are discussed.

The list of applications presented here is intended as an illustrative one and not an exhaustive one. But even then, it is clear that there are numerous possibilities that arise from the combination of materials and coatings. Especially noteworthy is the multidisciplinarity of the progress in this field. For example, the development of micro- or nanostructured membranes for biological application not only requires state-of-the-art techniques in fabrication and process design, but also a precise control of surface wetting and bioresistance. Another example is a antibody-based biosensor on photonic crystals, which needs a good characterization of the crystal structure and optical properties, combined with the accurate measurement of the loading and bioavailability of the immobilized proteins.

This convergence of different skills and knowledge enables the development of applications and furthers the collaboration of scientists from various fields. This, in turn causes new fields of research to emerge. Indeed, some of the techniques that are presented here (SPR, enzyme electrodes, microcontact printing…) have been highly successful, and whole fields of research are now dedicated to each of them.

Formation of covalent organic monolayers

The three main classes of covalent organic monolayers discussed here differ by the nature of the covalent bonds linking the alkyl chains to the inorganic surface (Figure 2): the formation of thiol monolayers on gold relies on the covalent interaction of sulfur with noble metals like gold.[9-11] The same chemistry can be applied for the formation of monolayers on silver or (oxide-free) copper surfaces. Alkylsilane monolayers can be formed by the reaction of a reactive silane (usually chloro- or alkoxysilane) with the surface hydroxyl groups of oxygen-containing materials, like glass, silica or aluminum oxide.[6,12] Alkene-based monolayers are in most cases formed by a hydrosilylation reaction between alkene molecules and hydrogen-terminated silicon surfaces,[7,8,13-15] although very recently this has also been shown to work on –OH terminated surfaces such as silicon carbide,[16,17] amorphous carbon[18,19] or oxidized silicon.[20]

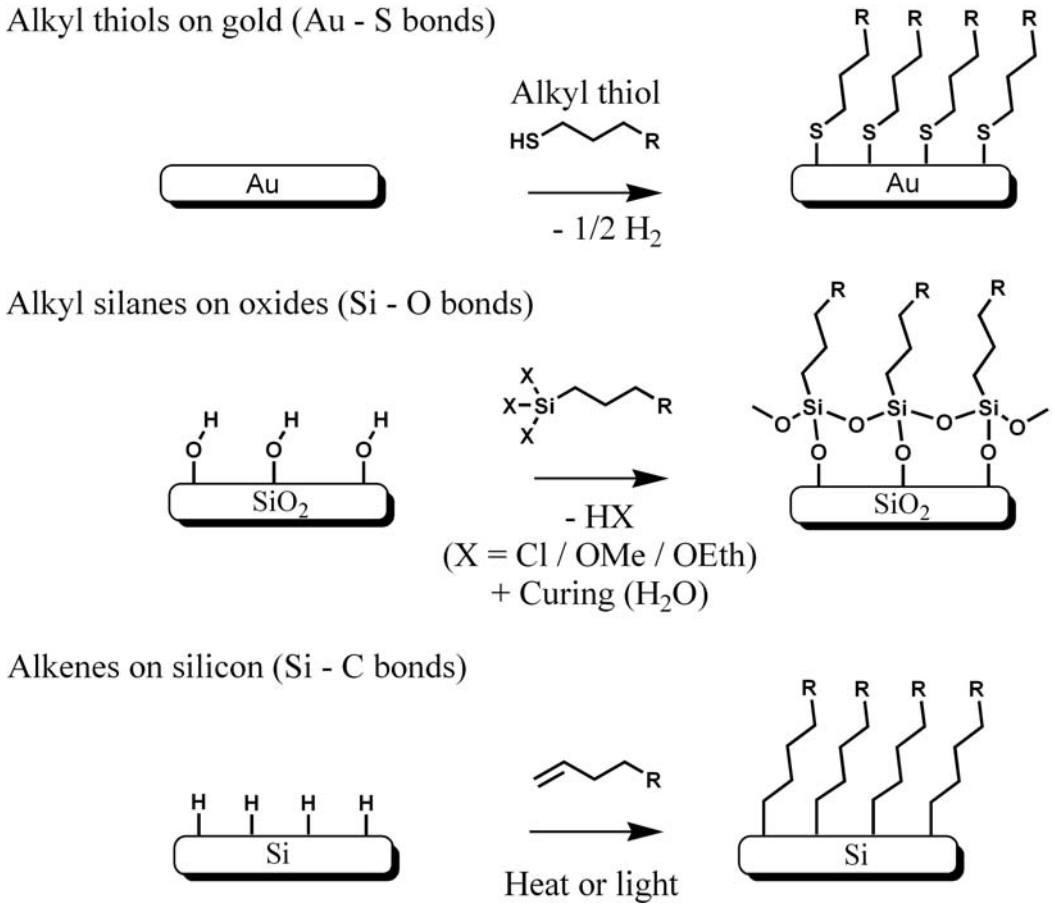

Figure 2. Formation of covalent organic monolayers on the surface of inorganic materials: alkylthiols onto gold, alkylsilanes onto oxides, and 1-alkenes onto hydrogen-terminated silicon.

Alkylthiol monolayers

Since the first studies reporting on the formation of thiol monolayers on gold surfaces,[9,11] these coatings have been widely studied and applied in numerous fields of interest, including self-assembly on surfaces, wettability, biocompatible coatings, molecular and organic electronics and affinity separations on surfaces.[1,21-23] A variety of sulfur-containing compounds can form self-assembled monolayers on gold surfaces: terminal alkyl thiols have been the most studied,[24,25] but dialkyl disulfides,[11,26] dialkyl sulfides,[27,28] cystein[29,30] or xanthates[31] also form ordered monolayers.

The mechanism of attachment of thiols can be described as an oxidative addition to form the gold (I) thiolate (RS^-) (Figure 2);[10] this mechanism has also been proposed for the formation of dialkyl disulfides.[32,33]

A wide variety of functional end groups can be grafted directly onto gold surfaces (Figure 3): next to methyl, ether,[34-36] ester or acid groups,[24,25] examples of complex thiols attached on surfaces also include ferrocenyl,[37-39] porphyrins,[40-42] DNA[43-45] or even nanoparticles[46] and complete vesicles[47]

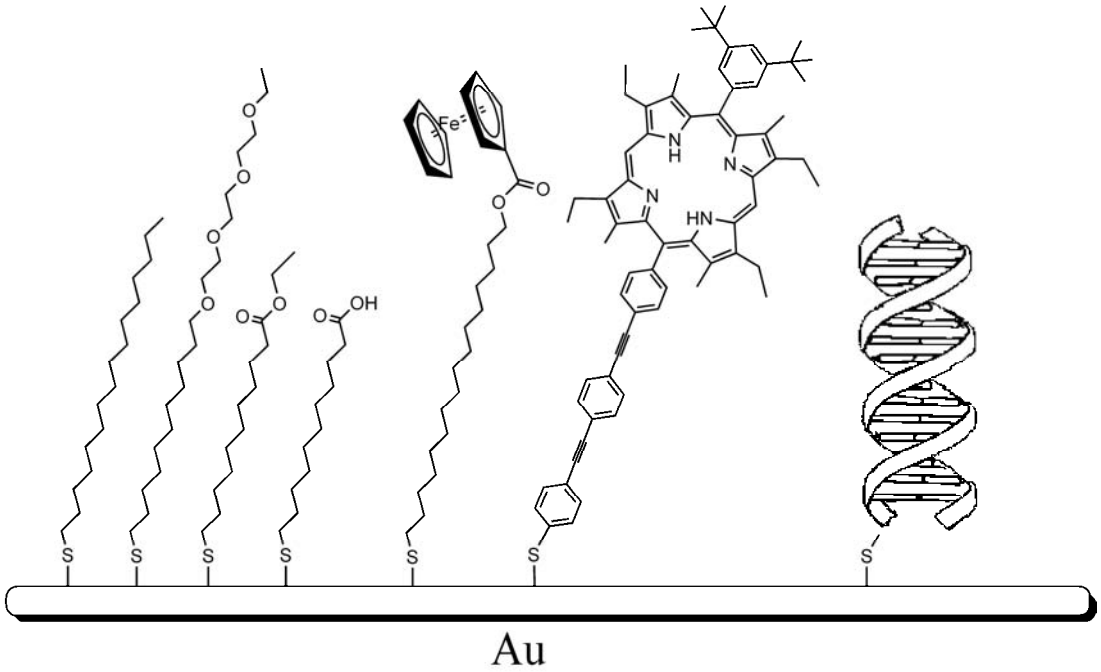

Figure 3. Functionalization of gold surfaces using alkyl thiols. From left to right: bound thiols functionalized with methyl, oligoethylene oxide, ester or acid moieties, ferrocene, porphyrin and ds-DNA.

This type of monolayer is not limited to gold surfaces: thiol compounds also form self-assembled monolayers onto silver and (oxide-free) copper surfaces,[48-52] although the reproducibility of the monolayer formation onto these metals is more difficult to control than on gold.[53] The same is true for other metals such as Pt[54,55] and Fe,[56] or even Hg[57] and Pd.[58] Alkyl thiols also bind to some semiconductor materials, such as GaAs[59,60] and InP,[61] which opens more applications for organic electronics or nanoparticle coatings.

Clearly, thiols represent one of the mildest and flexible way to covalently functionalize metal surfaces. This approach does not require special conditions, and such self-assembled monolayers do not require additional thermal or photochemical activation for their formation. As a result, they are the most used in nanotechnological applications, and the coating of metallic electrodes or nanoparticles with DNA to detect hybridization, or the fast writing of organic nanopatterns with dip-pen nanolithography are just two of numerous successful examples. However, the Au-S bond is also relatively weak, which causes the monolayer to be rather unstable under mechanical stress or long-term exposure to even neutral water. In addition, the thiolate is relatively rich in electrons, and as such prone to oxidation, especially in the presence of light.[62-64] Effectively the ease of formation is inversely related to their medium- or long-term stability.

Alkylsilane monolayers on oxide materials

Another widely used technique for the formation of covalently attached organic monolayers involves the adsorption of alkylsilanes onto oxidized inorganic materials.[6,12] These monolayers can be formed using chlorosilane or alkoxysilane precursors (usually methoxy or ethoxy precursors), as depicted in Figure 4. For chlorosilanes, the Cl-Si bond is readily attacked by the hydroxyl groups of the oxide surface, forming the more stable Si-O-Si linkage. However, trace amounts of water in the solvent or at the solid-liquid interface can also cause hydrolysis and polymerization of chlorosilanes without the involvement of surface hydroxyl groups.[65] The resulting formation of non-covalently linked aggregates can lead to a lower quality and stability of trichlosilane-based monolayers. Therefore, trichlorosilanes are sometimes substituted by precursors that have some of their chlorine atoms replaced by e.g. methyl groups, such as alkyldimethylchlorosilanes.

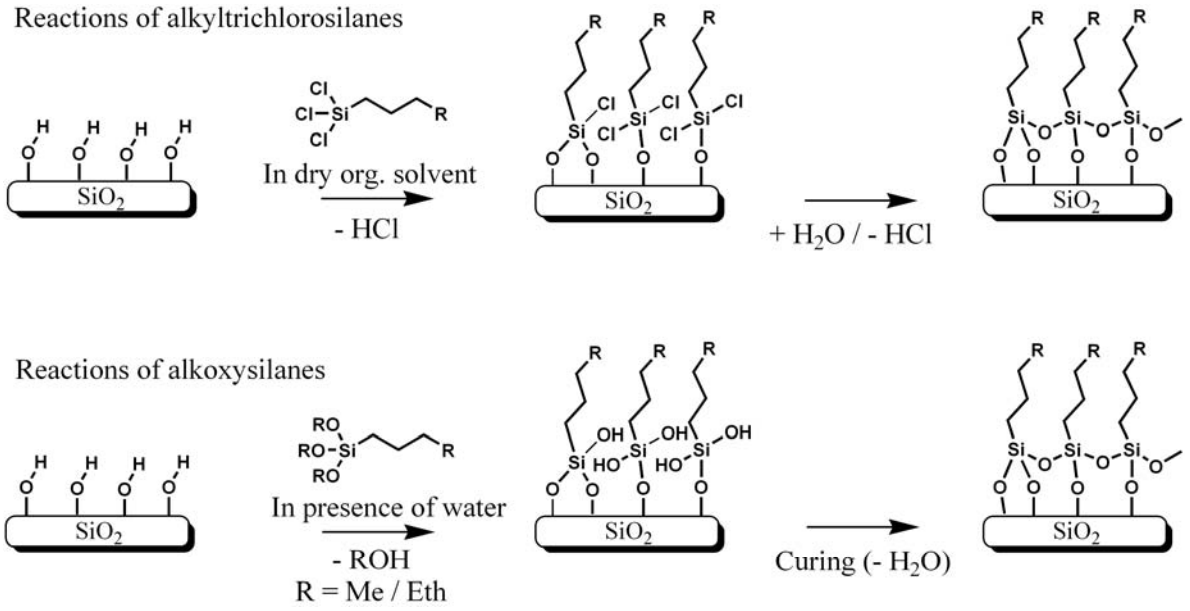

Figure 4. Monolayers formation from alkyltrichlorosilane and alkylalkoxysilanes precursors.

The formation of monolayers requires the hydrolysis of the alkoxy group by water in the presence of a basic or acidic catalyst, to give free silanol groups. These compounds then adsorb at the oxide surfaces and form covalent siloxane bonds by condensation with the surface, as well as between neighboring silanes. A final curing step (e.g. heating at 100 ºC in ambient air) finalizes the cross-linking of the coating and usually increases its stability).

Silane monolayers can be formed on any inorganic material, provided that this material presents stable hydroxyl groups at its surface. This is the case for most oxides such as glass, silica (SiO_2) or alumina (Al_2O_3), but also for materials such as silicon or silicon nitride (Si_xN_4) and silicon carbide (SiC) that are covered under ambient conditions with a top layer of native silicon dioxide, silicon oxynitride or silicon oxycarbide. In the case of SiC this is actually also the case for acid-etched surfaces.[66] The oxidation of these materials by harsh but controllable chemical (e.g. H_2O_2/H_2SO_4: 3/7)[67] or physical treatments (heat, O_2 plasma)[16,68] will then reproducibly provide reactive surfaces for the formation of organosilane monolayers.

Alkyl monolayers can be formed on SiC,[69-71] to develop, for example, sensors based on the electronic properties of this high-bandgap semiconductor.[66] Organosilane monolayers have also been used to covalently attach proteins on flat Si_xN_4 surfaces, and to develop sensing systems based on fluorescence[72] or electrical impedance,[73,74] to functionalize AFM tips[75] or to improve the colloidal properties of Si_3N_4 particles.[76]

However, obtaining a good reproducibility in the formation of organosilane monolayers is more difficult than with thiols on gold surfaces, because the monolayer formation is highly dependent on the reaction conditions.[1] In particular, the nature of the solvents,[77] the temperature,[78-80] and the water content and aging of solutions[81,82] play an important role in the quality of the obtained coatings. For example, water in the solvent can start the hydrolysis of the organosilane precursors, and the subsequent polymerization of silanes in the liquid can cause the formation of aggregates that deposit onto the surface, affecting the homogeneity of the final coatings. This will thus influence the quality and stability of the resulting monolayers in a negative way. Under some circumstances, small amounts of water can also remain between the self-assembled monolayer and the oxide surface: since the condensation reactions also occur between adjacent precursors within the monolayer, a significant fraction of silanol groups can remain unattached to the surface.[65,79,83,84] The monolayer then forms a "net" above the surface, which traps the water film adsorbed on the hydrophilic surface.

Although the preparation of organosilane monolayers can be fast in ambient conditions, they have a poor overall stability in basic conditions,[85-87] and even at pH 5 at 80 ºC.[86] Due to the presence of Si-O bonds, organosilane monolayers are also sensitive to hydrolysis with HF.[8] Even aqueous solutions at neutral pH can compromise the stability of organosilane compounds: polyethylene glycol coatings onto oxidized silicon substrates displayed a near-complete loss of biorepelling activity after a week even in aqueous buffer (pH = 7.5).[88] Other studies have reported the instability of similar coatings in physiological conditions[89,90] (PBS buffer pH 7.4, 37 ºC), with a decrease of more than half of the thickness of polyethylene glycol monolayers after 1 month.

Alkene-based monolayers on silicon-rich surfaces

Another method for the formation of covalently bound alkyl monolayers on silicon-containing surfaces involves the reaction of terminal alkenes or alkynes with HF-treated substrates.[7,8,13-15,91] In particular, this method avoids the need of an intermediate oxide layer between the organic functional groups and the silicon-containing bulk, as it does not need the presence of surface hydroxyl groups, like in the case of alkyl silanes. This reaction is a variation on the widely used hydrosilylation reaction between 1-alkenes and organo-silanes in solution: the hydrosilylation on silicon-containing surfaces occurs through the addition of Si-H on the terminal carbon-carbon double bond (Figure 5). Densely packed monolayers are

obtained from alkenes and alkynes on hydrogen-terminated silicon surfaces using thermal reactions[92-94] or photochemical initiation with UV[20,95-98] or visible light,[99-101] although some reports also mention the spontaneous formation of monolayers at room temperature.[102,103] The high quality and chemical versatility of monolayers formed with these methods allow a rapidly growing number of applications of modified silicon surfaces in molecular electronics and sensors.[104,105]

The mechanism of hydrosilylation of alkenes on pure silicon surfaces (Figure 5) is characterized by a radical chain reaction.[106] Nanometer-sized islands of alkyl chains are first formed, which then progressively cover the whole surface of the material. While this radical propagation mechanism is widely accepted, several mechanisms have been proposed to explain the initiation of the reaction. The success of high temperatures and UV light to initiate monolayer formation first lead to the hypothesis that a homolytic Si-H bond cleavage was needed to start the reaction.[95] The energy of UV light (3.5 eV for 350 nm light) is sufficient to break the Si-H bond (binding enthalpy ~ 3.5 eV) and form surface Si• radicals. However, this mechanism cannot explain the possibility to form monolayers with visible light (wavelengths > 400 nm, up to 700 nm) or at room temperature. In this case, a different initiation mechanism was put forward: after absorption, photons with energies lower than 3.5 eV, but higher than the band-gap of the semiconductor, are able to excite an electron and form an electron-hole pair (Figure 5). The hole localized on silicon atoms acts as an electrophile, and induces reactivity with alkenes (or other electron-rich compounds such as alkynes, halogens, O_2, etc), after which monolayer formation starts.[101,107]

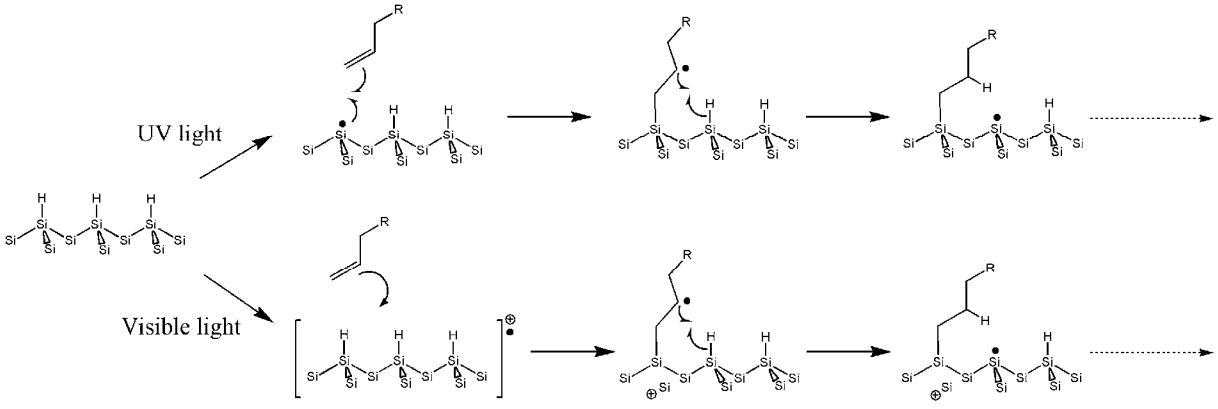

Figure 5. Mechanisms for the initiation of monolayer formation with alkenes on hydrogen-terminated silicon surfaces (adapted from Sun *et al.*[101]).

Alkene-based monolayers were also formed on flat Si_xN_4[108,109] and 6H-SiC and polycrystalline 3C-SiC[16] using thermal conditions close to those used for the surface modification of silicon. Good quality monolayers were obtained with several simple alkenes (e.g. water contact angles up to 107 ° for hexadecene-derived monolayers on both SiC and Si_xN_4). The UV-induced formation of monolayers of semi-carbazide on H-terminated Si_5N_4 surfaces prepared under UHV conditions was also reported by Coffinier *et al.*[110] In addition, methyl- and ester-terminated monolayers were also formed on $Si_{3.9}N_4$[108] and 3C-SiC substrates,[16,17] using wet etching with HF and UV irradiation in the presence of alkenes, under ambient conditions of temperature and pressure. Semi-carbazides and esters can be easily converted to amine[110] and acid groups,[17] respectively, which can serve for further attachment of biomolecules or biorepelling molecules and polymers.[111-113]

The advantage of alkene-based monolayers is their stability, mainly due to the absence of a silicon oxide layer, and the presence of stable and non-polar Si-C bonds, in the case of Si[92] and Si_xN_4,[108] and stable C-O-C bonds in the case of SiC surfaces.[16] Stability measurements revealed the outstanding stability of thermally produced 1-hexadecene monolayers on Si_xN_4 substrates, in acidic or basic conditions at 60 ºC, with changes in contact angles of less than 5º after 4 h of such a treatment.[108] On SiC substrates, a good stability is also obtained after 4 h treatments in 2M HCl at 90 ºC and at pH 11 at 60 ºC, with resulting water contact angle values of 106º and 96º, respectively (coming from 108/109º for the original alkyl monolayer).[17] Even after 1 h in 2.5% HF solution, under which Si-O-Si bonds dissolve rapidly, 1-hexadecene monolayers on SiC still displayed water contact angles of 99º, which indicates the presence of a stable hydrophobic coating.

Hydrogen-free diamond surfaces were also reacted under UHV conditions[114-116] with alkenes via a [2+2] cycloaddition or Diels-Alder mechanism. Hydrogen-terminated diamond surfaces could be functionalized with alkenes under UV irradiation.[117-120] The reaction forms new carbon-carbon bonds, ensuring a robust grafting of monolayers. The same modification can be applied to amorphous carbon.[18,121,122] Functional molecules, including DNA could be grafted in this way to diamond surfaces[117,123] and the hybridization with complementary DNA strands could be monitored on the surfaces. In this case, the surface reactivity differs from that of silicon: the reaction initiation on diamond and amorphous carbon surfaces is due to their negative electron affinity.[118] Upon irradiation with sub-bandgap wavelengths, electrons are ejected from the surface into the surrounding alkenes, causing the formation of charged reactive species in the liquid close to the diamond surface.[120]

Applications of Organic Monolayers

Biorepellent materials

For applications in which the devices come into contact with biological solutions, the non-specific adsorption of biomaterials onto surfaces is an inevitable problem. As an example, the unwanted non-specific adsorption of proteins or polysaccharides onto sensing areas will decrease the specificity and signal-to-noise ratio of any surface-based detection technique. In the case of other applications, such as microfiltration, the adsorption of biomaterials will decrease the performance of membranes and can eventually cause complete blocking of the pores. Other applications require materials with biocompatible surfaces, which can have a well-defined activity in biological environment. Such surfaces can, for example, promote the adhesion of cells without causing the denaturation of proteins, or adsorb an analyte in solution without the interference of other compounds. In biomedical applications especially, where synthetic materials are placed in the presence of complex biological solutions, protein denaturation and/or inflammatory responses can cause a failure of the intervention (installation of prosthesis or measuring probe). New developments involving nanomaterials, such as bioimaging with nanoparticles (*vide supra*), also require the application of coatings to dissolve the nanomaterials in aqueous conditions. In all these examples, biorepellent coatings have been developed to limit the unwanted adsorption onto surfaces. We present here the most illustrative examples for organic monolayers.

Biorepellent coatings are typically hydrophilic, as this property strongly minimizes the adsorption of proteins in aqueous solutions.[34,124-126] In this category, two approaches prevail, each with their own mode of action. For short oligomers, the high internal hydrophilicity of the grafted chains traps a water molecules at the liquid-solid interface. Colloids and proteins from the liquid phase cannot readily displace this strongly bound water.[127] In the case of long polymers, the biorepellence is mainly caused by the osmotic effect of hydrated chains. The adsorption of e.g. proteins is unfavorable, as the concomitant compression of the grafted chains would locally increase the concentration of polymer chains near the surface.[128,129]

Polyethylene glycols (PEG), also called polyethylene oxides (PEO), constitute one of the most widely used polymers to produce biorepellent surfaces.[130,131] Table 1 presents examples of other hydrophilic polymers that have been used to improve surface properties, in the

particular case of membranes. Most of these coatings have been prepared on organic substrates, but these modifications can be extended to inorganic membranes with a proper grafting method (*vide infra*).

Table 1. Examples of biorepellent hydrophilic polymers.

Monomer	Polymer structure	Reference
Ethylene glycol (EG)	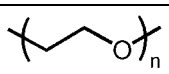	130,131
Acrylic acid (AA)	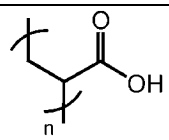	132-135
Polyethylene glycol methacrylate (PEG-MA)	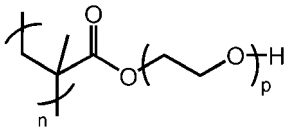	132,135,136
Diethylene glycol vinyl ether (DEGVE)	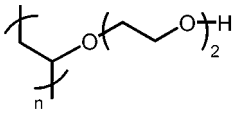	137
Vinyl acetate (VA)	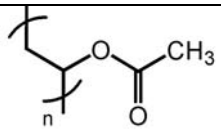	138
Vinylsulfonic acid (VSA)	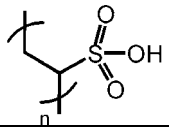	139

The grafting of oligomers and polymers onto surfaces can be done using two different approaches: “grafting-on” methods involve the attachment of pre-formed polymer chains onto surfaces, whereas “grafting-from” methods use the *in-situ* polymerization of monomers from the surface (See Figure 6).

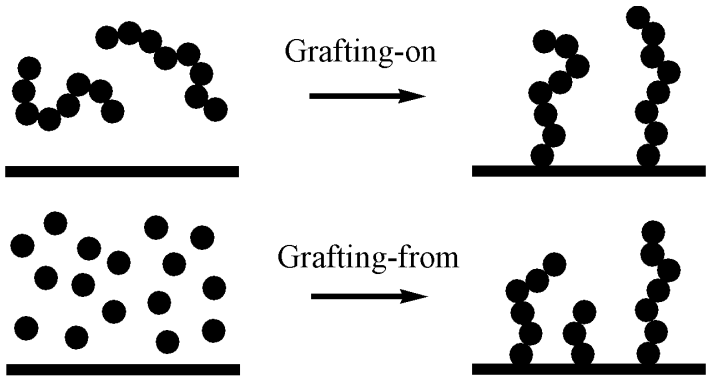

Figure 6. “Grafting-on” and “Grafting-from” strategies for the formation of polymer brushes on solid surfaces.

When applied to small oligomers, the "grafting-on" approach gives a close packing of the grafted chains and a good passivation of the substrate.[140] In addition, the grafted compounds can be precisely characterized before attachment, ensuring a good control of the coating. In particular, the use of monolayers functionalized with oligoethylene glycols has been reported extensively: monolayers formed on gold with thiol compounds end-functionalized with 3 to 9 ethylene glycol units have been extensively studied to obtain the key parameters for efficient biorepellent properties.[141-146] Beside the hydrophilicity of the oligomers, the packing density of the ethylene glycol chains is an important parameter,[34-36,147-152] since a too close packing of the grafted oligomers has been shown to reduce protein-repellent properties, compared to similar monolayers with lower packing densities (Figure 7). This can be explained by the reduced internal hydrophilicity of closely packed monolayer: the penetration of water inside the monolayer is a prerequisite for good biorepellent properties. In a similar way, temperature also has a significant effect on biorepellent properties, as it influences the packing density of ethylene glycols.[153]

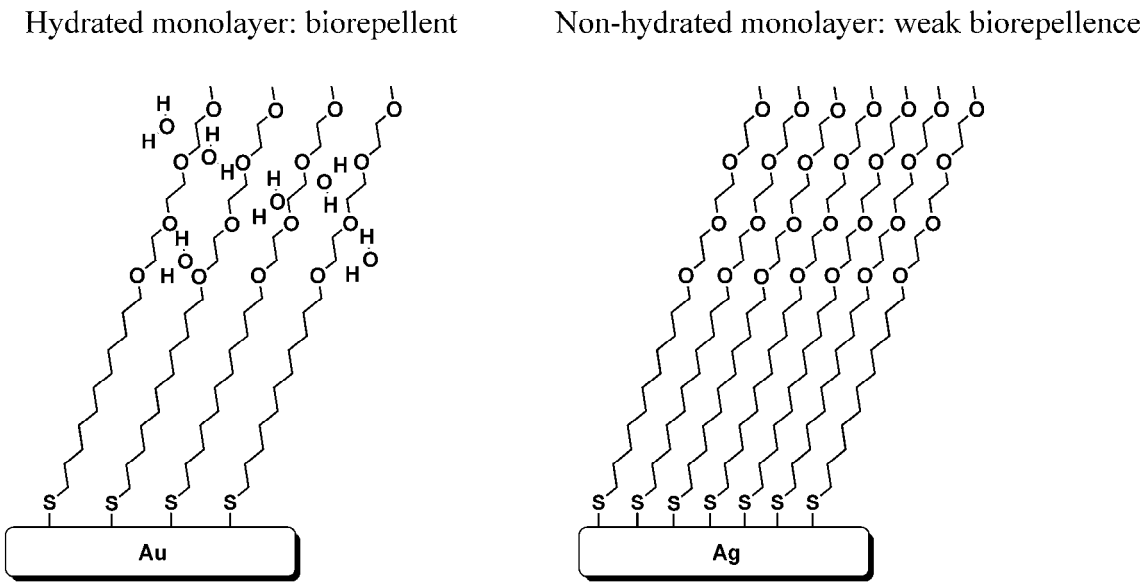

Figure 7. Influence of monolayer packing on biorepellent activity (adapted from Herrwerth *et al.*[35]).

On silica, ethylene glycol monolayers can also reduce the adsorption of proteins[88,154,155] and microorganisms.[156] Organosilane compounds were also used to form monolayers of oligoethylene glycol onto oxidized silicon nitride substrates,[157] but no studies on their protein resistance or hydrolytic stability have been reported. Besides ethylene glycols, other linear

compounds, such as some derivatives of zwitterionic phospholipids[158,159] ($-(CH_2)_{15}-(PO_4)^--(CH_2)_2-NR_3^+$ (R = CH_3 or H)) have been attached to oxide surfaces, reducing lysozyme or fibrinogen adsorption by about 90% compared to bare substrates.

On silicon surfaces, oligo ethylene glycol-containing monolayers could also be attached using the hydrosilylation reaction:[160-162] these biorepelling surfaces were used for example for the specific attachment of DNA molecules[163] or the formation of nano-patterned biorepellent surfaces.[164] In a recent study from our laboratories monolayers of alkene-based oligoethylene glycol compounds (3 and 6 repeating EG units) were formed on $Si_{3.9}N_4$ substrates,[165] which decreased the adsorption of proteins down to the detection limit of reflectometry. Complementary water contact angles and AFM measurements on surfaces coated with compounds containing 6 ethylene glycol units confirmed the absence of any contamination, when tested for BSA and fibrinogen adsorption. Since these monolayers display a very high hydrolytic stability, even in acidic or basic media,[108,109] this technique can be extended to silicon nitride nano- and microdevices such as microsieves membranes[166-169] (See Chapter 3), and studies on this topic are currently ongoing in our laboratories. Another development concerns the coating of bio-compatible microdevices, like silicon carbide-based medical prosthesis and micro-electrodes.[170-175] For sensing and biomedical applications, SiC surfaces would benefit from surface modification with biocompatible monolayers, which is also possible by all means, using thermal or light-initiated monolayer formation with alkenes.[16,17]

Some articles also reported on the attachment of linear PEG polymers onto Si_xN_4 cantilevers using polymer chains bearing NHS (N-hydrosuccinimide) esters that can form amide bonds with the surface NH_2 groups,[176-178] to study molecular recognition with atomic force microscopy. Another example mentions the grafting of PEG chains (MW: 5000) on flat silicon nitride substrates by direct condensation at 100ºC of –OH groups with the silanol groups at the surface to form strong Si-O-C bonds.[179]

If a silane group is present as part of the polymer, it can be grafted directly to the surfaces. This modification has been used for instance to attach long PEG chains (MW 750-5000) on silica[89,90] or glass[180] surfaces and on alumina membranes.[181] PEG methyl ether acrylate could also be included in a copolymer[182] with 3-(trimethoxysilyl)propyl methacrylate (poly(TMSMA-r-PEGMA), MW of PEG: 475) and attached onto oxidized silicon substrates. These coatings could dramatically reduce the adsorption of BSA and fibrinogen, but could also reduce the adhesion of fibroblast cells onto surfaces. Still using silane chemistry, the pre-formed poly(TMSMA-r-PEGMA) copolymer has also been applied to Si_xN_4 microsieves to

introduce PEG chains onto the membrane surfaces.[85] Such modified membranes displayed a more efficient filtration of BSA or skimmed milk than untreated microsieves, when using a backpulsing device, which repeatedly removes deposited particles from the surface. However, these coatings had a relatively low stability at pH 12, which can be related to the instability of silanes in alkaline solutions and to the poor control over polymer grafting. Silane pre-coatings also allowed the grafting of amines[183,184] or aldehydes,[185] which can then be grafted with PEG or dextran, respectively.

Since the "grafting-from" of polymer chains on solid substrates has been developed mainly for organic substrates[186-188] and organic membranes,[135,189-192] polymer grafting on inorganic surfaces requires the prior formation of organic monolayers. Indeed, using such a method, the polymerization of oligo(ethylene glycol) methyl methacrylate (OEGMA) could give protein-repellent glass surfaces. The polymerization was carried out by atom transfer radical polymerization (ATRP)[193] or ozone-induced graft polymerization[194] on glass surfaces modified with silanes bearing ATRP initiators or hydrocarbon chains, respectively. Besides ATRP and ozone initiation, UV irradiation,[133,195,196] plasma-induced graft polymerization,[134,135,189] or radical initiators such as azobisazobutyronitrile (AIBN)[197] and the redox couple $K_2S_2O_8$ - $Na_2S_2O_5$[132,136,139] can initiate graft polymerization. Although not all these methods have already been used to graft polymers onto organic monolayers, they represent an important route to exploit the chemistry of polymers on inorganic substrates.

Direct graft-polymerization can also be applied, like in the case of the plasma-induced graft polymerization of poly(ethylene glycol) methyl ether methacrylate (PEGMA, MW of PEG: 1000) onto oxidized silicon surfaces; the resulting polymer layers reduced significantly the adhesion of BSA and platelets.[198] This direct grafting of polymers onto inorganic surfaces represents a simple alternative to the use of preformed monolayers, but the quality of the grafting is then difficult to control and frequently a low packing density is obtained for long polymer chains. As a result, the nature of the polymer-inorganic substrate interface must be investigated in each case, and the layer properties must be optimized. In conclusion, the application of a well-defined monolayer, prior to the grafting of oligomers or polymers, is usually preferred, because of the flexibility of this approach, which allows many different substrates to be modified in a similar way.

Micro- and Nanopatterning of Surfaces

Two main approaches are generally presented for the formation of nanostructures (Figure 8): the first approach, called “top-down”, involves the use of bulk materials that are reduced to smaller dimensions. The classical photolithographic methods used for the industrial fabrication of microelectronic components falls into this category. A second method, called “bottom-up”, is characterized by the assembly of small preformed building units. This more elegant approach is the one used by nature, where the natural building blocks fabricated by the living cells (proteins, lipids, carbohydrates…) assemble according to a complex scheme predetermined by the structure of the individual components. The recent development of supramolecular chemistry promises more applications in the future by this fabrication strategy.

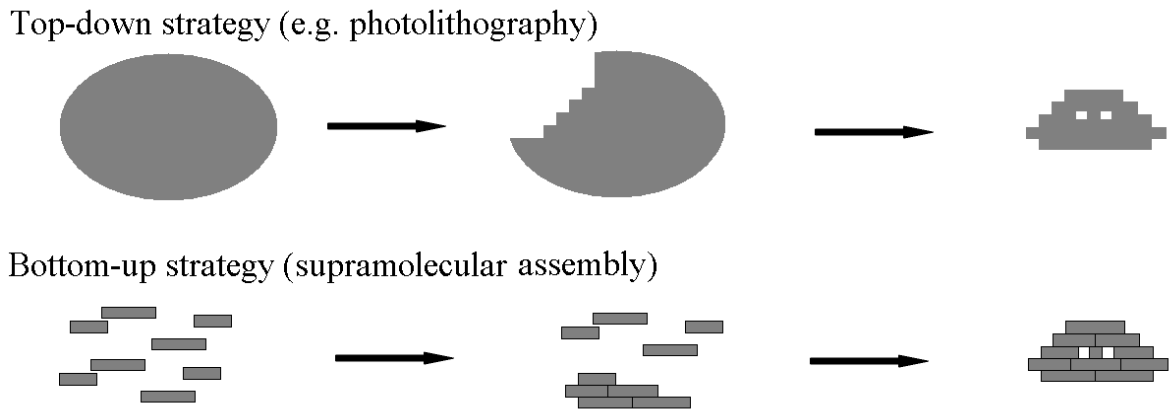

Figure 8: Top-down vs. bottom-up approaches for micro- and nanofabrication.

Organic monolayers can be prepared with extremely accurate spatial geometries: low-dimensional features on surfaces can be readily formed using techniques such as dip-pen lithography or microcontact printing. For this, surface patterning methods usually combine both top-down (fabrication of molds and masks), and bottom-up (self-assembly onto the patterned surfaces) strategies. Among all techniques known for micro- and nano-patterning of surfaces,[199-205] we present here two examples which have been particularly used for structuring of bioactive surfaces: dip-pen lithography and micro-contact printing.

Dip-pen lithography. Dip-pen lithography uses AFM to deposit controlled amounts of liquids over surfaces. Capillary forces are here the main driver for the deposition of the liquid from the AFM tip onto the surface (Figure 9). The use of thiol compounds as an “ink”, deposited over gold surfaces[206-209] allows the formation of small features, with widths of no

more than 30 nm. With the excellent horizontal control offered by the AFM, any two-dimensional structure can be reproduced. The use of functional thiols to pattern the surface can also be used to direct the self-assembly of other component on the surface, in a second step: carboxylic acid-terminated thiols,[210] for example can be used to form ordered arrays of charged polystyrene beads by electrostatic interactions. Such patterned monolayers can also be functionalized covalently, to form DNA arrays.[211] Later, the direct patterning of oligonucleotides[212] or proteins[213] was also demonstrated. The main advantage of this technique is the possibility to directly write on surfaces, while other techniques (lithography, micro-contact printing) can only reproduce a predefined pattern. However the parallelization of the writing, to reproduce quickly large areas of patterned surfaces, is a difficult task. This was made possible by using microfabricated arrays of AFM tips,[214-216] where up to 1024 synchronized AFM tips were used to write identical patterns over an area of 9 mm^2. From its initial simple writing function, dip-pen lithography can then perform the replication of nanoscale patterns.

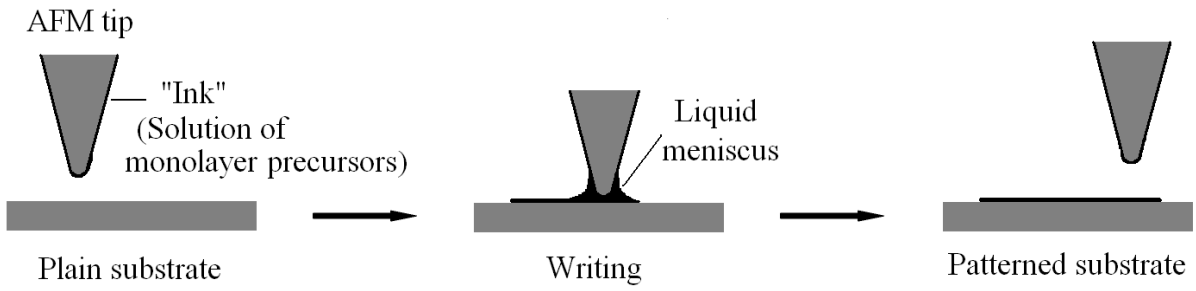

Figure 9. Principle of patterning by dip-pen lithography, using an AFM tip, wetted with the material to deposit on the surface (e.g. deposition of alkyl thiols onto gold surfaces).

The use of such parallel writing AFM tips has made possible the fast sub-micrometer patterning of active proteins such as collagen,[217] histidine-tagged proteins[218] or antigens of protein A/G[219] onto surfaces, or even the formation of arrays of immobilized mosaic viruses[220,221] with an absolute control on their position and orientation.

Similarly to dip-pen lithography, AFM can be used to perform electrochemical patterning of organic monolayers. Maoz et al.[222-224] first reported this technique, where an electrical bias applied between the sample to pattern and the AFM tip caused a reaction on the surface in a confined area. The most common reaction used with this technique is the tip-induced electrooxidation of organic monolayers, yielding oxidized surfaces that can be further reacted

with common chemical reactions. An example of this method is the oxidation of 18-nonadecenyl monolayers, which can then be further reacted with octadecyl trichlorosilane (Figure 10a). In a similar way, the use of functionalized silanes in the second step allows the formation of arrays of biomolecules such as fibronectin,[225] nanoparticle-labeled streptavidin,[226] ferritin[227] or other proteins and DNA molecules.[228,229] Electrical dip-pen nanolithography was also carried out onto H-terminated silicon surfaces (Figure 10b),[230] with the attachment of acetylene in the presence of the electrical bias of an AFM tip.

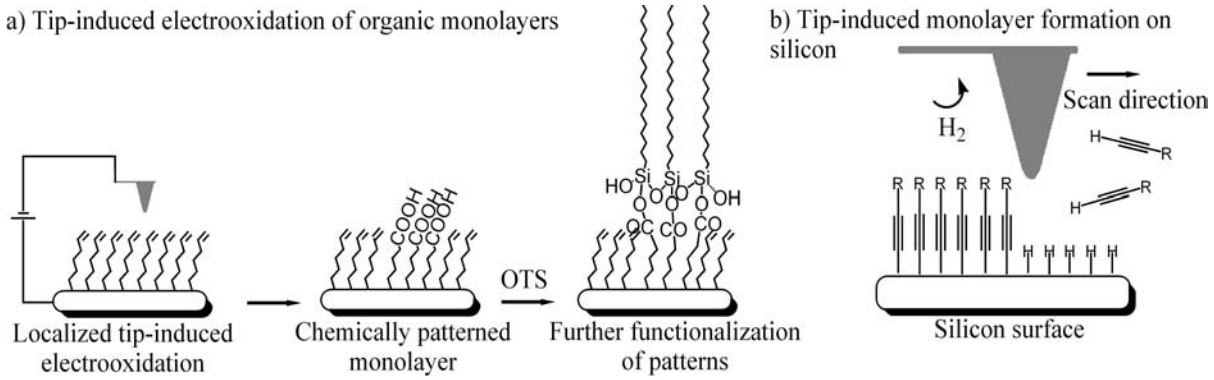

Figure 10. Principles of surface patterning by: a) Tip-induced electrooxidation of vinyl-terminated monolayer and subsequent reaction with octadecyl trichlorosilane (OTS), b) Tip-induced reaction of terminal alkynes with hydrogen terminated silicon surfaces.

Microcontact printing. Microcontact printing (or soft lithography) uses the mechanical properties of elastomeric materials to reproduce patterns with nanometers to centimeter resolution. The elastomer, usually polydimethylsiloxane is used as a stamp to transfer the "ink" onto surfaces, or as a mask to protect defined areas of the surface.

Self-assembled monolayers can be deposited on gold, using alkyl thiols as an ink,[231,232] to create features smaller than 1 μm.[233,234] After a physical contact between the stamp and the surface, facilitated by the flexibility of the PDMS, the ink is transferred and linked to the gold surface (Figure 11). Scanning electron microscopy even shows that the structure of monolayers obtained by microcontact printing is comparable to that of monolayers prepared from solution.[235]

Apart from the simple description of microcontact printing given here, variations using microfabricated molds for micro- and nanofabrication also include techniques such as replica molding, microtransfer molding, micromolding in capillaries or solvent-assisted micromolding.[201]

The formation of patterned monolayers by micro-contact printing has yielded numerous studies on the formation of bioactive arrays on metals or silicon surfaces. The concept of "molecular printboard" has been coined for the use of preformed patterns by microcontact printing, where biomolecules or nanoparticles can adsorb selectively from solution.[236-239] The biotin-streptavidin interaction has been widely used for this approach, for example by patterning surfaces with a biotin-containing thiol or silane, followed by the adsorption of streptavidin-tagged proteins or nanoparticles.

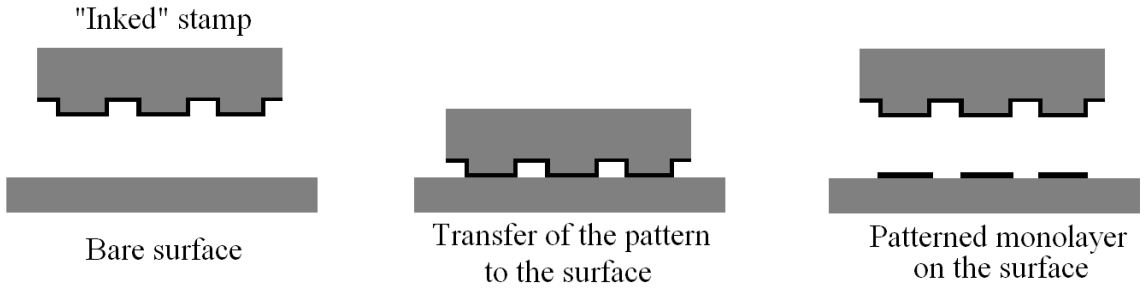

Figure 11. Principle of microcontact printing of organic monolayers on surface.

However, the direct deposition of active biomolecules is also possible: the direct printing of an extracellular matrix protein showed no adverse effects on the protein (inflammatory response, bioincompatibility) by the printing process.[240] In this same way, immunoglobulin,[241] ferritin,[242] concanavalin A[243] or polylysine[244] could be patterned on flat surfaces.

More challenging studies on surface biopatterning have been reported, including the production of guiding tracks to control the growth of actin filaments[245] or the printing of axon-guidance molecules to direct the growth of retinal ganglion cells.[246]

Bio- and Chemosensors

Covalent organic monolayers have found numerous applications in a third type of technology: the fabrication of surface-based sensing devices.[247-249] In such systems, the detection of specific analytes from a gas or a solution requires three main steps: first the analyte is transferred from the bulk phase (gas or liquid) to the surface and bound onto it specifically. We will discuss here the case where covalent organic monolayers are used for this recognition and binding. In a second step, the surface bound compound is detected in a physical way: the chemical binding information is then transformed into physical information: we describe here the electrical and optical detection methods. In a last important step, the detector is usually connected to an electronic system that allows the storage or read out of the detection. Although we do not treat this last topic here, the integration, packaging and efficiency of this part of the device is often a crucial parameter for the commercial success of a detection technique.

Optical sensors. Numerous examples of biodetection using organic monolayers have been described: for example, biosensors based on fluorescence,[72,250] Raman scattering,[251] ellipsometry,[252,253] infra-red[254] or simply visual techniques[255] have used the specificity of monolayer-functionalized surfaces. The geometry of the sensor also has a tremendous importance for the realization of the devices. Besides classical transmission and reflection modes, the need for compact sensors has favored the development of systems based on optic fibers and waveguide materials to transport light from the source to the binding area and to the detector.[256] Miniaturized microfluidics sensors, for example, can use silicon oxide or silicon nitride as waveguide and immobilization platform. In particular, Si_xN_4 is widely used, for example, as waveguide material in refractometric[257-259] or fluorescence[260] detection.

Among all optical techniques, one type of surface-based detection technique, surface plasmon resonance (SPR), has had tremendous success in the last 20 years.[261-267] Surface plasmons are longitudinal waves of charge density that propagate at the interface between a metal and a dielectric material. In a typical Kretchmann geometry (Figure 12), light travelling through a glass prism hits a thin layer of metal (usually gold or silver, with a thickness smaller than the light wavelength) and is totally reflected to a detector. However, a part of the light, called the evanescent wave, is able to penetrate some distance (in the order of micrometers) beyond the metal-glass interface, and to couple with the free electrons of the metal. This coupling results in a drop in intensity of the reflected light. Since this drop is related to the

refractive index of the material present at the external surface of the metal, any adsorption on that surface will cause a change in the SPR signal. The SPR signal is also highly dependent on the angle, wavelength[268] and also phase[269] of the reflected light, and all parameters can be used to monitor the adsorption on the metal surface.

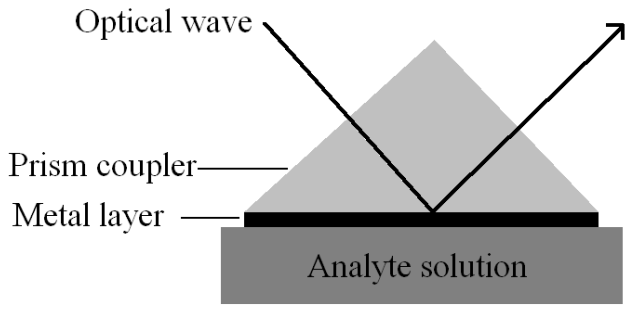

Figure 12. Kretchmann configuration for SPR detection: the light beam is directed towards the back side of a metal (gold or silver), by means of a prism. The front side of the metal is in contact with the solution to analyze. The adsorption of biomolecules on the metal causes a change in the refractive index close to the surface and affects the drop in intensity of the reflected light.

The success of SPR is due to many advantages: the sensors can be cleaned and reused indefinitely, the detection does not need any labeling of the analyte and it can be done in real time, allowing kinetic studies. The crucial role of gold or silver surfaces in SPR has naturally promoted the use of thiol-based monolayers to create specific surface interactions: the specific detection of DNA,[270] or organic pollutants[271,272] and pathogens[273] has been made possible by coupling of complementary strands of DNA or antibodies, respectively. A further step in sensitivity was achieved with the formation of more complex sensing architectures using the assembly of nanoparticles onto the gold surface of the SPR: the signal amplification caused by the coupling of the SPR signal with the localized surface plasmons of the metal or semiconductor nanoparticles[46,274] (Figure 13) has resulted in a 1000-fold increase in sensitivity, allowing the detection of picomolar concentrations, and approaches the performances of classical fluorescence based fluorescence based detection method of DNA-hybridation.[275,276]

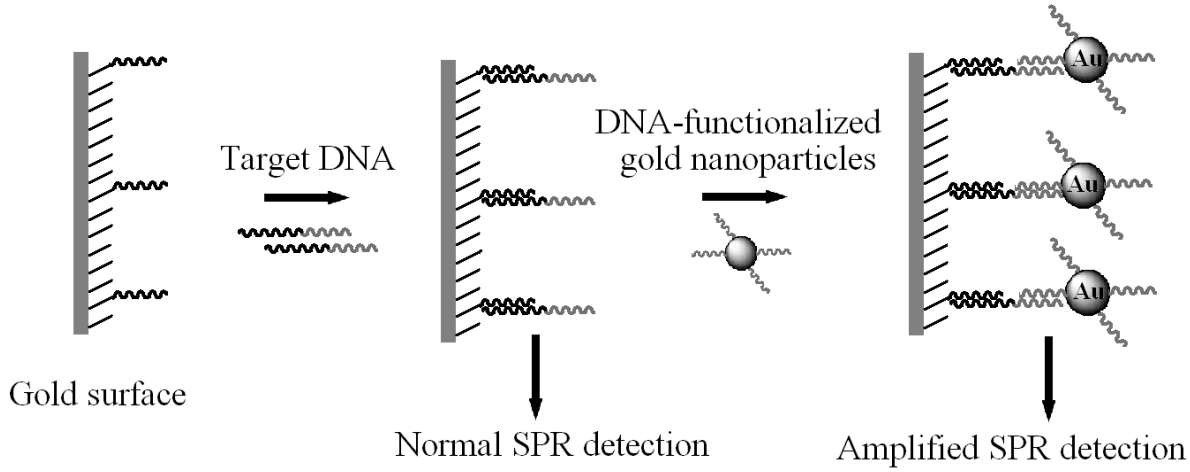

Figure 13. Example of amplified SPR detection: nanoparticle-enhanced SPR (adapted from He *et al*.[275]).

The fluorescence of metallic or semiconducting nanoparticles has opened their applications in biosensing and imaging.[277-279] Similarly to SPR, the free electrons oscillations (localized surface plasmons or LSP) in metal nanoparticles can be coupled with environmental factors that results in changes in optical properties.[280] In particular, the hybridization of DNA on surfaces functionalized with monolayers can cause the subsequent immobilization of functionalized nanoparticles (sandwich assay);[43,45] their presence on the glass sensor can then be monitored directly, or after an amplification step, often carried out by reduction of the metal salt to increase the size of nanoparticles.[45,281]

In a similar way, the aggregation of metal nanoparticles functionalized with thiol-modified DNA single strands in the presence of the complementary DNA will cause a change in their melting behavior that can be observed by a change in their optical absorption, fluorescence or simply the visual aspect of the nanoparticles (Figure 14).[282] Besides DNA, variations on this method have also enabled the detection of single amino-acids or metal ions.[283-285]

Another use of monolayer-functionalized metal nanoparticles involves the coupling of their localized plasmon resonance (LSP) with fluorescence[286-289] or chemiluminescence:[290] the attachment of fluorescent molecules to metallic nanoparticles via organic monolayers can result in dramatic increases in detection sensitivity, making single molecule detection and imaging possible.

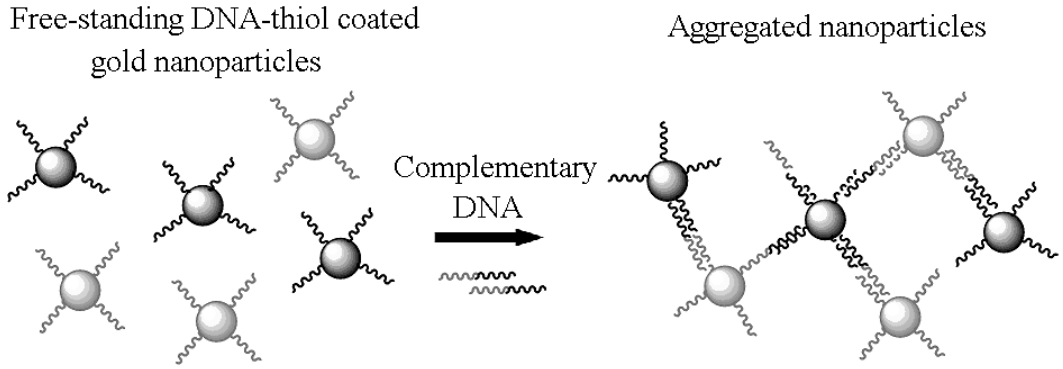

Figure 14. Two types of DNA-functionalized gold nanoparticles, which carry different parts of the sequence to detect, aggregate when the target DNA is introduced, causing a shift in optical properties and melting behavior (adapted from Elghanian et al.[282])

Another recent interesting sensing technique based on functionalized solid surfaces involves the use of photonic crystals, a type of mesoscopic structure formed by the periodical arrangement of nanosized objects. The resulting periodical variation of refractive index between bulk and void in the crystal causes the appearance of a photonic bang-gap: typically this causes sharp peaks in the transmission spectrum of the material. The position of these peaks is highly dependent on the refractive index in the voids of the crystal, allowing for an optical monitoring of adsorption processes at this location.[291,292] Even the binding of small molecules on the highly developed surface of the crystals can cause a significant frequency shift in the resonant photonic crystal mode.

Several studies have investigated the use of surface-modified photonic crystals for biosensing applications; in particular, silicon can be used as a material for the fabrication of photonic crystals sensors, when combined with surface modification by hydrosilylation reactions with alkenes. Indeed, alkene-based monolayers can be readily formed onto the surface of porous silicon structures and the attachment and subsequent surface binding events can be monitored by the shift of the crystal optical band-gap.[293,294] Such a silicon photonic crystal was developed to monitor the protease activity of biological samples[295] (Figure 15a), by immobilizing the protein angiotensine on the walls of the crystal: the degradation of the protein caused by the presence of a protease induces a shift in the photonic bandgap of the crystal.

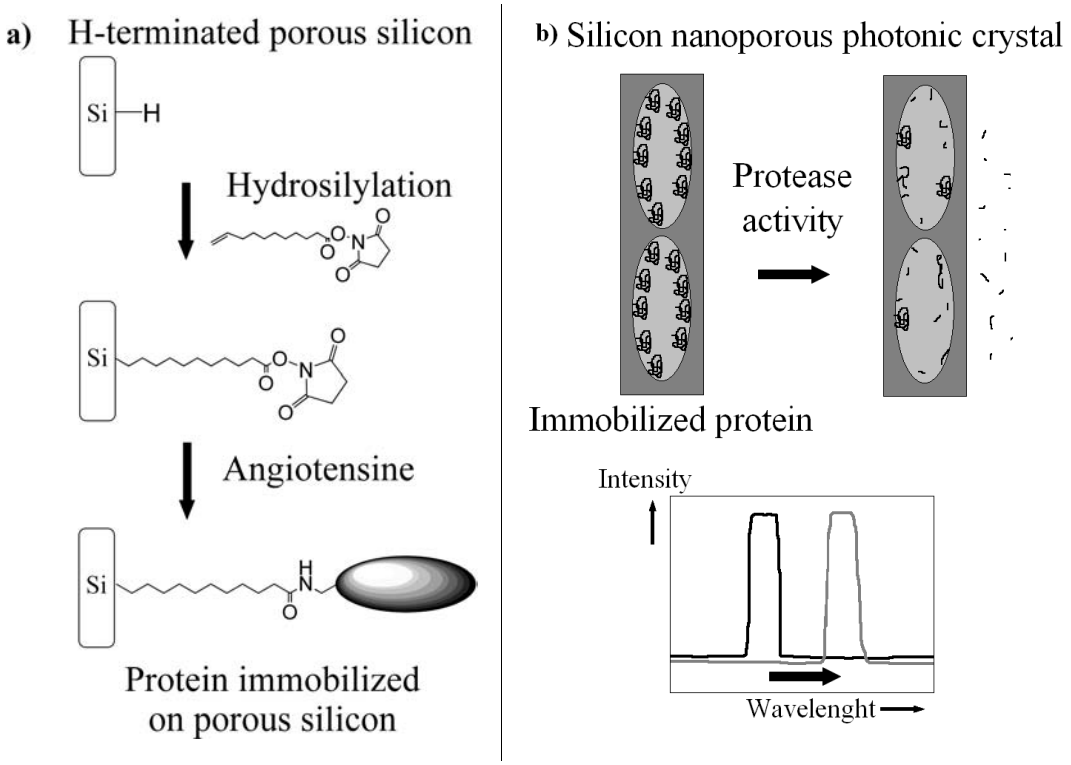

Figure 15. a) Immobilization of the protein angiotensine on the surface of porous silicon by hydrosilylation, b) Photonic crystal with immobilized protein in the voids: the removal of protein by a protease is monitored by a shift in the optical mode of the crystal (adapted from Kilian *et al*.[295]).

Electrical sensors. Besides optical techniques**,** electrical measurements have been intensively exploited for the development of biosensors. Metal and semiconductor surfaces coated with organic monolayers can be characterized by e.g. resistance, impedance or capacitance measurement.[247,248] The wealth of combinations of measurement modes and functionalized monolayers creates a large variety of sensor designs. Some examples of sensors include resistivity measurements to detect DNA hybridization,[44] capacitance measurements to monitor the adsorption of nanoparticle-functionalized antibodies[296] or the voltammetric detection of copper (II) ions on a gold electrode functionalized with a thiol-derived sequence of chelating amino-acids (Gly-Gly-His, Figure 16).[297] Impedance measurements were also used to detect antibody–antigen interaction, by coating of silicon nitride surfaces with antibodies with an alkylsilane linker.[73,74] The adsorption of rabbit immunoglobulin causes a change in the capacitance of the layer, which is used to monitor the interaction.

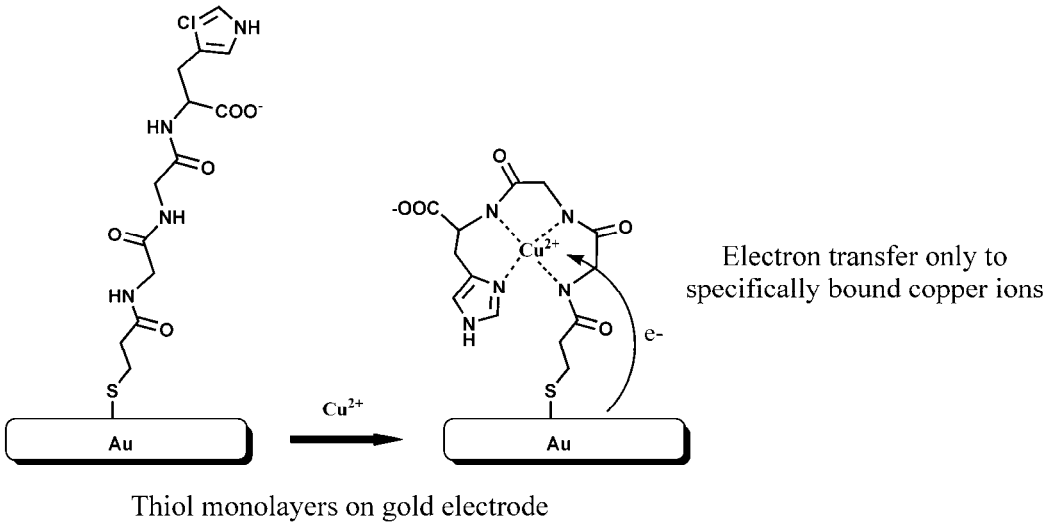

Figure 16. Specific binding of copper (II) ions onto gold electrode using a thiol-based monolayer of oligopeptide (Gly-Gly-His), the detection is carried out by voltammetry.[298]

An important class of electrical biosensors is constituted by enzymatic electrodes: enzymes are immobilized onto metal electrodes and usually kept in presence of a red-ox mediator. In the presence of the analyte to detect (e.g. glucose,[299] gluconic acid,[300] phenolic compounds[298]), the enzyme is converting the mediator into the other red-ox form, which is then detected at the electrode. Thiols have been extensively used to immobilize enzymes onto gold electrodes, often using acid-terminated monolayers and the subsequent formation of a strong amide bond with free amines of the enzyme.[301] For enzyme electrodes, numerous studies describe the use of artificial bilayer membranes deposited onto electrodes: the two-dimensional liquid environment of lipid bilayers not only stabilizes the enzyme on the surface but also allows enough conformational freedom for the enzyme to function like in a natural membrane. Although artificial membranes are out of the scope of this review, it is important to highlight the positive role of covalent organic monolayers in the stabilization if these membranes. Compact linear alkyl monolayers, for instance, have been shown to stabilize bilayers membranes sitting on top of them.[302] In other studies, the integration of some thiol compound within the bilayers also stabilizes the formation of synthetic membranes[303] or vesicles;[47] such glycolipid-containing vesicles attached to gold electrodes, upon binding with concanavalin A, can decrease the typical reduction current of a solution of $Fe(CN)_6^{3-}$ (Figure 17).

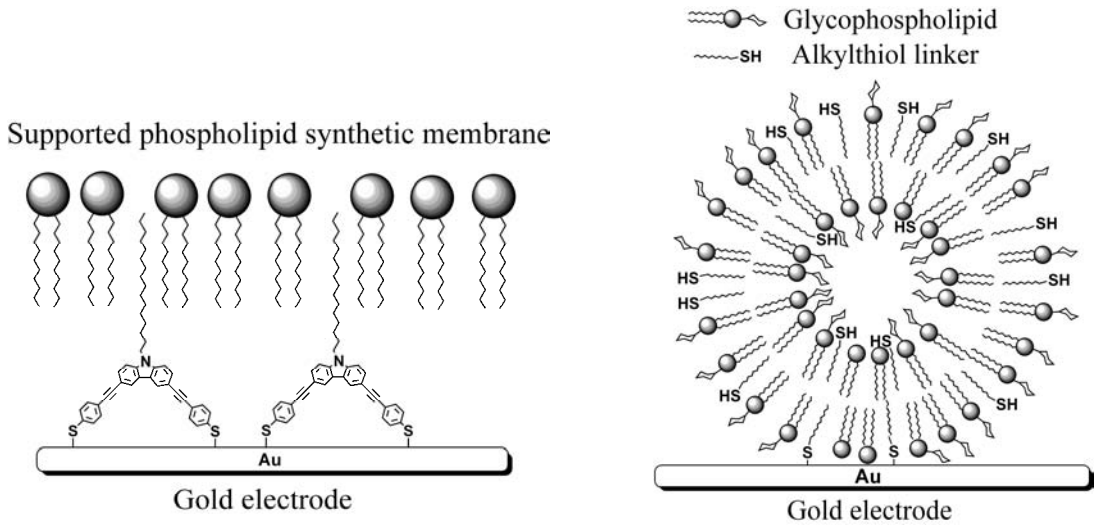

Figure 17. Two examples of biomimetic membrane: a) bulky alkyl thiol linker to anchor flat phospholipid membrane (adapted from Bao et al.[303]) and b) mixed vesicle prepared from glycophospholipids (for the specific binding of concanavalin A) and linear alkylthiol linkers (adapted from Guo et al.[47]).

Conclusion

The formation of covalent organic monolayers is an optimal way to control the surface of inorganic materials. The carefully designed bulk characteristics of a conducting, transparent or nanostructured inorganic device can be maintained even if surface properties need to be adapted to changing environments or applications. In this respect, they allow a supplementary freedom in the design of nano- and microdevices. However, monolayers not only serve material science in this secondary function; they are nowadays at the center of new fields of research, such as nanopatterning or biocompatible surfaces.

This review has presented three general methods for the formation of covalent organic monolayers onto inorganic surfaces and a number of relevant applications where these nanometer-thick structures play a central role.

Despite the wealth of applications, the fundamental aspects of monolayer formation are still undergoing intensive investigations; a basic internet query with ISI Web of Science on the topic “organic monolayers” shows an ever-increasing number of hits since 1990, which reaches almost 400 articles for the year 2008. Considering the current overwhelming trend in favor of nanotechnological research, which has brought an intense light upon a world dominated by interfacial effects, the interest in organic monolayers is likely to persist for a long time.

References

(1) Ulman, A. *Chem. Rev.* **1996,** *96*, 1533-1554.

(2) Templeton, A. C.; Wuelfing, M. P.; Murray, R. W. **2000,** *33*, 27-36.

(3) Love, J. C.; Estroff, L. A.; Kriebel, J. K.; Nuzzo, R. G.; Whitesides, G. M. **2005,** *105*, 1103-1169.

(4) Schreiber, F. **2000,** *65*, 151-256.

(5) Poirier, G. E. **1997,** *97*, 1117-1127.

(6) Onclin, S.; Ravoo, B. J.; Reinhoudt, D. N. *Angew. Chem., Int. Ed.* **2005,** *44*, 6282-6304.

(7) Buriak, J. M. *Chem. Rev.* **2002,** *102*, 1271-1308.

(8) Linford, M. R.; Fenter, P.; Eisenberger, P. M.; Chidsey, C. E. D. *J. Am. Chem. Soc.* **1995,** *117*, 3145-3155.

(9) Li, T. T. T.; Weaver, M. J. *J. Am. Chem. Soc.* **1984,** *106*, 6107-6108.

(10) Li, Y. Z.; Huang, J. Y.; McIver, R. T.; Hemminger, J. C. *J. Am. Chem. Soc.* **1992,** *114*, 2428-2432.

(11) Nuzzo, R. G.; Allara, D. L. *J. Am. Chem. Soc.* **1983,** *105*, 4481-4483.

(12) Sagiv, J. *J. Am. Chem. Soc.* **1980,** *102*, 92-98.

(13) Boukherroub, R. *Curr. Opin. Solid State Mater. Sci.* **2005,** *9*, 66-72.

(14) Shirahata, N.; Hozumi, A.; Yonezawa, T. *Chem. Rec.* **2005,** *5*, 145-159.

(15) Sieval, A. B.; Linke, R.; Zuilhof, H.; Sudhölter, E. J. R. *Adv. Mater.* **2000,** *12*, 1457-1460.

(16) Rosso, M.; Arafat, A.; Schroën, K.; Giesbers, M.; Roper, C. S.; Maboudian, R.; Zuilhof, H. *Langmuir* **2008,** *24*, 4007-4012.

(17) Rosso, M.; Giesbers, M.; Arafat, A.; Schroën, K.; Zuilhof, H. *Langmuir* **2009,** *25*, 2172-2180.

(18) Colavita, P. E.; Sun, B.; Tse, K. Y.; Hamers, R. J. *J. Vac. Sci. Technol. A* **2008,** *26*, 925-931.

(19) Colavita, P. E.; Sun, B.; Wang, X. Y.; Hamers, R. J. *J. Phys. Chem. C* **2009,** *113*, 1526-1535.

(20) Mischki, T. K.; Donkers, R. L.; Eves, B. J.; Lopinski, G. P.; Wayner, D. D. M. *Langmuir* **2006,** *22*, 8359-8365.

(21) Dubois, L. H.; Nuzzo, R. G. *Ann. Rev. Phys. Chem.* **1992,** *43*, 437-463.

(22) Lee, T. R.; Laibinis, P. E.; Folkers, J. P.; Whitesides, G. M. *Pure Appl. Chem.* **1991,** *63*, 821-828.

(23) Heimel, G.; Romaner, L.; Zojer, E.; Bredas, J. L. *Acc. Chem. Res.* **2008,** *41*, 721-729.

(24) Bain, C. D.; Evall, J.; Whitesides, G. M. *J. Am. Chem. Soc.* **1989,** *111*, 7155-7164.
(25) Bain, C. D.; Troughton, E. B.; Tao, Y. T.; Evall, J.; Whitesides, G. M.; Nuzzo, R. G. *J. Am. Chem. Soc.* **1989,** *111*, 321-335.
(26) Crivillers, N.; Mas-Torrent, M.; Vidal-Gancedo, J.; Veciana, J.; Rovira, C. *J. Am. Chem. Soc.* **2008,** *130*, 5499-5506.
(27) Katz, E.; Itzhak, N.; Willner, I. *J. Electroanal. Chem.* **1992,** *336*, 357-362.
(28) Troughton, E. B.; Bain, C. D.; Whitesides, G. M.; Nuzzo, R. G.; Allara, D. L.; Porter, M. D. *Langmuir* **1988,** *4*, 365-385.
(29) Cooper, J. M.; Greenough, K. R.; McNeil, C. J. *J. Electroanal. Chem.* **1993,** *347*, 267-275.
(30) Uvdal, K.; Bodo, P.; Liedberg, B. *J. Colloid Interf. Sci.* **1992,** *149*, 162-173.
(31) Ihs, A.; Uvdal, K.; Liedberg, B. *Langmuir* **1993,** *9*, 733-739.
(32) Biebuyck, H. A.; Bian, C. D.; Whitesides, G. M. *Langmuir* **1994,** *10*, 1825-1831.
(33) Nuzzo, R. G.; Fusco, F. A.; Allara, D. L. *J. Am. Chem. Soc.* **1987,** *109*, 2358-2368.
(34) Prime, K. L.; Whitesides, G. M. *Science* **1991,** *252*, 1164-1167.
(35) Herrwerth, S.; Eck, W.; Reinhardt, S.; Grunze, M. *J. Am. Chem. Soc.* **2003,** *125*, 9359-9366.
(36) Prime, K. L.; Whitesides, G. M. *J. Am. Chem. Soc.* **1993,** *115*, 10714-10721.
(37) Chidsey, C. E. D. *Science* **1991,** *251*, 919-922.
(38) Chidsey, C. E. D.; Bertozzi, C. R.; Putvinski, T. M.; Mujsce, A. M. *J. Am. Chem. Soc.* **1990,** *112*, 4301-4306.
(39) Collard, D. M.; Fox, M. A. *Langmuir* **1991,** *7*, 1192-1197.
(40) Hutchison, J. E.; Postlethwaite, T. A.; Murray, R. W. *Langmuir* **1993,** *9*, 3277-3283.
(41) Watcharinyanon, S.; Nilsson, D.; Moons, E.; Shaporenko, A.; Zharnikov, M.; Albinsson, B.; Martensson, J.; Johansson, L. S. O. *Phys. Chem. Chem. Phys.* **2008,** *10*, 5264-5275.
(42) Zak, J.; Yuan, H. P.; Ho, M.; Woo, L. K.; Porter, M. D. *Langmuir* **1993,** *9*, 2772-2774.
(43) Bailey, R. C.; Nam, J. M.; Mirkin, C. A.; Hupp, J. T. *J. Am. Chem. Soc.* **2003,** *125*, 13541-13547.
(44) Hianik, T.; Gajdos, V.; Krivanek, R.; Oretskaya, T.; Metelev, V.; Volkov, E.; Vadgama, P. *Bioelectrochem.* **2001,** *53*, 199-204.
(45) Taton, T. A.; Mirkin, C. A.; Letsinger, R. L. *Science* **2000,** *289*, 1757-1760.
(46) Hutter, E.; Fendler, J. H.; Roy, D. *J. Phys. Chem. B* **2001,** *105*, 11159-11168.
(47) Guo, C. X.; Boullanger, P.; Jiang, L.; Liu, T. *Coll. Surf. B* **2008,** *62*, 146-150.

(48) Heinz, R.; Rabe, J. P. *Langmuir* **1995,** *11*, 506-511.

(49) Ihs, A.; Liedberg, B. *Langmuir* **1994,** *10*, 734-740.

(50) Laibinis, P. E.; Whitesides, G. M. *J. Am. Chem. Soc.* **1992,** *114*, 1990-1995.

(51) Laibinis, P. E.; Whitesides, G. M. *J. Am. Chem. Soc.* **1992,** *114*, 9022-9028.

(52) Walczak, M. M.; Chung, C. K.; Stole, S. M.; Widrig, C. A.; Porter, M. D. *J. Am. Chem. Soc.* **1991,** *113*, 2370-2378.

(53) Laibinis, P. E.; Whitesides, G. M.; Allara, D. L.; Tao, Y. T.; Parikh, A. N.; Nuzzo, R. G. *J. Am. Chem. Soc.* **1991,** *113*, 7152-7167.

(54) Laiho, T.; Lukkari, J.; Meretoja, M.; Laajalehto, K.; Kankare, J.; Leiro, J. A. *Surf. Sci.* **2005,** *584*, 83-89.

(55) Chen, S. H.; Kimura, K. *J. Phys. Chem. B* **2001,** *105*, 5397-5403.

(56) Ruan, C. M.; Bayer, T.; Meth, S.; Sukenik, C. N. *Thin Solid Films* **2002,** *419*, 95-104.

(57) Demoz, A.; Harrison, D. J. *Langmuir* **1993,** *9*, 1046-1050.

(58) Love, J. C.; Wolfe, D. B.; Haasch, R.; Chabinyc, M. L.; Paul, K. E.; Whitesides, G. M.; Nuzzo, R. G. *J. Am. Chem. Soc.* **2003,** *125*, 2597-2609.

(59) Sheen, C. W.; Shi, J. X.; Martensson, J.; Parikh, A. N.; Allara, D. L. *J. Am. Chem. Soc.* **1992,** *114*, 1514-1515.

(60) Ding, X.; Moumanis, K.; Dubowski, J. J.; Frost, E. H.; Escher, E. *Appl. Phys. A: Mater. Sci. Process.* **2006,** *83*, 357-360.

(61) Gu, Y.; Lin, Z.; Butera, R. A.; Smentkowski, V. S.; Waldeck, D. H. *Langmuir* **1995,** *11*, 1849-1851.

(62) Hutt, D. A.; Cooper, E.; Leggett, G. J. *J. Phys. Chem. B* **1998,** *102*, 174-184.

(63) Brewer, N. J.; Foster, T. T.; Leggett, G. J.; Alexander, M. R.; McAlpine, E. *J. Phys. Chem. B* **2004,** *108*, 4723-4728.

(64) Brewer, N. J.; Janusz, S.; Critchley, K.; Evans, S. D.; Leggett, G. J. *J. Phys. Chem. B* **2005,** *109*, 11247-11256.

(65) Silberzan, P.; Leger, L.; Ausserre, D.; Benattar, J. J. *Langmuir* **1991,** *7*, 1647-1651.

(66) Schoell, S. J.; Hoeb, M.; Sharp, I. D.; Steins, W.; Eickhoff, M.; Stutzmann, M.; Brandt, M. S. *Appl. Phys. Lett.* **2008,** *92*, 153301 (1-3).

(67) King, S. W.; Nemanich, R. J.; Davis, R. F. *J. Electrochem. Soc.* **1999,** *146*, 1910-1917.

(68) Hijikata, Y.; Yaguchi, H.; Yoshikawa, M.; Yoshida, S. *Appl. Surf. Sci.* **2001,** *184*, 161-166.

(69) Sampathkumaran, U.; De Guire, M. R.; Heuer, A. H.; Niesen, T.; Bill, J.; Aldinger, F. *Ceram. Trans.* **1999,** *94*, 307-318.
(70) Petoral, R. M.; Yazdi, G. R.; Spetz, A. L.; Yakimova, R.; Uvdal, K. *Appl. Phys. Lett.* **2007,** *90*, 223904(1-3).
(71) Yakimova, R.; Petoral, R. M.; Yazdi, G. R.; Vahlberg, C.; Spetz, A. L.; Uvdal, K. *J. Phys. D Appl. Phys.* **2007,** *40*, 6435-6442.
(72) Anderson, A. S.; Dattelbaum, A. M.; Montano, G. A.; Price, D. N.; Schmidt, J. G.; Martinez, J. S.; Grace, W. K.; Grace, K. M.; Swanson, B. I. *Langmuir* **2008,** *24*, 2240-2247.
(73) Tlili, A.; Abdelghani, A.; Ameur, S.; Jaffrezic-Renault, N. *Mater. Sci. Eng., C* **2006,** *26*, 546-550.
(74) Tlili, A.; Jarboui, M. A.; Abdelghani, A.; Fathallah, D. M.; Maaref, M. A. *Mater. Sci. Eng., C* **2005,** *25*, 490-495.
(75) Headrick, J. E.; Berrie, C. L. *Langmuir* **2004,** *20*, 4124-4131.
(76) Colic, M.; Franks, G.; Fisher, M.; Lange, F. *J. Am. Ceram. Soc.* **1998,** *81*, 2157-2163.
(77) Rozlosnik, N.; Gerstenberg, M. C.; Larsen, N. B. *Langmuir* **2003,** *19*, 1182-1188.
(78) Glaser, A.; Foisner, J.; Friedbacher, G.; Hoffmann, H. *Anal. Bioanal. Chem.* **2004,** *379*, 653-657.
(79) Carraro, C.; Yauw, O. W.; Sung, M. M.; Maboudian, R. *J. Phys. Chem. B* **1998,** *102*, 4441-4445.
(80) Sung, M. M.; Carraro, C.; Yauw, O. W.; Kim, Y.; Maboudian, R. *J. Phys. Chem. B* **2000,** *104*, 1556-1559.
(81) Leitner, T.; Friedbacher, G.; Vallant, T.; Brunner, H.; Mayer, U.; Hoffmann, H. *Microchim. Acta* **2000,** *133*, 331-336.
(82) Vallant, T.; Brunner, H.; Mayer, U.; Hoffmann, H.; Leitner, T.; Resch, R.; Friedbacher, G. *J. Phys. Chem. B* **1998,** *102*, 7190-7197.
(83) Tripp, C. P.; Hair, M. L. *Langmuir* **1992,** *8*, 1120-1126.
(84) Tripp, C. P.; Hair, M. L. *Langmuir* **1995,** *11*, 1215-1219.
(85) Girones, M.; Bolhuis-Versteeg, L.; Lammertink, R.; Wessling, M. *J. Colloid Interf. Sci.* **2006,** *299*, 831-840.
(86) Geerken, M. J.; van Zonten, T. S.; Lammertink, R. G. H.; Borneman, Z.; Nijdam, W.; van Rijn, C. J. M.; Wessling, M. *Adv. Eng. Mater.* **2004,** *6*, 749-754.
(87) Wasserman, S. R.; Tao, Y. T.; Whitesides, G. M. *Langmuir* **1989,** *5*, 1074-1087.

(88) Cecchet, F.; De Meersman, B.; Demoustier-Champagne, S.; Nysten, B.; Jonas, A. M. *Langmuir* **2006,** *22*, 1173-1181.

(89) Sharma, S.; Johnson, R. W.; Desai, T. A. *Appl. Surf. Sci.* **2003,** *206*, 218-229.

(90) Sharma, S.; Johnson, R. W.; Desai, T. A. *Langmuir* **2004,** *20*, 348-356.

(91) Wayner, D. D. M.; Wolkow, R. A. *J. Chem. Soc., Perkin Trans. 2* **2002**, 23-34.

(92) Linford, M. R.; Chidsey, C. E. D. *J. Am. Chem. Soc.* **1993,** *115*, 12631.

(93) Sieval, A. B.; Demirel, A. L.; Nissink, J. W. M.; Linford, M. R.; van der Maas, J. H.; de Jeu, W. H.; Zuilhof, H.; Sudhölter, E. J. R. *Langmuir* **1998,** *14*, 1759-1768.

(94) Sieval, A. B.; Opitz, R.; Maas, H. P. A.; Schoeman, M. G.; Meijer, G.; Vergeldt, F. J.; Zuilhof, H.; Sudhölter, E. J. R. *Langmuir* **2000,** *16*, 10359-10368.

(95) Cicero, R. L.; Linford, M. R.; Chidsey, C. E. D. *Langmuir* **2000,** *16*, 5688.

(96) Effenberger, F.; Gotz, G.; Bidlingmaier, B.; Wezstein, M. *Angew. Chem., Int. Ed.* **1998,** *37*, 2462-2464.

(97) Strother, T.; Cai, W.; Zhao, X. S.; Hamers, R. J.; Smith, L. M. *J. Am. Chem. Soc.* **2000,** *122*, 1205-1209.

(98) Strother, T.; Hamers, R. J.; Smith, L. M. *Nucleic Acids Res.* **2000,** *28*, 3535-3541.

(99) de Smet, L. C. P. M.; Pukin, A. V.; Sun, Q. Y.; Eves, B. J.; Lopinski, G. P.; Visser, G. M.; Zuilhof, H.; Sudhölter, E. J. R. *Appl. Surf. Sci.* **2005,** *252*, 24-30.

(100) de Smet, L. C. P. M.; Stork, G. A.; Hurenkamp, G. H. F.; Sun, Q. Y.; Topal, H.; Vronen, P. J. E.; Sieval, A. B.; Wright, A.; Visser, G. M.; Zuilhof, H.; Sudhölter, E. J. R. *J. Am. Chem. Soc.* **2003,** *125*, 13916-13917.

(101) Sun, Q.-Y.; de Smet, L. C. P. M.; van Lagen, B.; Giesbers, M.; Thune, P. C.; van Engelenburg, J.; de Wolf, F. A.; Zuilhof, H.; Sudhölter, E. J. R. *J. Am. Chem. Soc.* **2005,** *127*, 2514-2523.

(102) Scheres, L.; Arafat, A.; Zuilhof, H. *Langmuir* **2007,** *23*, 8343-8346.

(103) Okano, T.; Inari, H.; Ishizaki, T.; Saito, N.; Sakamoto, W.; Takai, O. *Chem. Lett.* **2005,** *34*, 600-601.

(104) Aswal, D. K.; Lenfant, S.; Guerin, D.; Yakhmi, J. V.; Vuillaume, D. *Anal. Chim. Acta* **2006,** *568*, 84-108.

(105) Zhao, J. W.; Uosaki, K. *J. Phys. Chem. B* **2004,** *108*, 17129-17135.

(106) Eves, B. J.; Sun, Q. Y.; Lopinski, G. P.; Zuilhof, H. *J. Am. Chem. Soc.* **2004,** *126*, 14318-14319.

(107) Sun, Q.-Y.; de Smet, L. C. P. M.; van Lagen, B.; Wright, A.; Zuilhof, H.; Sudhölter, E. J. R. *Angew. Chem., Int. Ed.* **2004,** *43*, 1352-1355.
(108) Arafat, A.; Giesbers, M.; Rosso, M.; Sudhölter, E. J. R.; Schroën, K.; White, R. G.; Yang, L.; Linford, M. R.; Zuilhof, H. *Langmuir* **2007,** *23*, 6233-6244.
(109) Arafat, A.; Schroën, K.; de Smet, L. C. P. M.; Sudhölter, E. J. R.; Zuilhof, H. *J. Am. Chem. Soc.* **2004,** *126*, 8600-8601.
(110) Coffinier, Y.; Boukherroub, R.; Wallart, X.; Nys, J. P.; Durand, J. O.; Stievenard, D.; Grandidier, B. *Surf. Sci.* **2007,** *601*, 5492-5498.
(111) Coffinier, Y.; Olivier, C.; Perzyna, A.; Grandidier, B.; Wallart, X.; Durand, J.-O.; Melnyk, O.; Stiévenard, D. *Langmuir* **2005**, 1489-1496.
(112) Asanuma, H.; Noguchi, H.; Uosaki, K.; Yu, H. Z. *J. Phys. Chem. B* **2006,** *110*, 4892-4899.
(113) Love, J. C.; Estroff, L. A.; Kriebel, J. K.; Nuzzo, R. G.; Whitesides, G. M. *Chem. Rev.* **2005,** *105*, 1103-1169.
(114) Buriak, J. M. *Angew. Chem., Int. Ed.* **2001,** *40*, 532-534.
(115) Hovis, J. S.; Coulter, S. K.; Hamers, R. J.; D'Evelyn, M. P.; Russell, J. N.; Butler, J. E. *J. Am. Chem. Soc.* **2000,** *122*, 732-733.
(116) Wang, G. T.; Bent, S. F.; Russell, J. N.; Butler, J. E.; D'Evelyn, M. P. *J. Am. Chem. Soc.* **2000,** *122*, 744-745.
(117) Knickerbocker, T.; Strother, T.; Schwartz, M. P.; Russell, J. N.; Butler, J.; Smith, L. M.; Hamers, R. J. *Langmuir* **2003,** *19*, 1938-1942.
(118) Nichols, B. M.; Butler, J. E.; Russell, J. N.; Hamers, R. J. *J. Phys. Chem. B* **2005,** *109*, 20938-20947.
(119) Strother, T.; Knickerbocker, T.; Russell, J. N.; Butler, J. E.; Smith, L. M.; Hamers, R. J. *Langmuir* **2002,** *18*, 968-971.
(120) Wang, X.; Colavita, P. E.; Metz, K. M.; Butler, J. E.; Hamers, R. J. *Langmuir* **2007,** *23*, 11623-11630.
(121) Ababou-Girard, S.; Sabbah, H.; Fabre, B.; Zellama, K.; Solal, F.; Godet, C. *J. Phys. Chem. C.* **2007,** *111*, 3099-3108.
(122) Ababou-Girard, S.; Solal, F.; Fabre, B.; Alibart, F.; Godet, C. *J. Non-Cryst. Solids* **2006,** *352*, 2011-2014.
(123) Shin, D.; Rezek, B.; Tokuda, N.; Takeuchi, D.; Watanabe, H.; Nakamura, T.; Yamamoto, T.; Nebel, C. E. *Phys. Stat. Sol. A* **2006,** *203*, 3245-3272.

(124) Kane, R. S.; Deschatelets, P.; Whitesides, G. M. *Langmuir* **2003,** *19*, 2388-2391.

(125) Senaratne, W.; Andruzzi, L.; Ober, C. K. *Biomacromolecules* **2005,** *6*, 2427-2448.

(126) Ramsden, J. J. *Chem. Soc. Rev.* **1995,** *24*, 73-78.

(127) Wang, R. L. C.; Kreuzer, H. J.; Grunze, M. *J. Phys. Chem. B* **1997,** *101*, 9767-9773.

(128) Halperin, A. *Langmuir* **1999,** *15*, 2525-2533.

(129) Jeon, S. I.; Lee, J. H.; Andrade, J. D.; Degennes, P. G. *J. Colloid Interf. Sci.* **1991,** *142*, 149-158.

(130) Chan, Y. H. M.; Schweiss, R.; Werner, C.; Grunze, M. *Langmuir* **2003,** *19*, 7380-7385.

(131) Norde, W.; Gage, D. *Langmuir* **2004,** *20*, 4162-4167.

(132) Freger, V.; Gilron, J.; Belfer, S. *J. Membr. Sci.* **2002,** *209*, 283-292.

(133) Taniguchi, M.; Belfort, G. *J. Membr. Sci.* **2004,** *231*, 147-157.

(134) Ulbricht, M.; Belfort, G. *J. Membr. Sci.* **1996,** *111*, 193-215.

(135) Ulbricht, M.; Matuschewski, H.; Oechel, A.; Hicke, H. G. *J. Membr. Sci.* **1996,** *115*, 31-47.

(136) Belfer, S.; Purinson, Y.; Fainshtein, R.; Radchenko, Y.; Kedem, O. *J. Membr. Sci.* **1998,** *139*, 175-181.

(137) Bremmell, K. E.; Kingshott, P.; Ademovic, Z.; Winther-Jensen, B.; Griesser, H. J. *Langmuir* **2006,** *22*, 313-318.

(138) Kim, M.; Saito, K.; Furusaki, S.; Sugo, T.; Okamoto, J. *J. Membr. Sci.* **1991,** *56*, 289-302.

(139) Belfer, S.; Purinson, Y.; Kedem, O. *Acta Polym.* **1998,** *49*, 574-582.

(140) Papra, A.; Gadegaard, N.; Larsen, N. B. *Langmuir* **2001,** *17*, 1457-1460.

(141) Palegrosdemange, C.; Simon, E. S.; Prime, K. L.; Whitesides, G. M. *J. Am. Chem. Soc.* **1991,** *113*, 12-20.

(142) Rundqvist, J.; Hoh, J. H.; Haviland, D. B. *Langmuir* **2005,** *21*, 2981-2987.

(143) Seigel, R. R.; Harder, P.; Dahint, R.; Grunze, M.; Josse, F.; Mrksich, M.; Whitesides, G. M. *Anal. Chem.* **1997,** *69*, 3321-3328.

(144) Vanderah, D. J.; Meuse, C. W.; Silin, V.; Plant, A. L. *Langmuir* **1998,** *14*, 6916-6923.

(145) Vanderah, D. J.; Valincius, G.; Meuse, C. W. *Langmuir* **2002,** *18*, 4674-4680.

(146) Latham, A. H.; Williams, M. E. *Langmuir* **2006,** *22*, 4319-4326.

(147) Harder, P.; Grunze, M.; Dahint, R.; Whitesides, G. M.; Laibinis, P. E. *J. Phys. Chem. B* **1998,** *102*, 426-436.

(148) Laibinis, P. E.; Bain, C. D.; Nuzzo, R. G.; Whitesides, G. M. *J. Phys. Chem.* **1995,** *99*, 7663-7676.

(149) Unsworth, L. D.; Sheardown, H.; Brash, J. L. *Langmuir* **2005,** *21*, 1036-1041.

(150) Vanderah, D. J.; Arsenault, J.; La, H.; Gates, R. S.; Silin, V.; Meuse, C. W.; Valincius, G. *Langmuir* **2003,** *19*, 3752-3756.

(151) Vanderah, D. J.; Parr, T.; Silin, V.; Meuse, C. W.; Gates, R. S.; La, H. Y.; Valincius, G. *Langmuir* **2004,** *20*, 1311-1316.

(152) Vanderah, D. J.; Pham, C. P.; Springer, S. K.; Silin, V.; Meuse, C. W. *Langmuir* **2000,** *16*, 6527-6532.

(153) Balamurugan, S.; Ista, L. K.; Yan, J.; Lopez, G. P.; Fick, J.; Himmelhaus, M.; Grunze, M. *J. Am. Chem. Soc.* **2005,** *127*, 14548-14549.

(154) Hoffmann, C.; Tovar, G. E. M. *J. Colloid Interf. Sci.* **2006,** *295*, 427-435.

(155) Lee, S. W.; Laibinis, P. E. *Biomaterials* **1998,** *19*, 1669-1675.

(156) Finlay, J. A.; Krishnan, S.; Callow, M. E.; Callow, J. A.; Dong, R.; Asgill, N.; Wong, K.; Kramer, E. J.; Ober, C. K. *Langmuir* **2008,** *24*, 503-510.

(157) Cerruti, M.; Fissolo, S.; Carraro, C.; Ricciardi, C.; Majumdar, A.; Maboudian, R. **2008,** *24*, 10646-10653.

(158) Wang, Y. L.; Su, T. J.; Green, R.; Tang, Y. Q.; Styrkas, D.; Danks, T. N.; Bolton, R.; Liu, J. R. *Chem. Comm.* **2000**, 587-588.

(159) Feng, W.; Zhu, S. P.; Ishihara, K.; Brash, J. L. *Langmuir* **2005,** *21*, 5980-5987.

(160) Bocking, T.; Kilian, K. A.; Hanley, T.; Ilyas, S.; Gaus, K.; Gal, M.; Gooding, J. J. *Langmuir* **2005,** *21*, 10522-10529.

(161) Yam, C. M.; Gu, J. H.; Li, S.; Cai, C. Z. *J. Colloid Interf. Sci.* **2005,** *285*, 711-718.

(162) Yam, C. M.; Lopez-Romero, J. M.; Gu, J. H.; Cai, C. Z. *Chem. Comm.* **2004**, 2510-2511.

(163) Bocking, T.; Killan, K. A.; Gaus, K.; Gooding, J. J. *Langmuir* **2006,** *22*, 3494-3496.

(164) Gu, J. H.; Yam, C. M.; Li, S.; Cai, C. Z. *J. Am. Chem. Soc.* **2004,** *126*, 8098-8099.

(165) Rosso, M.; de Jong, E.; Giesbers, M.; Fokkink, R. G.; Norde, W.; Schroën, K.; Zuilhof, H., submitted.

(166) Kuiper, S.; Brink, R.; Nijdam, W.; Krijnen, G. J. M.; Elwenspoek, M. C. *J. Membr. Sci.* **2002,** *196*, 149-157.

(167) Kuiper, S.; van Wolferen, H.; van Rijn, G.; Nijdam, W.; Krijnen, G.; Elwenspoek, M. *J. Micromech. Microeng.* **2001,** *11*, 33-37.

(168) van Rijn, C. J. M.; Veldhuis, G. J.; Kuiper, S. *Nanotechnology* **1998,** *9*, 343-345.
(169) van Rijn, C. J. M. *Nano and Micro Engineered Membrane Technology*. Aquamarijn Research BV, The Netherlands: 2002.
(170) Singh, S.; Buchanan, R. C. *Mater. Sci. Eng., C* **2007,** *27*, 551-557.
(171) Cogan, S. F.; Edell, D. J.; Guzelian, A. A.; Liu, Y. P.; Edell, R. *J. Biomed. Mater. Res. A* **2003,** *67A*, 856-867.
(172) de Carlos, A.; Borrajo, J. P.; Serra, J.; Gonzalez, P.; Leon, B. *J. Mater. Sci. Mater. Med.* **2006,** *17*, 523-529.
(173) Rosenbloom, A. J.; Sipe, D. M.; Shishkin, Y.; Ke, Y.; Devaty, R. P.; Choyke, W. J. *Biomed. Microdev.* **2004,** *6*, 261-267.
(174) Santavirta, S.; Takagi, M.; Nordsletten, L.; Anttila, A.; Lappalainen, R.; Konttinen, Y. T. *Arch. Orthop. Trauma. Surg.* **1998,** *118*, 89-91.
(175) Sella, C.; Martin, J. C.; Lecoeur, J.; Lechanu, A.; Harmand, M. F.; Naji, A.; Davidas, J. P. *Mater. Sci. Eng., A* **1991,** *139*, 49-57.
(176) Ebner, A.; Wildling, L.; Kamruzzahan, A. S. M.; Rankl, C.; Wruss, J.; Hahn, C. D.; Holzl, M.; Zhu, R.; Kienberger, F.; Blaas, D.; Hinterdorfer, P.; Gruber, H. J. *Bioconjugate Chem.* **2007,** *18*, 1176-1184.
(177) Riener, C. K.; Stroh, C. M.; Ebner, A.; Klampfl, C.; Gall, A. A.; Romanin, C.; Lyubchenko, Y. L.; Hinterdorfer, P.; Gruber, H. J. *Anal. Chim. Acta* **2003,** *479*, 59-75.
(178) Wang, T.; Xu, J. J.; Qiu, F.; Zhang, H. D.; Yang, Y. L. *Polymer* **2007,** *48*, 6170-6179.
(179) Suo, Z. Y.; Arce, F. T.; Avci, R.; Thieltges, K.; Spangler, B. *Langmuir* **2006,** *22*, 3844-3850.
(180) Yang, Z. H.; Galloway, J. A.; Yu, H. U. *Langmuir* **1999,** *15*, 8405-8411.
(181) Popat, K. C.; Mor, G.; Grimes, C.; Desai, T. A. *J. Membr. Sci.* **2004,** *243*, 97-106.
(182) Jon, S. Y.; Seong, J. H.; Khademhosseini, A.; Tran, T. N. T.; Laibinis, P. E.; Langer, R. *Langmuir* **2003,** *19*, 9989-9993.
(183) Heyes, C. D.; Kobitski, A. Y.; Amirgoulova, E. V.; Nienhaus, G. U. *J. Phys. Chem. B* **2004,** *108*, 13387-13394.
(184) Massia, S. P.; Stark, J.; Letbetter, D. S. *Biomaterials* **2000,** *21*, 2253-2261.
(185) Schlapak, R.; Pammer, P.; Armitage, D.; Zhu, R.; Hinterdorfer, P.; Vaupel, M.; Fruhwirth, T.; Howorka, S. *Langmuir* **2006,** *22*, 277-285.
(186) Uyama, Y.; Kato, K.; Ikada, Y. *Adv. Polym. Sci.* **1998,** *137*, 1-39.

(187) Kato, K.; Uchida, E.; Kang, E. T.; Uyama, Y.; Ikada, Y. *Prog. Polym. Sci.* **2003,** *28*, 209-259.

(188) Hilal, N.; Ogunbiyi, O. O.; Miles, N. J.; Nigmatullin, R. *Sep. Sci. Tech.* **2005,** *40*, 1957-2005.

(189) Chen, H.; Belfort, G. *J. Appl. Polymer Sci.* **1999,** *72*, 1699-1711.

(190) Kilduff, J. E.; Mattaraj, S.; Zhou, M. Y.; Belfort, G. *J. Nanopart. Res.* **2005,** *7*, 525-544.

(191) Yamagishi, H.; Crivello, J. V.; Belfort, G. *J. Membr. Sci.* **1995,** *105*, 237.

(192) Yamagishi, H.; Crivello, J. V.; Belfort, G. *J. Membr. Sci.* **1995,** *105*, 249.

(193) Ma, H. W.; Li, D. J.; Sheng, X.; Zhao, B.; Chilkoti, A. *Langmuir* **2006,** *22*, 3751-3756.

(194) Beyer, M.; Felgenhauer, T.; Bischoff, F. R.; Breitling, F.; Stadler, V. *Biomaterials* **2006,** *27*, 3505-3514.

(195) Ma, H. M.; Bowman, C. N.; Davis, R. H. *J. Membr. Sci.* **2000,** *173*, 191-200.

(196) Susanto, H.; Balakrishnan, M.; Ulbricht, M. *J. Membr. Sci.* **2007,** *288*, 157-167.

(197) Asatekin, A.; Kang, S.; Elimelech, M.; Mayes, A. M. *J. Membr. Sci.* **2007,** *298*, 136-146.

(198) Zou, X. P.; Kang, E. T.; Neoh, K. G. *Plasmas Polym.* **2002,** *7*, 151-170.

(199) Xia, Y. N.; Rogers, J. A.; Paul, K. E.; Whitesides, G. M. *Chem. Rev.* **1999,** *99*, 1823-1848.

(200) Gates, B. D.; Xu, Q. B.; Stewart, M.; Ryan, D.; Willson, C. G.; Whitesides, G. M. *Chem. Rev.* **2005,** *105*, 1171-1196.

(201) Xia, Y. N.; Whitesides, G. M. *Angew. Chem.-Int. Edit.* **1998,** *37*, 551-575.

(202) Tseng, A. A.; Notargiacomo, A.; Chen, T. P. *J. Vac. Sci. Technol. A* **2005,** *23*, 877-894.

(203) Mukherjee, R.; Sharma, A.; Patil, G.; Faruqui, D.; Pattader, P. S. G. *Bull. Mat. Sci.* **2008,** *31*, 249-261.

(204) Mendes, P. M.; Yeung, C. L.; Preece, J. A. *Nanoscale. Res. Lett.* **2007,** *2*, 373-384.

(205) Guo, L. J. *Adv. Mater.* **2007,** *19*, 495-513.

(206) Ginger, D. S.; Zhang, H.; Mirkin, C. A. *Angew. Chem.-Int. Edit.* **2004,** *43*, 30-45.

(207) Piner, R. D.; Zhu, J.; Xu, F.; Hong, S. H.; Mirkin, C. A. *Science* **1999,** *283*, 661-663.

(208) Hong, S. H.; Mirkin, C. A. *Science* **2000,** *288*, 1808-1811.

(209) Hong, S. H.; Zhu, J.; Mirkin, C. A. *Science* **1999,** *286*, 523-525.

(210) Demers, L. M.; Mirkin, C. A. *Angew. Chem.-Int. Edit.* **2001,** *40*, 3069-3071.

(211) Demers, L. M.; Park, S. J.; Taton, T. A.; Li, Z.; Mirkin, C. A. *Angew. Chem.-Int. Edit.* **2001,** *40*, 3071-3073.

(212) Demers, L. M.; Ginger, D. S.; Park, S. J.; Li, Z.; Chung, S. W.; Mirkin, C. A. *Science* **2002,** *296*, 1836-1838.

(213) Lee, K. B.; Park, S. J.; Mirkin, C. A.; Smith, J. C.; Mrksich, M. *Science* **2002,** *295*, 1702-1705.

(214) King, W. P.; Kenny, T. W.; Goodson, K. E.; Cross, G. L. W.; Despont, M.; Durig, U. T.; Rothuizen, H.; Binnig, G.; Vettiger, P. *J. Microelectromech. Syst.* **2002,** *11*, 765-774.

(215) Wang, X. F.; Ryu, K. S.; Bullen, D. A.; Zou, J.; Zhang, H.; Mirkin, C. A.; Liu, C. *Langmuir* **2003,** *19*, 8951-8955.

(216) Zhang, M.; Bullen, D.; Chung, S. W.; Hong, S.; Ryu, K. S.; Fan, Z. F.; Mirkin, C. A.; Liu, C. *Nanotechnology* **2002,** *13*, 212-217.

(217) Noy, A.; Miller, A. E.; Klare, J. E.; Weeks, B. L.; Woods, B. W.; DeYoreo, J. J. *Nano Lett.* **2002,** *2*, 109-112.

(218) Agarwal, G.; Naik, R. R.; Stone, M. O. *J. Am. Chem. Soc.* **2003,** *125*, 7408-7412.

(219) Lee, S. W.; Oh, B. K.; Sanedrin, R. G.; Salaita, K.; Fujigaya, T.; Mirkin, C. A. *Adv. Mater.* **2006,** *18*, 1133-1136.

(220) Smith, J. C.; Lee, K. B.; Wang, Q.; Finn, M. G.; Johnson, J. E.; Mrksich, M.; Mirkin, C. A. *Nano Lett.* **2003,** *3*, 883-886.

(221) Vega, R. A.; Maspoch, D.; Salaita, K.; Mirkin, C. A. *Angew. Chem.-Int. Edit.* **2005,** *44*, 6013-6015.

(222) Maoz, R.; Frydman, E.; Cohen, S. R.; Sagiv, J. *Adv. Mater.* **2000,** *12*, 725-731.

(223) Maoz, R.; Frydman, E.; Cohen, S. R.; Sagiv, J. *Adv. Mater.* **2000,** *12*, 424-429.

(224) Maoz, R.; Cohen, S. R.; Sagiv, J. *Adv. Mater.* **1999,** *11*, 55-61.

(225) Sekine, S.; Kaji, H.; Nishizawa, M. *Anal. Bioanal. Chem.* **2008,** *391*, 2711-2716.

(226) Choi, I.; Kang, S. K.; Lee, J.; Kim, Y.; Yi, J. *Biomaterials* **2006,** *27*, 4655-4660.

(227) Yoshinobu, T.; Suzuki, J.; Kurooka, H.; Moon, W. C.; Iwasaki, H. *Electrochim. Acta* **2003,** *48*, 3131-3135.

(228) Yoshinobu, T.; Moon, W.; Nishikawa, A.; Suzuki, J.; Iwasaki, H. *Sens. Mater.* **2004,** *16*, 421-428.

(229) Suzuki, J.; Yoshinobu, T.; Moon, W.; Shanmugam, K.; Iwasaki, H. *Electrochemistry* **2006,** *74*, 131-134.

(230) Hurley, P. T.; Ribbe, A. E.; Buriak, J. M. *J. Am. Chem. Soc.* **2003,** *125*, 11334-11339.

(231) Kumar, A.; Biebuyck, H. A.; Whitesides, G. M. *Langmuir* **1994,** *10*, 1498-1511.

(232) Kumar, A.; Whitesides, G. M. *Appl. Phys. Lett.* **1993,** *63*, 2002-2004.

(233) Moffat, T. P.; Yang, H. *J. Electrochem. Soc.* **1995,** *142*, L220-L222.
(234) Xia, Y.; Kim, E.; Whitesides, G. M. *J. Electrochem. Soc.* **1996,** *143*, 1070-1079.
(235) Larsen, N. B.; Biebuyck, H.; Delamarche, E.; Michel, B. *J. Am. Chem. Soc.* **1997,** *119*, 3017-3026.
(236) Ludden, M. J. W.; Li, X.; Greve, J.; van Amerongen, A.; Escalante, M.; Subramaniam, V.; Reinhoudt, D. N.; Huskens, J. *J. Am. Chem. Soc.* **2008,** *130*, 6964-6973.
(237) Yanker, D. M.; Maurer, J. A. *Mol. Biosyst.* **2008,** *4*, 502-504.
(238) Ludden, M. L. W.; Mulder, A.; Schulze, K.; Subramaniam, V.; Tampe, R.; Huskens, J. *Chem. Eur. J.* **2008,** *14*, 2044-2051.
(239) Chelmowski, R.; Prekelt, A.; Grunwald, C.; Woll, C. *J. Phys. Chem. A* **2007,** *111*, 12295-12303.
(240) Trimbach, D. C.; Keller, B.; Bhat, R.; Zankovych, S.; Pohlmann, R.; Schroter, S.; Bossert, J.; Jandt, K. D. *Adv. Func. Mater.* **2008,** *18*, 1723-1731.
(241) Foley, J. O.; Fu, E.; Gamble, L. J.; Yager, P. *Langmuir* **2008,** *24*, 3628-3635.
(242) Pla-Roca, M.; Fernandez, J. G.; Mills, C. A.; Martinez, E.; Samitier, J. *Langmuir* **2007,** *23*, 8614-8618.
(243) Das, T.; Mallick, S. K.; Paul, D.; Bhutia, S. K.; Bhattacharyya, T. K.; Maiti, T. K. *J. Colloid Interface Sci.* **2007,** *314*, 71-79.
(244) Chang, J. C.; Brewer, G. J.; Wheeler, B. C. *Biomaterials* **2003,** *24*, 2863-2870.
(245) Interliggi, K. A.; Zeile, W. L.; Ciftan-Hens, S. A.; McGuire, G. E.; Purich, D. L.; Dickinson, R. B. *Langmuir* **2007,** *23*, 11911-11916.
(246) Von Philipsborn, A. C.; Lang, S.; Bernard, A.; Loeschinger, J.; David, C.; Lehnert, D.; Bastmeyer, M.; Bonhoeffer, F. *Nat. Protoc.* **2006,** *1*, 1322-1328.
(247) Chaki, N. K.; Vijayamohanan, K. *Biosens. Bioelectron.* **2002,** *17*, 1-12.
(248) Krull, U. J.; Heimlich, M. S.; Kallury, K. M. R.; Piunno, P. A. E.; Brennan, J. D.; Brown, R. S.; Nikolelis, D. P. *Can. J. Chem.* **1995,** *73*, 1239-1250.
(249) Shin, S. K.; Yoon, H. J.; Jung, Y. J.; Park, J. W. *Curr. Opin. Chem. Biol.* **2006,** *10*, 423-429.
(250) Cattaruzza, F.; Cricenti, A.; Flamini, A.; Girasole, M.; Longo, G.; Prosperi, T.; Andreano, G.; Cellai, L.; Chirivino, E. *Nucleic Acids Res.* **2006,** *34*, -.
(251) Yonzon, C. R.; Haynes, C. L.; Zhang, X. Y.; Walsh, J. T.; Van Duyne, R. P. *Anal. Chem.* **2004,** *76*, 78-85.
(252) Arwin, H. *Thin Solid Films* **2000,** *377*, 48-56.

(253) Arwin, H. *Phys. Stat. Sol. A* **2001,** *188*, 1331-1338.

(254) Liao, W.; Wei, F.; Liu, D.; Qian, M. X.; Yuan, G.; Zhao, X. S. *Sens. Actuators, B* **2006,** *114*, 445-450.

(255) Masuda, T.; Yamaguchi, A.; Hayashida, M.; Asari-Oi, F.; Matsuo, S.; Misawa, H. *Sens. Actuators, B* **2005,** *105*, 556-561.

(256) Sharma, A. K.; Jha, R.; Gupta, B. D. *IEEE Sens. J.* **2007,** *7*, 1118-1129.

(257) Karymov, M. A.; Kruchinin, A. A.; Tarantov, Y. A.; Balova, I. A.; Remisova, L. A.; Vlasov, Y. G. *Sens. Actuators, B* **1995,** *29*, 324-327.

(258) McDonagh, C.; Burke, C. S.; MacCraith, B. D. **2008,** *108*, 400-422.

(259) Ymeti, A.; Greve, J.; Lambeck, P. V.; Wink, T.; van Hovell, S. W. F. M.; Beumer, T. A. M.; Wijn, R. R.; Heideman, R. G.; Subramaniam, V.; Kanger, J. S. *Nano Lett.* **2007,** *7*, 394-397.

(260) Anderson, A. S.; Dattelbaum, A. M.; Montano, G. A.; Price, D. N.; Schmidt, J. G.; Martinez, J. S.; Grace, W. K.; Grace, K. M.; Swanson, B. I. **2008,** *24*, 2240-2247.

(261) Boozer, C.; Kim, G.; Cong, S. X.; Guan, H. W.; Londergan, T. *Curr. Opin. Biotechnol.* **2006,** *17*, 400-405.

(262) Green, R. J.; Frazier, R. A.; Shakesheff, K. M.; Davies, M. C.; Roberts, C. J.; Tendler, S. J. B. *Biomater.* **2000,** *21*, 1823-1835.

(263) Mullett, W. M.; Lai, E. P. C.; Yeung, J. M. *Methods (Oxford, U.K.)* **2000,** *22*, 77-91.

(264) Phillips, K. S.; Cheng, Q. *Anal. Bioanal. Chem.* **2007,** *387*, 1831-1840.

(265) Rich, R. L.; Myszka, D. G. *Curr. Opin. Biotechnol.* **2000,** *11*, 54-61.

(266) Hoa, X. D.; Kirk, A. G.; Tabrizian, M. *Biosens. Bioelectron.* **2007,** *23*, 151-160.

(267) Homola, J.; Yee, S. S.; Gauglitz, G. *Sens. Actuators, B* **1999,** *54*, 3-15.

(268) Liu, X.; Song, D. Q.; Zhang, Q. L.; Tian, Y.; Ding, L.; Zhang, H. Q. *Trends Anal. Chem.* **2005,** *24*, 887-893.

(269) Markowicz, P. P.; Law, W. C.; Baev, A.; Prasad, P. N.; Patskovsky, S.; Kabashin, A. V. *Opt. Express* **2007,** *15*, 1745-1754.

(270) Buhl, A.; Metzger, J. H.; Heegaard, N. H. H.; Von Landenberg, P.; Fleck, M.; Luppa, P. B. *Clin. Chem.* **2007,** *53*, 334-341.

(271) Farre, M.; Martinez, E.; Ramon, J.; Navarro, A.; Radjenovic, J.; Mauriz, E.; Lechuga, L.; Marco, M. P.; Barcelo, D. *Anal. Bioanal. Chem.* **2007,** *388*, 207-214.

(272) Mauriz, E.; Calle, A.; Montoya, A.; Lechuga, L. M. *Talanta* **2006,** *69*, 359-364.

(273) Lazcka, O.; Del Campo, F. J.; Munoz, F. X. *Biosens. Bioelectron.* **2007,** *22*, 1205-1217.

(274) Chah, S.; Hutter, E.; Roy, D.; Fendler, J. H.; Yi, J. *Chem. Phys.* **2001,** *272*, 127-136.
(275) He, L.; Musick, M. D.; Nicewarner, S. R.; Salinas, F. G.; Benkovic, S. J.; Natan, M. J.; Keating, C. D. *J. Am. Chem. Soc.* **2000,** *122*, 9071-9077.
(276) Hutter, E.; Pileni, M. P. *J. Phys. Chem. B* **2003,** *107*, 6497-6499.
(277) Zhong, Y.; Kaji, N.; Tokeshi, M.; Baba, Y. *Expert Rev. Proteomics* **2007,** *4*, 565-572.
(278) Bruchez, M.; Moronne, M.; Gin, P.; Weiss, S.; Alivisatos, A. P. *Science* **1998,** *281*, 2013-2016.
(279) Michalet, X.; Pinaud, F. F.; Bentolila, L. A.; Tsay, J. M.; Doose, S.; Li, J. J.; Sundaresan, G.; Wu, A. M.; Gambhir, S. S.; Weiss, S. *Science* **2005,** *307*, 538-544.
(280) Xu, H. X.; Kall, M. *Sens. Actuators, B* **2002,** *87*, 244-249.
(281) Yang, X. H.; Wang, Q.; Wang, K. M.; Tan, W. H.; Li, H. M. *Biosens. Bioelectron.* **2007,** *22*, 1106-1110.
(282) Elghanian, R.; Storhoff, J. J.; Mucic, R. C.; Letsinger, R. L.; Mirkin, C. A. *Science* **1997,** *277*, 1078-1081.
(283) Lee, J. S.; Ulmann, P. A.; Han, M. S.; Mirkin, C. A. *Nano Lett.* **2008,** *8*, 529-533.
(284) Han, M. S.; Lytton-Jean, A. K. R.; Oh, B. K.; Heo, J.; Mirkin, C. A. *Angew. Chem.-Int. Edit.* **2006,** *45*, 1807-1810.
(285) Storhoff, J. J.; Lazarides, A. A.; Mucic, R. C.; Mirkin, C. A.; Letsinger, R. L.; Schatz, G. C. *J. Am. Chem. Soc.* **2000,** *122*, 4640-4650.
(286) Enderlein, J. R. *Phys. Chem. Chem. Phys.* **2002,** *4*, 2780-2786.
(287) Fu, Y.; Lakowicz, J. R. *Anal. Chem.* **2006,** *78*, 6238-6245.
(288) Zhang, J.; Gryczynski, I.; Gryczynski, Z.; Lakowicz, J. R. *J. Phys. Chem. B* **2006,** *110*, 8986-8991.
(289) Tam, F.; Goodrich, G. P.; Johnson, B. R.; Halas, N. J. *Nano Lett.* **2007,** *7*, 496-501.
(290) Chowdhury, M. H.; Aslan, K.; Malyn, S. N.; Lakowicz, J. R.; Geddes, C. D. *J. Fluoresc.* **2006,** *16*, 295-299.
(291) Kang, C.; Weiss, S. M. *Opt. Express* **2008,** *16*, 18188-18193.
(292) Lee, M.; Fauchet, P. M. *Opt. Express* **2007,** *15*, 4530-4535.
(293) Alvarez, S. D.; Derfus, A. M.; Schwartz, M. P.; Bhatia, S. N.; Sailor, M. J. *Biomater.* **2009,** *30*, 26-34.
(294) Bocking, T.; Ilyas, S.; Salvador, G. P.; Reece, P. J.; Gaus, K.; Gooding, J. J.; Gal, M. *Commad Proc. 2004* **2005**, 217-220
414.

(295) Kilian, K. A.; Boecking, T.; Gaus, K.; Gal, M.; Gooding, J. J. *ACS Nano* **2007,** *1*, 355-361.

(296) Wang, J. B.; Profitt, J. A.; Pugia, M. J.; Suni, I. I. *Anal. Chem.* **2006,** *78*, 1769-1773.

(297) Liu, Z. M.; Liu, J.; Shen, G. L.; Yu, R. Q. *Electroanal.* **2006,** *18*, 1572-1577.

(298) Liu, G. Z.; Nguyen, Q. T.; Chow, E.; Bocking, T.; Hibbert, D. B.; Gooding, J. J. *Electroanal.* **2006,** *18*, 1141-1151.

(299) Alexander, P. W.; Rechnitz, G. A. *Electroanal.* **2000,** *12*, 343-350.

(300) Campuzano, S.; Gamella, M.; Serra, B.; Reviejo, A. J.; Pingarron, J. M. *J. Agric. Food Chem.* **2007,** *55*, 2109-2114.

(301) Gooding, J. J.; Hibbert, D. B. *Trends Anal. Chem.* **1999,** *18*, 525-533.

(302) Zhang, L. Q.; Longo, M. L.; Stroeve, P. *Langmuir* **2000,** *16*, 5093-5099.

(303) Bao, H. F.; Peng, Z. Q.; Wang, E. K.; Dong, S. J. *Langmuir* **2004,** *20*, 10992-10997.

Chapter 3

Biorepellent Organic Coatings for Improved Microsieve Filtration

Microsieves are a new type of silicon-based membrane, which are coated with a silicon-rich silicon nitride (Si_xN_4) top layer. Although Si_xN_4 is known to be relatively inert, surface contamination (fouling through e.g. protein adsorption) is critical for application in microfiltration. As a result, surface modification is needed to prevent or minimize these interactions. Functional coatings can be formed on the Si_xN_4 surfaces via several grafting methods which are presented here. Some stable modifications allow the covalent grafting of biorepellent oligomers and polymers whose effect on protein adsorption is shown.

This chapter will be published as:
"*Biorepellent Coatings for Improved Microsieve Filtration*", Rosso, M.; Schroën, K.; Zuilhof, H., in *New Membranes and Advanced Materials for Wastewater Treatment*, ACS books **2009**, in press.

Introduction

Microsieves are a new type of micro-perforated filtration membrane, produced using photolithography to create membrane pores with a very well-defined size and shape.[1-3] Crystalline silicon is used to form the well-defined 3-D support structure of microsieves by controlled anisotropic etching, while silicon-enriched silicon nitride (Si_xN_4; x typically 3.5 - 5) - deposited by chemical vapor deposition (CVD) - is used as outer coating with high mechanical and chemical stability.[4,5]

Studies have been done to assess and optimize the performance of microsieves in filtration, especially to purify fluids in food processes, like the removal of yeast from beer or the cold sterilization of milk.[2] The very thin effective membrane layer of microsieves (< 1 µm) results in a high permeability, and allows very low transmembrane pressures (< 100 mbar[6]) compared to ceramics membranes (with pressures of typically 0.5 to 5 bar[7,8]). Moreover, the possibility to accurately design the pore size and shape, the porosity and the thickness of membranes gives new degrees of freedom to optimize the filtration processes.[9-12] However, microsieves suffer, like other microfiltration membranes, from surface contamination, which causes a dramatic decrease in the permeate flux during the filtration.[13-15] Such membrane fouling is one of the main limitations for industrial microfiltration.[16,17]

For biological solutions in the food, beverage, or biotechnology industries, surface contamination is mainly due to proteins or protein aggregates. Protein fouling in microfiltration has been described as a combination of pore blockage, formation of a cake layer on top of the membrane and/or adsorption inside the pores (See Figure 1).[17-19] Mostly, protein adsorption is the first stage of irreversible fouling by other components, therefore tackling protein adsorption may be a solution to a bigger problem.

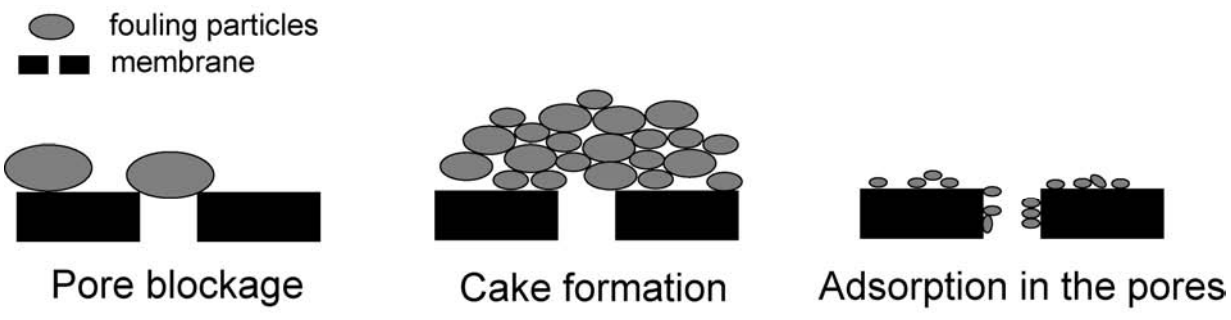

Figure 1. Sources of membrane fouling during microfiltration.

In this chapter, we present ways to control the surface properties of membranes to prevent the initial adsorption of proteins or other biomaterials. Protein adsorption is strongly reduced on hydrophilic substrates,[20,21] because the macromolecules then compete with water to interact with the solid surfaces. Although the use of hydrophilic surfaces may reduce fouling, it cannot totally prevent protein adsorption. To further improve this, strategies involving the grafting of organic monolayers or polymer brushes need to be applied, and we present here such approaches to prevent adsorption onto surfaces.

Besides biorepellence, hydrophilic coatings also provide a good wetting of membrane pores,[22] which is especially critical at the low transmembrane pressure and the high product throughput used during microsieve filtration.[23]

Surface Properties of Clean Microsieves

The Si_xN_4 outer coating of microsieves reinforces the spatial structure of the membranes and protects surfaces from corrosion by filtrated solutions, cleaning solutions, and exposure to air during storage. Silicon carbide (SiC) is also a very robust material[24,25] with a high potential in biocompatible devices.[26-28] The possibility to form homogeneous SiC coatings by CVD[29] offers a possible alternative to Si_xN_4 for the coating of microsieves. This chapter will therefore consider the surface modification of both materials.

Properties of Si_xN_4 and SiC Surfaces

Besides silicon, the clean surfaces of pure Si_xN_4 and SiC should contain only nitrogen and carbon, respectively. However, the composition of these surfaces changes upon oxidation and contamination from air, both occurring when the material is stored under ambient conditions. Firstly, the surface of both materials is usually covered with an oxygen-rich top layer after storage in air.[24,30] As a result, the oxidized surfaces of Si_xN_4[30,31] and SiC[32,33] behave very similar to the surface of pure silica, presenting mainly Si-OH groups and a point of zero charge at about pH 3. Consequently, at physiological pH, these surfaces are negatively charged because of $Si\text{-}O^-$ surface groups,[34,35] and the remaining surface Si-OH groups can also form strong electrostatic dipole interactions and hydrogen bonds with polar compounds, including water. Apart from this oxide layer, the solid surfaces are usually contaminated by organic compounds from the ambient air.[36]

When exposed to biological solutions, such oxidized surfaces are quickly covered with a layer of adsorbed proteins or polysaccharides, which in turn favors the adhesion of bigger aggregates or microorganisms and the growth of a biofilm.[37-39]

Cleaning of Si_xN_4 and SiC Surfaces

A sacrificial oxidation step is needed to obtain surfaces free from organic contamination. The oxidation of Si_xN_4 and SiC substrates can be carried out by chemical treatment with acidic, basic, or oxidizing solutions, or mixtures. The resulting clean oxide layer can be subsequently removed using aqueous solutions of pure or buffered HF. A typical oxidative cleaning procedure involves oxidation in "piranha" solution (H_2SO_4:30% H_2O_2, 3:1), followed by etching with a diluted HF solution (2-5%).[4] Etching with HF leaves the surface of Si_xN_4 deprived of carbon and oxygen,[40,41] whereas SiC surfaces still remain oxygen-terminated.[42,43] The resulting monolayer of surface hydroxyl groups on SiC cannot be removed unless high-temperature annealing in pure hydrogen or silicon vapor is applied.[44,45]

Alternative oxidation methods involve thermal or plasma treatments[40,43,46] in air or oxygen, which combine efficient oxidation with the convenience of dry treatments, and also allow a non-destructive treatment of porous microstructures such as microsieves. Apart from its common application in cleaning and oxidation, plasma treatment is also used to obtain highly hydrophilic organic membranes[21,47] and has as such been applied to Si_xN_4 microsieves.[23] This dry process can be easily scaled up from the dimensions of experimental microsieves (5 x 5 mm) to the wafer-sized membranes required for industrial processes. However, the effects of the plasma treatment are only temporary, as the high surface energy of the obtained oxide surface promotes the adsorption of new contaminants from air or water. As a result, the treatment must then be repeated to recover a highly hydrophilic, wettable surface, which again only remains this way for a short period.

Surface Coating of Microsieves

Attachment of Organic Monolayers

The formation of covalent organic monolayers has been widely used to attach specific functional groups onto inorganic substrates. Additionally, organic monolayers can serve as an anchoring base for further grafting of polymer brushes onto surfaces. The rich chemistry of organic polymers can then be explored to produce microsieves with tailored surface properties.

One of the most common methods to form organic monolayers involves the adsorption of alkylsilanes onto oxidized inorganic surfaces.[48,49] These monolayers can be formed by the reaction of chlorosilane or alkoxysilane precursors with any oxidic inorganic material that displays stable hydroxyl groups at their surface (See Figure 2a). This is the case for Si_xN_4 and SiC with a top layer of native silicon dioxide (or, in the case of SiC, also on bare etched surfaces[45]). Oxidation of these materials by controlled chemical or physical treatments (*vide infra*) will then reproducibly provide proper surfaces for the formation of organo-silane monolayers.[50-52] However, the specific hydrolytic stability of such layers is not as high as needed in a practical application where cleaning steps can be very severe. As a result, the potential use of silane-based monolayers is rather limited in membrane applications.

Another method to form stable alkyl monolayers on silicon-containing surfaces involves the reaction of terminal alkenes or alkynes with HF-treated substrates. This method is a variation on the widely used hydrosilylation reaction between 1-alkenes and hydrogen-terminated silicon surfaces.[53-57] That reaction occurs through the addition of Si-H on the terminal carbon-carbon double bond, following a thermal initiation,[58-60] or a photochemical initiation with UV[61-65] or visible light.[66-68] These reactions allow the use of a wider range of reactive moieties that are not compatible with silanes. They also do not need an oxide layer, since they do not require surface -OH groups, but even when hydroxyl-terminated, surfaces can be coated in similar conditions with alkene molecules.[43]

Alkene-based monolayers were formed on flat Si_xN_4[40,41] and 6H-SiC and polycrystalline 3C-SiC[43] using thermal initiation or UV irradiation[69] in conditions close to those used for the surface modification of silicon. Good quality monolayers were obtained with several simple alkenes (e.g. water contact angles up to 107° for hexadecene-derived monolayers on both SiC

and Si_xN_4). One advantage of alkene-based monolayers is their high stability. This is mainly due to the absence of a silicon oxide layer, and to the presence of stable Si-C and Si-N bonds, in the case of Si_xN_4,[40] and extremely stable C-O-C bonds that even survive boiling at pH = 0 for hours, in the case of SiC surfaces[43] (See Figure 2b and c).

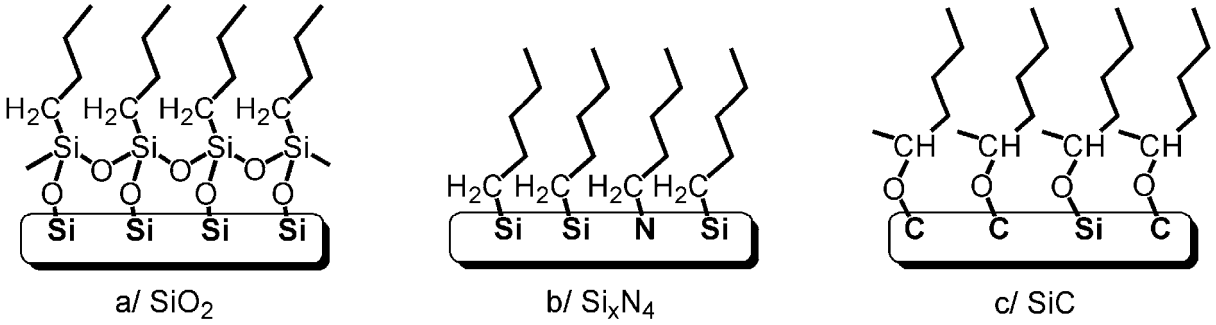

Figure 2. Monolayer formation on Si-based materials using a) organosilanes on oxide surfaces, and alkene-based coatings on b) Si_xN_4 and c) SiC.

Other less general methods can be used to graft small organic molecules or polymer chains onto inorganic surfaces: in particular, surface -NH_2 groups on Si_xN_4 can be reacted with alkyl bromides[70-72] or aldehydes.[73] Only a few examples of direct "grafting-on" polymerization to inorganic surfaces exist in the literature. Some reports mention the polymerization of methyl acrylate on Shirazu porous glass (SPG) membranes induced by plasma,[74,75] the grafting of vinyl-terminated polystyrene onto silicon oxide surfaces[76] or the electro-grafting of poly-*N*-succinimidylacrylate (PNSA) on SiN cantilevers.[77]

Biorepellent Oligomer and Polymer Coatings

Biorepellent coatings are typically hydrophilic, as this property strongly minimizes the adsorption of proteins.[78-81] In this category two approaches are present, each with their own mode of action. For short oligomers, the high internal hydrophilicity of the grafted chains traps a big amount of water at the liquid-solid interface, and the resulting layer forms a barrier for the adsorption of e.g. colloids from the liquid phase.[82] In the case of long polymers, the biorepellence is mainly caused by the osmotic effect of hydrated chains. The adsorption is unfavorable, as the concomitant compression of the grafted chains would locally increase the polymer concentration near the surface.[83,84]

Polyethylene glycols (PEG), also called polyethylene oxides (PEO), constitute one of the most widely used polymers to make surfaces biorepellent.[85,86] Table 1 presents examples of other hydrophilic polymers that have been used to improve the surface properties of membranes. Most of these coatings have been prepared on organic substrates, but these modifications can be extended to inorganic membranes with a proper grafting method (*vide infra*).

Table 1. Examples of biorepellent hydrophilic polymers.

Monomer	Polymer structure	Reference
Ethylene glycol (EG)	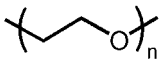	85,86
Acrylic acid (AA)	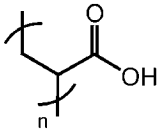	21,87-89
Polyethylene glycol methacrylate (PEG-MA)	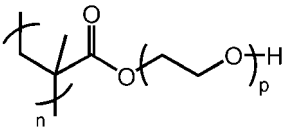	87,89,90
Diethylene glycol vinyl ether (DEGVE)	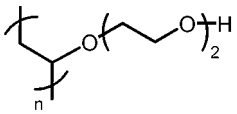	91
Vinyl acetate (VA)	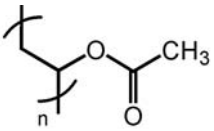	92
Vinylsulfonic acid (VSA)	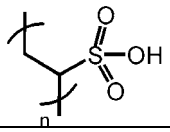	93

The grafting of oligomers and polymers onto surfaces can be done using two different approaches: “grafting-on” methods involve the attachment of pre-formed polymer chains onto surfaces, whereas “grafting-from” methods use the *in-situ* polymerization of monomers from the liquid onto the surface (See Figure 3).

When applied to small oligomers, the “grafting-on” approach gives a close packing of the grafted chains and a good passivation of the substrate.[94] In addition, the grafted compounds can be precisely characterized before attachment, ensuring a good control of the coating. In particular, the use of organosilanes functionalized with oligoethylene glycols has been reported extensively: chains with 3 to 9 ethylene glycol units are usually sufficient to

significantly reduce the adsorption of proteins[95-97] and microorganisms[98] on silica. Organosilane compounds were also used to form monolayers of oligoethylene glycol onto oxidized silicon nitride substrates,[99] but no studies on their protein resistance or hydrolytic stability has been reported.

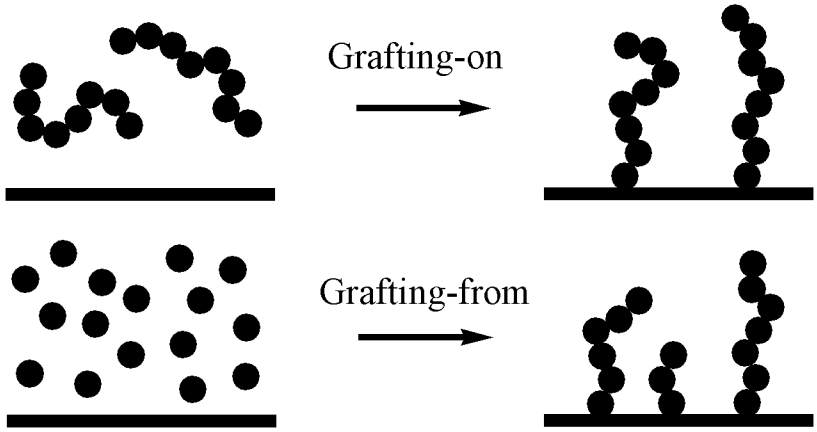

Figure 3. "Grafting-on" and "Grafting-from" strategies for the formation of polymer brushes on solid surfaces.

In a recent study from our laboratories monolayers of alkene-based oligoethylene glycol compounds (3 and 6 repeating EG units) were formed on $Si_{3.9}N_4$ substrates,[39] which decreased the adsorption of proteins down to the detection limit of reflectometry. Complementary water contact angles and AFM measurements on surfaces coated with compounds containing 6 ethylene glycol units confirmed the absence of any contamination, when tested for BSA and fibrinogen adsorption. Since these monolayers display a very high hydrolytic stability, even in acidic or basic media,[40,41] this technique can be applied to microsieves, and studies on this topic are currently ongoing in our laboratories.

Some articles also reported on the attachment of linear PEG polymers attached onto Si_xN_4 cantilevers using polymer chains bearing NHS (N-hydrosuccinimide esters, forming amide bonds with the surface NH_2 groups,[100-102] to study molecular recognition with atomic force microscopy. Another example mentions the grafting of PEG chains (MW: 5000) on flat silicon nitride substrates by direct condensation at 100 ºC of –OH groups with the silanol groups at the surface to form strong Si-O-C bonds.[103] Besides PEG, other linear compounds, such as some derivatives of zwitterionic phospholipids[104,105] (-$(CH_2)_{15}$-$(PO_4)^-$-$(CH_2)_2$-NR_3^+ (R

= CH_3 or H)) have been attached to oxide surfaces, reducing lysozyme or fibrinogen adsorption by about 90% compared to bare substrates.

If a silane group is present as part of the polymer, it can be grafted directly to the surfaces. This modification has been used for instance to attach long PEG chains (MW 750-5000) on silica[106,107] or glass[108] surfaces and on alumina membranes.[109] PEG methyl ether acrylate could also be included in a copolymer[110] with 3-(trimethoxysilyl)propyl methacrylate (poly(TMSMA-r-PEGMA), MW of PEG: 475) and attached onto oxidized silicon substrates. These coatings could reduce dramatically the adsorption of BSA and fibrinogen, but could also reduce the adhesion of fibroblast cells onto surfaces. Still using silane chemistry, the pre-formed poly(TMSMA-r-PEGMA) copolymer has also been applied to Si_xN_4 microsieves to introduce PEG chains onto the membrane surfaces.[14] Such modified membranes displayed a more efficient filtration of BSA or skimmed milk than untreated microsieves, when using backpulsing. However, these coatings had a relatively low stability at pH 12, which can be related to the instability of silanes in alkaline solutions. Silane pre-coatings also allowed the grafting of amines[111,112] or aldehydes,[113] which were then grafted with PEG or dextran, respectively.

Since the "grafting-from" of polymer chains on solid substrates has been developed mainly for organic substrates[114-116] and organic membranes,[89,117-120] polymer grafting on Si_xN_4 or SiC surfaces requires the prior formation of organic monolayers. Indeed, using such a method, the polymerization of oligo(ethylene glycol) methyl methacrylate (OEGMA) was carried out by atom transfer radical polymerization (ATRP)[121] and ozone-induced graft polymerization,[122] to give protein-repellent glass surfaces. Besides ATRP and ozone initiation, UV irradiation,[88,123,124] plasma-induced graft polymerization,[21,89,117] or radical initiators such as azobisazobutyronitrile (AIBN)[125] and the redox couple $K_2S_2O_8$ - $Na_2S_2O_5$[87,90,93] can initiate graft polymerization. Although not all these methods have already been used to graft polymers onto organic monolayers, they represent an important route to exploit the chemistry of polymers on inorganic substrates.

Direct graft-polymerization was also applied in plasma-induced graft polymerization of poly(ethylene glycol) methyl ether methacrylate (PEGMA, MW of PEG: 1000) onto oxidized silicon surfaces; the resulting polymer layers reduced significantly the adhesion of BSA and platelets.[126] This direct grafting of polymers onto inorganic surfaces represents a simple alternative to the use of preformed monolayers, but the quality of the grafting is then difficult to control and frequently a low packing density is obtained for long polymer chains. As a

result, the nature of the polymer-inorganic substrate interface and the possibilities to optimize the layer properties must be investigated in each case.

A possible adverse effect of polymer coatings is an increase of the membrane resistance, due to the growth of thick layers within the pores. In addition, poorly defined polymerizations may yield polymer layers with irreproducible thicknesses and other properties (stability, protein resistance). However, when properly controlled, the attachment of an organic polymer layer of well-defined thickness can tune small pore sizes, especially in ultrafiltration membranes, and thus in fact turn a potential problem into a potential benefit.

Conclusions

Modification of the surface properties of silicon nitride and silicon carbide substrates can be achieved via various techniques. These can rigorously change the surface properties and biorepellent behavior. The most extensively studied monolayers involve organosilane-based monolayers, either as a fully functional layer or as a reactive intermediate layer from which e.g. grafting-on or grafting-from polymerization can be started. In view of its superior stability, use of milder chemicals, ease of practical use and wider range of allowed functionalities, the more recently developed alkene-based chemistry represents an important improvement as a grafting technique for functional coatings (oligomers, polymers) on silicon nitride and silicon carbide.

Using the wide range of grafting techniques and available biorepellent compounds, surface chemistry can provide efficient ways to improve filtration with microsieves and thus expand their range of applications.

Acknowledgments.

The authors thank Graduate School VLAG and MicroNed (Project no. 6163510395) for financial support.

References

(1) van Rijn, C. J. M.; Nijdam, W.; Kulper, S.; Veldhuis, G. J.; van Wolferen, H.; Elwenspoek, M. *J. Micromech. Microeng.* **1999,** *9,* 170-172.

(2) van Rijn, C. J. M. *Nano and Micro Engineered Membrane Technology*. Aquamarijn Research BV, The Netherlands: 2002.

(3) Kuiper, S.; van Wolferen, H.; van Rijn, G.; Nijdam, W.; Krijnen, G.; Elwenspoek, M. *J. Micromech. Microeng.* **2001,** *11*, 33-37.

(4) Bermudez, V. M.; Perkins, F. K. *Appl. Surf. Sci.* **2004,** *235*, 406-419.

(5) Rathi, V. K.; Gupta, M.; Agnihotri, O. P. *Microelectron. J.* **1995,** *26*, 563.

(6) Brans, G.; Kromkamp, J.; Pek, N.; Gielen, J.; Heck, J.; van Rijn, C. J. M.; Van der Sman, R. G. M.; Schroën, C. G. P. H.; Boom, R. M. *J. Membr. Sci.* **2006,** *278*, 344-348.

(7) Brans, G.; Schroën, C. G. P. H.; van der Sman, R. G. M.; Boom, R. M. *J. Membr. Sci.* **2004,** *243*, 263-272.

(8) Daufin, G.; Escudier, J. P.; Carrere, H.; Berot, S.; Fillaudeau, L.; Decloux, M. *Food Bioprod. Process.* **2001,** *79*, 89-102.

(9) Brans, G.; Van der Sman, R. G. M.; Schroën, C. G. P. H.; van der Padt, A.; Boom, R. M. *J. Membr. Sci.* **2006,** *278*, 239-250.

(10) Kuiper, S.; Brink, R.; Nijdam, W.; Krijnen, G. J. M.; Elwenspoek, M. C. *J. Membr. Sci.* **2002,** *196*, 149-157.

(11) Chandler, M.; Zydney, A. *J. Membr. Sci.* **2006,** *285*, 334-342.

(12) Kuiper, S.; van Rijn, C.; Nijdam, W.; Raspe, O.; van Wolferen, H.; Krijnen, G.; Elwenspoek, M. *J. Membr. Sci.* **2002,** *196*, 159-170.

(13) Mulder, M. *Basic Principles of Membrane Technology*. 2 ed.; Kluver Academic Publishers: Dordrecht, 1996; p 418.

(14) Girones, M.; Bolhuis-Versteeg, L.; Lammertink, R.; Wessling, M. *J. Colloid Interf. Sci.* **2006,** *299*, 831-840.

(15) Girones, M.; Lammertink, R. G. H.; Wessling, M. *J. Membr. Sci.* **2006,** *273*, 68-76.

(16) Belfort, G.; Davis, R. H.; Zydney, A. L. *J. Membr. Sci.* **1994,** *96*, 1-58.

(17) Palacio, L.; Ho, C. C.; Pradanos, P.; Hernandez, A.; Zydney, A. L. *J. Membr. Sci.* **2003,** *222*, 41-51.

(18) Bowen, W. R.; Calvo, J. I.; Hernandez, A. *J. Membr. Sci.* **1995,** *101*, 153.

(19) Ho, C. C.; Zydney, A. L. *J. Colloid Interf. Sci.* **2000,** *232*, 389-399.

(20) Koehler, J. A.; Ulbricht, M.; Belfort, G. *Langmuir* **1997,** *13*, 4162-4171.
(21) Ulbricht, M.; Belfort, G. *J. Membr. Sci.* **1996,** *111*, 193-215.
(22) Franken, A. C. M.; Nolten, J. A. M.; Mulder, M. H. V.; Bargeman, D.; Smolders, C. A. *J. Membr. Sci.* **1987,** *33*, 315-328.
(23) Girones, M.; Borneman, Z.; Lammertink, R. G. H.; Wessling, M. *J. Membr. Sci.* **2005,** *259*, 55-64.
(24) Choyke, W. J.; Matsunami, H.; Pensl, G. *Silicon Carbide, Recent Major Advances*. Springer: Berlin, 2003.
(25) Saddow, S. E.; Agarwal, A. *Advances in Silicon Carbide: Processing and Applications*. Artech House Inc.: Boston, 2004.
(26) Cogan, S. F.; Edell, D. J.; Guzelian, A. A.; Liu, Y. P.; Edell, R. *J. Biomed. Mater. Res. A* **2003,** *67A*, 856-867.
(27) Rosenbloom, A. J.; Sipe, D. M.; Shishkin, Y.; Ke, Y.; Devaty, R. P.; Choyke, W. J. *Biomed. Microdev.* **2004,** *6*, 261-267.
(28) Sella, C.; Martin, J. C.; Lecoeur, J.; Lechanu, A.; Harmand, M. F.; Naji, A.; Davidas, J. P. *Mater. Sci. Eng., A* **1991,** *139*, 49-57.
(29) Roper, C. S.; Radmilovic, V.; Howe, R. T.; Maboudian, R. *J. Electrochem. Soc.* **2006,** *153*, C562-C566.
(30) Bousse, L. J.; Mostarshed, S.; Hafeman, D. *Sens. Actuators, B* **1992,** *10*, 67-71.
(31) Harame, D. L.; Bousse, L. J.; Shott, J. D.; Meindl, J. D. *IEEE T. Electron Dev.* **1987,** *34*, 1700-1707.
(32) Popping, B.; Deratani, A.; Sebille, B.; Desbois, N.; Lamarche, J. M.; Foissy, A. *Colloid Surface* **1992,** *64*, 125-133.
(33) Whitman, P. K.; Feke, D. L. *J. Am. Ceram. Soc.* **1988,** *71*, 1086-1093.
(34) Bolt, G. H. *J. Phys. Chem.* **1957,** *61*, 1166-1169.
(35) Hiemstra, T.; Dewit, J. C. M.; Vanriemsdijk, W. H. *J. Colloid Interf. Sci.* **1989,** *133*, 105-117.
(36) Patton, S. T.; Eapen, K. C.; Zabinski, J. S. *Tribol. Int.* **2001,** *34*, 481-491.
(37) Marshall, A. D.; Munro, P. A.; Tragardh, G. *Desalination* **1993,** *91*, 65-108.
(38) Vanloosdrecht, M. C. M.; Lyklema, J.; Norde, W.; Zehnder, A. J. B. *Microbiol. Rev.* **1990,** *54*, 75-87.
(39) Rosso, M.; de Jong, E.; Giesbers, M.; Fokkink, R. G.; Norde, W.; Schroën, K.; Zuilhof, H., submitted.

(40) Arafat, A.; Giesbers, M.; Rosso, M.; Sudhölter, E. J. R.; Schroën, K.; White, R. G.; Yang, L.; Linford, M. R.; Zuilhof, H. *Langmuir* **2007,** *23*, 6233-6244.

(41) Arafat, A.; Schroën, K.; de Smet, L. C. P. M.; Sudhölter, E. J. R.; Zuilhof, H. *J. Am. Chem. Soc.* **2004,** *126*, 8600-8601.

(42) King, S. W.; Nemanich, R. J.; Davis, R. F. *J. Electrochem. Soc.* **1999,** *146*, 1910-1917.

(43) Rosso, M.; Arafat, A.; Schroën, K.; Giesbers, M.; Roper, C. S.; Maboudian, R.; Zuilhof, H. *Langmuir* **2008,** *24*, 4007-4012.

(44) Bernhardt, J.; Schardt, J.; Starke, U.; Heinz, K. *Appl. Phys. Lett.* **1999,** *74*, 1084-1086.

(45) Starke, U. *Phys. Stat. Sol. B* **1997,** *202*, 475-499.

(46) Chen, L.; Guy, O. J.; Pope, G.; Teng, K. S.; Maffeis, T.; Wilks, S. P.; Mawby, P. A.; Jenkins, T.; Brieva, A.; Hayton, D. J. *Mater. Sci. Forum* **2004,** *457-460*, 1337-1340.

(47) Ulbricht, M.; Belfort, G. *J. Appl. Polymer Sci.* **1995,** *56*, 325-343.

(48) Onclin, S.; Ravoo, B. J.; Reinhoudt, D. N. *Angew. Chem., Int. Ed.* **2005,** *44*, 6282-6304.

(49) Sagiv, J. *J. Am. Chem. Soc.* **1980,** *102*, 92-98.

(50) Petoral, R. M.; Yazdi, G. R.; Spetz, A. L.; Yakimova, R.; Uvdal, K. *Appl. Phys. Lett.* **2007,** *90*, 223904(1-3).

(51) Sampathkumaran, U.; De Guire, M. R.; Heuer, A. H.; Niesen, T.; Bill, J.; Aldinger, F. *Ceram. Trans.* **1999,** *94*, 307-318.

(52) Schoell, S. J.; Hoeb, M.; Sharp, I. D.; Steins, W.; Eickhoff, M.; Stutzmann, M.; Brandt, M. S. *Appl. Phys. Lett.* **2008,** *92*, 153301 (1-3).

(53) Boukherroub, R. *Curr. Opin. Solid State Mater. Sci.* **2005,** *9*, 66-72.

(54) Buriak, J. M. *Chem. Rev.* **2002,** *102*, 1271-1308.

(55) Linford, M. R.; Fenter, P.; Eisenberger, P. M.; Chidsey, C. E. D. *J. Am. Chem. Soc.* **1995,** *117*, 3145-3155.

(56) Shirahata, N.; Hozumi, A.; Yonezawa, T. *Chem. Rec.* **2005,** *5*, 145-159.

(57) Sieval, A. B.; Linke, R.; Zuilhof, H.; Sudhölter, E. J. R. *Adv. Mater.* **2000,** *12*, 1457-1460.

(58) Linford, M. R.; Chidsey, C. E. D. *J. Am. Chem. Soc.* **1993,** *115*, 12631.

(59) Scheres, L.; Arafat, A.; Zuilhof, H. *Langmuir* **2007,** *23*, 8343-8346.

(60) Sieval, A. B.; Demirel, A. L.; Nissink, J. W. M.; Linford, M. R.; van der Maas, J. H.; de Jeu, W. H.; Zuilhof, H.; Sudhölter, E. J. R. *Langmuir* **1998,** *14*, 1759-1768.

(61) Cicero, R. L.; Linford, M. R.; Chidsey, C. E. D. *Langmuir* **2000,** *16*, 5688.

(62) Effenberger, F.; Gotz, G.; Bidlingmaier, B.; Wezstein, M. *Angew. Chem., Int. Ed.* **1998,** *37*, 2462-2464.

(63) Mischki, T. K.; Donkers, R. L.; Eves, B. J.; Lopinski, G. P.; Wayner, D. D. M. *Langmuir* **2006,** *22*, 8359-8365.
(64) Strother, T.; Cai, W.; Zhao, X. S.; Hamers, R. J.; Smith, L. M. *J. Am. Chem. Soc.* **2000,** *122*, 1205-1209.
(65) Strother, T.; Hamers, R. J.; Smith, L. M. *Nucleic Acids Res.* **2000,** *28*, 3535-3541.
(66) de Smet, L. C. P. M.; Pukin, A. V.; Sun, Q. Y.; Eves, B. J.; Lopinski, G. P.; Visser, G. M.; Zuilhof, H.; Sudhölter, E. J. R. *Appl. Surf. Sci.* **2005,** *252*, 24-30.
(67) de Smet, L. C. P. M.; Stork, G. A.; Hurenkamp, G. H. F.; Sun, Q. Y.; Topal, H.; Vronen, P. J. E.; Sieval, A. B.; Wright, A.; Visser, G. M.; Zuilhof, H.; Sudhölter, E. J. R. *J. Am. Chem. Soc.* **2003,** *125*, 13916-13917.
(68) Sun, Q.-Y.; de Smet, L. C. P. M.; van Lagen, B.; Giesbers, M.; Thune, P. C.; van Engelenburg, J.; de Wolf, F. A.; Zuilhof, H.; Sudhölter, E. J. R. *J. Am. Chem. Soc.* **2005,** *127*, 2514-2523.
(69) Rosso, M.; Giesbers, M.; Arafat, A.; Schroën, K.; Zuilhof, H. *Langmuir* **2009,** *25*, 2172-2180.
(70) Cattaruzza, F.; Cricenti, A.; Flamini, A.; Girasole, M.; Longo, G.; Mezzi, A.; Prosperi, T. *J. Mater. Chem.* **2004,** *14*, 1461-1468.
(71) Cricenti, A.; Longo, G.; Luce, M.; Generosi, R.; Perfetti, P.; Vobornik, D.; Margaritondo, G.; Thielen, P.; Sanghera, J. S.; Aggarwal, I. D.; Miller, J. K.; Tolk, N. H.; Piston, D. W.; Cattaruzza, F.; Flamini, A.; Prosperi, T.; Mezzi, A. *Surf. Sci.* **2003,** *544*, 51-57.
(72) Karymov, M. A.; Kruchinin, A. A.; Tarantov, Y. A.; Balova, I. A.; Remisova, L. A.; Vlasov, Y. G. *Sens. Actuators, B* **1995,** *29*, 324-327.
(73) Yin, L. T.; Chou, J. C.; Chung, W. Y.; Sun, T. P.; Hsiung, S. K. *IEEE T. Bio-Med. Eng.* **2001,** *48*, 340-344.
(74) Kai, T.; Suma, Y.; Ono, S.; Yamaguchi, T.; Nakao, S. I. *J. Polym. Sci. Pol. Chem.* **2006,** *44*, 846-856.
(75) Kai, T.; Yamaguchi, T.; Nakao, S. *Ind. Eng. Chem. Res.* **2000,** *39*, 3284.
(76) Maas, J. H.; Stuart, M. A. C.; Sieval, A. B.; Zuilhof, H.; Sudhölter, E. J. R. *Thin Solid Films* **2003,** *426*, 135-139.
(77) Gabriel, S.; Jerome, C.; Jerome, R.; Fustin, C. A.; Pallandre, A.; Plain, J.; Jonas, A. M.; Duwez, A. S. *J. Am. Chem. Soc.* **2007,** *129*, 8410-8411.
(78) Kane, R. S.; Deschatelets, P.; Whitesides, G. M. *Langmuir* **2003,** *19*, 2388-2391.
(79) Senaratne, W.; Andruzzi, L.; Ober, C. K. *Biomacromolecules* **2005,** *6*, 2427-2448.

(80) Ramsden, J. J. *Chem. Soc. Rev.* **1995,** *24*, 73-78.
(81) Prime, K. L.; Whitesides, G. M. *Science* **1991,** *252*, 1164-1167.
(82) Wang, R. L. C.; Kreuzer, H. J.; Grunze, M. *J. Phys. Chem. B* **1997,** *101*, 9767-9773.
(83) Halperin, A. *Langmuir* **1999,** *15*, 2525-2533.
(84) Jeon, S. I.; Lee, J. H.; Andrade, J. D.; Degennes, P. G. *J. Colloid Interf. Sci.* **1991,** *142*, 149-158.
(85) Chan, Y. H. M.; Schweiss, R.; Werner, C.; Grunze, M. *Langmuir* **2003,** *19*, 7380-7385.
(86) Norde, W.; Gage, D. *Langmuir* **2004,** *20*, 4162-4167.
(87) Freger, V.; Gilron, J.; Belfer, S. *J. Membr. Sci.* **2002,** *209*, 283-292.
(88) Taniguchi, M.; Belfort, G. *J. Membr. Sci.* **2004,** *231*, 147-157.
(89) Ulbricht, M.; Matuschewski, H.; Oechel, A.; Hicke, H. G. *J. Membr. Sci.* **1996,** *115*, 31-47.
(90) Belfer, S.; Purinson, Y.; Fainshtein, R.; Radchenko, Y.; Kedem, O. *J. Membr. Sci.* **1998,** *139*, 175-181.
(91) Bremmell, K. E.; Kingshott, P.; Ademovic, Z.; Winther-Jensen, B.; Griesser, H. J. *Langmuir* **2006,** *22*, 313-318.
(92) Kim, M.; Saito, K.; Furusaki, S.; Sugo, T.; Okamoto, J. *J. Membr. Sci.* **1991,** *56*, 289-302.
(93) Belfer, S.; Purinson, Y.; Kedem, O. *Acta Polym.* **1998,** *49*, 574-582.
(94) Papra, A.; Gadegaard, N.; Larsen, N. B. *Langmuir* **2001,** *17*, 1457-1460.
(95) Cecchet, F.; De Meersman, B.; Demoustier-Champagne, S.; Nysten, B.; Jonas, A. M. *Langmuir* **2006,** *22*, 1173-1181.
(96) Hoffmann, C.; Tovar, G. E. M. *J. Colloid Interf. Sci.* **2006,** *295*, 427-435.
(97) Lee, S. W.; Laibinis, P. E. *Biomaterials* **1998,** *19*, 1669-1675.
(98) Finlay, J. A.; Krishnan, S.; Callow, M. E.; Callow, J. A.; Dong, R.; Asgill, N.; Wong, K.; Kramer, E. J.; Ober, C. K. *Langmuir* **2008,** *24*, 503-510.
(99) Cerruti, M.; Fissolo, S.; Carraro, C.; Ricciardi, C.; Majumdar, A.; Maboudian, R. *Langmuir* **2008**, ASAP article.
(100) Ebner, A.; Wildling, L.; Kamruzzahan, A. S. M.; Rankl, C.; Wruss, J.; Hahn, C. D.; Holzl, M.; Zhu, R.; Kienberger, F.; Blaas, D.; Hinterdorfer, P.; Gruber, H. J. *Bioconjugate Chem.* **2007,** *18*, 1176-1184.
(101) Riener, C. K.; Stroh, C. M.; Ebner, A.; Klampfl, C.; Gall, A. A.; Romanin, C.; Lyubchenko, Y. L.; Hinterdorfer, P.; Gruber, H. J. *Anal. Chim. Acta* **2003,** *479*, 59-75.
(102) Wang, T.; Xu, J. J.; Qiu, F.; Zhang, H. D.; Yang, Y. L. *Polymer* **2007,** *48*, 6170-6179.

(103) Suo, Z. Y.; Arce, F. T.; Avci, R.; Thieltges, K.; Spangler, B. *Langmuir* **2006,** *22*, 3844-3850.

(104) Wang, Y. L.; Su, T. J.; Green, R.; Tang, Y. Q.; Styrkas, D.; Danks, T. N.; Bolton, R.; Liu, J. R. *Chem. Comm.* **2000**, 587-588.

(105) Feng, W.; Zhu, S. P.; Ishihara, K.; Brash, J. L. *Langmuir* **2005,** *21*, 5980-5987.

(106) Sharma, S.; Johnson, R. W.; Desai, T. A. *Appl. Surf. Sci.* **2003,** *206*, 218-229.

(107) Sharma, S.; Johnson, R. W.; Desai, T. A. *Langmuir* **2004,** *20*, 348-356.

(108) Yang, Z. H.; Galloway, J. A.; Yu, H. U. *Langmuir* **1999,** *15*, 8405-8411.

(109) Popat, K. C.; Mor, G.; Grimes, C.; Desai, T. A. *J. Membr. Sci.* **2004,** *243*, 97-106.

(110) Jon, S. Y.; Seong, J. H.; Khademhosseini, A.; Tran, T. N. T.; Laibinis, P. E.; Langer, R. *Langmuir* **2003,** *19*, 9989-9993.

(111) Heyes, C. D.; Kobitski, A. Y.; Amirgoulova, E. V.; Nienhaus, G. U. *J. Phys. Chem. B* **2004,** *108*, 13387-13394.

(112) Massia, S. P.; Stark, J.; Letbetter, D. S. *Biomaterials* **2000,** *21*, 2253-2261.

(113) Schlapak, R.; Pammer, P.; Armitage, D.; Zhu, R.; Hinterdorfer, P.; Vaupel, M.; Fruhwirth, T.; Howorka, S. *Langmuir* **2006,** *22*, 277-285.

(114) Uyama, Y.; Kato, K.; Ikada, Y. *Adv. Polym. Sci.* **1998,** *137*, 1-39.

(115) Kato, K.; Uchida, E.; Kang, E. T.; Uyama, Y.; Ikada, Y. *Prog. Polym. Sci.* **2003,** *28*, 209-259.

(116) Hilal, N.; Ogunbiyi, O. O.; Miles, N. J.; Nigmatullin, R. *Sep. Sci. Tech.* **2005,** *40*, 1957-2005.

(117) Chen, H.; Belfort, G. *J. Appl. Polymer Sci.* **1999,** *72*, 1699-1711.

(118) Kilduff, J. E.; Mattaraj, S.; Zhou, M. Y.; Belfort, G. *J. Nanopart. Res.* **2005,** *7*, 525-544.

(119) Yamagishi, H.; Crivello, J. V.; Belfort, G. *J. Membr. Sci.* **1995,** *105*, 237.

(120) Yamagishi, H.; Crivello, J. V.; Belfort, G. *J. Membr. Sci.* **1995,** *105*, 249.

(121) Ma, H. W.; Li, D. J.; Sheng, X.; Zhao, B.; Chilkoti, A. *Langmuir* **2006,** *22*, 3751-3756.

(122) Beyer, M.; Felgenhauer, T.; Bischoff, F. R.; Breitling, F.; Stadler, V. *Biomaterials* **2006,** *27*, 3505-3514.

(123) Ma, H. M.; Bowman, C. N.; Davis, R. H. *J. Membr. Sci.* **2000,** *173*, 191-200.

(124) Susanto, H.; Balakrishnan, M.; Ulbricht, M. *J. Membr. Sci.* **2007,** *288*, 157-167.

(125) Asatekin, A.; Kang, S.; Elimelech, M.; Mayes, A. M. *J. Membr. Sci.* **2007,** *298*, 136-146.

(126) Zou, X. P.; Kang, E. T.; Neoh, K. G. *Plasmas Polym.* **2002,** *7*, 151-170.

Chapter 4

Covalent Biofunctionalization of Silicon Nitride Surfaces

Covalently attached organic monolayers on etched silicon nitride (Si_xN_4; $x \geq 3$) surfaces were prepared by reaction of Si_xN_4-coated wafers with 1-alkenes and 1-alkynes, neat or diluted in refluxing mesitylene. The surface modification was monitored with static water contact angle, XPS, IRRAS, AFM and ToF-SIMS measurements, which give evidence for the formation of Si–C bonds. After etching in diluted HF solutions, yielding both Si–H and N–H surface groups, the resulting Si_xN_4 surfaces were functionalized by terminal carboxylic acid groups in either of two ways: a) via attachment of a 10-undecenoic acid 2,2,2-trifluoroethyl ester (trifluoro ethanol ester) and subsequent thermal acid hydrolysis; b) through attachment of a photocleavable ester, and subsequent photochemical cleavage, as this would allow photopatterned functionalized Si_xN_4. The carboxylic acids were successfully used for the attachment of oligopeptides (aspartame) and complete proteins using EDC/NHS-chemistry. Finally, an amino-terminated organic monolayer was formed by reaction of HF-treated Si_xN_4 surfaces with an *N*-(ω-undecylenyl)-phthalimide, which yielded an amino-terminated surface upon deprotection with hydrazine.

This chapter is published as:
"*Covalent biofunctionalization of silicon nitride surfaces*" Arafat, A.; Giesbers, M.; Rosso, M.; Sudhölter, E. J. R.; Schroën, K.; White, R. G.; Yang, L.; Linford, M. R.; Zuilhof, H. *Langmuir* **2007**, *23*, 6233-6244.

Introduction

Silicon nitride (Si_xN_4; $x \geq 3$) is one of the most frequently used materials in the semiconductor industry.[1] Films of this material inhibit diffusion of water, oxygen and sodium ions, and are widely used as passivation layer in integrated circuits.[2] The wide use of Si_xN_4 is mainly motivated by its superior physical and chemical inertness,[3] as it provides an excellent alternative to silicon dioxide[4] in microelectronic[5] and membrane applications.[6-9]

Silicon nitride itself has been functionalized via modification of the native SiO_2 layer that is present as a poorly defined, thin layer on Si_xN_4 surfaces. This has especially found use in the modification of AFM tips, and interactions of such tips with various substrates[10-13] and proteins.[14] However, the surface roughness of silicon nitride and the chemical composition of its surface change over time under ambient conditions or in aqueous media. This hampers the application of this material, for example, in durable membranes (microsieves).[8,15,16]

One way to solve the problems posed by the surface of silicon nitride is to provide a well-controlled and stable modification of oxide-free Si_xN_4 surfaces using the covalent attachment of organic monolayers, which proved to be very successful for silicon surfaces[17-20] and opened up many new opportunities for applications including optoelectronics,[21,22] biosensors,[23,24] and micro- and nano-electromechanical systems (MEMS and NEMS).[25,26] Several approaches have been applied to attach organic molecules onto crystalline hydrogen-terminated silicon surfaces using thermal methods,[17,18,27-29] UV irradiation,[30,31] electrochemistry,[32-34] hydrosilylation catalysis,[35-37] and very recently visible light irradiation.[38] These methods provide stable, densely packed monolayers with tailor-made surface properties, including the covalent attachment of biomolecules[39] such as DNA[40] and fragile carbohydrates.[41]

In contrast to the situation with SiO_2 and Si surfaces, covalent attachment of organic monolayers onto Si_xN_4 was not explored in detail until recently. In addition, no method has been reported to photopattern Si_xN_4 itself, rather than the oxide layer on it. A few independent modification examples have been reported, which include poorly defined monolayers of 1-octadecene (static water contact angle $\theta = 83^o$),[42] and attachment of a carboxylic acid-functionalized monolayer via *N*-alkylation with an ω-bromoalkanoic acid.[43,44] However, a reaction analogous to the reaction of Si–H sites on silicon was unknown, while it would be highly useful.

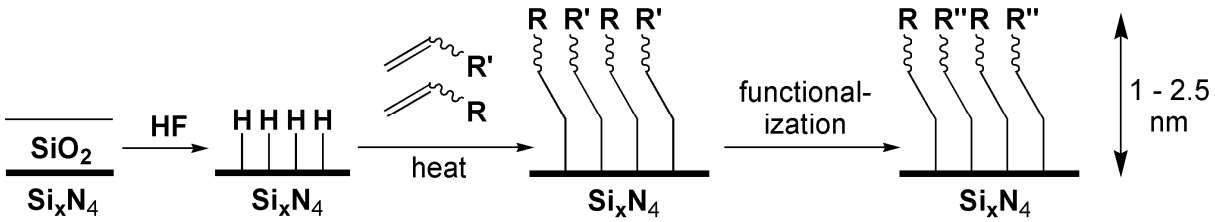

Figure 1. Formation of covalently attached organic monolayers onto Si_xN_4 surfaces.

This prompted us to investigate such surface functionalization in detail, and we reported recently preliminary data regarding the development of a method for the thermal functionalization and passivation of hydrogen-terminated Si_xN_4 via the reaction sequence presented in Figure 1.[45] Non-functionalized and functionalized 1-alkenes and 1-alkynes were used to form organic monolayers covalently bound to the Si_xN_4 surface by Si–C and N–C bonds, and hydrophobic surfaces were obtained (Water contact angle: θ = 107°). Infrared reflection absorption spectroscopy (IRRAS) confirmed the formation of organic monolayers, but also displayed a smaller degree of ordering of these monolayers in comparison to flat Si and SiO_2 surfaces, which was hypothesized to be related to the roughness of these surfaces (rms roughness of at least 4.3 nm).[45] Apart from a preliminary, base-induced ester hydrolysis, no further functionalization was reported. Recently, Cattaruza *et al.* have independently reported on HF-treated Si_xN_4 that could be functionalized via the attachment of long chain carboxylic acid-terminated monolayers.[43,44]

An investigation of the possibilities and limitations of further functionalization of Si_xN_4 would be of interest, given the different properties of Si_xN_4 (very robust, insulating) in comparison to e.g. Si (brittle, semiconductor). For example, a recent report on the direct functionalization of HF-treated Si_xN_4 to form DNA microarrays presented a higher density of surface functionalization than observed for analogous Si surfaces.[46] In addition, mild methods for the formation of highly hydrophilic Si_xN_4 surfaces without the involvement of an unstable SiO_x interlayer would be desirable, as this would yield *stable* Si_xN_4 surface properties that are out of reach from currently reported methods.

Therefore, we present in this paper the first detailed investigation on monolayer formation of highly flattened hydrogen-terminated Si_xN_4 surfaces, and their functionalization with esters, carboxylic acids, amine groups, amino-acids and proteins. Static water contact angle measurements were used to study changes that occur during the different steps of the monolayer formation, and Atomic Force Microscopy (AFM) was used to study the effect of

HF treatment on the roughness of the Si_xN_4 surface. On modified surfaces, AFM was also used to image any changes in the surface topography and to get information about the quality of the layers. IRRAS and X-ray Photoelectron Spectroscopy (XPS) were used to follow the progress of the reaction and to characterize the resulting surfaces. Time-of-Flight Secondary Ion Mass Spectroscopy (ToF-SIMS) was used to get information about the sites of attachment (Si and/or N) during the attachment of the organic monolayer. In addition, the stability of the formed monolayers towards different media (acidic and alkaline) was investigated, in regard of the practical importance for cleaning procedures normally used for Si_xN_4–based durable membranes. Finally, we introduce the use of covalently attached photo-cleavable esters to yield highly hydrophilic and photopatternable Si_xN_4 under neutral conditions at room temperature.

Experimental Section

Materials

Chemicals

Petroleum ether (PE 40/60), methanol (MeOH), ethanol (EtOH), toluene, and dichloromethane (CH_2Cl_2) were distilled prior to use. Acetone was used as obtained (Acros, > 99%). Mesitylene (Fluka, 99%) was distilled twice and stored on $CaCl_2$. The dried mesitylene was filtered through filter paper to remove any $CaCl_2$ particles before mixing with the 1-alkenes or 1-alkynes. 1-Decene (Fluka, 97%), 1-dodecene (Fluka, 99%), 1-tetradecene (Sigma, 99%), 1-hexadecene (Sigma, ~ 99%) and 1-hexadecyne (Alpha Aesar, 98%) were distilled twice at reduced pressure. 1-octadecene (Fluka, 95%) was distilled three times and further purified by column chromatography. 1-Octadecyne was synthesized and purified by recrystallization according to the procedure published by Sieval et al.[17] HF (Fluka, 50% p.a. plus) was diluted with demineralized H_2O to get a 2.5% solution. (**Warning:** HF is a hazardous material: it can readily penetrate skin, destroy soft tissue, and decalcify bone, and should be handled with care!) All reactions were performed under a nitrogen atmosphere. 2-Bromo-4′-methoxyacetophenone (Aldrich), bovine milk κ-casein (Sigma, purity > 90%), *N*-hydroxysuccinimide (NHS, Sigma), 1,8-diazabicyclo[5.4.0.]undec-7-ene (DBU, Aldrich), *N*-ethyl-*N'*-(3-dimethylaminopropyl) carbodiimide hydrochloride (EDC, Sigma), *n*-octylamine (Sigma) and aspartame (Sigma) were used without further purification.

Purification and analysis of the synthesized compounds

Thin-layer chromatography (TLC) was performed on Merck silica gel 60F254 plastic sheets, and detection was performed by oxidation with solution of 10% v/v H_2SO_4 in EtOH. Column chromatography was conducted by elution of a column of Merck silica gel, 230-400 mesh (Merck) using eluents as specified below. ^{1}H and ^{13}C NMR spectra were recorded on a Bruker AC-E 400 spectrometer in $CDCl_3$ (dried over Al_2O_3). Gas chromatography (GC) measurements were performed on a Hewlett-Packard 5890 series II chromatograph that was equipped with a DB-17 reverse phase column and an FID detector. GC samples were prepared in ethyl acetate or diethyl ether.

Synthesis of 10-undecenoic acid 2-(4-methoxyphenyl)-2-oxo-ethyl ester (I)

2-Bromo-4′-methoxyacetophenone (9.16 g, 40 mmol) was added to a mixture of 10-undecylenic acid (10 g, 54 mmol) and DBU (7.69 g, 50 mmol) in toluene (100 mL). The solution was stirred for 2 h under nitrogen at room temperature The suspension was then neutralized with 50 mL of 10% v/v HCl in water and extracted 3 times with toluene. The organic fraction was washed with water, and dried over $MgSO_4$. The solvent was evaporated to give **I** as a yellowish oily compound. Column chromatography on silica gel with dichloromethane (product: rf = 0.6; 10-undecylenic acid: rf < 0.1) yielded 10.5 g (80%) of **I**. 1H-NMR (CDCl3): δ = 1.33 (br., 10H), 1.7 (m, 2H), 2.06 (m, 2H), 2.5 (t, J = 7 Hz, 2H), 3.89 (s, 3H), 4.97 (m, 2H), 5.31 (s, 2H), 5.83, (m, 1H), 6.96 (d, J = 9 Hz, 2H), 7.91 (d, J = 9 Hz, 2H); 13C-NMR (CDCl3): δ = 25-30 (6C), 33.8, 33.9, 55.5, 65.6, 114.1 (3C), 127.3, 129.6, 130.0, 139.2, 164.0, 173.3, 190.8.

Synthesis of 2,2,2-trifluoroethyl undec-10-enoate (II)

This compound was synthesized according to the procedure published by Sun et al.[47]

Synthesis of *N*-(ω-undecylenyl)-phthalimide (III)

(III) was prepared according to the procedure reported by Sieval et al.[48] and recrystallized from distilled methanol.

Monolayer Formation

Silicon nitride-coated silicon (single side-polished wafers; thickness of Si_xN_4: 100, 144 or 200 nm, sample size: 10 x 10 x 0.5 mm^3) were supplied by Aquamarijn B.V., The Netherlands. Si_xN_4 samples were first cleaned by rinsing several times in chemically pure

acetone, followed by wiping the sample several times with a tissue paper saturated with acetone. Thereafter, the samples were placed in c.a. 5 mL of acetone and further cleaned in an ultrasonic bath for at least 15 min. Finally, the surfaces were cleaned with an air-based plasma in a plasma cleaner/sterilizer (Harrick PDC-32G) for 3 min. To facilitate the subsequent removal of the native oxide layer the surface was first oxidized by exposure to oxygen plasma for 5 min.[49] Immediately after the oxygen plasma treatment, hydrogen–termination of Si_xN_4 samples was carried out by placing the samples in 2.5% v/v HF for 2 min in an ultrasonic bath, prior to placing it in the alkene reaction mixture.

A solution of a 1-alkene or 1-alkyne in mesitylene (10 mL, 0.4 M) was placed in a 20 mL three-necked flask fitted with a nitrogen inlet, a condenser with a $CaCl_2$ tube, and a stopper. The solution was deoxygenated for at least 45 min, by refluxing it using a metal bath (temperature ~ 165 ºC), while slowly bubbling dry nitrogen through the solution. Subsequently, a freshly etched Si_xN_4 wafer was placed into the refluxing solution by quickly removing and replacing the stopper. The reaction time varied from 2-72 h (see Results and Discussion section), after which the reaction mixture was allowed to cool down to room temperature Subsequently, the sample was removed from the solution, and rinsed extensively with distilled PE 40/60, EtOH, and CH_2Cl_2.

Stability tests

The stability of hexadecyl-modified Si_xN_4 surfaces was tested by placing modified samples in pure water, 0.1 M HCl, 0.1 M NaOH and 0.001 M NaOH. The effects were followed via static water contact angle and IRRAS measurements. Tests were carried out twice; stability in alkaline solutions was measured three times.

Formation of NHS-functionalized Si_xN_4 surfaces

A carboxylic acid-terminated Si_xN_4 surface was covered with an aqueous solution of 500 µL of 0.1 M NHS and 500 µL of 0.4 M EDC, and allowed to react at room temperature for 1 h at pH = 6.3.[40] The wafer was then rinsed copiously with deionized water and CH_2Cl_2, and dried under a stream of nitrogen.

Attachment of n-octylamine

An NHS-activated Si_xN_4 surface was covered by a solution of 30 µL of *n*-octylamine in 2 mL of DMF for 1 h at room temperature The surface was then rinsed thoroughly with deionized water and 1,1,1-trichloroethane, respectively, and dried under a stream of nitrogen.

Attachment of protein molecules

Protein solutions of bovine milk κ-casein in H_2O were prepared in different concentrations, ranging from 0.1 - 100 mg/mL in 20 mM phosphate buffer at pH 6.8 prepared from NaH_2PO_4 and K_2HPO_4.[50] The protein was covalently attached by placing the Si_xN_4 sample in 10 mL of protein solution for 1 h at room temperature, followed by copious rinsing with the phosphate buffer, after which the surface was dried under a stream of nitrogen gas. Non-covalent protein attachment onto protein-modified Si_xN_4 samples was quantitatively monitored using reflectometry measurements.[51] First, EDC/NHS-modified samples were exposed to aqueous phosphate buffer, pH 6.8 for 5 min. Subsequently, the sample was exposed to protein solution and adsorption was recorded until a plateau was observed indicating "equilibrium" at room temperature At this stage, the modified sample was again exposed to a stream of the same buffer solution and/or surfactant solution to record the possible removal of unbound proteins.

Formation of oligopeptide-substituted surfaces

An NHS-functionalized Si_xN_4 surface was further functionalized by placing the modified wafer in a 0.1 mg/mL aqueous solution of aspartame **(IV)**, for 1 h at room temperature Covalent attachment of aspartame was characterized by IRRAS measurements.

Formation of amino-terminated silicon nitride surface

A mixture of *N*-(ω-undecylenyl)-phthalimide (**III)** and 1-decene (**C10)** was attached to H-terminated Si_xN_4 by refluxing 0.4 M solutions with 1:1 and 2:1 molar ratios of **III** and **C10**, respectively. The formed mixed monolayers were characterized with static water contact angle measurements and IRRA spectroscopy. Deprotection of the phthalimide-functionalized monolayers was carried out by placing the modified Si_xN_4 in 5% (v/v) solution of hydrazine in distilled ethanol for 48 h. The solution was agitated by bubbling nitrogen gas. Subsequently, the samples were removed from the solution and cleaned as described previously.

Monolayer Characterization

Contact angle measurements

Static water contact angles were obtained using an Erma Contact Angle Meter G-1 (drop volume of ultrapure water = 3.5 μL). Contact angles of two or three independent drops were measured. The experimental error in the reported values of contact angles is ± 1º.

Infrared Reflection-Absorption Spectroscopy (IRRAS)

FT IRRA spectra were recorded on a Bruker Tensor 27 equipped with a variable-angle reflection Auto Seagull accessory. A Harrick grid polarizer installed in front of the detector for measuring spectra with *p*-polarized (parallel) radiation with respect to the plane of incidence at the sample surface. Single channel transmittance spectra (4096 scans) were recorded using a spectral resolution of 2-4 cm^{-1}. The spectra shown in this paper are ratios of single channel data of the modified samples to that of a plasma-cleaned Si_xN_4 sample (i.e. plasma-cleaned sample data are treated as background), and baseline-corrected.

X-ray Photoelectron Spectroscopy (XPS)

XPS spectra were obtained in normal emission at ~ 10^{-9} mbar on either of two systems: 1) a VG Ionex system operating with a Clam II analyzer and a standard Al K_α X-ray source. On this instrument, all C_{1s} peaks corresponding to hydrocarbons were calibrated to a binding energy of 285.0 eV to correct for the energy shift caused by static charging. 2) ARXPS analyses were performed on a Theta Probe (Thermo VG Scientific, UK) by using a monochromatic Al K_α X-ray source with a 400 micrometer spot runs at 100W under UHV conditions. XPS data were acquired in angle-resolved mode (8 angles from 23.75 to 76.25 deg.) by using scanned spectra at a pass energy of 50 eV. Quantifications were done by collapsing all angle-resolved data. Results are also a summation of 36 acquisition points through the whole wafer."

Atomic Force Microscopy (AFM)

AFM images were obtained on a Nanoscope III Multimode AFM (Digital Instruments, Santa Barbara, CA) operating in contact mode in air. The scan size was 2.5 μm at a scan rate of 1.0 Hz. Standard silicon nitride contact-mode cantilevers (Digital Instruments; force constant ~0.58 $N.m^{-1}$) were used.

X-ray Reflectivity

X-ray reflectivity measurements were performed on a Panalytical X'Pert Pro diffractometer using Cu K_α radiation (tube settings 40 kV / 40 mA). The data were collected using a fixed divergence slit of 1/32° and a parallel plate collimator on the diffracted beam side. The layer thickness was calculated from the interference fringes. The error in the measurement was depicted as the standard deviation of 5 measurements on the same sample.

ToF-SIMS Measurements

Time-of-flight secondary ion mass spectrometry (ToF-SIMS)[52] was performed on samples made by immersion in refluxing neat 1-hexadecene for different periods of time. Each sample was analyzed at two points on its surface. To deal with the enormous quantity of data produced by ToF-SIMS and to rapidly find the chemical variation in the data without introducing user bias, principal components analysis (PCA)[53-55] was performed on the resulting spectra.

ToF-SIMS was performed with an ION-TOF ToF-SIMS IV with monoisotopic 25 keV $^{69}Ga^+$ primary ions in "bunched mode." The primary ion (target) current was typically 1.319 pA, with a pulse width of 20 ns before bunching, and the raster area of the beam was 51.8 x 51.8 μm^2.

For the principal components analysis (PCA), 192 peak regions from the positive ion ToF-SIMS spectra were selected and integrated over in the instrument software. The following spectral regions were integrated in the positive ion spectra over two ranges -0.2 and +0.2 amu around these values: 12, 13, 14, 15, 19, 23, 24, 26, 27, 28, 29, 30, 31, 32, 38, 39, 40, 41, 42, 43, 44, 45, 46, 47, 48, 49, 50, 51, 52, 53, 54, 55, 56, 57, 58, 59, 62, 63, 65, 66, 67, 68, 69, 70, 71, 72, 73, 74, 75, 77, 78, 79, 80, 81, 83, 84, 85, 87, 89, 91, 93, 95, 97, 100, 101, 103, 105, 109, 112, 113, 114, 115, 116, 117, 119, 128, 131, 133, 135, 137, 147, 148, 149, 150, 151, 163, 169, 185, 201, 207, 213, 216, 221, 251, 281. The following two regions were also included: 1 to 1.2 and 81.9 to 82.1. Each region was either the "mass excess" region from the integer value of a mass up to 0.2 mass units above it, e.g., m/z 55.0 to 55.2, or the "mass deficit" region from the integer value of a mass down to 0.2 mass units below it, e.g., m/z 46.0 to 45.8. The purpose of binning the data in this manner was to separate the organic fragments in the mass excess region from the inorganic fragments in the mass deficit region. The entire spectra were then normalized by dividing each area by the total area of the spectrum (all the integrated regions). The PLS Toolbox 3.0 (Eigenvector Research) in Matlab (Version 6.5) was then used to mean center the data and to perform PCA. These preprocessing methods have been shown to be effective in PCA analysis of ToF-SIMS data from monolayers on gold[53] and silicon.[56-58]

Results and Discussion

Hydrogen-termination of silicon nitride surfaces

The silicon nitride samples used consisted of a thin layer of Si_xN_4 (100, 144 or 200 nm) deposited onto a Si wafer by low-pressure chemical vapor deposition (LPCVD) of NH_3 and SiH_4/N_2. The resulting material is somewhat heterogeneous in chemical nature (*vide infra*), but frequently used due to its excellent mechanical properties.[8] Hydrogen termination of such a silicon-enriched Si_xN_4 ($x \geq 3$) surface can be achieved using etching with aqueous HF.

The static water contact angle θ of as-received silicon nitride samples after an oxygen plasma cleaning step was ~18°, which indicates a very hydrophilic surface. Dipping the samples in an aqueous solution of 2.5% (v/v) HF for different time intervals (10-360 s) gradually increased θ up to 57-59° after 4 min (see Figure 2, left). This result is consistent with the formation of both Si–H (2170 cm^{-1}) and N–H bonds (3330 cm^{-1}) on the surface, as can also be seen from the IRRAS data (Figure 2, right). Similar results were recently reported by Bermudez *et al.*[59] As a result of the etching step, the hydrophobicity of the surface increased, but to lower contact angle values than measured for e.g. H-terminated Si surfaces (~ 70°) due to the presence of the polar N–H bonds at the surface.

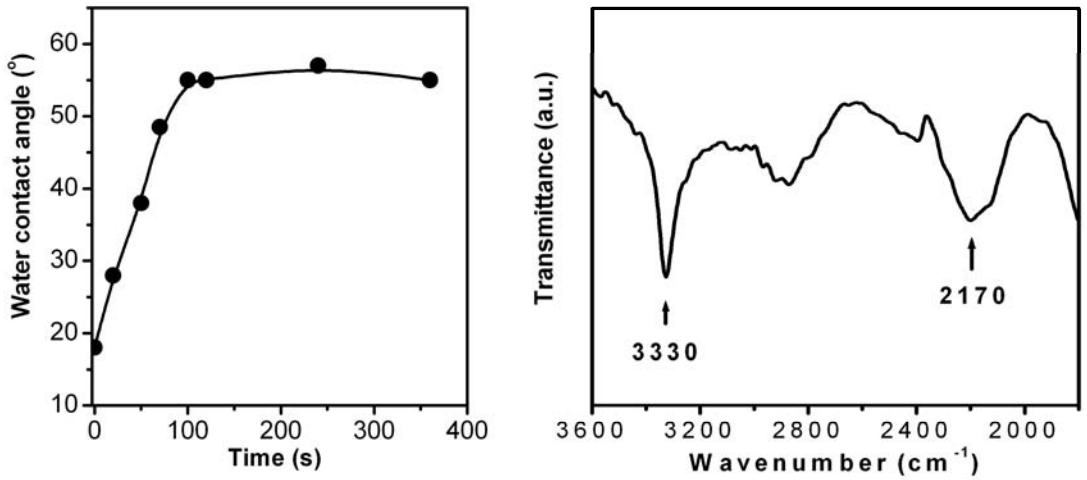

Figure 2. (left) Water contact angles as a function of etching time of Si_xN_4 samples (thickness 200 nm), and (right) IRRA spectrum recorded immediately after 2 min etching in 2.5% HF solution (without sonication).

A contact mode AFM image of a plasma–cleaned, unmodified silicon nitride sample is shown in Figure 3 (left). The image clearly shows that the surface of as-received Si_xN_4 substrates was very rough, e.g. compared to nearly atomically flat silicon surfaces. The root mean square (rms) variation across the surface amounted to 2.36 nm, compared to ~ 0.2 nm in case of a polished Si(100) surface on a commercial Si wafer. The removal of these irregularities on the Si_xN_4 surface is desirable prior to the attachment of the organic monolayer, as it is expected to retard the formation of a densely packed monolayer. Therefore, we studied the effect of the HF treatment on the Si_xN_4 roughness with contact mode AFM. Reaction with HF strongly reduced the surface roughness (rms from 2.36 to 0.84 nm in 3 min; see Table 1), although it did not lead to complete removal of the irregularities and even corrugates the surface after 5-10 min of dipping in the etching solution. However, the average surface roughness (rms values) is not the only determining factor for obtaining high quality monolayers, as the etching also yields surface Si–F sites (XPS data not shown). Such highly stable Si–F surface sites can result in a lower packing density of the monolayer, and thereby, also in a reduced stability. We found an optimum monolayer quality after etching for 2 min with 2.5% (v/v) HF solution, apparently as the compromise between reduced surface roughness and an increasing number of Si–F sites.

Table 1. Surface roughness of Si_xN_4 samples (AFM rms values in nm, ± 2%) after different etching times in 2.5% HF.

Etching time (min)	0	1	2	3	5	7	10
r.m.s. Surface roughness (nm)	2.36	2.09	0.97	0.84	1.07	1.51	1.64

Interestingly, the surface roughness could be further reduced upon performing the etching step while the wafer was placed vertically in an ultrasonic bath. Etching for 2 min then yielded a surface roughness of 0.80 nm (compared to 0.97 nm without sonication) and, more importantly, lead to the near-complete removal of the biggest surface irregularities. This indicates that such wet etching of Si_xN_4 can be best performed in combination with sonication (See Figure 3).

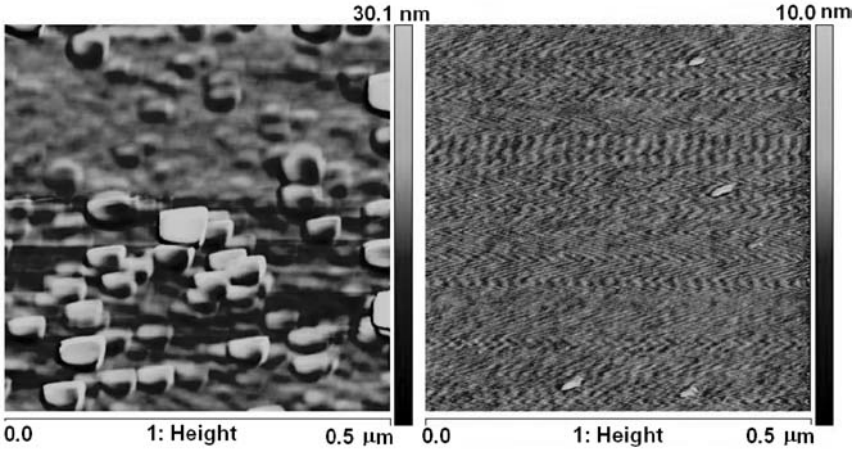

Figure 3. Contact mode AFM images of cleaned as-received Si_xN_4 surface (left) and Si_xN_4 surface after HF treatment in ultrasonic bath (right).

The chemical composition of the silicon nitride surface was investigated by XPS (Figure 4). This analysis shows that the silicon nitride surfaces under study are composed of five elements. From the XPS survey scan the atomic concentration at the surface was found to correspond to 35% Si, 30% N, 24% O, 7% C and 3% F. Similar findings regarding the presence of carbon in the as-received surface of Si_xN_4 are reported to be due to environmental contamination during growth of silicon nitride in presence of carbon or fluorine.[42]

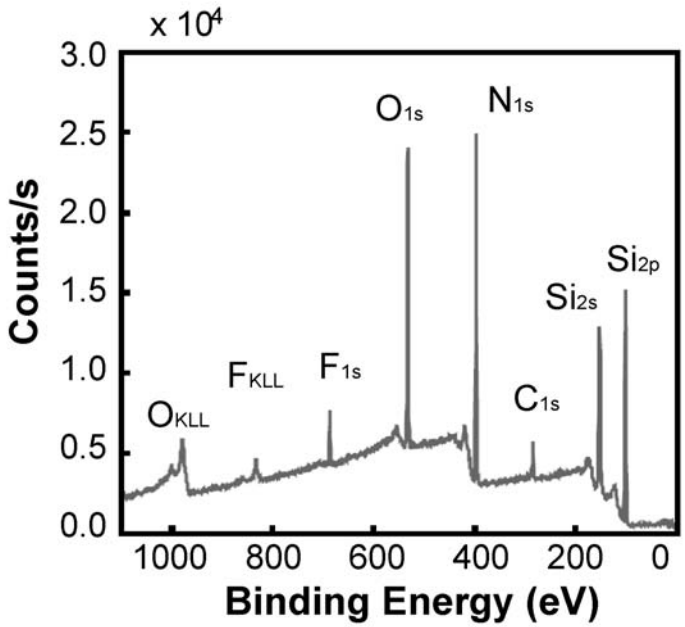

Figure 4. XPS measurement on a solvent-cleaned, unmodified Si_xN_4 surface (200 nm thickness) before etching.

Like the surface roughness, the composite chemical nature of this surface has also a negative effect on the production of high quality monolayers. Both the surface roughness and the stoechiometry of Si_xN_4 are significantly changed by the preparation method of this material. For example, plasma-enhanced CVD produces Si–H, N–H and O–H bonds at the surface that are not produced when low-pressure CVD is used.[60]

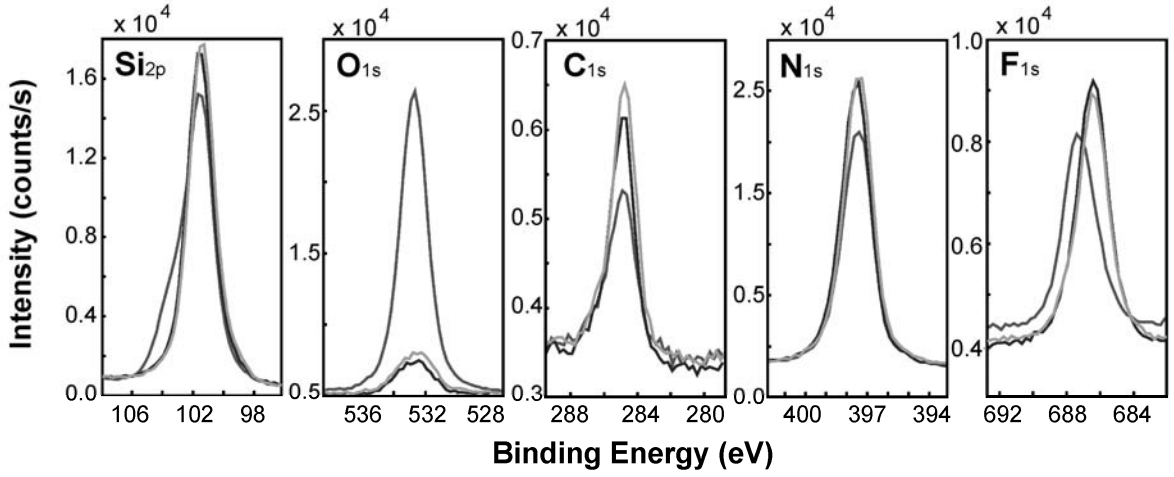

Figure 5. XPS measurements of as-received, solvent-cleaned Si_xN_4 (200 nm) (dark gray), and after wet etching with 2.5% HF for 2 min (black) and 4 min (light gray).

XPS analyses of HF-treated Si_xN_4 surfaces at different treatment times are depicted in Figure 5. After 2 min of etching, the surface composition (atomic %) changed to: Si = 37.8, N = 42.6, C = 9.0, F = 6.2 and O = 4.4. It is obvious that the native oxide layer originally present in the as-received samples was almost completely removed upon reaction with the HF solution. However, even prolonged exposure of the surface to HF solution did not lead to the complete removal of oxygen, as some of it is apparently buried in sub-surface levels. While the XPS peak corresponding to N–O bonds could not be resolved in the N_{1s} spectra of this sample, this peak was very clear in another batch with silicon nitride thickness of 100 nm (data not shown). Such silicon oxynitride is not removable by reaction with HF solutions.[61] The removal of the native surface oxide layer can also be seen in the Si_{2p} spectra, where the oxide shoulder present in as-received samples at 105 eV has been completely removed as shown in the spectra of the HF-treated samples (Figure 5, most left spectrum). Removal of this oxide layer also yields a concomitant increase in the Si_{2p} and N_{1s} signals.

The 2 eV shift in F_{1s} spectra of the original and etched samples can be attributed to the formation of new fluorinated species on the surface by the action of HF, via reactions of F^- and HF_2^- as suggested by Knotter and Denteneer:[62]

$$(\text{-N-})_3\text{Si-NH}_3^+ + F^- \longrightarrow (\text{-N-})_3\text{Si-F} + \text{NH}_3 \qquad \text{or}$$

$$(\text{-N-})_3\text{Si-NH}_2 + HF_2^- \longrightarrow (\text{-N-})_3\text{Si-F} + F^-$$

Monolayer formation on the silicon nitride surface

The H-terminated Si_xN_4 surface obtained after HF treatment was successfully used for attachment of monolayers from 1-alkenes and 1-alkynes. Table 2 lists the static water contact angles measured on Si_xN_4 samples modified with a variety of 1-alkenes and 1-alkynes. We previously reported static water contact angle values[45] (values shown in parentheses in Table 2) for Si_xN_4 surfaces that were not smoothed using sonication. Currently reported contact angles are slightly higher, which we attribute to the reduced surface roughness obtained using sonication. This improved etching step allows for a better/denser packing of the monolayers. The contact angles of alkyl monolayers indicate a high hydrophobicity, and the values of θ approach those of high-quality alkyl monolayers prepared under thermal conditions on crystalline silicon (109-110°).[19,38]

So far, the roughness of the as-received samples had prevented any measurement of the monolayer thickness with X-ray reflectivity. However, with the strongly reduced surface roughness achieved upon sonication, the thickness could be measured, and gave for an *n*-$C_{18}H_{37}$ monolayer a value of 18 ± 1 Å. This result implies an average tilt angle of 36° with the surface normal, assuming a linear conformation of the alkyl chain. This angle is comparable to a tilt angle of ~ 30° for the corresponding *n*-$C_{18}H_{37}$ monolayers on hydrogen-terminated silicon (111), and confirms the high packing density of alkyl chains on H-terminated Si_xN_4 surfaces. The reduced surface roughness obtainable via the new sonication-etching method is also clear from the slower intensity fall-off of the specularly reflected X-ray beam.

Table 2. Static water contact angles (θ) of Si_xN_4 substrates modified by different 1-alkenes and 1-alkynes (refluxing solutions in mesitylene for 24 h; experimental error ± 1°). Values in parentheses are the values obtained without sonication during etching.

Compound (concentration)	Contact angles (°)
CH_2=CH-$C_{20}H_{41}$ (0.4 M)	106 (102)
CH_2=CH-$C_{16}H_{33}$ (Neat)	108 (107)
CH_2=CH-$C_{16}H_{33}$ (0.4 M)	108 (104)
CH_2=CH-$C_{14}H_{29}$ (Neat)	107 (107)
CH_2=CH-$C_{14}H_{29}$ (0.4 M)	106 (106)
CH_2=CH-$C_{12}H_{25}$ (0.4 M)	106 (105)
CH_2=CH-$C_{10}H_{21}$ (0.4 M)	106 (106)
CH≡C-$C_{16}H_{33}$ (0.4 M)	106 (104)
CH≡C-$C_{14}H_{33}$ (0.4 M)	108 (103)

XPS spectra were recorded at different reaction times to study the attachment sites of the alkenes onto silicon nitride (see Figure 6). The amount of C_{1s} increases gradually during the reaction, which indicates attachment of the alkyl chains onto the surface. A shoulder around 287 eV appears in the C_{1s} spectra, which can be assigned to attachment of the alkyl chain to the (electronegative) surface nitrogen. The detected amount of Si and N decreased gradually during the reaction, indicating the formation of an organic overlayer, in line with the observed reduction of the detected amount of F, which is thought to be all Si-bound. The amount of surface oxygen was found to slightly increase during the reaction, which suggests a competitive reaction of O_2 with the H-terminated Si_xN_4 surface during the formation of the monolayer. The increase is, however, small, as can be seen from the near-absence of a SiO_2 peak in the Si_{2p} spectrum at 104-105 eV.

Generally, the formation of a complete monolayer on the H-terminated Si_xN_4 surface is much slower than the same reaction on crystalline silicon surfaces (24 *vs.* 2 h under identical thermal conditions). We attribute this to the still higher surface roughness, which will reduce the chain length of any radical chain process, and to the presence of N-H sites (BDE ~ 93 kcal/mol), which has a lower reactivity towards carbon-centered radicals then Si-H (BDE ~ 76 kcal/mol).

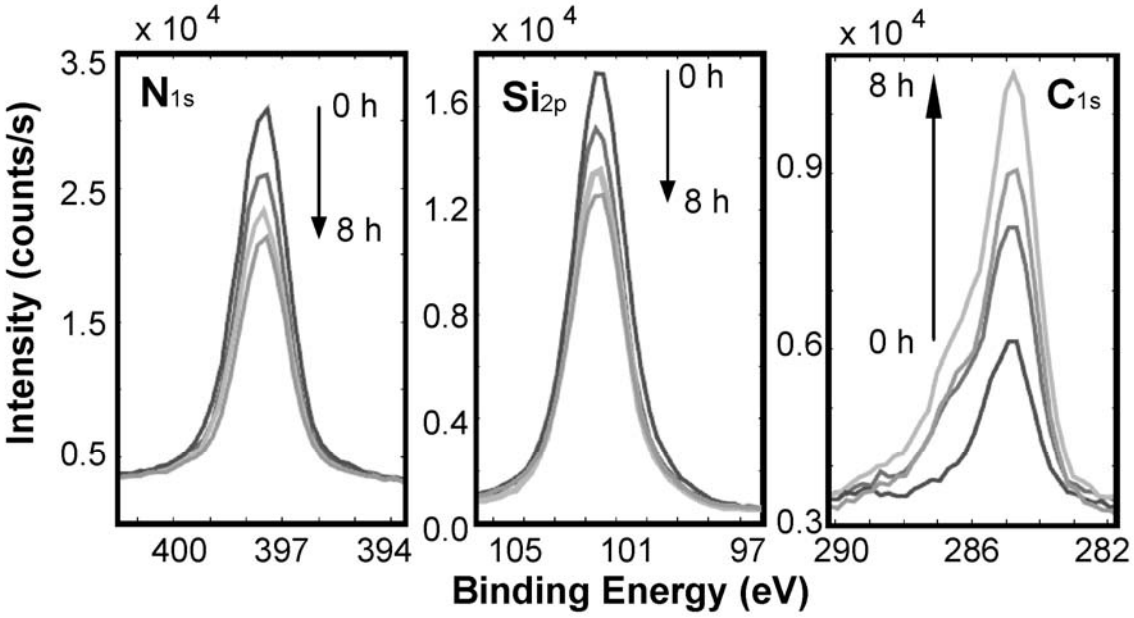

Figure 6. XPS measurements following monolayer formation, from 0 to 8 h of reaction: 0 h (solvent-cleaned Si_xN_4), 2 h, 4 h and 8 h reaction with 1-hexadecene. (Shades of gray are only a help to the reader).

ToF-SIMS analysis of alkyl monolayers on the Si_xN_4 surface

ToF-SIMS analysis can provide direct structural information about the attachment reaction. A combined analysis of selected peaks or spectral regions[56] together with a multivariate analysis method, such as principal component analysis (PCA), can prove unambiguously the attachment of the monolayer and even yield detailed information about the nature of the chemical bonds linking the monolayer to the surface. PCA can be viewed as a tool that first "plots" a complete spectrum as a single point in a hyperspace, where a series of spectra appear as a set of points in this space. The axes of the hyperspace correspond to the spectral regions that one selects for analysis, and the distance a point is plotted along an axis is given by the peak area or areas in a particular spectral region. PCA then rotates the axes of this coordinate system to find the axis that corresponds to the largest fraction of the variation in the data. This axis is known as the first principal component (PC1). The remaining axes are then rotated to find the axis that contains the next largest fraction of the variation in the data (PC2). Higher PCs are found in a similar manner. The projections of the data points (spectra) on the PCs in the hyperspace are known as their scores. Scores plots are often valuable in revealing trends between spectra. The projections of the original axes in the hyperspace on the PCs are known

as loadings. Therefore, the loadings plot of a particular PC gives the chemical variation that corresponds to that PC.

The scores of the spectra on the first principal component (PC1), which accounts for 87.5% of the variation in the data, are plotted in Figure 7. This high percentage indicates that many of the peaks in the spectrum are highly correlated.[58] Clearly the main variation in the samples correlates with the amount of time they spent in the hot alkene. The largest variation between the spectra in PC1 occurs at short reaction times when the greatest amount of monolayer formation is expected to occur. As the reaction time progresses, the spectra appear to asymptotically approach a limiting value, which corresponds to a complete monolayer formation. A loading plot for PC1 was also generated, and the ten largest peaks from this plot are given in Table 3. These data show that samples made at longer (or shorter) times have greater contributions from the positive (or negative) peaks in the loadings plot. The positive peaks correspond to organic fragments expected from the monolayer and the negative peaks correspond to inorganic fragments expected from the substrate. These results are a strong confirmation of monolayer formation on silicon nitride during immersion in hot 1-hexadecene. That is, the spectra from samples that were immersed for longer periods of time in the 1-alkene are richer in organic fragments coming from the organic monolayer, and the spectra from samples that were immersed for shorter periods of time are richer in fragments that are expected from the substrate.

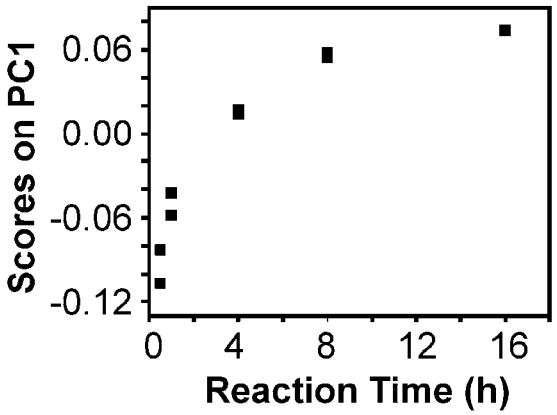

Figure 7. Scores on PC1 of TOF-SIMS positive ion spectra of 1-hexadecene-derived monolayers on silicon nitride for different reaction times.

One of the most important findings of this ToF-SIMS study is the presence of peaks that appear to contain silicon, carbon, and nitrogen, such as SiCH, $SiCH_5$, SiC_3H_9, and $SiC_3H_{13}N_3$ (Table 3).

Because of the low ion fluxes in ToF-SIMS, ion recombination above the surface is not a favored process. Therefore, the presence of fragments that contain silicon, carbon, and nitrogen, is strongly suggestive of covalent binding between alkyl chains in the monolayer and the silicon nitride substrate. While ToF-SIMS clearly points to the formation of Si–C bonds, the formation of N–C bonds can neither be proven nor disproved conclusively based on these data.

Table 3. Largest peaks from loading plots of PC1 from mean-centered positive and negative ion spectra of 1-hexadecyl monolayers on Si_xN_4 surface**.**

m/z	PC1 loadings	Species	m/z	PC1 loadings	Species
118.9918	-0.3751	$Si_3H_7N_2$ or $SiCH_3N_2O_3$	68.9942	-0.1443	$^{29}SiC_2H_2N$ or $^{30}SiC_2H_3$
43.0539	0.3664	C_3H_7	39.0225	0.1289	C_3H_3
41.0385	0.3454	C_3H_5	49.9957	-0.1087	$^{30}SiH_4O$
46.9893	-0.3231	SiH_3O	27.9772	-0.1064	Si
29.0387	0.2725	C_2H_5	119.0083	-0.0987	$SiC_3H_{13}N_3$
27.0228	0.2657	C_2H_3	44.9792	-0.0925	SiHO
99.9925	-0.2251	$Si_2CH_4N_2$	31.0193	-0.0915	CH_3O
55.0548	0.2172	C_4H_7	40.9846	0.0715	SiCH or ^{29}SiC
30.9979	-0.195	^{30}SiH	1.0078	-0.0653	H
57.0711	0.1828	C_4H_9	67.0548	0.0541	C_5H_7

Stability of organic monolayers on Si_xN_4.

(a) In air and water. The stability of alkyl monolayers was studied by exposing modified Si_xN_4 surfaces to different media: air, water, acid and alkaline solutions. The stability of these monolayers was monitored using water contact angle and IRRAS measurements. Si_xN_4 samples modified with 1-hexadecene-derived monolayers were exposed to ambient conditions in air for one week, and did not show any change in either the static water contact angle θ or the IRRAS spectrum of the samples. A decrease of only ~ 2° in θ was observed on several samples left in air under ambient conditions (including humid summer months) for five months.

The stability of 1-hexadecyl modified silicon nitride surfaces towards water was tested for different time intervals up to seven days by placing a modified substrate in water at room temperature. Over this week θ decreased gradually by ~ 2°. Analogous hot water treatment of similar samples at 60 °C at different time intervals up to 5 h caused a decrease in θ by ~ 3°, in which it was noticed that in the first 2 h there was almost no decrease. Once the contact angle starts to drop, which is indicative of growing defects in the monolayer, the decrease speeds up autocatalytically.

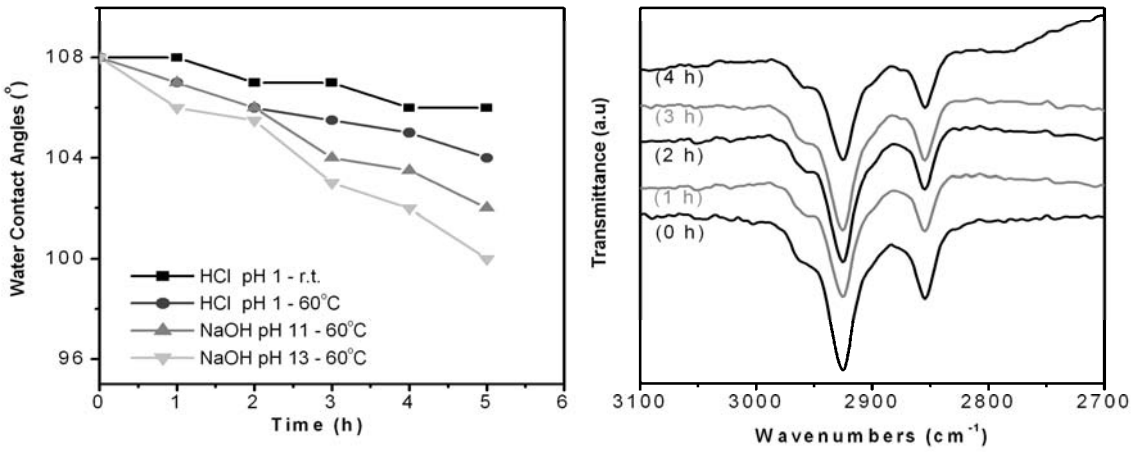

Figure 8. (left) Variation of the static water contact angle θ of 1-hexadecene-derived monolayers on Si_xN_4 upon treatment with 0.1 M HCl and NaOH solutions. (right) Changes of CH_2 stretching bands on alkyl-modified Si_xN_4 upon treatment with 0.1 M NaOH solutions for different time intervals up to 4 hrs.

(b) In acid solutions. The stability of 1-hexadecyl monolayers in acid and alkaline solutions are represented in Figure 8. The value of θ was not affected by more than 2° for up to 4 h in both cold (room temperature) and warm (60 °C) acid solutions (0.1 M HCl). Only moderate decreases of θ from 108° to 103° were observed after 20 h in a warm acid solution. 1-Hexadecyl monolayers on Si_xN_4 even partially resisted dipping in 2% HF solution in methanol for 5 min, as θ decreased with about 10° while the CH_2 stretching vibrations at 2928 and 3857 cm^{-1} could also still clearly be seen in IRRAS. In all cases, the best stability was observed for monolayers that showed the highest initial water contact angles, again indicating that monolayer removal starts at defects in the monolayer.

(c) In very alkaline solutions (pH 13). Figure 8 (right) also shows the changes in the quality of the 1-hexadecyl monolayers treated in alkaline solution. Only small changes in both θ and the IRRAS spectra were observed for up to 3 h in either cold or warm 0.1 M NaOH solution. Thereafter, the contact angle in hot alkaline solution decreased rapidly to 90°, while at room temperature the monolayer remains largely intact for ≥ 5 h ($\theta \geq 100°$). This monolayer stability compares very favorably to that of monolayers on crystalline Si, which more or less completely disappear after placement in warm 0.1 M NaOH for 100 min. The relatively high stability of alkyl monolayers attached to the Si_xN_4 surface can be attributed to the outstanding chemical stability of the silicon nitride surface itself, which is not etched away easily under these conditions, and which thus minimizes the growth of defects in the monolayer structure.

(d) In 'milder' alkaline solution (pH=11): 1-alkenes vs. 1-alkynes. Modified silicon nitride surfaces were prepared according to the improved etching procedure (HF + sonication) using 1-octadecene and 1-hexadecyne. The resulting monolayers both displayed water contact angles of 108°. Both sets of samples were then dipped in alkaline solution (pH = 11) at 60°C for different time intervals up to 4 h, and the monolayer stability was monitored via θ. The values of θ for a 1-octadecene-derived monolayer attached to the Si_xN_4 surface decreased from 108 to 102° (± 1°) after 6 h under these conditions. 1-Hexadecyne-derived monolayers showed a much higher stability, as θ only decreased from 108 to 104° (± 1) after 6 h under the same conditions, while θ was still at least 102° even after 22 h. We tentatively suggest that this implies a double bonding of 1-alkynes to the etched Si_xN_4 surface, which would require the cleavage of two covalent bonds, before a real defect in the monolayer structure can arise or be enlarged. Therefore we would expect the growth of defects, as indicated by a decrease in θ, to be significantly slowed down in the case of 1-alkyne-derived monolayers, which is as observed.

Carboxylic acid-terminated monolayers on Si_xN_4 surface

The carboxylic acid functional group is one of the most sought-after candidates as terminal group for organic monolayers, because of its chemical versatility and wetting properties. Together with the amine functionality (*vide infra*) it can be considered as the key linker group for the attachment of biomolecules.[40] We presently report two different methods for obtaining acid-terminated monolayers.

a) Chemical hydrolysis of an ester. An acid-terminated monolayer was obtained via the thermal reaction of 2,2,2-trifluoroethyl undec-10-enoate **(II)** with the H-terminated Si_xN_4 surface, followed by hydrolysis in acid medium. The IRRA spectra recorded before (Figure 9a) and after acid hydrolysis in aqueous 2 M HCl solution at 80°C (Figure 9b), give evidence for the attachment and the hydrolysis of **(II)** on Si_xN_4 surfaces. The presence of the antisymmetric/symmetric CH_2 bands in Figure 9a, at 2924/2854 cm^{-1} and the C=O band at 1735 cm^{-1} prove the formation of a covalent monolayer. However, while the surface could be further functionalized, and thus can be modified with some trifluoroester moieties, the position of this vibration is different from the vibration of the liquid compound **(II)** at 1765 cm^{-1}. We attribute this difference to the partial reaction of the activated ester with surface amine groups to form surface amides. The intensities and positions of the CH_2 stretching peak in Figure 9b are unaffected by the acid hydrolysis conditions, which indicates that the quality of the monolayer was not significantly affected by the relatively high acid concentration. The carbonyl vibration shifts to 1719 cm^{-1} corresponding to the carbonyl (C=O) stretching of the formed COOH group. The formation of the acid-terminated monolayer was also confirmed by the change of the static water contact angle from 84^o to 23^o. These data are an improvement over our previously reported basic hydrolysis, as that step more strongly influenced the monolayer quality,[63] while the current acidic procedure also yields lower contact angles (23 versus 44 degrees for the basic hydrolysis). While the use of the trifluoro ester seems to be advantageous over the use of methyl esters, near-complete deprotection is not yet achieved ($\theta \neq 0°$).

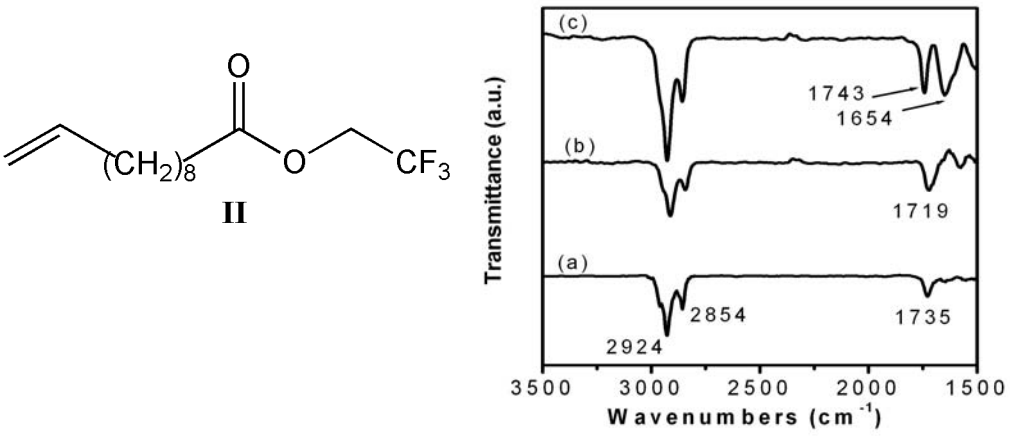

Figure 9. IRRA spectra of a Si_xN_4 wafer modified with (a) ester **II**, (b) carboxylic acid obtained after hydrolysis (2 M HCl, 2 h, 80 ºC) and the subsequently attached (c) NHS-terminated monolayer.

The attachment and hydrolysis of the trifluoroester to Si_xN_4 was further investigated with XPS. Figure 10 shows the C_{1s} and F_{1s} XPS spectra before (top) and after (bottom) hydrolysis. The C_{1s} spectrum of the ester-modified sample (top right) shows peaks at 285, 288, 289.65 and 293.9 eV, which can be assigned to the different carbons in the trifluoroethanol ester.[67] The peaks at 288 and 293.9 eV in the C_{1s} spectrum and at 689 eV in the F_{1s} spectrum indicate the covalent attachment of the trifluoroester to the Si_xN_4 surface, although the low intensity of the CF_3 peak at 293.9 eV confirms the partial disappearance (~ 50%) of the trifluoroester moiety upon monolayer formation that was observed in IRRAS. The peaks characteristic for the CF_3CH_2 moiety were removed for ~ 90% upon hydrolysis in aqueous HCl solution as clearly shown in the XPS spectra of the hydrolyzed sample. The F_{1s} spectrum also clearly points to the presence of two different fluorine binding sites, which we attribute to Si-bound F (~ 688 eV) and C-bound F (~ 691 eV).

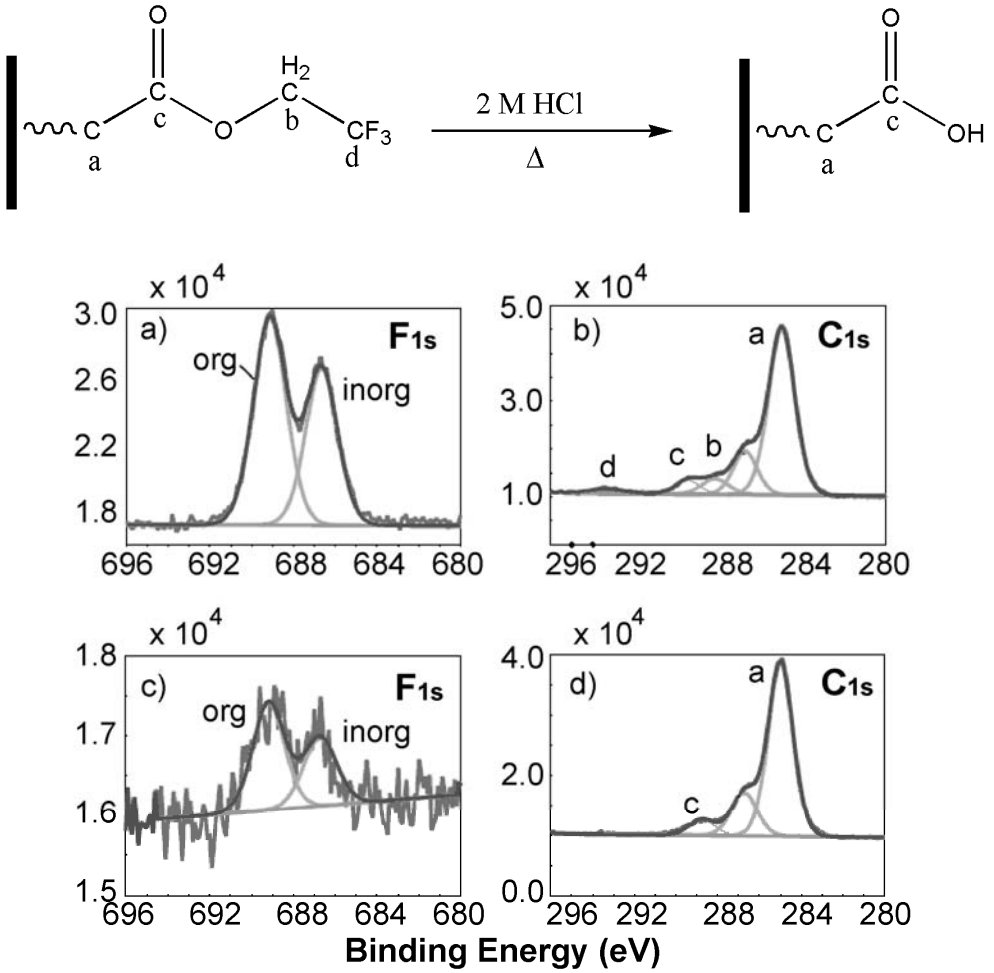

Figure 10. F_{1s} and C_{1s} XPS spectra of trifluoroethanol ester attached to a Si_xN_4 samples before (a, b) and after (c, d) hydrolysis in 2 M HCl for 2 h at 80 °C.

b) Photochemical hydrolysis of an ester. The formation of a terminal carboxylic acid under milder conditions, as compared to basic and acidic hydrolysis, can be very useful in view of the stability of the monolayers and for the formation of patterned monolayers. Therefore, we investigated the use of a light-induced deprotection. The ester **I** was thermally attached to the Si_xN_4 surface and characterized by both water contact angle (θ = 82°) and IRRAS measurements (Figure 11a). The characteristic bands due to the aromatic C=C, the aromatic C=O and the ester C=O groups appeared at 1600, 1695 and 1732 cm^{-1}, respectively.[64] The irradiation of this sample (λ = 371 nm) in ethanol for 20 h at room temperature lead to the formation of a more hydrophilic surface (θ = 34°) and to the disappearance of the aromatic carbonyl band (1695 cm^{-1}) and the aromatic C=C band (1600 cm^{-1}). While the contact angles are not as low as obtained with the acid hydrolysis (θ = 23°), the mild conditions of this photochemical deprotection make it a very valuable additional tool in the formation of acid-functionalized surfaces.

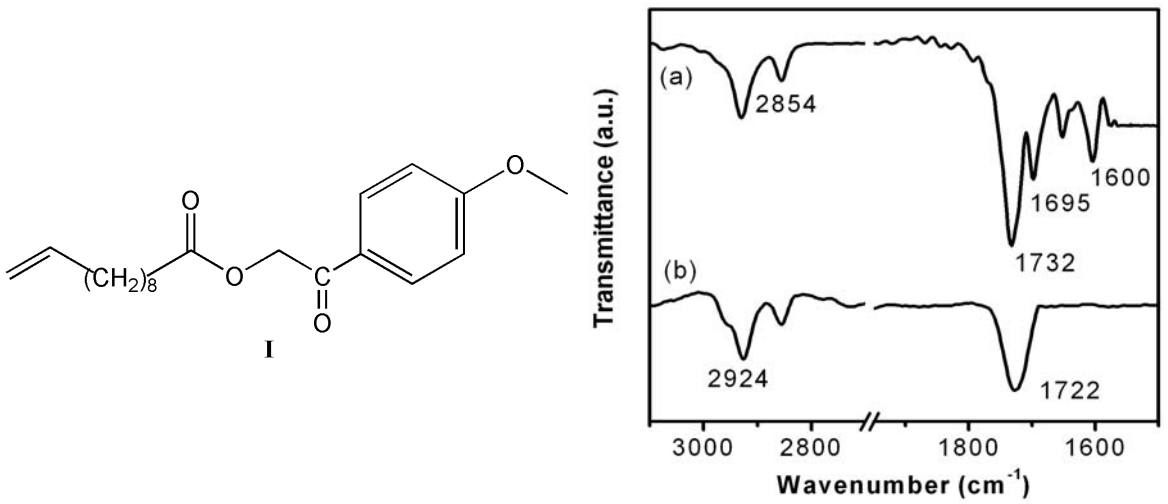

Figure 11. (a) IRRA spectra of ester **(I)** attached to Si_xN_4 and (b) the same sample after irradiation in absolute ethanol (λ = 371 nm) for 20 h.

Bio-activation: formation of NHS-esters and their reaction with octylamine

The presence of free carboxylic acid was also demonstrated by carrying out further reactions. The chemical activation of the acid function with N-hydroxy succinimide (NHS) was used to prepare surface-bound NHS-activated esters.[40]

$$Si_xN_4—C_{10}H_{20}COOH + NHS/EDC \xrightarrow{r.t., 1h} Si_xN_4—C_{10}H_{20}COONHS$$

Figure 9c represents an IRRA spectrum of an acid-terminated surface that was chemically activated with aqueous NHS/EDC for 1 h at room temperature. It shows the complete disappearance of the peak due to the acid-terminated surface at 1720 cm^{-1}, while the appearance of the new peaks at 1743 cm^{-1} can be assigned to the NHS ester. These results are consistent with a hydrosilylation reaction mainly taking place at the carbon-carbon double bond. The availability of the NHS groups on the surface was demonstrated by reaction of the NHS-terminated surface with *n*-octylamine. Figure 12a displays the IRRA spectrum measured on a Si_xN_4 samples after reaction of the surface NHS ester with *n*-octylamine. The figure shows the disappearance of the NHS ester (characteristic peaks at 1743 cm^{-1}; see Figure 9c), and the appearance of new peaks at 1665 and 1565 cm^{-1}, assigned to the NH-C=O groups. An additional peak at 3330 cm^{-1} is also observed and attributed to an N–H stretching vibration.

$$Si_xN_4\text{—}C_{10}H_{20}COONHS + C_8H_{17}\text{-}NH_2 \xrightarrow[1\text{-}2\ h]{r.t.} Si_xN_4\text{—}C_{10}H_{20}CONH\text{-}C_8H_{17}$$

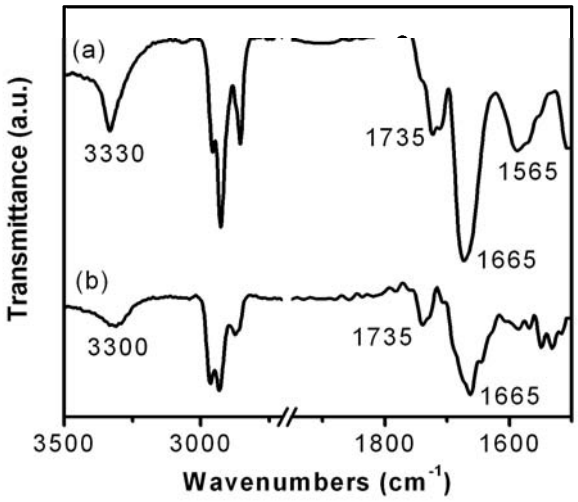

Figure 12. IRRA spectra of the NHS-modified Si_xN_4 surface modified after (a) reaction with *n*-octylamine, and (b) with bovine milk *κ*-casein.

Attachment of proteins

Figure 12b shows an IRRA spectrum recorded on a NHS-modified Si_xN_4 sample after reaction with a protein, in this case bovine milk *κ*-casein. The IRRA spectrum indicates that the amount of carbonyl and methylene groups significantly increased after reaction. The attachment of the protein to the surface was further detected by the in-growing NH_2 band at

3300 cm^{-1}. Figure 13 (left) shows the AFM height image of a sample with *κ*-casein attached to the surface. The protein layer seems to be relatively structured with protein globules. Reflectometry measurements (Figure 13, right) showed that the amount of protein near the surface increases until after ~ 2.5 min of exposure to the protein solution. Upon subsequent rinsing with buffer, only a small fraction of the protein (~ 25%) was removed, which is in line with a substantial covalent attachment, next to irreversible protein adsorption that will definitively also contribute to the total amount of attached protein. A tight binding was also confirmed by a washing with 0.5 M dodecylbenzene sulfonate solution, as this resulted in no additional loss of κ-casein.

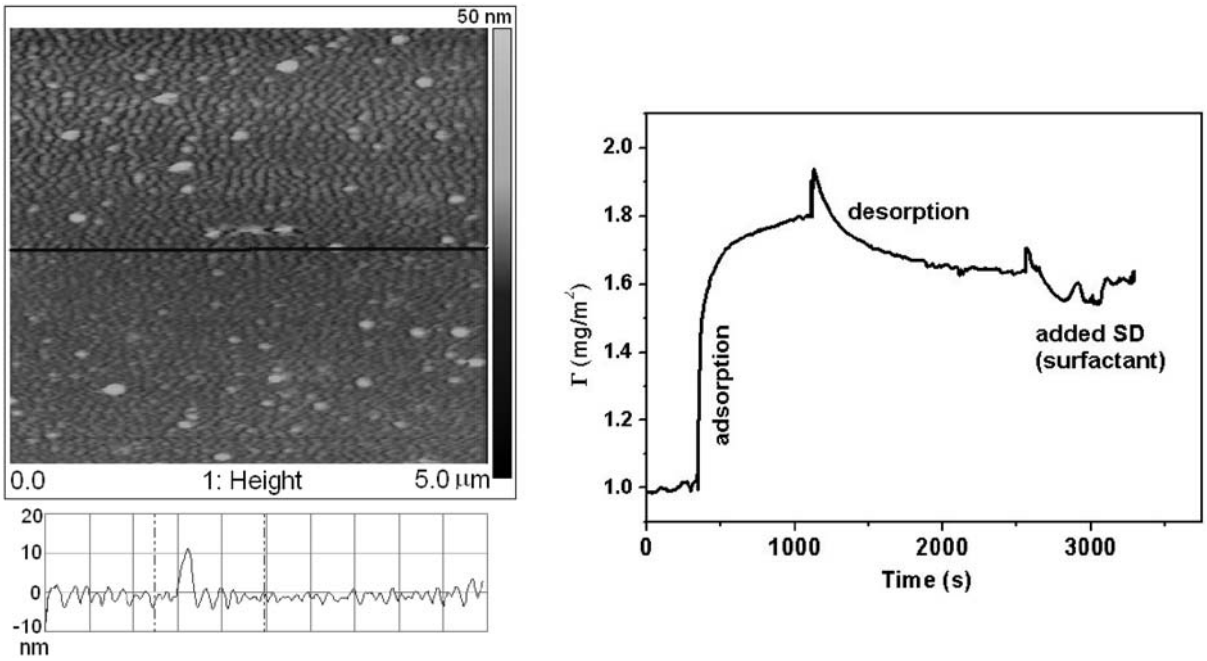

Figure 13. (left) AFM image and section analysis of a NHS-modified Si_xN_4 sample after reaction with *κ*-casein. (right) Adsorption-desorption isotherm of *κ*-casein on NHS-terminated Si_xN_4 surface.

Attachment of oligopeptides

Figure 14 presents the IRRA spectrum recorded on a NHS-functionalized Si_xN_4 sample after reaction with diamino-acid aspartame **(IV)**. A strong C=O band appears at 1744 cm^{-1}, which indicates the successful attachment of the aspartame molecule to the monolayer. The spectrum is also characterized by the high intensity of the antisymmetric and symmetric CH_2 bands at 2925 and 2854 cm^{-1}, respectively. A characteristic sharp NH stretching band appears

at 3328 cm^{-1}. These peaks strongly indicate the covalent attachment of the aspartame molecule to the NHS-functionalized Si_xN_4 surface, to form a super-sweet monolayer.

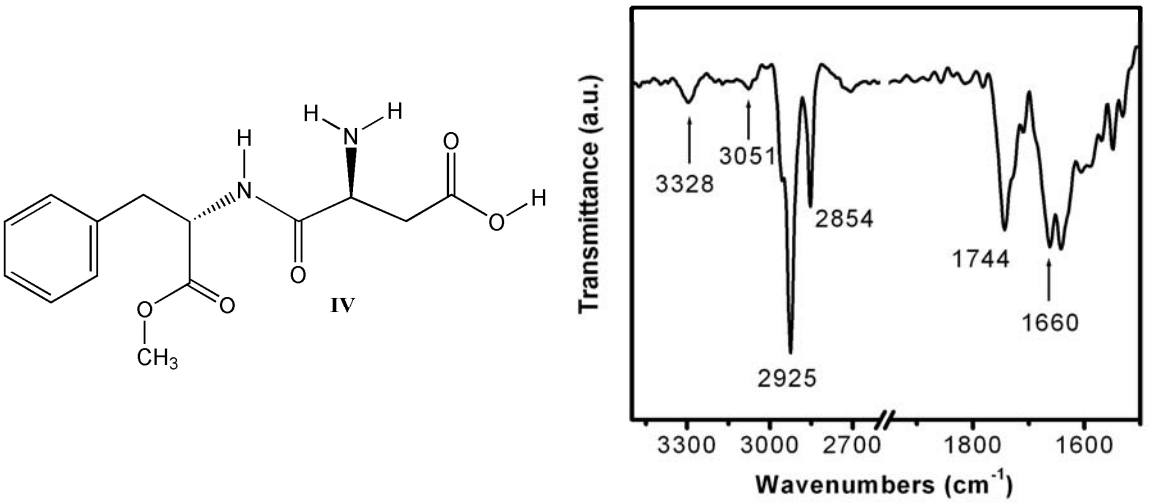

Figure 14. IRRA spectrum of NHS-functionalized Si_xN_4 reacted with aspartame at room temperature.

Amino-terminated monolayers

Mixed monolayers with different surface densities of amino groups can be prepared by using mixtures of the protected amine derivative *N*-(ω-undecylenyl)-phtalimide **(III)** and 1-decene **(C10)** in the surface modification of Si_xN_4. Two different **C10** : **III** ratios were used (1:1 and 2:1) in the thermal reaction with HF-treated Si_xN_4. As previously reported,[48] incorporation of the phtalimide group to the surface is expected to lower the water contact angle of the modified sample. This was indeed observed: contact angles of 84^o and 86^o were obtained for **C10** : **III** ratios of 1:1 and 2:1, respectively. Similar results were reported for mixed monolayers on silicon,[65] and oxidized silicon surfaces.[66] The incorporation of a higher percentage of **III** in the monolayer decreased the contact angles, which can be attributed to both the polarity of the phthalimide group and the increased disorder –partially by steric effects of the bulky phthalimide group[48]– upon increase of the relative amount of phthalimide groups.

The IRRA spectra of the carbonyl group and the C–H regions of the 2:1 monolayer of **C10** and **III** are shown in Figure 15. The C=O vibration of the phthalimide group is clearly visible at 1715 cm^{-1} in the spectrum of the as prepared monolayer (Figure 15a). The maxima of the

methylene C–H stretching vibrations are visible at 2925 and 2854 cm^{-1}, values that are somewhat higher than those of a monolayer of a pure **C10**-modified Si_xN_4 surface (2923 and 2853 cm^{-1}). This again indicates that this mixed monolayer of **C10** and **III** is not as ordered as those of neat 1-alkenes. No frequency change in either the CH_2 or C=O stretching vibrations was observed when **C10** / **I** ratios increased from 1 : 1 to 2 : 1.

The phthalimide-containing monolayers were deprotected by reaction with hydrazine hydrate for two days, to form amino-terminated monolayers. After the monolayer was reacted with the hydrazine solution, the C=O vibration disappeared completely (Figure 15b). In addition, a small peak around 3300 cm^{-1} appeared, while the water contact angle dropped significantly upon deprotection, from 84° to 57°. This value approaches that of monolayers that are fully terminated with NH_2 groups.[67,68]

These observations confirm that phthalimide groups have been removed by conversion into amine groups via reaction with hydrazine. In contrast to observations during the deprotection reaction on silicon surfaces,[48] the peaks for the methylene vibrations have in the current case changed towards more ordered monolayers (2923 and 2852 cm^{-1}). The increase in the ordering of the monolayer was achieved by the removal of the bulky phthalimide group.

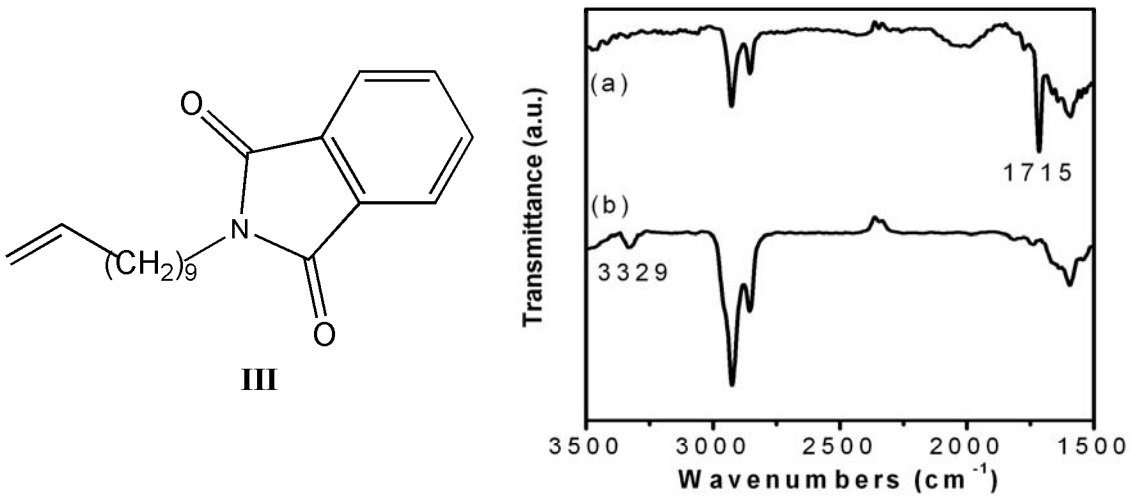

Figure 15. IRRA spectra showing the C=O and CH_2 regions of Si_xN_4 samples modified with 1-decene and phthalimide **III** (ratio 2 : 1) before (a), and after (b) deprotection with hydrazine hydrate for 2 days.

Conclusions

Silicon nitride surfaces can be successfully modified via a thermal covalent attachment of organic monolayers of 1-alkenes and 1-alkynes. HF treatment in combination with sonication provides a smooth silicon nitride surface and the resulting monolayers are of good quality: the water contact angle for alkyl monolayers is up to 108°. This is slightly lower than measured on e.g. Si surfaces, due to the chemical heterogeneity of silicon nitride surfaces, which contain both reactive Si–H and N–H sites, and their increased roughness. Both XPS and ToF-SIMS data point to the formation of Si–C bonds, while the involvement of N–C bonds can be neither really proven nor disproved based on our data.

The resulting monolayers have two important characteristics. First, they are far more stable than any corresponding monolayer on silicon, silicon oxide, or gold under both acidic and alkaline conditions. Second, they can be functionalized at will, as was shown by the formation of monolayers with –COOH and $–NH_2$ moieties, and the attachment of oligopeptides and proteins onto such monolayers via standard coupling techniques. Given the complementary properties of silicon nitride (insulator, very robust) in comparison to either silicon, silicon oxide or gold, this reveals the wide potential of such monolayers.

Acknowledgments.

We thank graduate school VLAG for funding of a graduate student position to M. R. and a postdoctoral fellowship to A. A.

References

(1) Patil, L. S.; Pandey, R. K.; Bang, J. P.; Gaikwad, S. A.; Gautam, D. K. *Opt. Mater.* **2005,** *27*, 663-670.

(2) Bermudez, V. M.; Perkins, F. K. *Appl. Surf. Sci.* **2004,** *235*, 406-419.

(3) Antsiferov, V. N.; V. G. Gilev, V. G.; Karmanov, V. I. *Refract. Ind. Ceram*$^{+}$ **2003,** *44*, 108-114.

(4) Rathi, V. K.; Gupta, M.; Agnihotri, O. P. *Microelectron. J.* **1995,** *26*, 563-567.

(5) Wong, J. S.; Yen, Y.-S. *Appl. Spectrosc.* **1988,** *42*, 598-604.

(6) Van Rijn, C. J. M.; Nijdam, W.; Kuiper, S.; Veldhuis, G. J.; van Wolferen, H.; Elwenspoek, M. *J. Micromechan. Microeng.* **1999,** *9*, 170-172.

(7) Van Rijn, C. J. M.; Veldhuis, G. J.; Kuiper, S. *Nanotechnology* **1998,** *9*, 343-345.

(8) Van Rijn, C. J. M. *Nano and Micro Engineered Membrane Technology*. Aquamarijn Research BV, The Netherlands: 2002.

(9) Kuiper, S.; van Wolferen, H.; van Rijn, G.; Nijdam, W.; Krijnen, G.; Elwenspoek, M. *J. Micromech. Microeng.* **2001,** *11*, 33-37.

(10) Kölbel, M.; Tjerkstra, R. W.; Kim, G.; Brugger, J.; van Rijn, C. J. M.; Nijdam, W.; Huskens, J.; Reinhoudt, D. N. *Adv. Funct. Mat.* **2003,** *13*, 219.

(11) Ren, S.; Yang, S.; Zhao, Y. *Langmuir* **2003,** *19*, 2763-2767.

(12) Tsukruk, V. V.; Bliznyuk, V. N. *Langmuir* **1998,** *14*, 446-455.

(13) Qian, L. M.; Xiao, X. D.; Wen, S. Z. *Langmuir* **2000,** *16*, 662-670.

(14) Gao, H.; Luginbuhl, R.; Sigrist, H. *Sensor Actuator B* **1997,** *38*, 38.

(15) Girones, M.; Borneman, Z.; Lammertink, R. G. H.; Wessling, M. *J. Membrane Sci.* **2005,** *259*, 55-64.

(16) Brans, G.; Kromkamp, J.; Pek, N.; Gielen, J.; Heck, J.; Rijn, C. J. M. v.; Sman, R. G. M. v. d.; Schroën, C. G. P. H.; Boom, R. M. *J. Membrane Sci.* **2006,** *In Press*.

(17) Sieval, A. B.; Optiz, R.; Maas, H. P. A.; Schoeman, M. G.; Meijer, G.; Vergeldt, F. J.; Zuilhof, H.; Sudhölter, E. J. R. *Langmuir* **2000**, 10359-10368.

(18) Sieval, A. B.; Demirel, A. L.; Nissink, J. W. M.; Linford, M. R.; van der Maas, J. H.; de Jeu, W. H.; Zuilhof, H.; Sudhölter, E. J. R. *Langmuir* **1998,** *14*, 1759-1768.

(19) Sieval, A. B.; Vleeming, V.; Zuilhof, H.; Sudhölter, E. J. R. *Langmuir* **1999,** *15*, 8288-8291.

(20) Sieval, A. B.; Linke, R.; Zuilhof, H.; Sudhölter, E. J. R. *Adv. Mater.* **2000,** *12*, 1457-1460.

(21) Reed, M. A.; Zhou, C.; Muller, C. J.; Burgin, T. P.; Tour, J. M. *Science* **1997,** *278*, 252-254.

(22) Zhou, C.; Deshpande, M. R.; Reed, M. A.; Jones, L.; Tour, J. M. *Appl. Phys. Lett.* **1997,** *71*, 611-613.

(23) Tsuzuki, H.; Watanabe, T.; Okawa, Y.; Yoshida, S.; Yano, S.; Koumoto, K.; Komiyama, M.; Nihei, Y. *Chem. Lett.* **1988**, 1265-1268.

(24) Watanabe, T.; Okawa, Y.; Tsuzuki, H.; Yoshida, S.; Nihei, Y. *Chem. Lett.* **1988**, 1183-1186.

(25) Evoy, S.; Carr, D. W.; Sekaric, L.; Olkhovets, A.; Parpia, J. M.; Craighead, H. G. *J. Appl. Phys.* **1999,** *86*, 6072-6077.

(26) Knapp, H. F.; Stemmer, A. *Surf. Interface Anal.* **1999,** *27*, 324-331.

(27) Linford, M. R.; Chidsey, C. E. D. *J. Am. Chem. Soc.* **1993,** *115*, 12631-12632.

(28) Linford, M. R.; Fenter, P.; Eisenberger, P. M.; Chidsey, C. E. D. *J. Am. Chem. Soc.* **1995,** *117*, 3145-3155.

(29) Sieval, A. B.; van den Hout, B.; Zuilhof, H.; Sudhölter, E. J. R. *Langmuir* **2001,** *17*, 2172-2181.

(30) Cicero, R. L.; Linford, M. R.; Chidsey, C. E. D. *Langmuir* **2000,** *16*, 5688-5695.

(31) Effenberger, F.; Gotz, G.; Bidlingmaier, B.; Wezstein, M. *Angew. Chem. Int. Ed.* **1998,** *37*, 2462-2464.

(32) Allongue, P.; de Villeneuve, C. H.; Pinson, J.; Ozanam, F.; Chazalviel, J. N.; Wallart, X. *Electrochimica Acta* **1998,** *43*, 2791-2798.

(33) De Villeneuve, C. H.; Pinson, J.; Bernard, M. C.; Allongue, P. *J. Phys. Chem. B* **1997,** *101*, 2415-2420.

(34) Robins, E. G.; Stewart, M. P.; Buriak, J. M. *Chem. Commun.* **1999**, 2479-2480.

(35) Buriak, J. M. *Chem. Rev.* **2002,** *102*, 1271-1308.

(36) Buriak, J. M.; Stewart, M. P.; Geders, T. W.; Allen, M. J.; Choi, H. C.; Smith, J.; Raftery, D.; Canham, L. T. *J. Am. Chem. Soc.* **1999,** *121*, 11491-11502.

(37) Holland, J. M.; Stewart, M. P.; Allen, M. J.; Buriak, J. M. *J. Solid State Chem.* **1999,** *147*, 251-258.

(38) Sun, Q.-Y.; de Smet, L. C. P. M.; van Lagen, B.; Giesbers, M.; Thune, P. C.; van Engelenburg, J.; de Wolf, F. A.; Zuilhof, H.; Sudhölter, E. J. R. *J. Am. Chem. Soc.* **2005,** *127*, 2514-2523.

(39) Pike, A. R.; Lie, L. H.; Eagling, R. A.; Ryder, L. C.; Patole, S. N.; Connolly, B. A.; Horrocks, B. R.; Houlton, A. *Angew. Chem. Int. Ed.* **2002,** *41*, 615.

(40) Voicu, R.; Boukherroub, R.; Bartzoka, V.; Ward, T.; Wojtyk, J.; Wayner, D. *Langmuir* **2004,** *20*, 11713-11720.

(41) De Smet, L. C. P. M.; Stork, G. A.; Hurenkamp, G. H. F.; Sun, Q.-Y.; Topal, H.; Vronen, P. J. E.; Sieval, A. B.; Wright, A.; Visser, G. M.; Zuilhof, H.; Sudhölter, E. J. R. *J. Am. Chem. Soc.* **2003,** *125*, 13916.

(42) Pignataro, B.; Grasso, G.; Renna, L.; Marletta, G. *Surf. Interf. Anal.* **2002,** *33*, 54-58.

(43) Cricenti, A.; Longo, G.; Luce, M.; Generosi, R.; Perfetti, P.; Vobornik, D.; Margaritondo, G.; Thielen, P.; Sanghera, J. S.; Aggarwal, I. D.; Miller, J. K.; Tolk, N. H.; Piston, D. W.; Cattaruzza, F.; Flamini, A.; Prosperi, T.; Mezzi, A. *Surf. Sci.* **2003,** *544*, 51-57.

(44) Cattaruzza, F.; Cricenti, A.; Flamini, A.; Girasole, M.; Longo, G.; Mezzi, A.; Prosperi, T. *J. Mat. Chem.* **2004,** *14*, 1461-1468.

(45) Arafat, A.; Schroën, K.; de Smet, L. C. P. M.; Sudhölter, E. J. R.; Zuilhof, H. *J. Am. Chem. Soc.* **2004,** *126*, 8600-8601.

(46) Manning, M.; Redmond, G. *Langmuir* **2005,** *21*, 395-402.

(47) Sun, Q.-Y.; de Smet, L. C. P. M.; van Lagen, B.; Wright, A.; Zuilhof, H.; Sudhölter, E. J. R. *Angew. Chem. Int. Ed.* **2004,** *43*, 1352-1355.

(48) Sieval, A. B.; Linke, R.; Heij, G.; Meijer, G.; Zuilhof, H.; Sudhölter, E. J. R. *Langmuir* **2001,** *17*, 7554-7559.

(49) Hicks, S.; Murad, S.; Sturrock, I.; Wilkinson, C. *Microelectron. Eng.* **1997,** *35*, 41-44.

(50) Jeffery, G. H.; Bassett, J.; Mendham, J.; Denney, R. C. *Vogel's Textbook of Quantitative Chemical Analysis*. 5th ed.; John Wiley & Sons Inc 1989.

(51) Dijt, J. C.; Stuart, M. A. C.; Hofman, J. E.; Fleer, G. J. *Coll. Surf.* **1990,** *51*, 141-158.

(52) *ToF-SIMS. Surface Analysis by Mass Spectrometry*. IM Publications: Huddersfield, UK, 2001.

(53) Graham, D. J.; Ratner, B. D. *Langmuir* **2002,** *18*, 5861-5868.

(54) Wagner, M. S.; Pasche, S.; Castner, D. G.; Textor, M. *Anal. Chem.* **2004,** *76*, 1483-1492.

(55) Wang, H.; Castner, D. G.; Ratner, B. D.; Jiang, S. *Langmuir* **2004,** *20*, 1877-1887.

(56) Belu, A. M.; Graham, D. J.; Castner, D. G. *Biomaterials* **2003,** *24*, 3635-3653.

(57) Lua, Y. Y.; Fillmore, W. J. J.; Linford, M. R. *Appl. Surf. Sci.* **2004,** *231-2*, 323-327.

(58) Yang, L.; Lua, Y. Y.; Jiang, G. L.; Tyler, B. J.; Linford, M. R. *Anal. Chem.* **2005,** *77*, 4654-4661.

(59) Bermudez, V. M. *Surf. Sci.* **2005,** *579*, 11-20.

(60) Beshkov, G.; Shi Lei; Lazarova, V.; Nedev, N.; Georgiev, S. S. *Vacuum* **2003,** *69*, 301-305.

(61) Bermudez, V. M. *J. Electrochem. Soc.* **2005,** *152*, F31-F36.

(62) Knotter, D. M.; Denteneer, T. J. J. *J. Electrochem. Soc.* **2001,** *148*, F43-F46.

(63) Liu, Y. J.; Navasero, N. M.; Yu, H. Z. *Langmuir* **2004,** *20*, 4039-4050.

(64) Socrates, G. *Infrared Characteristic Group Frequencies: Tables and Charts*. John Wiley & Sons: Brunel, The University of West London, Middlesex, UK, 2004.

(65) Sieval, A. B.; Linke, R.; Heij, G.; Meijer, G.; Zuilhof, H.; Sudholter, E. J. R. *Langmuir* **2001,** *17*, 7554-7559.

(66) Heid, S.; Effenberger, F. *Langmuir* **1996,** *12*, 2118-2120.

(67) Balachander, N.; Sukenik, C. N. *Langmuir* **1990,** *6*, 1621-1627.

(68) Heise, A.; Menzel, H.; Yim, H.; Foster, M. D.; Wieringa, R. H.; Schouten, A. J.; Erb, V.; Stamm, M. *Langmuir* **1997,** *13*, 723-728.

Chapter 5

Covalent Attachment of Organic Monolayers to Silicon Carbide Surfaces

This work presents the first covalently bound alkyl monolayers on HF-treated silicon carbide surfaces (SiC) through thermal reaction with 1-alkenes. Treatment of SiC with diluted aqueous HF solutions removes the native oxide layer (SiO_2) and provides a reactive hydroxyl-covered surface. Very hydrophobic methyl-terminated surfaces (water contact angle $\theta = 107°$) were obtained on flat SiC, whereas attachment of ω-functionalized 1-alkenes also yields well-defined functionalized surfaces. Infrared reflection absorption spectroscopy (IRRAS), ellipsometry and X-ray photoelectron spectroscopy (XPS) measurements were used to characterize the monolayers and show their covalent attachment. The resulting surfaces were extremely stable under harsh acidic conditions (e.g., no change in θ after 4 hrs in 2 M HCl at 90 °C), while their stability in alkaline conditions (pH = 11, 60 °C) also superseded that of analogous monolayers such as those on Au, Si and SiO_2. These results are very promising for applications involving functionalized silicon carbide.

This chapter is published as:
"*Covalent attachment of organic monolayers to silicon carbide surfaces*", Rosso, M.; Arafat, A.; Schroën, K.; Giesbers, M.; Roper, C. S.; Maboudian, R.; Zuilhof, H. *Langmuir* **2008,** *24*, 4007-4012.

Introduction

The modification of inorganic surfaces with covalently bound organic monolayers is an attractive and rapidly expanding research area from both fundamental and applied perspectives.[1] Well-known examples include monolayers of alkyl thiols onto gold surfaces,[2] of alkyl chlorosilanes onto silica surfaces,[3] and of alkenes and alkynes onto silicon[1,4-11] and germanium.[1,12] One of the major challenges in this area is the stable surface functionalization of mechanically and physicochemically robust materials. A few groups have succeeded in the covalent attachment of organic monolayers on diamond,[13-15] and amorphous carbon surfaces.[16-19] In the same direction, we recently reported on the modification of silicon nitride with covalently attached, highly stable functionalized monolayers.[20,21] To further expand the modification of mechanically robust and chemically stable materials, we explore in the current work the functionalization of silicon carbide (SiC) surfaces. This semiconducting material is mechanically extremely hard (Mohr's index = 9) with a large energy band-gap (2.3 to 3.2 eV, depending on the crystalline polytype). Because of these properties, SiC has been pursued for high-power, high-voltage applications, and for sensing in harsh environments.[22,23] The recent development of a method to obtain single-crystalline SiC with a low density of defects promises to further expand the application base for this material.[24] In addition, well-controlled use of poly-crystalline 3C-SiC has made it possible to measure zeptogram (10-21 g) quantities of material. These results open up the opportunity to extremely sensitive biosensors[25] if functionalization with specific recognition moieties would be feasible. Some theoretical studies have been reported on the chemisorption of organic molecules onto clean or hydroxylated SiC surfaces,[26,27] which show the potential of this material to form hybrid structures for biotechnological applications. This is of interest, since the biocompatibility of SiC itself allows its use in medical applications, for instance as a supporting material of bioactive layers for sensing, or as a passivation coating for prosthesis or microelectrodes.[28-32]

The current paper presents the first example of the covalent functionalization of SiC with alkyl monolayers, in analogy to organic monolayers on Si, Si_xN_4, and Ge. However, the surface chemistry of SiC leads to a different bonding of the monolayers, as indicated by X-ray photo-electron spectroscopy (XPS), infrared reflection absorption spectroscopy (IRRAS) and the analogy of reactions with organosilanes, which are all discussed in detail below. Finally, ester-terminated SiC surfaces were also prepared by this method, as they are one of the most

potent functionalities for further (bio-) functionalizations, via hydrolysis and formation of activated esters.[2,33]

Experimental Section

Materials

1-Decene (> 97%), 1-dodecene (> 99%), 1-tetradecene (> 97%), 1-hexadecene (99%), and methyl 10-undecenoate (96%) were purchased from Sigma-Aldrich and distilled twice under reduced pressure before use. 1-Octadecene (> 95%, Sigma-Aldrich) and 1-docosene (> 99%, TCI Europe) were recrystalized twice at 4 ºC in ethyl acetate with ethanol as anti-solvent. 2,2,2-Trifluoroethyl 10-undecenoate[34] and 11-fluoroundecene[8] were synthesized as described elsewhere.

Monolayer Formation

Three different types of SiC surfaces were investigated, namely polished Si-rich and C-rich faces of 6H-SiC substrate from TDI USA, and polycrystalline 3C-SiC films (thickness of 250 nm) obtained by chemical vapor deposition on Si(100).[35] Overall, polished 6H-SiC surfaces (both C-face and Si-face) gave similar results to the polycrystalline 3C-SiC (poly-SiC) films, hence only the latter is discussed here. With the exception of contact angle data depicted in Figure 4, all data reported were obtained on poly-SiC samples with a root-mean-square roughness of < 1 nm. SiC samples (1×1 cm^2 or 3×1.5 cm^2 for IRRAS) were cleaned first by sonication in acetone, followed by oxidation in air-based plasma for 10 min and wet-etching of the native oxide with a 2.5% solution of HF for 2 min. Right after this step, wafers were placed into heated neat alkenes at 130 ºC under argon atmosphere, and left to react for at least 6 h. After this time, samples were removed and rinsed several times with petroleum ether, ethanol and dichloromethane, and sonicated in the same solvents.

Monolayer Characterization

Static Water Contact Angle

Silicon carbide surfaces were characterized by static water contact angle measurements performed using an Erma Contact Angle Meter G-1 (volume of the drop of demineralized water = 3.5 μl).

X-ray Photoelectron Spectroscopy (XPS)

The XPS analysis was performed using a JPS-9200 Photoelectron Spectrometer (JEOL, Japan). The high-resolution spectra were obtained under UHV conditions using monochromatic Al K_α X-ray radiation at 12 kV and 25 mA, with an analyzer pass energy of 10 eV. High-resolution spectra were corrected using a linear background subtraction before any peak deconvolution.

Fourier Transform Infrared Reflection Absorption Spectroscopy (FT-IRRAS)

Spectra were obtained with a Bruker Tensor 27 FT-IR spectrometer, using a commercial variable-angle reflection unit (Auto Seagull, Harrick Scientific). A Harrick grid polarizer was installed in front of the detector, and was used for measuring spectra with p-polarized (parallel) radiation with respect to the plane of incidence at the sample surface. Single channel transmittance spectra were collected using a spectral resolution of 4 cm^{-1} and 1024 scans in each measurement. The optimal angle for data collection was found to be 68º; hence, all the reported measurements were performed at this angle. The raw data were divided by the data recorded on a plasma-oxidized reference SiC, to give the reported spectra.

Ellipsometry

Ellipsometric thickness measurements were performed on poly-SiC samples with a computer-controlled null-ellipsometer (Sentech SE-400) using a He-Ne laser (λ = 632.8 nm) and an incident angle of 70º. The mode 'polarizer + retarder, aperture, strict' was used. The layer thickness was determined using a three-layer model in the ellipsometry software from Sentech. Values of 3.85 and 0.02 were used for the refractive index (n) and the imaginary refractive index (k) of silicon, respectively. Refractive index values of 2.64 and 1.46 were used for silicon carbide[36] and organic monolayers,[5] respectively.

Atomic force microscopy (AFM)

Images were obtained with an MFP-3D AFM from Asylum Research (Santa Barbara, CA). Imaging was performed in AC mode in air using OMCL-AC240 silicon cantilevers (Olympus Corporation, Japan), and was mainly used for assessing the surface roughness and the cleanliness after modification.

Results and Discussion

Attachment of covalently bound organic monolayers onto SiC (vide infra) required a pre-treatment that provided the surface of this material with a reproducible reactivity. This pre-treatment involved cleaning of as-received SiC with organic solvents, subsequent oxidation by air plasma, and wet etching in 2.5% aqueous HF solution. The XPS wide scans after these two last steps (Figure 1, a and d), obtained with minimal exposure to air, show the significant decrease of the O_{1s} signal upon etching, relative to the silicon and carbon signals, while a small amount of fluorine is observed after exposure to HF. The removal of the native oxide is also seen on the high-resolution scan of the Si_{2p} region (Figure 1b, and e). The SiO_2 layer on top of the SiC substrate can be observed at 103 eV, while the two components of Si_{2p} in SiC can be resolved at 101.1 and 100.4 eV. Upon wet etching in HF, the peak at 103 eV disappeared completely, to be replaced with a small peak at 101.8 eV, indicating a small amount of Si singly bound to oxygen. The disappearance of the electrically insulating SiO_2 layer also becomes apparent from the significant increase in the XPS signal, which manifests as a significant improvement in the signal/noise ratio (compare Figure 1b, and 1c with 1e, and 1f, respectively). The high-resolution C_{1s} region (Figure 1c, and f) also shows intermediary oxidation states of carbon via the wide shoulder at 283.8 eV: the relatively large width at half maximum of this peak (1.5 eV, instead of 0.9 eV) indicates that it consists of partially overlapping peaks, likely due to C–C, Si–C–O, C–O and C=O species.[37,38] This etching method was reported to leave silicon carbide surfaces terminated with a thin silicon oxycarbide layer with terminal -OH groups.[22,39-42] Removal of the hydroxylic groups would require exposure to pure hydrogen under UHV conditions,[43,44] treatment with HCl/HF followed by hydrogen plasma treatment at elevated temperatures,[45] or heating to temperatures exceeding 1000 ºC.[46,47] This -OH termination was confirmed by measurement of the water contact angle (θ), which was still close to 0º after the HF etching.

The availability of the surface hydroxyl group for subsequent chemical reactions was investigated by immersing an etched wafer in a solution of octadecyl chlorosilane in toluene for 1h. A hydrophobic monolayer was indeed formed (static water contact angle of 111º), which remained stable upon sonication in toluene. However, an exposure to 2.5% HF solution removed this monolayer after 10 min (water contact angle < 40º).

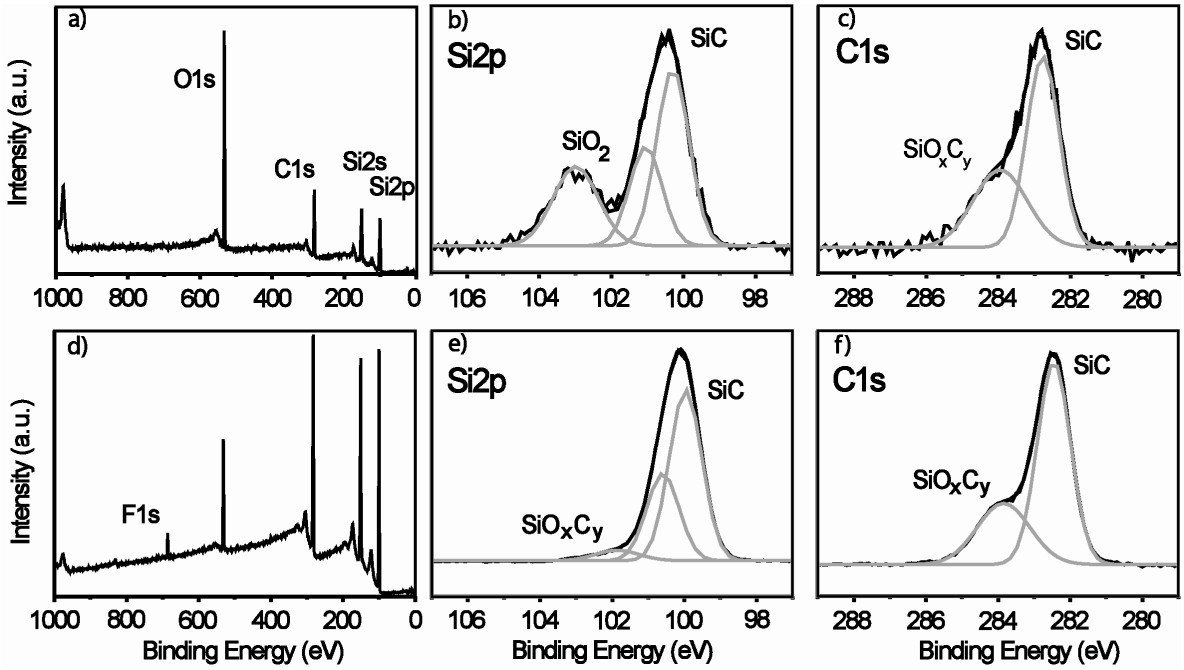

Figure 1. XPS data measured on plasma-oxidized SiC (1a, 1b, and 1c) and HF-etched SiC (1d, 1e and 1f), respectively wide scan, Si2p and C1s regions.

The –OH terminated SiC surface was modified with various alkyl monolayers by immersing them into neat 1-alkenes under an argon atmosphere for at least 6 hrs, at a temperature of 130 ºC. The surface wettability, measured via the water contact angle was a rapid indicator for the quality of alkyl-terminated surfaces. Table 1 presents the static water contact angles measured on SiC wafers after monolayer formation with several 1-alkenes. These values did not change upon sonication of modified wafers in petroleum ether and dichloromethane.

Table 1. Static water contact angle values for monolayers formed on poly-SiC, for alkenes with different chain lengths.

Alkenes	Water contact angle, on poly-SiC (± 1º)
CH_2=CH-C_8H_{17}	95
CH_2=CH-$C_{10}H_{21}$	101
CH_2=CH-$C_{12}H_{25}$	106
CH_2=CH-$C_{14}H_{29}$	106
CH_2=CH-$C_{16}H_{33}$	107
CH_2=CH-$C_{20}H_{41}$	105

The high water contact angle values obtained show the formation of hydrophobic monolayers, with an optimal value for alkyl chains containing at least 14 carbon atoms. These contact angle values approach those obtained for highly packed monolayers, such as thiol monolayers on gold or alkene monolayers on H-terminated silicon.

To support the covalent attachment of alkyl monolayers on SiC surfaces, IRRAS measurements were carried out on crystalline 6H-SiC samples and poly-SiC samples modified with a hexadecyl monolayer (Figure 2). The C–H stretching area shows a CH_3 stretching band at 2957 cm^{-1}, and antisymmetric and symmetric stretching bands of CH_2 at 2925 and 2854 cm^{-1}, respectively, independent of whether flat poly-SiC or the much rougher crystalline SiC was used. Such values are characteristics of disordered monolayers, in contrast with values for closely packed monolayers observed on crystalline Si (2920 and 2850 cm^{-1} for antisymmetric and symmetric CH_2 stretching, respectively).[48] Ellipsometry measurements on poly-SiC modified with 1-docosene ($C_{22}H_{44}$) revealed a monolayer thickness of 20 ± 2 Å, which is about 70% of the theoretical length of 1-docosene in an all-*trans* conformation (27 Å). Since the optical model does not include the thin oxycarbide layer, these values are only semi-quantitative and do not allow the assignment of a specific tilt angle, as is possible for monolayers on H-terminated silicon[8] or with alkyl silanes on silicon oxide[49] with values between 15 and 26º.

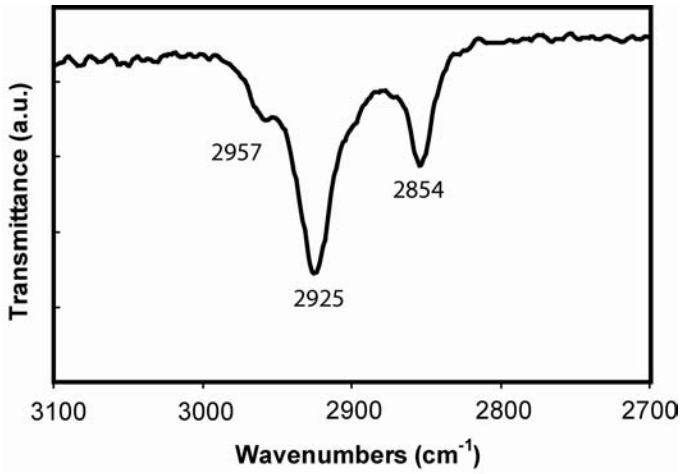

Figure 2. IRRA spectrum of 1-hexadecene modified poly-SiC.

Figure 3a shows the C_{1s} region of several XPS spectra recorded on SiC wafers after monolayer formation with a series of alkenes with chain lengths of 10, 14, 18 and 22 carbons. The spectra are normalized by aligning their baseline and setting the peak height at 282.5 eV at the same value.

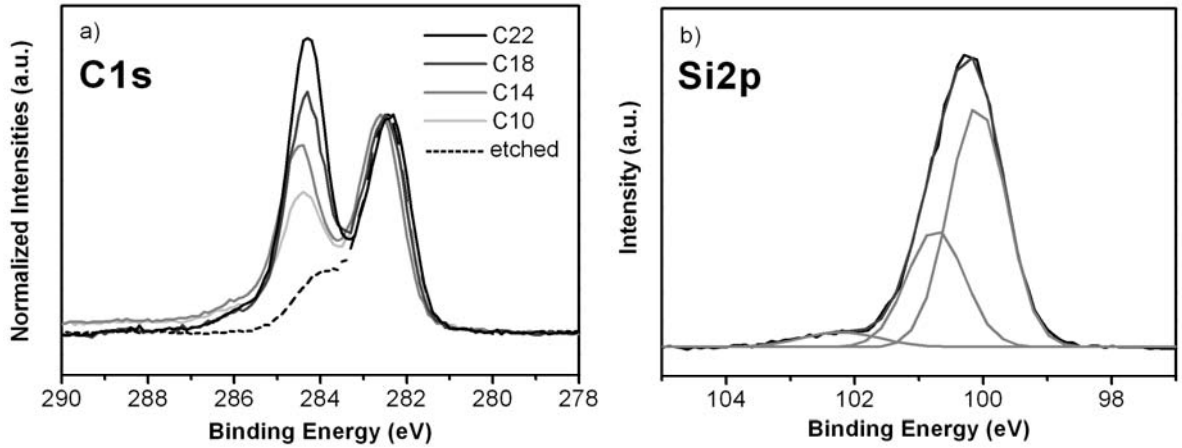

Figure 3. XPS of alkene monolayers on poly-SiC. (a) C_{1s} region for HF-etched SiC, and SiC wafer coated with monolayers of 1-decene (C_{10}), 1-tetradecene (C_{14}), 1-octadecene (C_{18}) and 1-docosene (C_{22}). (b) Si_{2p} region of a typical monolayer-coated SiC wafer.

With increased monolayer chain length, the signal at the binding energy of 284.4 eV increases with respect to the signal of the bulk silicon carbide at 282.5 eV. The relative increase of the high-binding energy C_{1s} signal – attributed to alkyl $CH_{2/3}$ carbon atoms not bound to oxygen – follows very closely the increase of chain length. More specifically, for the C_{10}, C_{14}, C_{18} and C_{22} monolayers, peak area ratios of 8.9 : 13.0 : 16.6 : 21.3 (normalized on the C_{14} monolayer) are obtained, closely following the expected ratios of 9 : 13 : 17 : 21, in absence of any significant electron attenuation effects. The spectra clearly indicate formation of an alkyl monolayer on the etched SiC surface.

An extra shoulder can be detected at about 285.9 eV, corresponding to carbon bound to oxygen.[37] The ratio of the areas under the $\underline{C}$-$H_{2/3}$ to $\underline{C}$-O carbon peaks, at 284.4 and 285.9 eV, respectively, is found to be 3.2 : 3.8 : 5.0 : 5.8 for the C_{10}, C_{14}, C_{18} and C_{22} monolayers. Again, a clear increase of this ratio is found for the longer alkyl chains, indicating the formation of a monolayer. From a comparison of the peaks at 102.3 eV in the Si_{2p} spectra of the modified samples (the Si_{2p} region of a wafer with a C_{14} monolayer, as a typical example of monolayer-coated wafer, is shown in Figure 3b) with that of HF-treated SiC wafers (see Figure 1e), it is clear that the oxycarbide signal does not change significantly. This confirms the formation of an incrementally thicker organic monolayer on top of the oxycarbide layer of fixed thickness that is present after HF etching. Since the XPS peak at 285.9 eV is attributed to both the oxycarbide layer already present, and to the $\underline{C}H_2$-O atoms of the monolayer, an

increase of the overall C-H/C-O ratio is expected for longer alkyl chains but with a slower rate than for the $\underline{C}$-$H_{2/3}$ signal itself (at 284.4. eV). This is indeed observed.

The monolayer properties (based on wettability and IR data) did not change within experimental error upon storage under ambient conditions for 1 year. The stability of monolayers prepared from 1-hexadecene was further assessed by exposing them to rather severe acidic and alkaline conditions (2M HCl at 90 ºC and 0.001 M NaOH at 60 ºC, respectively). Under hot acidic conditions, only small changes were observed, especially on the rougher surfaces, on which the decrease was within the experimental error (Figure 4a). While a similar stability in acidic environment has been reported for alkyl monolayers bound to Si_xN_4,[20,21] the stability under warm basic conditions is unparalleled (Figure 4b). While monolayers of thiol on gold, silanes on glass, and alkenes on silicon display a very weak stability under basic conditions, even alkene-derived monolayers on Si_xN_4 cannot withstand such harsh environments as the monolayers attached onto SiC could. Even after exposure for 4 h, all samples retained water contact angles higher than 85º (see Figure 4), which should be compared to the completely hydrophilic surface ($\theta < 15$º) of bare hydroxyl-terminated SiC. We attribute this stability to the formation of carbon-enriched SiC surfaces upon HF etching, and thus to the predominant formation of C-O-C bonds rather than Si-O-C bonds, as the latter would display poorer stability under basic conditions. Predominance of C-O-C bond formation is confirmed by stability tests in 2.5% HF solution, which yield even upon prolonged exposure water contact angles > 90º.

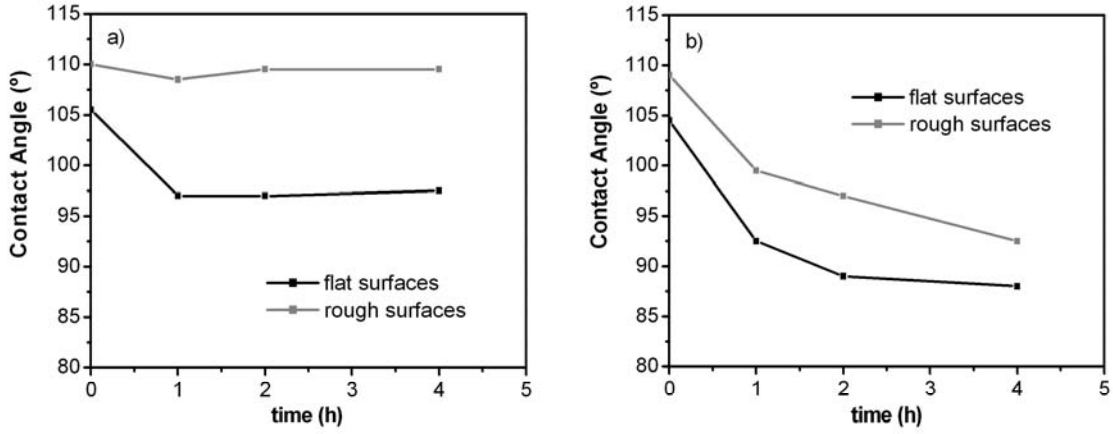

Figure 4. Water contact angle measured on 1-hexadecene-modified SiC surfaces exposed to a): 2M HCl at 90 ºC, b): 0.001M NaOH at 60 ºC. The flat surface corresponds to rms < 1 nm, and rough surface to rms ≈ 120 nm.

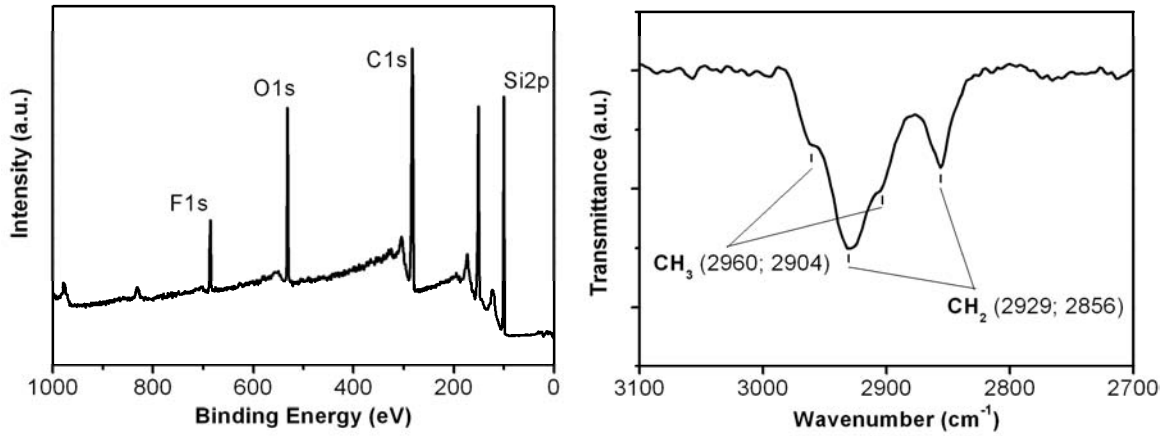

Figure 5. XPS (left) and IRRAS (right) of 11-fluoroundec-1-ene attached onto SiC.

This very high stability opens prospects for the use of these monolayers in applications where stable and well-defined surface properties are required under a wide range of chemical conditions.

To get more insight into the attachment mechanism, monolayers were prepared with 11-fluoroundec-1-ene, H_2C=CH-$(CH_2)_9$-F, an alkene without a terminal methyl group. These monolayers were studied with XPS (Figure 5, left) and IRRAS (Figure 5, right). On the wide scan XPS (Figure 5, left), a significantly increased F_{1s} signal is clearly observed (cf., Figure 1d for the amount of F present after HF etching), confirming the formation of a fluorine-terminated monolayer on SiC. The IRRA spectrum reveals the appearance of a shoulder at 2960 cm^{-1} that is absent in the FT-IR of the liquid compound. This can be attributed to the formation of a methyl group upon attack of a hydroxylic oxygen on the secondary carbon of the double bond. This evidence suggests that the thermal formation of alkyl monolayers from alkenes on hydroxyl-terminated surfaces occurs via a Markovnikov addition, as depicted in Figure 6. These results are similar to the quantitative IRRAS study of decyl monolayers on oxidized silicon surfaces by Wayner et al.,[50] in which the addition was proposed to take place via an acid-catalyzed process. However, monolayers obtained in that work did not have the extremely high stability observed in the present study for monolayers on silicon carbide. This can be explained by the stability of the superficial oxycarbide layer, compared to the SiO_2 layer formed on silicon. More specifically, in the case of defects in the monolayers, the underlying substrates can be exposed and etched by corrosive environment. Due to the

presence of Si-C bonds, SiOC compounds are very resistant to the nucleophilic attack of OH^- or F^- ions[51,52] under conditions where SiO_2 is soluble.[53]

The binding of 1-alkenes via the second carbon of the chain, instead of the first one as was the case for reaction with hydrogen-terminated silicon surfaces, is also probably the explanation for the formation of somewhat less ordered monolayers.

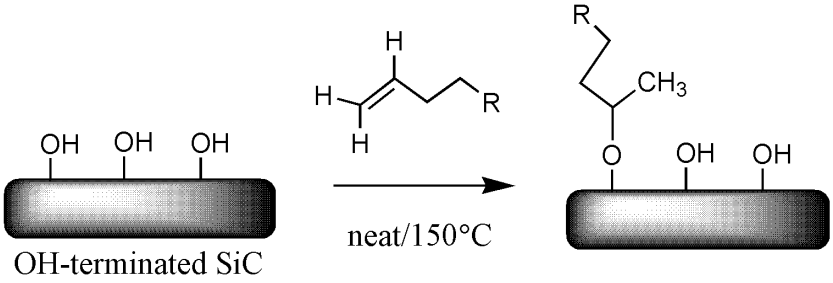

Figure 6. Attachment of alkyl monolayers on hydroxyl-terminated SiC surfaces

Apart from the stability of methyl-terminated surfaces, the integration of organic functionalities onto inorganic materials opens an extended field of research. Functional groups like amines[54,55] or carboxylic acids[56,57] have been covalently bound onto several materials. From these, carboxyl groups are one of the most investigated groups, because of the possibility of easy functionalization with biomolecules via the widely-used chemistry of activated esters. However, esters are often used as protective groups[33,58] to be hydrolyzed after attachment, since direct attachment of acids can cause interferences with the monolayer formation.[59] Our hydroxyl-terminated surfaces could as well be reactive towards carboxyl groups, and thus hinder the formation of a proper functional monolayer by decreasing the density of -COOH groups available.

Ester monolayers were prepared on SiC, from methyl undec-10-enoate and 2,2,2-trifluoroethyl undec-10-enoate. XPS data (Figure 7) for these monolayers clearly show the characteristic oxidation states of each carbon of the ester functions. In Figure 7a, the peaks at 292.8 (-***C***F_3), 289 (O-***C***=O) and 287.5 eV (O-***C***H_2-CF_3) show comparable areas, confirming that attachment of the trifluoroester at least predominantly occurs via the alkene moiety, leaving the functionality available for further reactions. The same can be observed for the methyl ester (Figure 7b), although the resolution of the characteristic peaks is poorer because of the overlapping peaks around 286 eV.

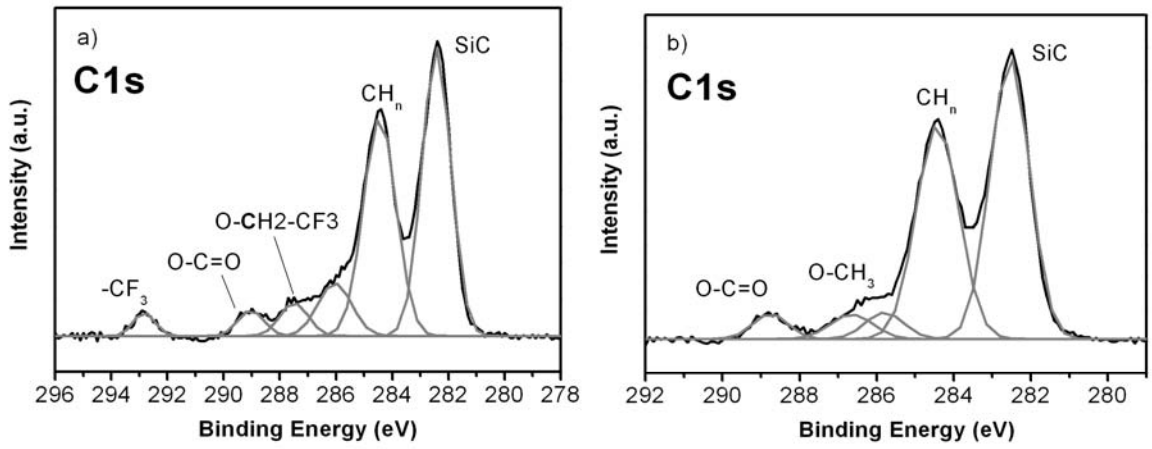

Figure 7. High-resolution C_{1s} XPS data of monolayers attached onto poly-SiC, derived from (a) 2,2,2-trifluoroethyl undec-10-enoate, and (b) methyl undec-10-enoate.

These observations are in line with IRRAS data (Figure 8), which depict that besides the usual methylene and/or methyl stretching bands, the carbonyl stretching of the trifluoroethyl and methyl esters are at essentially the wavenumbers observed for the pure liquid alkenes (1760 and 1745 cm^{-1}, respectively). In other words, the SiC surface can be readily functionalized with esters via the attachment of ω-ester-1-alkenes.

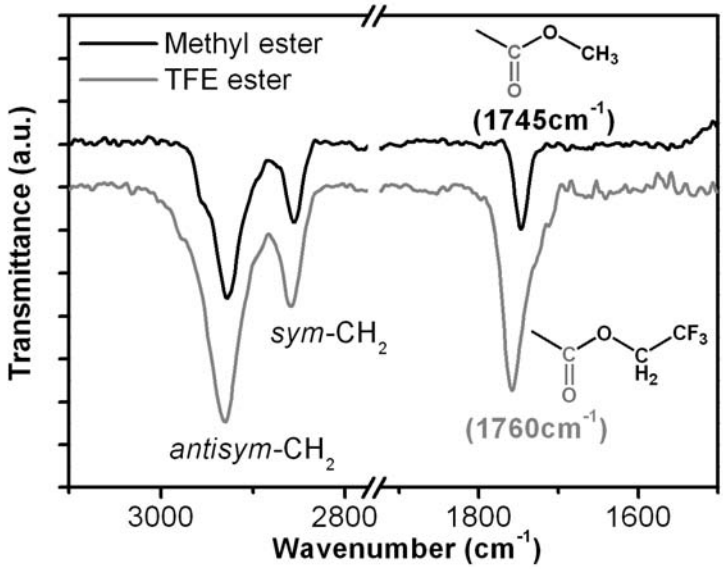

Figure 8. IRRA spectra of monolayers of 2,2,2-trifluoroethyl undec-10-enoate (bottom) and methyl undec-10-enoate (top) on poly-SiC.

Conclusions

This work presents the first covalently bound alkyl monolayers on silicon carbide surfaces, by reaction of neat alkenes with HF-etched surfaces to produce well-defined, chemically tunable, and highly stable coatings. IRRAS and XPS provide evidence that the covalent attachment of alkenes occurs via a Markovnikov-type addition of oxygen on the double bond. The obtained layers show a lower degree of order than monolayers obtained with 1-alkenes on hydrogen-terminated silicon or with thiols on gold. However, the coatings on SiC are extremely stable under acidic conditions, relatively stable in alkaline media, and do not show any significant degradation in ambient conditions over a year. The attachment reaction is compatible with esters, allowing the formation of functionalized surfaces, ready for further modification with organic and/or biologic moieties that would retain their activity upon immobilization, and provide coatings usable in sensing and other biotechnology applications.

Acknowledgments

The authors thank Graduate School VLAG, MicroNed (Project no. 6163510395), DARPA MTO (grant # N66001-03-1-8915) and NSF (grant #0355339 and graduate fellowship to C.S.R.) for financial support, and Professors Remko Boom (Wageningen University) and Ernst Sudhölter (Technical University of Delft) for stimulating discussions.

References

(1) Buriak, J. M. *Chem. Rev.* **2002,** *102*, 1271-1308.

(2) Love, J. C.; Estroff, L. A.; Kriebel, J. K.; Nuzzo, R. G.; Whitesides, G. M. *Chem. Rev.* **2005,** *105*, 1103-1169.

(3) Cotton, F. A.; Wilkinson, G.; Murillo, C. A.; Bochman, M. *Advanced Inorganic Chemistry*. 6th ed.; John Wiley & Sons: New York, 1999; p 259.

(4) Boukherroub, R. *Curr. Opin. Solid State Mater. Sci.* **2005,** *9*, 66-72.

(5) Linford, M. R.; Fenter, P.; Eisenberger, P. M.; Chidsey, C. E. D. *J. Am. Chem. Soc.* **1995,** *117*, 3145-3155.

(6) Shirahata, N.; Hozumi, A.; Yonezawa, T. *Chem. Rec.* **2005,** *5*, 145-159.

(7) Sieval, A. B.; Linke, R.; Zuilhof, H.; Sudhölter, E. J. R. *Adv. Mater.* **2000,** *12*, 1457-1460.

(8) Sun, Q.-Y.; de Smet, L. C. P. M.; van Lagen, B.; Giesbers, M.; Thune, P. C.; van Engelenburg, J.; de Wolf, F. A.; Zuilhof, H.; Sudhölter, E. J. R. *J. Am. Chem. Soc.* **2005,** *127*, 2514-2523.

(9) Sun, Q.-Y.; de Smet, L. C. P. M.; van Lagen, B.; Wright, A.; Zuilhof, H.; Sudhölter, E. J. R. *Angew. Chem., Int. Ed.* **2004,** *43*, 1352-1355.

(10) Wayner, D. D. M.; Wolkow, R. A. *J. Chem. Soc., Perkin Trans. 2* **2002**, 23-34.

(11) Scheres, L.; Arafat, A.; Zuilhof, H. *Langmuir* **2007,** *23*, 8343-8346.

(12) Choi, K.; Buriak, J. M. *Langmuir* **2000,** *16*, 7737-7741.

(13) Lasseter, T. L.; Clare, B. H.; Abbott, N. L.; Hamers, R. J. *J. Am. Chem. Soc.* **2004,** *126*, 10220-10221.

(14) Nichols, B. M.; Butler, J. E.; Russell, J. N.; Hamers, R. J. *J. Phys. Chem. B* **2005,** *109*, 20938-20947.

(15) Yang, W. S.; Auciello, O.; Butler, J. E.; Cai, W.; Carlisle, J. A.; Gerbi, J.; Gruen, D. M.; Knickerbocker, T.; Lasseter, T. L.; Russell, J. N.; Smith, L. M.; Hamers, R. J. *Nat. Mater.* **2003,** *2*, 63-63.

(16) Ababou-Girard, S.; Sabbah, H.; Fabre, B.; Zellama, K.; Solal, F.; Godet, C. *J. Phys. Chem. C.* **2007,** *111*, 3099-3108.

(17) Ababou-Girard, S.; Solal, F.; Fabre, B.; Alibart, F.; Godet, C. *J. Non-Cryst. Solids* **2006,** *352*, 2011-2014.

(18) Devadoss, A.; Chidsey, C. E. D. *J. Am. Chem. Soc.* **2007,** *129*, 5371-5372.

(19) Nakamura, T.; Ohana, T.; Suzuki, M.; Ishihara, M.; Tanaka, A.; Koga, Y. *Surf. Sci.* **2005,** *580*, 101-106.

(20) Arafat, A.; Schroën, K.; de Smet, L. C. P. M.; Sudhölter, E. J. R.; Zuilhof, H. *J. Am. Chem. Soc.* **2004,** *126*, 8600-8601.

(21) Arafat, A.; Giesbers, M.; Rosso, M.; Sudhölter, E. J. R.; Schroën, K.; White, R. G.; Yang, L.; Linford, M. R.; Zuilhof, H. *Langmuir* **2007,** *23*, 6233-6244.

(22) Choyke, W. J.; Matsunami, H.; Pensl, G. *Silicon Carbide, Recent Major Advances*. Springer: Berlin, 2003.

(23) Saddow, S. E.; Agarwal, A. *Advances in Silicon Carbide: Processing and Applications*. Artech House Inc.: Boston, 2004.

(24) Nakamura, D.; Gunjishima, I.; Yamaguchi, S.; Ito, T.; Okamoto, A.; Kondo, H.; Onda, S.; Takatori, K. *Nature* **2004,** *430*, 1009-1012.

(25) Yang, Y. T.; Callegari, X. L.; Ekinci, K. L.; Roukes, M. L. *Nano Lett.* **2006,** *6*, 583-586.

(26) Cicero, G.; Catellani, A. *J. Chem. Phys.* **2005,** *122*, 214716.1-5.

(27) Kanai, Y.; Cicero, G.; Selloni, A.; Car, R.; Galli, G. *J. Phys. Chem. B* **2005,** *109*, 13656-13662.

(28) Sella, C.; Martin, J. C.; Lecoeur, J.; Lechanu, A.; Harmand, M. F.; Naji, A.; Davidas, J. P. *Mater. Sci. Eng., A* **1991,** *139*, 49-57.

(29) Santavirta, S.; Takagi, M.; Nordsletten, L.; Anttila, A.; Lappalainen, R.; Konttinen, Y. T. *Arch. Orthop. Trauma. Surg.* **1998,** *118*, 89-91.

(30) Rosenbloom, A. J.; Sipe, D. M.; Shishkin, Y.; Ke, Y.; Devaty, R. P.; Choyke, W. J. *Biomed. Microdev.* **2004,** *6*, 261-267.

(31) de Carlos, A.; Borrajo, J. P.; Serra, J.; Gonzalez, P.; Leon, B. *J. Mater. Sci. Mater. Med.* **2006,** *17*, 523-529.

(32) Cogan, S. F.; Edell, D. J.; Guzelian, A. A.; Liu, Y. P.; Edell, R. *J. Biomed. Mater. Res. A* **2003,** *67A*, 856-867.

(33) Asanuma, H.; Noguchi, H.; Uosaki, K.; Yu, H. Z. *J. Phys. Chem. B* **2006,** *110*, 4892-4899.

(34) de Smet, L. C. P. M.; Pukin, A. V.; Sun, Q. Y.; Eves, B. J.; Lopinski, G. P.; Visser, G. M.; Zuilhof, H.; Sudhölter, E. J. R. *Appl. Surf. Sci.* **2005,** *252*, 24-30.

(35) Roper, C. S.; Radmilovic, V.; Howe, R. T.; Maboudian, R. *J. Electrochem. Soc.* **2006,** *153*, C562-C566.

(36) Harris, G. L. *Properties of Silicon Carbide*. INSPEC: London, 1995.

(37) Avila, A.; Montero, I.; Galan, L.; Ripalda, J. M.; Levy, R. *J. Appl. Phys.* **2001,** *89*, 212-216.

(38) Hijikata, Y.; Yaguchi, H.; Yoshikawa, M.; Yoshida, S. *Appl. Surf. Sci.* **2001,** *184*, 161-166.

(39) Guy, O. J.; Chen, L.; Pope, G.; Teng, K. S.; Maffeis, T.; Wilks, S. P.; Mawby, P. A.; Jenkins, T.; Brieva, A.; Hayton, D. J. *Mater. Sci. Forum* **2006,** *527-529*, 1027-1030.

(40) Muehlhoff, L.; Bozack, M. J.; Choyke, W. J.; Yates, J. T. *J. Appl. Phys.* **1986,** *60*, 2558-2563.

(41) Roccaforte, F.; La Via, F.; Raineri, V.; Musumeci, P.; Calcagno, L.; Condorelli, G. G. *Appl. Phys. Mater. Sci. Process.* **2003,** *77*, 827-833.

(42) Starke, U. *Phys. Stat. Sol. B* **1997,** *202*, 475-499.

(43) vanElsbergen, V.; Janzen, O.; Monch, W. *Mater. Sci. Eng.* **1997,** *B46*, 366-369.

(44) Lin, M. E.; Strite, S.; Agarwal, A.; Salvador, A.; Zhou, G. L.; Teraguchi, N.; Rockett, A.; Morkoc, H. *Appl. Phys. Lett.* **1993,** *62*, 702-704.

(45) Losurdo, M.; Giangregorio, M. M.; Capezzuto, P.; Bruno, G.; Brown, A. S.; Kim, T. H.; Yi, C. H. *J. Electron. Mater.* **2005,** *34*, 457-465.

(46) Bernhardt, J.; Schardt, J.; Starke, U.; Heinz, K. *Appl. Phys. Lett.* **1999,** *74*, 1084-1086.

(47) Sieber, N.; Seyller, T.; Graupner, R.; Ley, L.; Mikalo, R.; Hoffmann, P.; Batchelor, D. R.; Schmeisser, D. *Appl. Surf. Sci.* **2001,** *184*, 278-283.

(48) Sieval, A. B.; Demirel, A. L.; Nissink, J. W. M.; Linford, M. R.; van der Maas, J. H.; de Jeu, W. H.; Zuilhof, H.; Sudholter, E. J. R. *Langmuir* **1998,** *14*, 1759-1768.

(49) Onclin, S.; Ravoo, B. J.; Reinhoudt, D. N. *Angew. Chem., Int. Ed.* **2005,** *44*, 6282-6304.

(50) Mischki, T. K.; Donkers, R. L.; Eves, B. J.; Lopinski, G. P.; Wayner, D. D. M. *Langmuir* **2006,** *22*, 8359-8365.

(51) Onneby, C.; Pantano, C. G. *J. Vac. Sci. Tech. A* **1997,** *15*, 1597-1602.

(52) Soraru, G. D.; Modena, S.; Guadagnino, E.; Colombo, P.; Egan, J.; Pantano, C. *J. Am. Ceram. Soc.* **2002,** *85*, 1529-1536.

(53) Iler, R. K. *The Chemistry of Silica*. New York, 1979.

(54) Knickerbocker, T.; Strother, T.; Schwartz, M. P.; Russell, J. N.; Butler, J.; Smith, L. M.; Hamers, R. J. *Langmuir* **2003,** *19*, 1938-1942.

(55) Lin, Z.; Strother, T.; Cai, W.; Cao, X. P.; Smith, L. M.; Hamers, R. J. *Langmuir* **2002,** *18*, 788-796.

(56) Bain, C. D.; Evall, J.; Whitesides, G. M. *J. Am. Chem. Soc.* **1989,** *111*, 7155-7164.

(57) Faucheux, A.; Gouget-Laemmel, A. C.; de Villeneuve, C. H.; Boukherroub, R.; Ozanam, F.; Allongue, P.; Chazalviel, J. N. *Langmuir* **2006,** *22*, 153-162.

(58) Strother, T.; Cai, W.; Zhao, X. S.; Hamers, R. J.; Smith, L. M. *J. Am. Chem. Soc.* **2000,** *122*, 1205-1209.

(59) Sieval, A. B.; Demirel, A. L.; Nissink, J. W. M.; Linford, M. R.; van der Maas, J. H.; de Jeu, W. H.; Zuilhof, H.; Sudhölter, E. J. R. *Langmuir* **1998,** *14*, 1759-1768.

Chapter 6

Covalently Attached Organic Monolayers on SiC and Si_xN_4 Surfaces: Formation using UV Light at Room Temperature

We describe the formation of alkyl monolayers on silicon carbide (SiC) and silicon-rich silicon nitride (Si_xN_4) surfaces, using UV irradiation in the presence of alkenes. Both the surface preparation and the monolayer attachment were carried out under ambient conditions. The stable coatings obtained in this way were studied by water contact angle measurements, infrared reflection absorption spectroscopy (IRRAS), X-ray reflectivity and X-ray photoelectron spectroscopy (XPS). Besides unfunctionalized 1-alkenes, methyl undec-10-enoate and 2,2,2-trifluoroethyl undec-10-enoate were also grafted onto both substrates. The resulting ester-terminated surfaces could then be further reacted after hydrolysis using amide chemistry, to easily allow the attachment of amine-containing compounds.

This chapter is published as:
"Covalently Attached Organic Monolayers on SiC and Si_xN_4 Surfaces: Formation Using UV Light at Room Temperature", Rosso, M.; Giesbers, M.; Arafat, A.; Schroën, K.; Zuilhof, H. *Langmuir* **2009,** *25*, 2172-2180.

Introduction

Several methods have been developed over the last two decades to covalently attach organic monolayers onto semiconductor surfaces. Silicon surfaces[1-6] have been the most widely investigated: stable and densely packed monolayers were obtained from alkenes and alkynes on hydrogen-terminated silicon surfaces using thermal reactions[7-10] or photochemical initiation with UV[11-15] or visible light.[16-18] The high quality and chemical versatility of monolayers formed with these methods allowed various applications for modified silicon surfaces in molecular electronics and sensors.[19,20]

Alkenes and alkynes were also attached onto flat hydrogen-terminated germanium surfaces[2,21] in conditions close to those used for silicon, but only few results were obtained so far on this material. Diamond surfaces were recently studied: hydrogen-free surfaces were reacted under UHV conditions[22-24] with alkenes via a [2+2] cycloaddition or Diels-Alder mechanism, and hydrogen-terminated diamond surfaces could also be functionalized with alkenes under UV irradiation.[25-28]

The development of methods to tune the surface properties of two other robust high-bandgap materials, silicon-rich silicon nitride (Si_xN_4, $3.5 < x < 4.5$) and silicon carbide (SiC) would significantly increase the possible use of these materials as well. Si_xN_4 is widely used, for example, as waveguide material in refractometric[29-31] or fluorescence[32] detection, and as coating material for sensors based on electrical impedance[33,34] or vibrating microcantilevers.[35] SiC has a high potential for similar applications.[36-41] Another development concerns the coating of bio-compatible microdevices, like micro-fabricated Si_xN_4 membranes (microsieves),[42-45] or SiC-based medical prosthesis and micro-electrodes.[46-51] For such sensing and biomedical applications, both materials would benefit from specific surface modification. In this regard, we reported recently on the thermal modification of flat Si_xN_4[52,53] and 6H-SiC and polycrystalline 3C-SiC[54] using thermal conditions close to those used for the surface modification of silicon. We obtained stable and good quality monolayers from several simple alkenes (e.g. contact angles up to 107° for octadecene-derived monolayers on SiC). In addition, ester-functionalized monolayers could be prepared, allowing further (bio-)chemical surface modifications. Coffinier[55] *et al.* also reported on the formation of monolayers of protected amines on H-terminated Si_5N_4 surfaces prepared and irradiated under UHV conditions in the presence of alkenes.

In this work, we investigated the UV-assisted formation of organic monolayers on 3C-SiC and Si_xN_4, using only wet chemistry under ambient conditions (temperature and pressure), as this would significantly increase the range of monolayer functionalities that can be attached. Indeed, photochemical reactions at room temperature would allow the attachment of reactants that can not withstand the reaction conditions required for the thermal attachments (typically > 150 ºC). In addition, photochemical reactions strongly reduce the required amount of material (only the irradiated surface needs to be covered with a thin film containing the molecule to attach), and allow the patterning of surfaces using common photolithographic techniques.

The attachment of a variety of 1-alkenes was investigated, starting from unfunctionalized alkenes (CH_2=CH-(CH_2)$_n$$CH_3$) providing methyl-terminated monolayers, to ω-functionalized 1-alkenes (esters, fluoroalkene) on SiC and Si_xN_4 surfaces, after a standard cleaning and etching procedure. The wavelength dependence of the attachment reaction was studied in the range from 254 to 330 nm. Static water contact angle measurements, infra-red reflection-absorption spectroscopy (IRRAS), X-ray photoelectron spectroscopy (XPS) and X-ray reflectivity were used to characterize the modified surfaces. The stability of alkyl monolayers was tested in acidic and alkaline conditions, and further chemical modifications were performed on ester-terminated surfaces. After hydrolysis of ester monolayers and subsequent N-hydrosuccinimide (NHS) activation of the obtained carboxylic acid-terminated surfaces, amide formation with *m*-(trifluoromethyl)benzylamine (TFBA) showed the possibility of easy surface (bio-)functionalization of both SiC and Si_xN_4.

Experimental Section

Materials

1-Hexadecene (99%) was purchased from Sigma-Aldrich and distilled twice under reduced pressure before use. Undec-10-enoic acid (98%), undec-10-en-1-ol (98%), *N*-hydroxysuccinimide (NHS), 1-(ethyl-3-(3-dimethylaminopropyl)carbodiimide (EDC) and *m*-(trifluoromethyl)benzylamine (TFBA, 97%) were purchased from Sigma-Aldrich and used as received for synthesis. 2,2,2-Trifluoroethyl undec-10-enoate[16] and 11-fluoroundec-1-ene[18] were synthesized as described elsewhere.

Monolayer Formation

The alkyl monolayers were formed on stoechiometric polycrystalline 3C-SiC films (stoechiometric SiC, thickness: 250 nm, surface rms roughness determined with AFM: 1.5 ± 0.5 nm) obtained by chemical vapor deposition (CVD) on Si(100),[56] and on CVD-deposited Si_xN_4 (x ~ 3.9, thickness 140 nm, surface rms roughness determined with AFM: 0.45 ± 0.05 nm, Lionix B.V., The Netherlands) onto Si(100). SiC and Si_xN_4 samples (standard: 1 × 1 cm^2; for IRRAS measurements samples of 3 × 1.5 cm^2 were used) were cleaned first by sonication in acetone, followed by an air-based plasma treatment for 15 min. The resulting oxidized surfaces were etched with a 2.5% solution of HF for 2 min. Right after this step, wafers were dipped into argon-saturated neat alkenes, in fused silica (for wavelengths < 300 nm) or glass flasks. After 30 more min under an argon flow, the UV pen lamps (low pressure mercury vapor, double bore lamp, Jelight Company, Irvine, California, USA) were placed 4 mm away from the sample surface and turned on for the desired time. At the end of the experiment, samples were removed and rinsed several times with petroleum ether, acetone and dichloromethane, and sonicated in the same solvents. After these cleaning steps, no loss of surface bound material was observed with IRRAS and XPS after further rinsing; moreover, the homogeneity of water contact angle measurements showed all physisorbed species had been removed.

Further surface functionalization

Basic hydrolysis of esters

TFE-terminated surfaces were exposed to 0.25 M potassium *tert*-butoxide in DMSO, for 1 to 3 min at room temperature. The samples were then rinsed with 1 M HCl, with demineralized water and acetone, and finally sonicated in acetone before drying in a nitrogen flow.

NHS ester activation

Acid-terminated samples were placed in 2 ml of an aqueous solution of EDC and NHS (0.04 and 0.01 M, respectively), and reacted for 1 h at room temperature. Samples were then rinsed and dried as described previously.

Amide formation

NHS-terminated samples were placed in 5 ml of a 0.1 M solution of TFBA in dry DMSO, and let to react at room temperature for 24 h. Surfaces were then rinsed thoroughly with DMSO and acetone, sonicated in the same solvents and dried in a nitrogen flow.

Monolayer Characterization

Static water contact angle measurements

The wetting properties of modified surfaces were characterized by automated static water contact angle measurements performed using an Erma Contact Angle Meter G-1 (volume of the drop of demineralized water = 3.5 μl).

X-ray Photoelectron Spectroscopy (XPS)

The XPS analysis was performed using a JPS-9200 Photoelectron Spectrometer (JEOL, Japan). The high-resolution spectra were obtained under UHV conditions using monochromatic Al K_α X-ray radiation at 12 kV and 25 mA, using an analyzer pass energy of 10 eV. All high-resolution spectra were corrected with a linear background before fitting. Binding energies were calibrated at 285.0 eV for the C_{1s} peak corresponding to carbon in alkyl chains, to eliminate charging effects on these high-bandgap materials coated with insulating monolayers and compare the data on both SiC and Si_xN_4. To facilitate comparison between different samples, XPS intensities measured on SiC were normalized to the intensity of the substrate C_{1s} peak at 283.2 eV and XPS intensities measured on Si_xN_4 were normalized to the intensity of the N_{1s} peak from the Si_xN_4 substrate at 398.1 eV. Under the conditions used in this study, no significant X-ray-induced degradation of monolayers was observed, even for repeated XPS measurements on the same spot and sequential surface functionalizations.

Thickness calculations from XPS

Thicknesses of monolayers on SiC substrates were calculated from XPS electron attenuation using the following equation,[57] which involves the ratio of C_{1s} XPS signals from the substrate and the film. This approach can be used when the kinetic energies of electrons from both film and substrate are comparable:

$$t = \lambda_{CH}.\cos(\theta).\ln\left(1+\frac{I_{CH}.\rho_S.\lambda_S}{I_S.\rho_{CH}.\lambda_{CH}}\right)$$

θ is the take-off angle (θ = 1º) of electrons relative to the surface normal. The thickness of the organic film (t) was determined as a function of I_{CH} and I_s, which are the intensities of the C_{1s} XPS signal originating from the organic film and from the substrate, respectively. For electrons originating from the C_{1s} level (kinetic energy E_k ~ 1200 eV) an attenuation length for the alkyl monolayer (λ_{CH} = 2.8 nm) was chosen by extrapolating data from previous reports.[58,59] Under the conditions used for XPS measurements (θ < 60º, E_k > 100 eV), the attenuation length of C_{1s} electrons in silicon carbide could be approximated to their inelastic mean free path (IMFP = 2.35 nm),[60] within 15% of its value.[61] The element density of carbon in the monolayer (ρ_{CH}), and in silicon carbide (ρ_S) were estimated at 0.054 and 0.08 mol.cm^{-3}, respectively.

For monolayers on silicon nitride, the calculation was done using the ratio of C_{1s} signal in the film and Si_{2p} signal in the substrate. The element density of silicon in the Si_xN_4 (ρ_S) was estimated at 0.07 mol.cm^{-3}. A value of 3.1 nm was then taken for both the IMFP of Si_xN_4 and the electron attenuation length of Si_{2p} electrons (E_k = 1386 eV) in the monolayer, and the intensity ratio in the logarithm was corrected for the different sensitivity factors of the C_{1s} (s_C) and Si_{2p} (s_{Si}) peaks (1 and 0.865, respectively), according to the modified equation:

$$t = \lambda_{CH} . \cos(\theta) . \ln\left(1 + \frac{I_{CH} . \rho_S . \lambda_S . s_{Si}}{I_S . \rho_{CH} . \lambda_{CH} . s_C}\right)$$

Fourier Transform Infrared Reflection Absorption Spectroscopy (FT-IRRAS)

IRRA Spectra were measured with a Bruker Tensor 27 FT-IR spectrometer, using a commercial variable-angle reflection unit (Auto Seagull, Harrick Scientific). A Harrick grid polarizer was installed in front of the detector, and was used to measure spectra with *p*-polarized (parallel) radiation with respect to the plane of incidence at the sample surface. Single channel transmittance spectra were collected using a spectral resolution of 4 cm^{-1}, using 1024 scans in each measurement. The optimal angle for data collection was found to be 68º for all the surfaces studied. All the reported measurements were performed at this angle. Raw data files were divided by data recorded on a plasma-oxidized reference surface, to give the reported spectra.

Results and Discussion

Wet etching of SiC and Si_xN_4 surfaces

Immediately after oxidation and etching with an aqueous solution of 2.5% HF for 2 min, the surfaces of both materials were hydrophilic, but SiC surfaces exhibited lower static water contact angles ($\theta < 10^o$) than Si_xN_4 surfaces ($\theta \sim 35^o$). The wide-scan XPS data measured on both SiC and Si_xN_4 ($x \sim 3.9$) (Figure 1) clearly shows the removal of SiO_2 with HF, evidenced by the decrease of the O_{1s} peak at 532 eV. The quantification of the surface oxygen also shows different surface terminations: the SiC surface retained a significant amount of oxygen (8%) after etching, while this element was almost absent from etched Si_xN_4 surfaces (< 2%). In addition, a significant F_{1s} signal can be observed at 687 eV on both materials (SiC: 1.2%, Si_xN_4: 3%), resulting from the inclusion of fluorine in the surfaces during exposure to HF. The carbon contamination after wet etching was very low in Si_xN_4 substrates (~ 2%), while it was not possible to determine it on SiC, due to the intrinsic carbon content of the material.

These results are in agreement with our previous work published on the HF etching of both substrates.[52,54] XPS analysis of etched Si_xN_4 surfaces suggests a bulk composition corresponding to $Si_{3.9\pm0.1}N_4$. Previous XPS and XRD analysis of the used SiC wafers revealed the exclusive presence of a 3C-SiC phase in the bulk material,[56,62] without significant contamination by other elements.

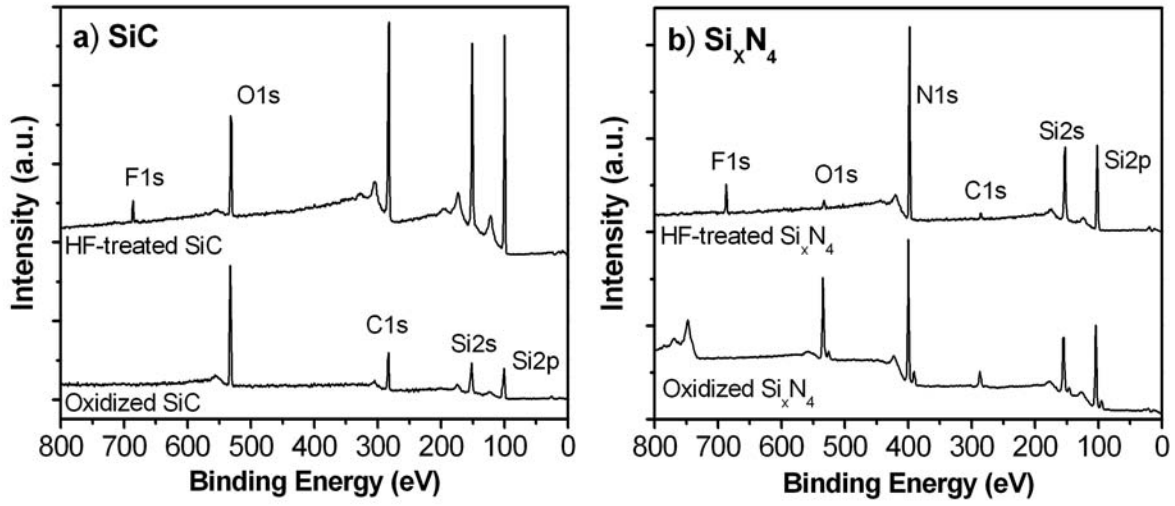

Figure 1. XPS wide scans measured on (a) SiC and (b) Si_xN_4 substrates, before (oxidized surfaces) and after 2 min etching with 2.5% HF in water.

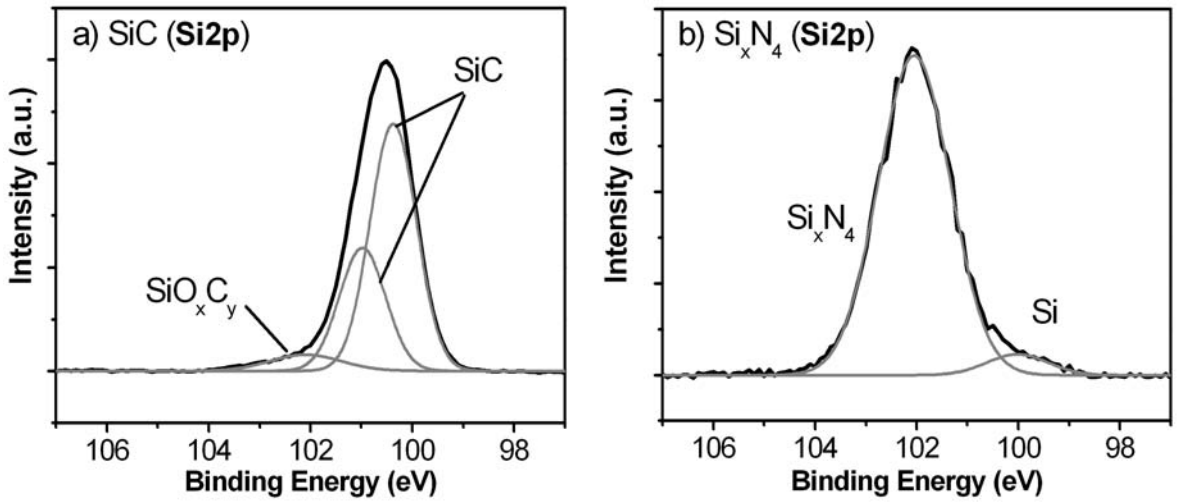

Figure 2. Si_{2p} XPS narrow-scan data measured on (a) SiC and (b) Si_xN_4 substrates after 2 min etching in 2.5% HF.

A more detailed picture of the surface chemistry was obtained from narrow-scan data of the Si_{2p} region. In Figure 2, the spectrum measured on etched SiC surfaces shows the presence of partially oxidized silicon (101.8 eV), next to the peak corresponding to bulk silicon carbide, which could still be resolved into its two spin-orbit components, at 100.4 ($Si_{2p}3/2$) and 101.0 eV ($Si_{2p}1/2$). As reported earlier,[54,63-65] treatment of SiC with HF leaves a residual silicon oxycarbide layer with a high density of surface hydroxyl groups. The oxygen originated mainly from surface adsorbed species, as previous SIMS measurements on the same wafers yielded values of only 0.04% of bulk oxygen content.[56]

The etched Si_xN_4 surfaces, however, only show the main peak of bulk silicon nitride (Si-N, 102.0 eV), and a small component (~ 6% of the total Si_{2p} signal) at lower binding energy, close to the value measured on pure silicon surfaces (100.0 eV). This observation has been attributed to the presence of silicon clusters within the CVD-Si_xN_4,[66] or to the diffusion of silicon into the Si_xN_4 coating during high-temperature annealing.[67] Since no annealing was carried out on the used substrates, this 100.0 eV peak is most likely due to the presence of silicon clusters.

As reported before[52,53] the HF treatment of Si_xN_4 surfaces decreased the oxygen content to close to the detection limit of the XPS, and left surfaces mainly covered with Si-H or N-H bonds. However, we cannot rule out the presence of a small amount of surface hydroxyl groups, which is difficult to resolve from nitrogen-bound silicon in the Si_{2p} XPS data. Additionally, the presence of a small fraction of silicon clusters at the surface could also

affect the chemistry of HF-treated Si_xN_4 surfaces, since pure silicon surfaces react readily with alkenes in much milder conditions than the ones presented here. In this respect, the surface chemistry of silicon-rich silicon nitride (Si_xN_4) is expected to differ significantly from that of stoichiometric silicon nitride (Si_3N_4), which yields hydroxyl-covered surfaces upon etching with HF.[68]

Monolayer formation onto SiC and Si_xN_4 surfaces

The attachment of alkyl monolayers on SiC and Si_xN_4 surfaces using a variety of wavelengths was first monitored with static water contact angles. As the reaction took place, the surfaces became more hydrophobic (Figure 3). The fastest reaction was obtained using a 254 nm lamp, and this also gave the highest final contact angles ($\theta \geq 107^o$). Irradiation with a 330 nm lamp through a glass vessel (cut-off wavelength of 300 nm), or a 285 nm lamp with a filter (cut-off wavelength of 275 ± 5 nm, data not shown) never gave water contact angles above 95º indicative of the formation of incomplete monolayers. Clearly, a wavelength below 270 nm was needed to form good monolayers onto both materials. For comparison, samples placed into 1-hexadecene and left in the dark for 24 h gave low water contact angle values of 40 ± 5º. These small values, close to those measured on the initial etched surfaces; show the near-absence of thermal reactivity at room temperature of etched SiC and Si_xN_4 surfaces.

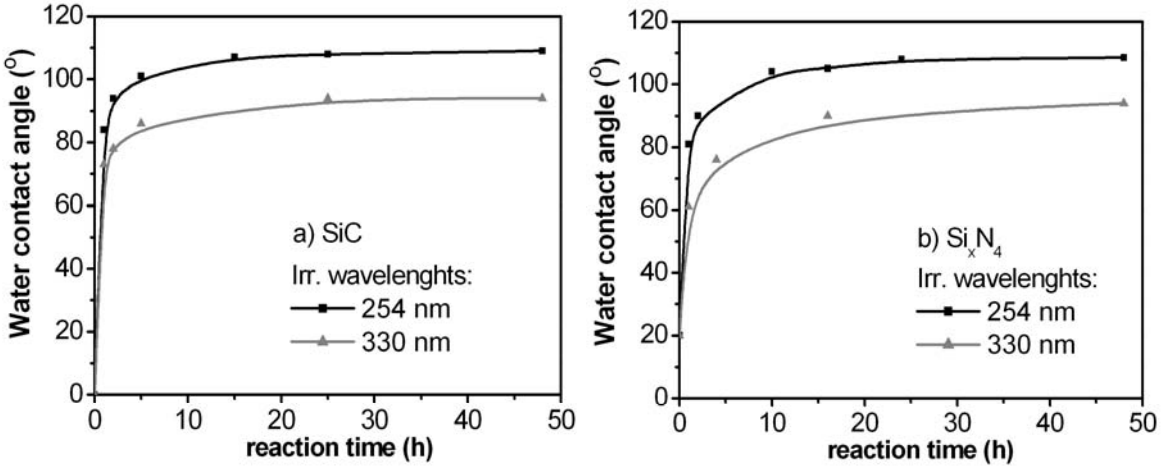

Figure 3. Static water contact angles measured on (a) SiC and (b) Si_xN_4 substrates modified with 1-hexadecene using irradiation at 254 and 330 nm for different reaction times.

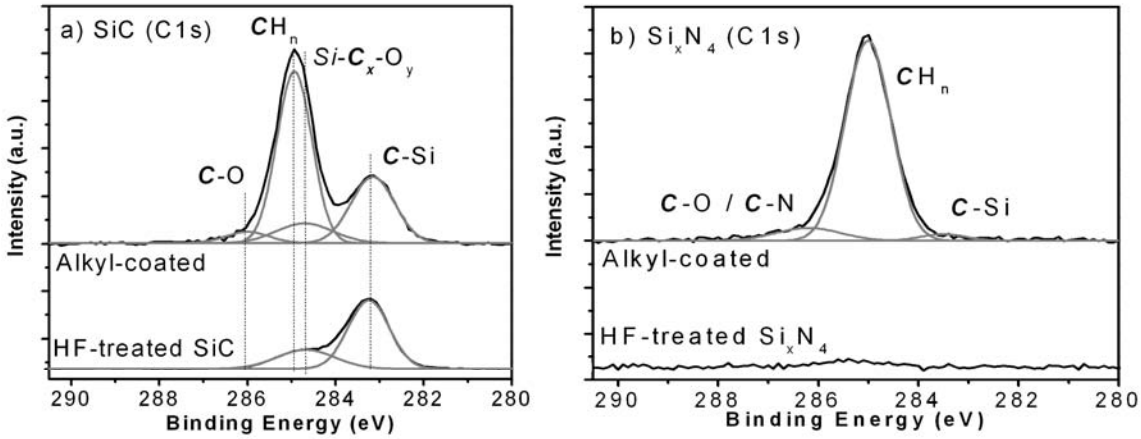

Figure 4. Normalized narrow-scan XPS data (C_{1s} region) measured on (a) SiC and (b) Si_xN_4 substrates etched (HF-treated) and coated with 1-hexadecene for 24 h under irradiation with 254 nm wavelength.

The formation of hexadecyl monolayers was confirmed by narrow-scan XPS C_{1s} regions measured on SiC and Si_xN_4 surfaces after 24 h of reaction (Figure 4), specifically by the clear increase in intensity of the peak at 285.0 eV, corresponding to alkyl chains on top of both substrates. Next to the main peak at 285.0 eV on both substrates, the fitted lines displayed in Figure 4 allow a more detailed description of the coatings. The spectrum measured on a 1-hexadecyl-coated SiC surface was fitted with 4 components, taking into account reference data measured on a bare etched SiC surface. Two components are related to the SiC substrate: a peak at 283.2 eV, corresponding to bulk silicon-bound carbon (Si***C***), and a peak at 284.7 eV corresponding to the carbon contained in the silicon oxycarbide ($Si\boldsymbol{C}_xO_y$) surface layer present after etching.[69] Before fitting, the ratio $A(Si\boldsymbol{C})/A(Si\boldsymbol{C}_xO_y)$ was fixed at 2.5, in accordance to the ratio observed on bare surfaces right after etching. The two remaining components were not present in the etched surfaces, but appear after reaction with hexadecene. The main peak at 285.0 eV is characteristic for the attached alkyl chains ($\boldsymbol{C}H_n$), and a small peak at higher binding energy (286.0 eV) reveals the presence of ***C***-O bonds, which probably results from the attachment of alkyl chains via an ether or silyl ether bond (C-O-C or Si-O-C). The ($\boldsymbol{C}H_n$)/(***C***-O) ratio of 12 indicates that probably all the alkyl chains are linked to the SiC surface via a C-O bond, as was reported for the thermal reaction. The ratio of 12 instead of 16 can be due to the low precision associated with the integration of the small signal at 286.0 eV. Stability measurements (*vide supra*) would tentatively suggest that all alkenes are reacted via ether formation. Similar XPS observations were made on Si_xN_4 (Figure 4b); the monolayer

formation caused a main alkyl peak at 285.0 eV. For these surfaces, no substrate carbon contributions were taken into account for the fitting of the C_{1s} region, since etched Si_xN_4 surfaces did not contain significant amounts of carbon. In addition, small peaks appeared at 286.2 eV (attributed to the formation of mainly C-N bonds), and at 283.5 eV, which can only be explained by the formation of Si-C bonds between a fraction of the alkyl chains and the substrate.[70] The ($\boldsymbol{C}H_n$)/($\boldsymbol{C}$-N) ratio approached a value of about 11, while the ($\boldsymbol{C}H_n$)/($\boldsymbol{C}$-Si) ratio was around 33. These results imply alkene attachment to the surface via both N and Si sites, but with a clear preference for C-N bond formation.

When surfaces were irradiated with wavelengths higher than 270 nm, the relative C_{1s} intensities measured ($\boldsymbol{C}H_n$ peak at 285.0 eV) after 24 h of irradiation displayed only 8% (on SiC) and 32% (on Si_xN_4) of the intensity measured on samples modified with 254 nm irradiation. This indicates formation of incomplete monolayers, even after prolonged irradiation. The significantly higher reactivity of Si_xN_4 surfaces with wavelengths > 270 nm, seems to confirm for these etched Si_xN_4 surfaces the presence of surface sites with different reactivities (e.g. Si clusters), as was suggested in the analysis of the etched samples (*vide infra*).

Figure 5 shows XPS data measured on surfaces coated with 1-hexadecene using 254 nm light for different irradiation times. SiC and Si_xN_4 displayed similar behavior: when the irradiation was carried out for a longer time than 24 h, which ensured an optimal monolayer formation (water contact angle $\geq 107^o$), the relative intensity of the XPS peak at 285.0 eV further increased, implying that the grafting of hydrocarbon chains went on even after the monolayer formation.

X-ray reflectivity (XRR) was used to measure the thickness of the 1-hexadecyl layers. While no proper signal was obtained on surfaces irradiated for 24 h or less (implying a layer thickness < 2 nm), the surfaces irradiated for 48 h showed a thickness of 4.0 ± 0.2 nm, much higher than the expected thickness of a hexadecyl monolayer (1.6 to 1.8 nm.[9,10]). The thickness of monolayers at intermediate irradiation times were calculated from XPS data (See the experimental part for the details of the calculation method). Thicknesses of alkyl monolayers on SiC substrates of 0.5, 0.8, 1.8 and 2.7 nm (± 15%) were obtained for irradiation times of 1, 5, 24, and 48 h, respectively. On Si_xN_4, the calculated thickness values were 0.7, 1.0, 1.5 and 2.3 nm (± 15%).

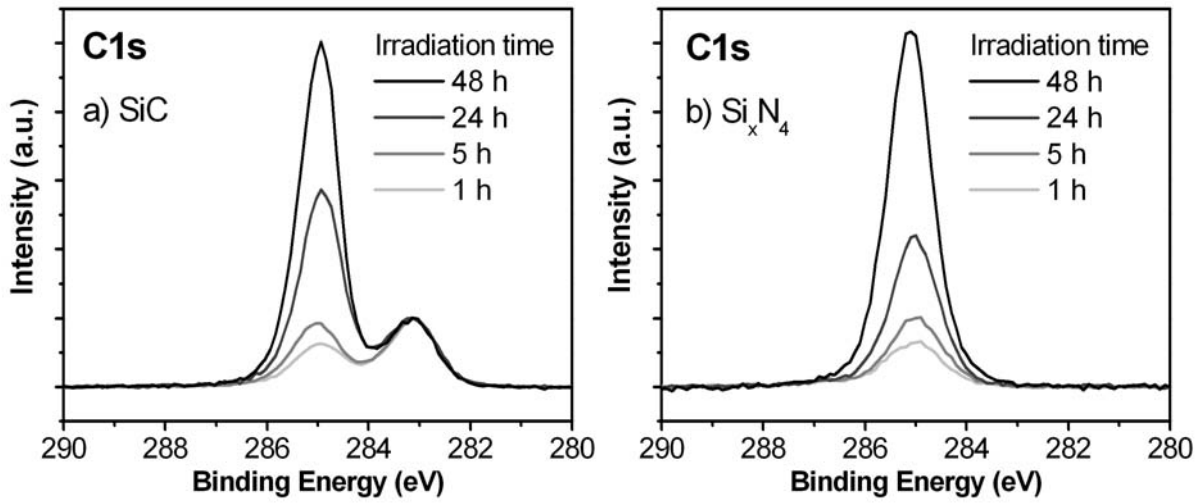

Figure 5. Normalized XPS (C_{1s} region) data measured on (a) SiC and (b) Si_xN_4 substrates modified with 1-hexadecene with 254 nm wavelength, as a function of irradiation time.

For both substrates, these calculations show a progressive increase of the monolayer thicknesses and a value after 24 h of reaction close to the expected thickness of hexadecyl monolayers (within the 15% precision of the calculation), which is confirmed by the maximum value of water contact angle measured at that time. After 48 h of irradiation, a lower thickness than the 4.0 ± 0.2 nm determined by XRR is found, which can perhaps be attributed to the assumptions used in the calculations. This approach confirms the formation of more than a monolayer for irradiation times longer than 24 h.

A GC/MS study of the irradiated alkenes (after up to 7 days of irradiation at 254 nm, in the presence of SiC or Si_xN_4 substrates) only revealed the presence of the initial 1-hexadecene, excluding the UV-initiated formation of rearrangement products or dimers of the alkene as these would still be detectable by GC.

Fluoroalkyl monolayers

In the previously reported case of the thermal modification of SiC, IRRAS measurements[54] provided evidence for a Markovnikov-type β-attachment of the 1-alkenes via the formation of an ether bond between the second carbon of the double bond and the abundantly present OH groups on SiC surfaces. This ether bond formation was also observed during the formation of alkene monolayers on silicon oxide.[13] We performed a similar IRRAS study on photochemically prepared monolayers with 11-fluoroundec-1-ene on SiC and Si_xN_4 surfaces, using 254 nm irradiation for 24 h. Figure 6 shows the C-H stretching region of IRRA spectra

measured on such surfaces. Both materials displayed after monolayer attachment symmetric and antisymmetric CH_2 stretching vibrations at 2856 ± 2 cm^{-1} and 2926 ± 2 cm^{-1}, respectively. These frequencies are typical for disordered monolayers.[8,9] This is in line with the maximum values of water contact angles measured on these alkyl layers (~ 107 ± 1°), which are significantly lower than values measured on more densely packed monolayers on silicon (~ 111 – 112°).[8]

More importantly, a clear methyl stretching is also observed at 2965 ± 2 cm^{-1} on both surfaces, while no methyl group is initially present in the starting alkene. This indicates that UV-induced monolayers are also formed via a Markovnikov-type addition. The methyl stretching peak is well resolved on SiC, and this is attributed to clean reactivity of the hydroxyl-terminated SiC surfaces via an addition on the second carbon of the double bond, as was observed with the thermal reactions. It is more difficult to assign a unique mechanism for the attachment on Si_xN_4 surfaces, where broader methyl features are observed in the IRRAS spectrum. This could be due to the more complex surface composition of this material, allowing several modes of attachment.

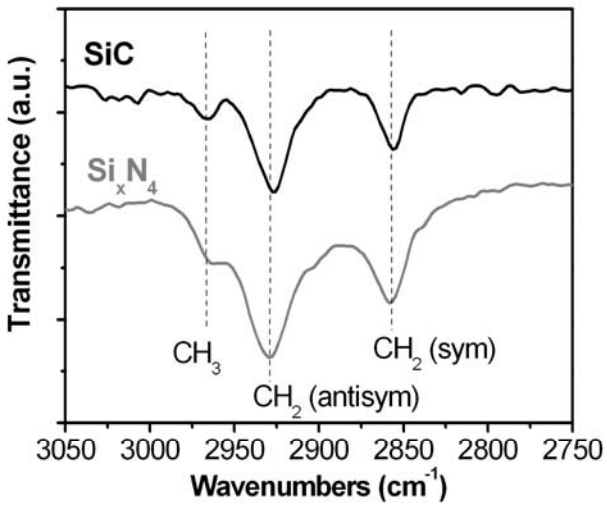

Figure 6. IRRA spectra measured on 11-fluoroundec-1-ene monolayers on SiC and Si_xN_4 substrates.

Mechanism of attachment

For the formation of organic monolayers on hydrogen-terminated silicon, radical initiation via Si-H homolytic cleavage was first used to explain the reaction initiation for UV methods.[3] The Si-H bond could be cleaved using an irradiation wavelength ≤ 350 nm (3.5 eV). However, irradiation with wavelengths above 600 nm also induces monolayer formation; electron-hole pair formation at the surface of silicon can then explain the reaction initiation, by creating positively charged species at the surface that can react with nucleophiles, like unsaturated C-C bonds.[70-72]

In the case of SiC and Si_xN_4, GC/MS analysis of 1-alkenes after reaction showed no formation of by-products, even after 7 days of irradiation, ruling out reactions in solution. It can thus be assumed that the grafting of alkenes is initiated by the formation of activated species at the surface of the substrates. Indeed, the 254 nm irradiation has enough energy per photon (4.9 eV) to overcome the bandgap of both materials (2.3 to 3 eV for SiC,[36] and 3 to 5 eV for Si_xN_4[66,73]), and to break chemical bonds with bond enthalpies < 4.9 eV. In particular, once the radiation has been absorbed by the material, a wide variety of bonds can, in principle, be broken, including Si-H (3.5 eV)[11,74], Si-Si (2.3 eV), or even the stronger Si-C, Si-O, Si-N or O-H bonds (all with bond enthalpies ≤ 4.9 eV[75,76]). Such cleavage reactions can form surface radicals, thus leading to the formation of a monolayer by reaction with alkenes. While this may indeed play a part on Si_xN_4, the formation of new methyl groups after reaction on etched SiC points to an ionic process (Markovnikov addition).

Stability of alkyl monolayers

The monolayers formed via 254 nm irradiation for 24 h were very stable under ambient conditions, and could withstand several cleaning and sonication steps in various solvents (acetone, petroleum ether and dichloromethane). The stability of hexadecyl monolayers in aqueous solutions was determined by XPS measurements after dipping these methyl-terminated monolayers into a 2 M HCl solution at 90 ºC or a 0.001 M NaOH solution at 60 ºC. The stability was monitored by normalizing the proportions of $\boldsymbol{C}H_n$ to the area of the substrate-related peaks: $C_{1s}(\boldsymbol{C}H_n)$ / $C_{1s}(\boldsymbol{C}$-Si) for SiC, and $C_{1s}(\boldsymbol{C}H_n)$ / N_{1s} for Si_xN_4 (Figure 7).

The hexadecyl monolayers on silicon carbide display a very good stability: even hot acid at negative pH only yields a marginal reduction of the XPS signal, and measurement of the static water contact angle does not lead to more than 1° difference after several hours.

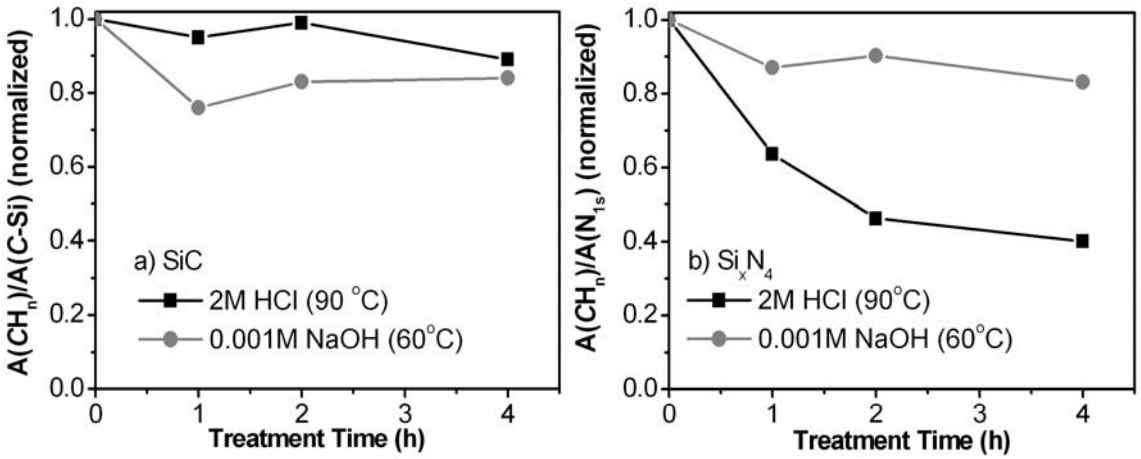

Figure 7. Stability of 1-hexadecene monolayers: normalized ratio of (a) $C_{1s}(\boldsymbol{C}H_n)$ / $C_{1s}(\boldsymbol{C}$-Si) measured on modified SiC and (b) $C_{1s}(\boldsymbol{C}H_n)$ / N_{1s} measured on modified Si_xN_4.

Under warm basic conditions both XPS C_{1s} data and water contact angle measurement indicate a somewhat reduced monolayer quality (water contact angle value of 96 ± 1° after 4 h versus 107 ± 1° directly after monolayer preparation), but the overall stability is still very good in comparison to any other organic monolayer that we know. For modified Si_xN_4 surfaces a good stability was again found under these warm basic conditions (pH = 11, 60 ºC), with a reduction of the XPS C_{1s} signal of 17% after 4 h and a concomitant reduction of the water contact angle from 107 ± 1° to 86 ± 1°. In the case of modified Si_xN_4, however, the stability under acidic conditions was unsatisfactory: only 40% of the signal corresponding to the alkyl coating remained after 4 hours of hot acidic treatment. This could be caused by the initial formation of N-C bonds, which may be prone to hydrolysis after protonation. Apparently, on SiC no such hydrolyzable bonds are present at the surface.

Organic monolayers on specifically SiC also display a remarkable stability towards hydrogen fluoride. Upon exposure of 1-hexadecyl monolayers to a 2.5% HF solutions for 1 h the water contact angle for monolayers on Si_xN_4 drops to 65º, but on SiC surfaces a superior stability is indicated by the contact angle value of 99º. This value is even higher than the value of 91º obtained after a similar treatment of thermally induced monolayers on SiC surfaces.[54] This increased stability could be due to the cross linking caused by UV irradiation: absorption of photons of 4.9 eV can provide homolytic bond cleavage of all surface-bound elements, which can provide surface-bound radicals. These can, even if with low efficiency, react with the formed monolayer. This would effect some degree of crosslinking in the

monolayer, allowing the retention of a nearly complete monolayer, even if some Si-O-C bonds were cleaved by HF. Applications of alkene-based monolayers on SiC and Si_xN_4 surfaces under aqueous conditions (in sensors or microsystems) can greatly benefit from the increased stability of modified surfaces in acidic and basic aqueous conditions, compared to organosilane monolayers that have been previously reported on SiC surfaces.[77]

Functional monolayers

Beside alkyl monolayers, functional coatings from covalently attached ω-functionalized 1-alkenes can be successfully formed onto both SiC and Si_xN_4 surfaces. Methyl undec-10-enoate and 2,2,2-trifluoroethyl undec-10-enoate (TFE) were successfully attached onto these materials using UV light. Figure 8 shows IRRA spectra of SiC surfaces modified with these two esters, displaying the expected values of 1747 ± 1 cm^{-1} and 1763 ± 1 cm^{-1} that correspond to the carbonyl stretching vibration of the methyl and trifluoroethyl ester, respectively.

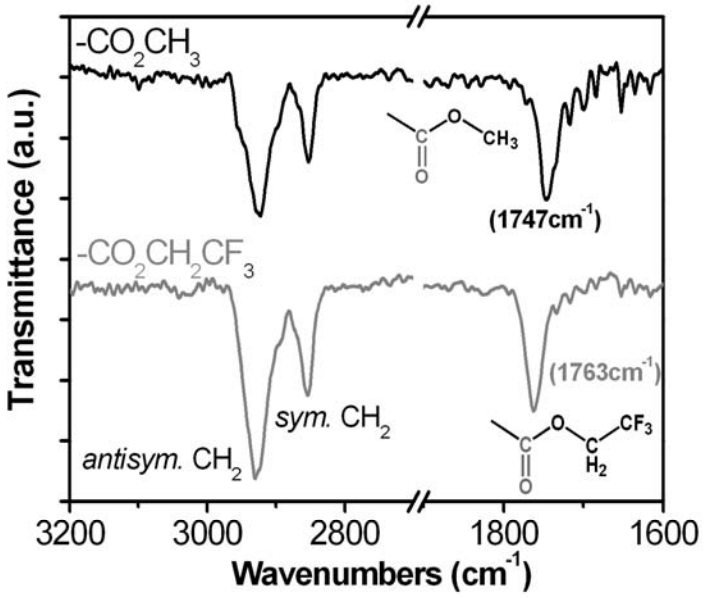

Figure 8. IRRA spectra of SiC substrates modified with methyl undec-10-enoate (up) and 2,2,2-trifluoroethyl undec-10-enoate (TFE, down).

To check that the UV-induced attachment could preserve the ester functionality, the TFE monolayers were also studied in more detail with XPS, as the $-CH_2-C(=O)OCH_2CF_3$ moiety can be used as a versatile handle to attach other amine-containing molecules to surfaces.[14,78] Figure 9 displays the XPS data measured on such a TFE-terminated SiC surface. The survey spectrum (Figure 9a) shows a high amount of fluorine at 689 eV (see for comparison the much smaller amount resulting from etching in Figure 1a). The narrow-scan XPS C_{1s} region

(Figure 9b) shows the characteristic binding energies associated with this compound: 293.4 eV (1: ***C***F_3), 289.8 eV (2: ***C***=O), 288.0 eV (3: CF_3-***C***H_2-O), 286.2 eV (4: -***C***H_2-CO), 285.0 eV (5: -***C***H_2-) and 283.2 eV (6: Si***C***). The relative areas of the signals of carbons 1, 2 and 3 (after background correction, *vide infra*) were 1.1 : 1 : 1.1, in very good agreement with the expected 1 : 1 : 1 ratio, and showing that the ester functionality can be attached in an intact manner. Due to the overlap with the large ***C***H_2 peaks (285.0 eV), it is hard to quantify the components corresponding to carbon 4 (-***C***H_2-CO) or to the carbon atom bound to the oxygen at the substrate (SiC-O-***C***H_2). However, the summed intensities of these 2 C atoms together with the remaining ***C***H_2 intensities is indeed in line with fully intact attachment of TFE-terminated monolayers.

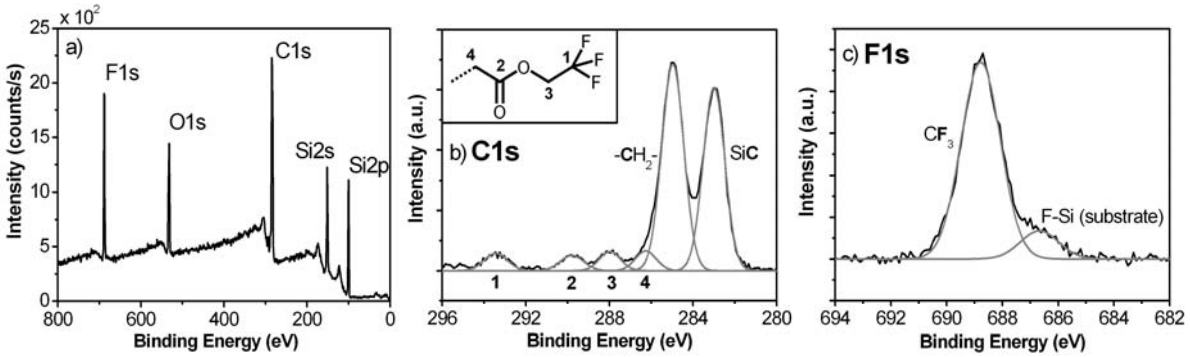

Figure 9. (a) XPS survey spectrum measured on a 2,2,2-trifluoroethyl undecyl monolayer on SiC and C_{1s} (b) and F_{1s} (c) regions of the XPS data measured on the same sample. Inset: assignment of the peaks to the corresponding carbon atoms of the ester.

The F_{1s} region of the XPS (Figure 9c) reveals the presence of two types of fluorine: a small amount of silicon-bound fluorine resulting from the HF treatment (686.7 eV), as was already seen in Figure 1, and the fluorine of the C***F***$_3$ group at 688.9 eV. The calculated C_{1s}(monolayer)/F_{1s}(C***F***$_3$) ratio of 4.5, is in excellent agreement with the expected theoretical value of 13/3 = 4.333, after correction for the contribution of the initial SiC substrate and the respective XPS sensitivities of carbon and fluorine.

TFE monolayers were subsequently subjected to further reactions at room temperature, including hydrolysis with a 0.25 M solution of potassium *tert*-butoxide in DMSO, followed by a NHS activation of the obtained carboxylic acids and subsequent reaction with *m*-(trifluoromethyl)benzylamine (TFBA), as depicted in Figure 10.

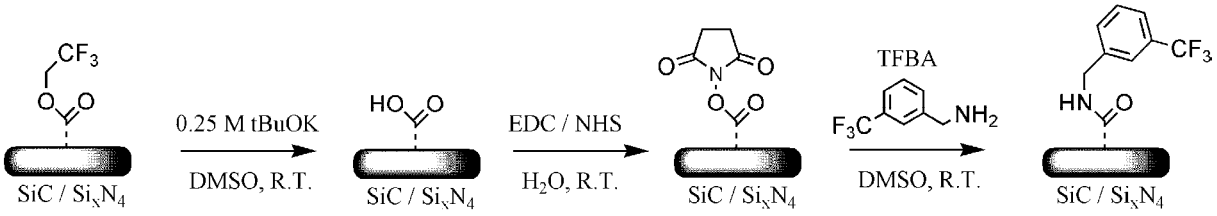

Figure 10. Functionalization of TFE monolayers on SiC or Si_xN_4 surfaces.

The different reaction steps were monitored with XPS (Figure 11): the main features observed in the high-resolution C_{1s} region clearly provide evidence for the expected reactivity: the hydrolysis (Figure 11b) caused the nearly complete disappearance of the ***C***F_3 signal at 293.4 eV. The unperturbed intensity of the peak corresponding to the alkyl chain at 285.0 eV demonstrates the stability of such monolayers under these hydrolysis conditions. The ***C***F_3 signal was then brought back upon coupling with TFBA, together with an increase of the signal between 285 and 286 eV, corresponding to the other carbon atoms of this compound.

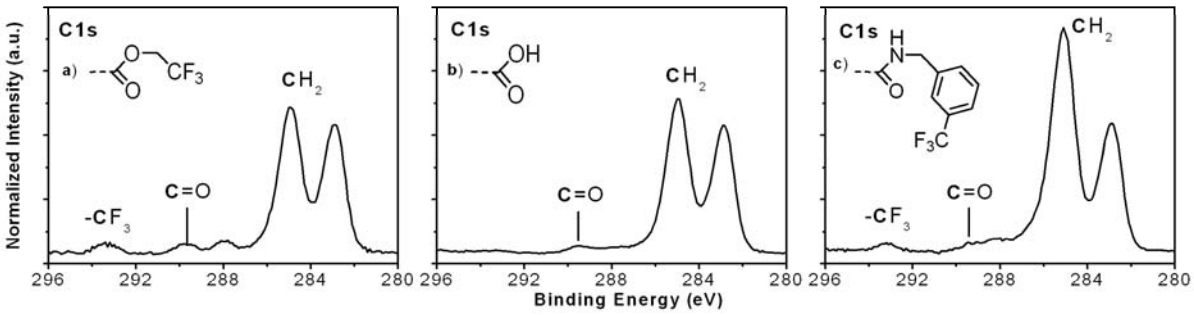

Figure 11. C_{1s} regions of the high-resolution XPS spectra measured on SiC substrates coated with (a) TFE monolayers, and subsequently subjected to (b) hydrolysis and (c) coupling with TFBA.

While the C_{1s} spectra monitor the overall reaction progress, the XPS F_{1s} region (Figure 12) allows a more precise determination of the efficiencies of the various reactions. Exposure of the TFE ester to tBuOK in DMSO brought the fluorine signal to 10 to 15% of its initial value, indicating an almost complete hydrolysis. The total removal of the trifluoroethyl moieties is likely hampered by surface roughness or disorder in the monolayers, causing some hindrance to the bulky *tert*-butoxide base. The coupling with TFBA after NHS activation restored the F_{1s} signal to about 70% of its initial value in the TFE monolayers.

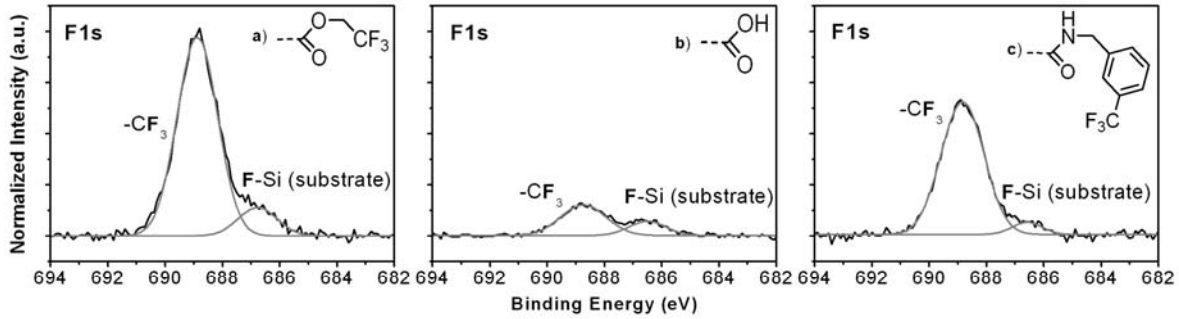

Figure 12. F_{1s} regions of the high-resolution XPS spectra measured on SiC substrates coated with (a) TFE monolayers, and subsequently subjected to (b) hydrolysis and (c) coupling with TFBA.

The less than 100% reaction yield is likely caused by several factors, including the size of the reagents used for the NHS-formation. In particular, partial hydrolysis of the NHS ester during the reaction with amines in aqueous media, and the size of the bulky EDC molecules – hampering the formation of a 100% NHS monolayer – will result in a less than 100% conversion.[79] The overall reaction yield will, however, be higher than the 70% suggested by the recovery of the F_{1s} signal: the different attenuation of electrons through the TFE and TFBA monolayers requires an additional step to translate the 70% of recovery in the F_{1s} signal to a quantitative reaction yield. The longer TFBA molecules (about 0.5 nm more than TFE, considering that the bulkier TFBA will likely adopt a more extended conformation) will likely cause the intensity of the substrate signal to be attenuated by 15 to 20% of its value in TFE monolayers.[58,59,80-82] Since all the reported spectra were normalized to the signal of this substrate (C_{1s}, Si***C*** at 283.2 eV), the reported signal intensities for F_{1s} (C***F***$_3$) can be corrected by the same values. The maximum measured recovery of 70% of the normalized F_{1s}(C***F***$_3$) signal would then correspond to an actual recovery of 80 to 85%, respectively, of the ester groups bearing the CF_3 functionalities. This result is in good agreement with the nearly quantitative reaction of amines with NHS ester.[83,84]

The same reaction sequence could be performed on Si_xN_4 substrates and monitored by XPS (Figure 13 and Figure 14), although the charging of the more insulating Si_xN_4 substrate decreased the XPS signal-to-noise ratio, compared to measurements on SiC surfaces. In this case, hydrolysis of the ester with potassium *tert*-butoxide caused a decrease of 95% of the F_{1s}(C***F***$_3$) signal and reaction with NHS and TFBA yielded a recovery of about 65% of this signal, similar to the results obtained on SiC surfaces.

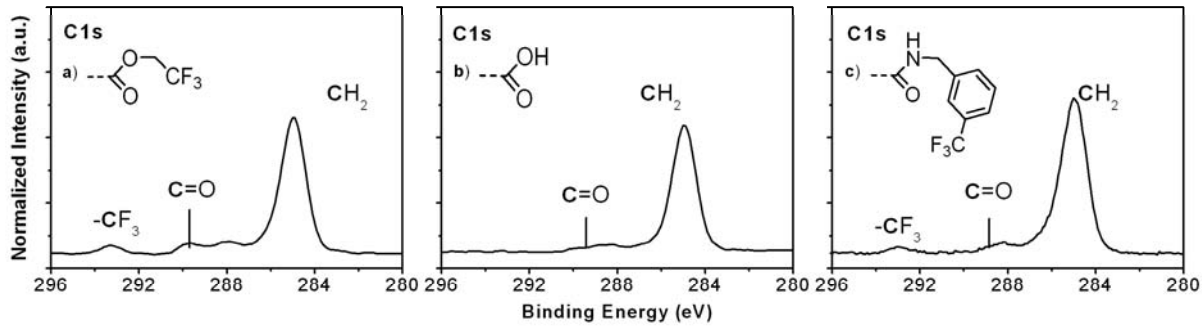

Figure 13. C_{1s} regions of the high-resolution XPS spectra measured on Si_xN_4 substrates coated with (a) TFE monolayers, and subsequently subjected to (b) hydrolysis and (c) coupling with TFBA.

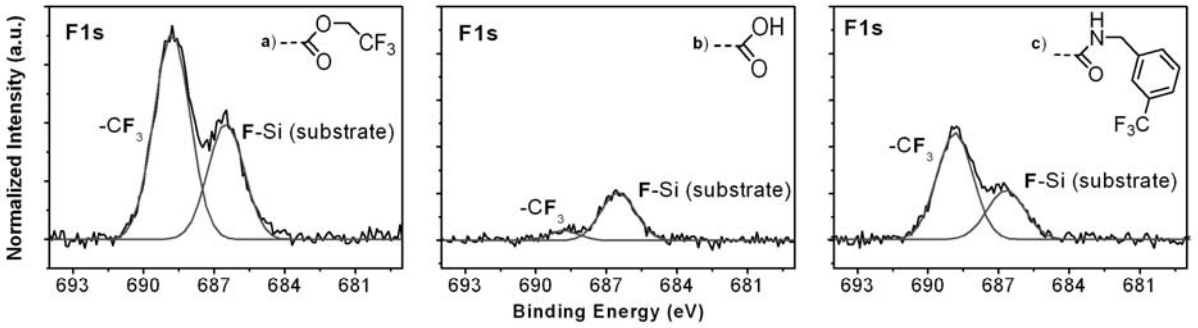

Figure 14. F_{1s} regions of the high-resolution XPS spectra measured on Si_xN_4 substrates coated with (a) TFE monolayers, and subsequently subjected to (b) hydrolysis and (c) coupling with TFBA.

Conclusions

A new way to produce very stable, covalently linked monolayers on SiC and Si_xN_4 surfaces, using UV irradiation at room temperature is presented. As shown previously in the case of thermally produced monolayers,[54] the attachment of the alkyl chains on SiC surfaces seems to occur via the formation of an ether bond between a thin oxycarbide layer and the second carbon of the double bond. On silicon nitride, the attachment seems to occur via several mechanisms, including most likely the formation of Si-C and N-C bonds, but the complex surface composition of etched Si_xN_4 surfaces makes it difficult to give a more precise description. Such UV-modified SiC and Si_xN_4 surfaces could withstand alkaline solutions, and alkyl-coated SiC surfaces even showed an excellent stability in both boiling 2M HCl and

2.5% HF. The possibility to form multilayers and the increased stability of these layers points to the involvement of radicals, which may provide further stability to the monolayers via internal cross-linking within the monolayers.

Robust functionalization of Si_xN_4 and SiC surfaces with a wide variety of (bio-)functional moieties is possible using a protecting trifluoethyl ester. This opens access to surface-bound amide chemistry that offers a convenient route for the attachment of biomolecules like peptides or DNA. A rich chemistry, similar to the one developed for organic monolayers on silicon surfaces,[8,17,18,85] including surface patterning can then be performed. Protein-repellent monolayers can also be formed with these methods, using oligoethylene glycol compounds.[86] This can be used in numerous microtechnological applications that involve SiC and Si_xN_4 as coating materials, when controlled sensing or antifouling properties are required.

Acknowledgments.

The authors thank Graduate School VLAG, MicroNed (Project no. 6163510395) for financial support, Professors Remko Boom (Wageningen University) and Ernst Sudhölter (Technical University of Delft) for stimulating discussions, and 2 reviewers of a previous version of this manuscript for helpful comments.

References

(1) Boukherroub, R. *Curr. Opin. Solid State Mater. Sci.* **2005,** *9*, 66-72.

(2) Buriak, J. M. *Chem. Rev.* **2002,** *102*, 1271-1308.

(3) Linford, M. R.; Fenter, P.; Eisenberger, P. M.; Chidsey, C. E. D. *J. Am. Chem. Soc.* **1995,** *117*, 3145-3155.

(4) Shirahata, N.; Hozumi, A.; Yonezawa, T. *Chem. Rec.* **2005,** *5*, 145-159.

(5) Sieval, A. B.; Linke, R.; Zuilhof, H.; Sudhölter, E. J. R. *Adv. Mater.* **2000,** *12*, 1457-1460.

(6) Wayner, D. D. M.; Wolkow, R. A. *J. Chem. Soc., Perkin Trans. 2* **2002**, 23-34.

(7) Linford, M. R.; Chidsey, C. E. D. *J. Am. Chem. Soc.* **1993,** *115*, 12631.

(8) Scheres, L.; Arafat, A.; Zuilhof, H. *Langmuir* **2007,** *23*, 8343-8346.

(9) Sieval, A. B.; Demirel, A. L.; Nissink, J. W. M.; Linford, M. R.; van der Maas, J. H.; de Jeu, W. H.; Zuilhof, H.; Sudhölter, E. J. R. *Langmuir* **1998,** *14*, 1759-1768.

(10) Sieval, A. B.; Opitz, R.; Maas, H. P. A.; Schoeman, M. G.; Meijer, G.; Vergeldt, F. J.; Zuilhof, H.; Sudhölter, E. J. R. *Langmuir* **2000,** *16*, 10359-10368.

(11) Cicero, R. L.; Linford, M. R.; Chidsey, C. E. D. *Langmuir* **2000,** *16*, 5688.

(12) Effenberger, F.; Gotz, G.; Bidlingmaier, B.; Wezstein, M. *Angew. Chem., Int. Ed.* **1998,** *37*, 2462-2464.
(13) Mischki, T. K.; Donkers, R. L.; Eves, B. J.; Lopinski, G. P.; Wayner, D. D. M. *Langmuir* **2006,** *22*, 8359-8365.
(14) Strother, T.; Cai, W.; Zhao, X. S.; Hamers, R. J.; Smith, L. M. *J. Am. Chem. Soc.* **2000,** *122*, 1205-1209.
(15) Strother, T.; Hamers, R. J.; Smith, L. M. *Nucleic Acids Res.* **2000,** *28*, 3535-3541.
(16) de Smet, L. C. P. M.; Pukin, A. V.; Sun, Q. Y.; Eves, B. J.; Lopinski, G. P.; Visser, G. M.; Zuilhof, H.; Sudhölter, E. J. R. *Appl. Surf. Sci.* **2005,** *252*, 24-30.
(17) de Smet, L. C. P. M.; Stork, G. A.; Hurenkamp, G. H. F.; Sun, Q. Y.; Topal, H.; Vronen, P. J. E.; Sieval, A. B.; Wright, A.; Visser, G. M.; Zuilhof, H.; Sudhölter, E. J. R. *J. Am. Chem. Soc.* **2003,** *125*, 13916-13917.
(18) Sun, Q.-Y.; de Smet, L. C. P. M.; van Lagen, B.; Giesbers, M.; Thune, P. C.; van Engelenburg, J.; de Wolf, F. A.; Zuilhof, H.; Sudhölter, E. J. R. *J. Am. Chem. Soc.* **2005,** *127*, 2514-2523.
(19) Aswal, D. K.; Lenfant, S.; Guerin, D.; Yakhmi, J. V.; Vuillaume, D. *Anal. Chim. Acta* **2006,** *568*, 84-108.
(20) Zhao, J. W.; Uosaki, K. *J. Phys. Chem. B* **2004,** *108*, 17129-17135.
(21) Choi, K.; Buriak, J. M. *Langmuir* **2000,** *16*, 7737-7741.
(22) Buriak, J. M. *Angew. Chem., Int. Ed.* **2001,** *40*, 532-534.
(23) Hovis, J. S.; Coulter, S. K.; Hamers, R. J.; D'Evelyn, M. P.; Russell, J. N.; Butler, J. E. *J. Am. Chem. Soc.* **2000,** *122*, 732-733.
(24) Wang, G. T.; Bent, S. F.; Russell, J. N.; Butler, J. E.; D'Evelyn, M. P. *J. Am. Chem. Soc.* **2000,** *122*, 744-745.
(25) Knickerbocker, T.; Strother, T.; Schwartz, M. P.; Russell, J. N.; Butler, J.; Smith, L. M.; Hamers, R. J. *Langmuir* **2003,** *19*, 1938-1942.
(26) Nichols, B. M.; Butler, J. E.; Russell, J. N.; Hamers, R. J. *J. Phys. Chem. B* **2005,** *109*, 20938-20947.
(27) Strother, T.; Knickerbocker, T.; Russell, J. N.; Butler, J. E.; Smith, L. M.; Hamers, R. J. *Langmuir* **2002,** *18*, 968-971.
(28) Wang, X.; Colavita, P. E.; Metz, K. M.; Butler, J. E.; Hamers, R. J. *Langmuir* **2007,** *23*, 11623-11630.

(29) Karymov, M. A.; Kruchinin, A. A.; Tarantov, Y. A.; Balova, I. A.; Remisova, L. A.; Vlasov, Y. G. *Sens. Actuators, B* **1995,** *29*, 324-327.

(30) McDonagh, C.; Burke, C. S.; MacCraith, B. D. *Chem. Rev.* **2008,** *108*, 400-422.

(31) Ymeti, A.; Greve, J.; Lambeck, P. V.; Wink, T.; van Hovell, S. W. F. M.; Beumer, T. A. M.; Wijn, R. R.; Heideman, R. G.; Subramaniam, V.; Kanger, J. S. *Nano Lett.* **2007,** *7*, 394-397.

(32) Anderson, A. S.; Dattelbaum, A. M.; Montano, G. A.; Price, D. N.; Schmidt, J. G.; Martinez, J. S.; Grace, W. K.; Grace, K. M.; Swanson, B. I. *Langmuir* **2008,** *24*, 2240-2247.

(33) Tlili, A.; Jarboui, M. A.; Abdelghani, A.; Fathallah, D. M.; Maaref, M. A. *Mater. Sci. Eng., C* **2005,** *25*, 490-495.

(34) Tlili, C.; Korri-Youssoufi, H.; Ponsonnet, L.; Martelet, C.; Jaffrezic-Renault, N. J. *Talanta* **2005,** *68*, 131-137.

(35) Goeders, K. M.; Colton, J. S.; Bottomley, L. A. *Chem.Rev.* **2008,** *108*, 522-542.

(36) Choyke, W. J.; Matsunami, H.; Pensl, G. *Silicon Carbide, Recent Major Advances*. Springer: Berlin, 2003.

(37) Godignon, P. *Mater. Sci. Forum* **2005,** *483*, 1009-1014.

(38) Saddow, S. E.; Agarwal, A. *Advances in Silicon Carbide: Processing and Applications*. Artech House Inc.: Boston, 2004.

(39) Stutzmann, M.; Garrido, J. A.; Eickhoff, M.; Brandt, M. S. *Phys. Stat. Sol. A* **2006,** *203*, 3424-3437.

(40) Yakimova, R.; Petoral, R. M.; Yazdi, G. R.; Vahlberg, C.; Spetz, A. L.; Uvdal, K. *J. Phys. D Appl. Phys.* **2007,** *40*, 6435-6442.

(41) Yang, Y. T.; Callegari, C.; Feng, X. L.; Ekinci, K. L.; Roukes, M. L. *Nano Lett.* **2006,** *6*, 583-586.

(42) Kuiper, S.; Brink, R.; Nijdam, W.; Krijnen, G. J. M.; Elwenspoek, M. C. *J. Membr. Sci.* **2002,** *196*, 149-157.

(43) Kuiper, S.; van Wolferen, H.; van Rijn, G.; Nijdam, W.; Krijnen, G.; Elwenspoek, M. *J. Micromech. Microeng.* **2001,** *11*, 33-37.

(44) van Rijn, C. J. M.; Veldhuis, G. J.; Kuiper, S. *Nanotechnology* **1998,** *9*, 343-345.

(45) van Rijn, C. J. M. *Nano and Micro Engineered Membrane Technology*. Aquamarijn Research BV, The Netherlands: 2002.

(46) Singh, S.; Buchanan, R. C. *Mater. Sci. Eng., C* **2007,** *27*, 551-557.

(47) Cogan, S. F.; Edell, D. J.; Guzelian, A. A.; Liu, Y. P.; Edell, R. *J. Biomed. Mater. Res. A* **2003,** *67A*, 856-867.
(48) de Carlos, A.; Borrajo, J. P.; Serra, J.; Gonzalez, P.; Leon, B. *J. Mater. Sci. Mater. Med.* **2006,** *17*, 523-529.
(49) Rosenbloom, A. J.; Sipe, D. M.; Shishkin, Y.; Ke, Y.; Devaty, R. P.; Choyke, W. J. *Biomed. Microdev.* **2004,** *6*, 261-267.
(50) Santavirta, S.; Takagi, M.; Nordsletten, L.; Anttila, A.; Lappalainen, R.; Konttinen, Y. T. *Arch. Orthop. Trauma. Surg.* **1998,** *118*, 89-91.
(51) Sella, C.; Martin, J. C.; Lecoeur, J.; Lechanu, A.; Harmand, M. F.; Naji, A.; Davidas, J. P. *Mater. Sci. Eng., A* **1991,** *139*, 49-57.
(52) Arafat, A.; Giesbers, M.; Rosso, M.; Sudhölter, E. J. R.; Schroen, K.; White, R. G.; Yang, L.; Linford, M. R.; Zuilhof, H. *Langmuir* **2007,** *23*, 6233-6244.
(53) Arafat, A.; Schroën, K.; de Smet, L. C. P. M.; Sudhölter, E. J. R.; Zuilhof, H. *J. Am. Chem. Soc.* **2004,** *126*, 8600-8601.
(54) Rosso, M.; Arafat, A.; Schroen, K.; Giesbers, M.; Roper, C. S.; Maboudian, R.; Zuilhof, H. *Langmuir* **2008,** *24*, 4007-4012.
(55) Coffinier, Y.; Boukherroub, R.; Wallart, X.; Nys, J. P.; Durand, J. O.; Stievenard, D.; Grandidier, B. *Surf. Sci.* **2007,** *601*, 5492-5498.
(56) Roper, C. S.; Radmilovic, V.; Howe, R. T.; Maboudian, R. *J. Electrochem. Soc.* **2006,** *153*, C562-C566.
(57) Cumpson, P. J. *Surf. Interface Anal.* **2000,** *29*, 403-406.
(58) Laibinis, P. E.; Bain, C. D.; Whitesides, G. M. *J. Phys. Chem.* **1991,** *95*, 7017-7021.
(59) Lamont, C. L. A.; Wilkes, J. *Langmuir* **1999,** *15*, 2037-2042.
(60) Tanuma, S.; Powell, C. J.; Penn, D. R. *Surf. Interface Anal.* **1993,** *20*, 77-89.
(61) Jablonski, A.; Powell, C. J. *Surf. Sci. Rep.* **2002,** *47*, 33-91.
(62) Wijesundara, M. B. J.; Valente, G.; Ashurst, W. R.; Howe, R. T.; Pisano, A. P.; Carraro, C.; Maboudian, R. *J. Electrochem. Soc.* **2004,** *151*, C210-C214.
(63) Muehlhoff, L.; Bozack, M. J.; Choyke, W. J.; Yates, J. T. *J. Appl. Phys.* **1986,** *60*, 2558-2563.
(64) Roccaforte, F.; La Via, F.; Raineri, V.; Musumeci, P.; Calcagno, L.; Condorelli, G. G. *Appl. Phys. Mater. Sci. Process.* **2003,** *77*, 827-833.
(65) Starke, U. *Phys. Stat. Sol. B* **1997,** *202*, 475-499.
(66) Pei, Z. W.; Hwang, H. L. *Appl. Surf. Sci.* **2003,** *212*, 760-764.

(67) Andersen, K. N.; Svendsen, W. E.; Stimpel-Lindner, T.; Sulima, T.; Baumgartner, H. *Appl. Surf. Sci.* **2005,** *243*, 401-408.

(68) Bermudez, V. M. *J. Electrochem. Soc.* **2005,** *152*, F31-F36.

(69) Avila, A.; Montero, I.; Galan, L.; Ripalda, J. M.; Levy, R. *J. Appl. Phys.* **2001,** *89*, 212-216.

(70) Terry, J.; Linford, M. R.; Wigren, C.; Cao, R. Y.; Pianetta, P.; Chidsey, C. E. D. *J. Appl. Phys.* **1999,** *85*, 213-221.

(71) Reboredo, F. A.; Schwegler, E.; Galli, G. *J. Am. Chem. Soc.* **2003,** *125*, 15243-15249.

(72) Stewart, M. P.; Buriak, J. M. *J. Am. Chem. Soc.* **2001,** *123*, 7821-7830.

(73) Dal Negro, L.; Yi, J. H.; Hiltunen, M.; Michel, J.; Kimerling, L. C.; Hamel, S.; Williamson, A. J.; Galli, G.; Chang, T.-W. F.; Sukhovatin, V.; Sargent, E. H. *J. Exp. Nanosci.* **2006,** *1*, 29-50.

(74) Kanabuskaminska, J. M.; Hawari, J. A.; Griller, D.; Chatgilialoglu, C. *J. Am. Chem. Soc.* **1987,** *109*, 5267-5268.

(75) Sanderson, R. T. *Chemical bonds and bond energy*. 2nd ed.; Academic Press: New York, 1976.

(76) Mercs, D.; Briois, P.; Demange, V.; Lamy, S.; Coddet, C. *Surf. Coat. Technol.* **2007,** *201*, 6970-6976.

(77) Schoell, S. J.; Hoeb, M.; Sharp, I. D.; Steins, W.; Eickhoff, M.; Stutzmann, M.; Brandt, M. S. *Appl. Phys. Lett.* **2008,** *92*, -.

(78) Kohler, N.; Fryxell, G. E.; Zhang, M. Q. *J. Am. Chem. Soc.* **2004,** *126*, 7206-7211.

(79) Yang, M.; Teeuwen, R. L. M.; Giesbers, M.; Baggerman, J.; Arafat, A.; de Wolf, F. A.; van Hest, J. C. M.; Zuilhof, H. *Langmuir* **2008,** *24*, 7931-7938.

(80) Harder, P.; Grunze, M.; Dahint, R.; Whitesides, G. M.; Laibinis, P. E. *J. Phys. Chem. B* **1998,** *102*, 426-436.

(81) Laibinis, P. E.; Bain, C. D.; Nuzzo, R. G.; Whitesides, G. M. *J. Phys. Chem.* **1995,** *99*, 7663-7676.

(82) Popat, K. C.; Mor, G.; Grimes, C. A.; Desai, T. A. *Langmuir* **2004,** *20*, 8035-8041.

(83) Guo, D. J.; Xiao, S. J.; Xia, B.; Shuai-Wei; Pei, J.; Pan, Y.; You, X. Z.; Gu, Z. Z.; Lu, Z. H. *J. Phys. Chem. B* **2005,** *109*, 20620-20628.

(84) Voicu, R.; Boukherroub, R.; Bartzoka, V.; Ward, T.; Wojtyk, J. T. C.; Wayner, D. D. M. *Langmuir* **2004,** *20*, 11713-11720.

(85) Sun, Q.-Y.; de Smet, L. C. P. M.; van Lagen, B.; Wright, A.; Zuilhof, H.; Sudhölter, E. J. R. *Angew. Chem., Int. Ed.* **2004,** *43*, 1352-1355.
(86) Rosso, M.; de Jong, E.; Giesbers, M.; Fokkink, R. G.; Norde, W.; Schroen, K.; Zuilhof, H., submitted.

Chapter 7

Protein-Repellent Silicon Nitride Surfaces: UV-Induced Formation of Oligoethylene Glycol Monolayers

Grafting of polymers and oligomers of ethylene oxide onto surfaces has been widely used to prevent non-specific adsorption of biologic material on sensors and membrane surfaces. In this work, we show for the first time the covalent attachment of short oligoethylene oxide-terminated alkenes onto silicon-rich silicon nitride (Si_xN_4) surfaces at room temperature using UV light. Reflectometry was then used to monitor *in situ* the non-specific adsorption of BSA and fibrinogen onto plasma-oxidized surfaces, and the reduction or complete prevention thereof on modified surfaces. Furthermore, we used atomic force microscopy (AFM), X-Ray photoelectron spectroscopy (XPS), X-ray reflectivity and water contact angle measurements to characterize the modified surfaces before protein adsorption, while AFM and contact angles were used to evaluate the surfaces after exposure to protein. EO_n-coated Si_xN_4 surfaces displayed a dramatically lowered protein adsorption. The performance of the obtained EO_n layers is comparable to those of similar, highly effective monolayers formed on gold or silver surfaces, but the stability of covalently attached monolayers on Si_xN_4 is clearly superior. This combination of stability and protein repellence allows a significant improvement of silicon nitride-coated microdevices, and in particular micro-fabricated membranes.

This chapter will be published as:
"Protein-Repellent Silicon Nitride Surfaces: UV-Induced Formation of Oligoethylene Glycol Monolayers", Rosso, M.; de Jong, E.; Giesbers, M.; Fokkink, R. G.; Norde, W.; Schroën, K.; Zuilhof, H., submitted.

Introduction

Silicon-rich silicon nitride (Si_xN_4) is a widely used insulator for microelectronics and microsystem coatings.[1] Films of this material inhibit diffusion of water, oxygen and sodium ions and are widely used as passivation layers in integrated circuits.[2] Si_xN_4 is not only popular because of its superior physical robustness and chemical inertness,[3] but also because it provides an excellent alternative to silicon dioxide[4] in microelectronic and membrane applications.[5-7]

Biocompatibility is an important issue for the use of Si_xN_4 films as coatings for biosensors or filtration membranes. In particular, the development of microfabricated filtration membranes (microsieves) is hindered by non-specific adsorption of biomolecules on surfaces during filtration, especially proteins (aggregates),[8,9] which dramatically affect the performance of the devices. Furthermore, the adsorption of the first protein layer is a decisive step in surface fouling as it usually initiates surface contamination, creating suitable conditions for the subsequent adsorption of more protein aggregates,[10] but also of cells, bacteria and other microorganisms.[11]

Increasing the hydrophilic properties of Si_xN_4 surfaces partially solves the problem of protein fouling. Indeed, hydrophilic membranes are less subject to fouling and have a longer operational life.[12-14] An air-based plasma treatment, for instance, that superficially oxidizes the silicon nitride surfaces, can improve the wettability and performance of membranes; however, the hydrophilic character obtained this way is only temporary.[15]

Widely used alternative solutions to reduce protein adsorption onto surfaces include self-assembled monolayers (SAMS) of ethylene oxide (EO) oligomers. This approach has been applied to polymers,[16-21] gold and silver,[22-30] glass and other oxides,[31-39] and etched silicon surfaces.[18,40-44] The application to silicon nitride would require a method for the robust attachment of such EO-based materials. Several studies reported on the specific modification of AFM tips[45-50] with polyethylene glycol chains, for applications where only a few attached chains were sufficient. Some work has been carried out on the attachment of long polyethylene glycol chains on oxidized silicon nitride,[51] but these heterogeneous coatings were not stable in water. Organosilane compounds have been used to graft polyethylene glycol methacrylate[52] onto oxidized silicon nitride, giving layers with some protein-repellent properties, but the obtained layers were not stable in alkaline conditions, probably because of the hydrolysis of Si-O bonds. Another report on organosilane-based monolayers of linear

oligoethylene glycol molecules (3 to 12 ethylene oxide units) on oxidized silicon nitride substrates[53] also mentioned a good thermal stability, but details on the stability in aqueous solutions were not given. Recently, we have shown that it was possible to covalently attach an organic monolayer onto a silicon nitride[54,55] or silicon carbide[56] surface, using conditions close to those used for the thermal hydrosilylation of silicon surfaces.[57-59] Stable and good-quality monolayers were obtained with several simple alkenes, as well as esters, allowing further (bio-)chemical surface modifications. The layers were stable in aqueous solutions, which is essential for application on e.g. microsieves.

Very recently we demonstrated that this modification can also be initiated by UV light at room temperature using less compound and a simpler experimental set-up.[60] This extends the method to monolayers formed with more labile and/or more expensive alkenes. In the current paper, we report on the use of this last method to attach oligo-EO-terminated monolayers onto silicon-rich silicon nitride surfaces in a single step procedure. In particular, methoxy-tri(ethylene oxide) undec-1-ene ($CH_3O(CH_2CH_2O)_3(CH_2)_9CH=CH_2$; EO_3), and methoxy-hexa(ethylene oxide) undec-1-ene ($CH_3O(CH_2CH_2O)_6(CH_2)_9CH=CH_2$; EO_6) were synthesized and grafted onto etched silicon-rich silicon nitride (Si_xN_4) surfaces. The obtained monolayers were characterized with X-ray photoelectron spectroscopy (XPS), static water contact angle measurements, X-ray reflectivity, and atomic force microscopy (AFM). Subsequently, the protein-repelling properties of surfaces were investigated by studying the adsorption of bovine serum albumin (BSA) and fibrinogen from solution, both *in situ* by reflectometry and *ex situ* by static water contact angle measurement and AFM. In each case, the anti-fouling properties of modified surfaces were compared to those of plasma-treated Si_xN_4 surfaces, to reveal the potential of EO-modified monolayers.

Experimental Section

Materials

Bovine serum albumin (fraction V, min 96% lyophilized powder) and fibrinogen (fraction I from pig plasma, 78% in protein) were purchased from Sigma. Sodium phosphate dibasic (analytical grade, Acros), potassium dihydrogenophosphate (ACS grade, Merck), potassium chloride (pro analysis, Merck) and sodium chloride (puriss., Riedel-de-Haën) were used to prepare the PBS buffer. Triethylene glycol (> 99%), triethylene glycol monomethyl ether (>

97%) and anhydrous DMF (99.5%) were purchased from Fluka. 11-Undecen-1-ol (98%), tosyl chloride (98%), sodium hydride (60% dispersion in mineral oil) were purchased from Aldrich. All solvents were distilled before use.

Synthesis of EO_3 and EO_6

EO_3 and EO_6 were synthesized according the scheme presented in Figure 1. The asymmetric oligoethylene oxide moieties were synthesized via a method from Yam et al.,[44] without the use of protecting groups, but using an excess of triethylene glycol **3**. The slightly less polar CH_3-$(OCH_2CH_2)_6$-OH (compound **4**), and the even longer CH_3-$(OCH_2CH_2)_9$-OH (not shown) could be easily extracted using CH_2Cl_2 or $CHCl_3$.

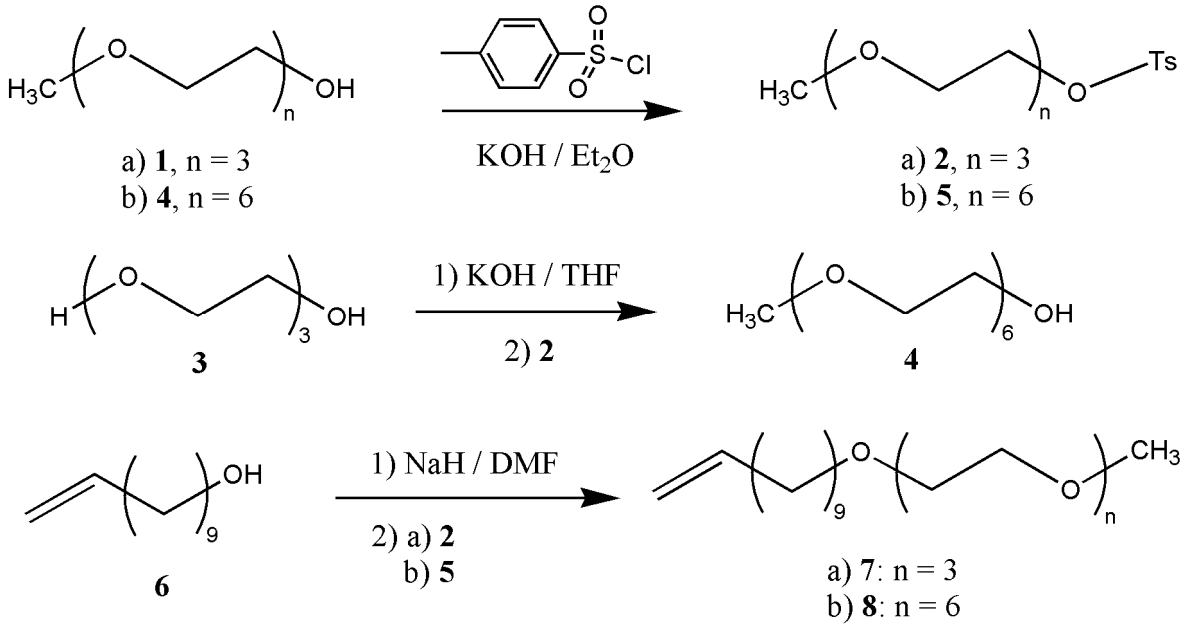

Figure 1. Scheme for the synthesis of EO_3 and EO_6 molecules.

Triethylene glycol methyl ether ω-methylbenzenesulfonate (2).

Triethylene glycol monomethyl ether (**1**, 34.14 g, 208 mmol) and *p*-toluenesulfonyl chloride (43.80 g, 230 mmol) were dissolved in 100 mL of diethyl ether. Freshly ground KOH (46.70 g, 830 mmol) was then added in several portions to the ice-cooled solution, keeping the temperature below 5 °C. After 3 hours of reaction, 75 mL of ice and water were added, the organic phase was extracted 3 times with diethyl ether. The combined organic fractions were washed with water, dried on Na_2SO_4, filtered, and the solvent was evaporated under reduced pressure to give **2** as a colorless oil (63.5 g, 96%). **^{1}H-NMR** (300 MHz, $CDCl_3$): δ 2.45 (s, 3H), 3.38 (s, 3H), 3,53 (t, 2H), 3.61 (m, 6H), 3.70 (t, *J* = 6, 2H); 4.17 (t, *J* = 6, 2H), 7.35 (d, *J*

= 7.5, 2H), 7.80 (d, *J* = 7.5, 2H); **^{13}C-NMR** (300 MHz, $CDCl_3$): δ 21.58, 58.95, 68.64, 69.23, 70.51, 70.71, 71.88, 127.93, 129.80, 133.06, 144.77.

Hexaethylene glycol monomethyl ether (4).

Under argon atmosphere, triethylene glycol (**3**, 42 g, 283 mmol) was dissolved in anhydrous THF (40 mL), and the resulting solution was brought to reflux. Freshly ground KOH (3 g, 52 mmol) was added in small portions. After complete dissolution, the solution was cooled to room temperature, and **2** (15 g, 47 mmol) in 20 mL of THF was added drop by drop. The solution was then refluxed under argon overnight. After evaporation of THF under vacuum, water was added to the resulting mixture, and the solution was extracted with dichloromethane until no product was detected by TLC (eluent: ethyl acetate). **4** was obtained as a pale yellow oil (11.3 g, 81%). **^{1}H-NMR** (300 MHz, $CDCl_3$): δ 2.70 (m, 1H), 3.32 (s, 3H), 3.47-3.62 (m, 24H); **^{13}C-NMR** (300 MHz, $CDCl_3$): δ 60.96, 69.99, 70.04, 70.15, 71.61, 72.34.

Hexaethylene glycol methyl ether ω-methylbenzenesulfonate (5).

The synthesis was carried out as for **2**. After evaporation of solvents, **5** was obtained as colorless oil (11.15 g, 89%). **^{1}H-NMR** (300 MHz, $CDCl_3$): δ 2.45 (s, 3H), 3.38 (s, 3H), 3.53-3.71 (m, 22H), 4.16 (t, 2H), 7.35 (d, J = 6, 2H), 7.81 (d, J = 6, 2H); **^{13}C-NMR** (300 MHz, $CDCl_3$): δ 21.63, 59.01, 68.67, 69.23, 70.51, 70.55, 70.60, 70.74, 71.93, 127.97, 129.81, 133.03, 144.77.

EO_3: Triethylene glycol methyl ω-undecenyl ether (7).

In a dry vessel, under Argon atmosphere, NaH (2 g of 60% dispersion in mineral oil, 27.7 mmol) was cleaned three times with pentane, and 20 mL of dry DMF were eventually added. The vessel being kept at 0 ºC in an ice bath, 10-undecen-1-ol (**6**, 4.71 g, 27.7 mmol) in THF was added dropwise. After 4 hours, hydrogen evolution being finished, **2** (8 g, 25.1 mmol) was added dropwise. The reaction was left stirring overnight under argon. After quenching with water, the mixture was extracted 3 times with ether. The combined organic phases were washed with brine, dried over Na_2SO_4, and the solvent was evaporated to give a pale yellow oil. After purification with silica gel column chromatography, with a 2/1 mixture of ethyl acetate/petroleum ether (40/60), 6.1 g (73%) of **7** were obtained as a colorless oil. **^{1}H-NMR** (300 MHz, $CDCl_3$): δ 1.25-1.4 (br, 14H), 1.58 (t, J = 6, 2H), 2.06 (m, 2H), 3.39 (s, 3H), 3.46 (t, J = 6, 2H), 3.55-3.68 (m, 10H), 4.97 (m, 2H), 5.82 (m, 1H). **^{13}C-NMR** (300 MHz, $CDCl_3$):

δ 26.08, 28.92, 29.11, 29.42, 29.46, 29.53, 29.63, 33.80, 59.03, 70.05, 70.53, 70.60, 70.64, 71.53, 70.95, 114.09, 139.22.

EO_6: Hexaethylene glycol methyl ω-undecenyl ether (8).

The synthesis was carried out as for **7**. After evaporation of the solvents, **8** was obtained as pale yellow oil. After purification on column chromatography (eluent: ethyl acetate), 4.52 g (65%) of colorless oil was obtained. **^{1}H-NMR** (300 MHz, $CDCl_3$): δ 1.3-1.45 (m, 14H), 1.58 (t, J = 6, 2H), 2.05 (m, 2H), 3.39 (s, 3H), 3.46 (t, J = 6, 2H), 3.55-3.75 (m, 22H), 4.95 (m, 2H), 5.82 (m, 1H). **^{13}C-NMR** (300 MHz, $CDCl_3$): δ 26.08, 28.92, 29.12, 29.43, 29.46, 29.53, 29.63, 33.80, 59.03, 70.06, 70.53, 70.59, 71.54, 71.95, 114.09, 139.23.

Monolayer Formation

Silicon-rich silicon nitride samples (CVD Si_xN_4 on Si100, thickness of 147 nm, obtained from Lionix B.V., The Netherlands, with sizes of 1 × 1 cm for XPS or 4 × 0.75 cm for reflectometry) were cleaned by sonication in acetone, followed by oxidation in air-based plasma for 15 min. The oxidized samples were then etched with a 2.5% aqueous solution of HF for 2 min and dried in a nitrogen flow. The substrates were then immediately dipped into argon-saturated neat alkenes in a quartz flask. After 30 more min under argon flow, a UV pen lamp (254 nm, low pressure mercury vapor, double bore lamp from Jelight Cie, California) was placed 4 mm above the Si_xN_4 surface and the sample was irradiated for 24 h. Afterwards, samples were removed and rinsed several times with ethyl acetate, ethanol and dichloromethane, and sonicated in the same solvents. Reference hydrophilic surfaces were only plasma-treated for 10 min. Angle-resolved XPS revealed that such plasma-treated surfaces presented a thin hydrophilic layer of silicon oxy-nitride (Atomic composition of the first 10 nm: 40% Si_2p, 30% N_{1s}, 20% O_{1s}, 10% C_{1s}, values obtained from XPS ± 5%).

Monolayer Characterization

Static water contact angle measurements

The wetting properties of modified surfaces were characterized by automated static water contact angle measurements performed using an Erma Contact Angle Meter G-1 (volume of the drop of demineralized water = 3.5 μl).

X-ray Photoelectron Spectroscopy (XPS)

The XPS analysis of surfaces was performed using a JPS-9200 Photoelectron Spectrometer (JEOL, Japan). The high-resolution spectra were obtained under UHV conditions using monochromatic Al K_α X-ray radiation at 12 kV and 25 mA, using an analyzer pass energy of 10 eV. High-resolution spectra were corrected with a linear background before fitting.

X-ray reflectivity

X-ray reflectivity measurements were performed on a Panalytical X'Pert Pro diffractometer using nickel filtered Cu K_α radiation (tube settings 50 kV and 40 mA). The data were collected using a fixed divergence slit 1/32°, and a parallel plate collimator on the diffracted beam side. The layer thickness was calculated from the interference fringes.

Atomic force microscopy (AFM)

Images were obtained with an MFP-3D AFM from Asylum Research (Santa Barbara, CA). Imaging was performed in AC mode in air using OMCL-AC240 silicon cantilevers (Olympus Corporation, Japan). The root mean square (RMS) roughness was calculated from the fluctuations of the surface height around the average height in the image. In this way, the RMS value describes the topography of the surface. The RMS is the standard deviation, i.e. the square root of the variance, of the Z-values within the image, according to: RMS = $\sqrt{(\sum(Z_i)^2/n)}$

Reflectometry

In a typical reflectometer (Figure 2), a monochromatic light beam (He-Ne laser; 632.8 nm) is linearly polarized and passes a 45° glass prism. This beam arrives at the interface with an angle of incidence of 66º for the solvent/substrate interface. After reflection at the interface and refraction in the prism, the beam is split into its p- and s-polarized components relative to the plane of incidence by means of a beam splitter. Both components are separately detected by two photodiodes and the ratio between the intensity of the parallel and perpendicular components is the output signal S ($S = I_p/I_s$) (the output signal given by the detection box is 10 × S). It is combined with a stagnation point flow cell, allowing the introduction of buffer or protein solutions, to study homogeneous adsorption on surfaces in diffusion-controlled conditions.

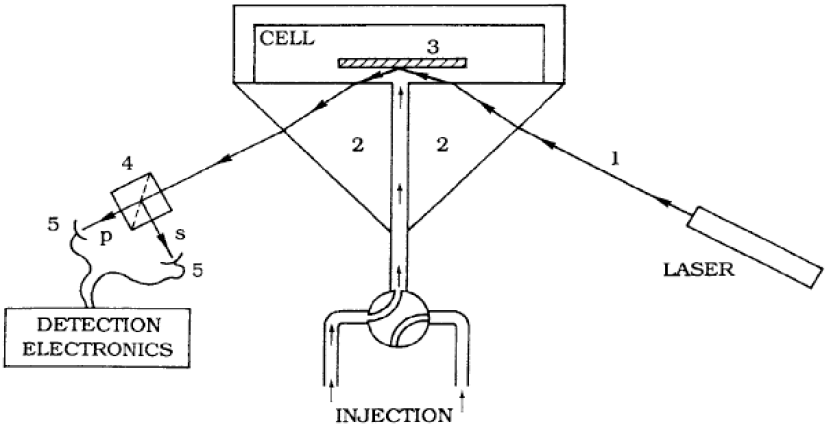

Figure 2. Schematic representation of the fixed angle reflectometer: 1) laser beam, 2) glass prism, 3) sample, 4) beam splitter, 5) photodiodes.

Strips of Si_xN_4-coated silicon wafer (typical size of 4 × 0.75 cm) were modified with alkenes on one end (about half of the sample length), while the other end was used to hold the strip in the measuring cell of the reflectometer. The BSA and fibrinogen solutions (0.1 mg/L) were freshly prepared in PBS buffer (pH 6.75, ionic strength 0.08 M). All reflectometry experiments were performed at 23 ºC. Before measurements were taken, surfaces were incubated 1 h in buffer to avoid artifacts due to initial surface wetting (especially relevant in the case of EO_n-modified samples).

After placing the samples in the reflectometer, the buffer solution was injected until the output signal was nearly constant: fluctuations of less than 0.01 V over 2 min were considered satisfactory. Each experiment involved at least one adsorption phase, in which protein solutions were injected onto the surface, and one subsequent desorption phase, in which only buffer was injected. The adsorbed amounts were calculated from equation 1, where Γ = adsorbed amount (mg/m^2), Q_f = sensitivity factor (mg/m^2), S_0 (mV) = signal given by the reflectometer before introducing protein solutions, and ΔS (mV) = recorded difference in signal before and after introduction of the protein solutions:[61]

$$\Gamma = Q_f \cdot \frac{\Delta S}{S_0} \qquad (1)$$

Q_f was determined for each measurement with Prof. Huygens software (www.dullware.nl): Q_f depends on the signal change (ΔS) and the system parameters (laser incident angle, thicknesses, real and imaginary refractive indexes of solid substrates and monolayers, refractive index of solutions, and differential refractive index of protein solutions (dn/dC) (see

values in Table 1). The values of 0.185 l/kg were chosen for d*n*/d*C* of both proteins; the possible variations encountered in the literature about these values (± 0.003 l/kg) didn't have a significant influence on our calculations. The same Prof. Huygens software was used to determine the optimal angle of incidence (66º) at the solvent/substrate interface and to minimize the error in the calculation of Q_f due to the angular position of each sample. The thickness of the adsorbed protein layer was shown to be unimportant for regular adsorption (calculated variation of ± 2% in Q_f for values of 3 to 10 nm). However, it is difficult to calculate Q_f accurately for low adsorbed amounts (d_3 < 2 nm; see discussion of the experimental results).

Table 1. Parameter values for the calculation of adsorbed amounts of protein.

parameter	Value
Si100 real ref. index (n_1)	3.85
Si100 im. ref. index (k_1)	0.02
Si_xN_4 real ref. index (n_2)	2.15
Si_xN_4 layer thickness (d_2)	147 nm
Assumed protein layer thickness (d_3)	5 nm
Solution ref. index (n_4)	1.33
BSA diff. ref. index (dn_{bsa}/dC)[a]	0.185 ± 0.003 l/kg
Fibrinogen diff. ref. index (dn_{fib}/dC)[a]	0.185 ± 0.003 l/kg
Laser incident angle on the surface (θ)	66º
Laser wavelength (λ)	632.8 nm

a) De Feijter, J. A.; Benjamins, J.; Veer, F. A., *Biopolymers* **1978,** *17*, 1759-1772.

Results and Discussion

Silicon nitride surface modification with EO_3 and EO_6

UV-modified surfaces with EO_3 and EO_6 monolayers exhibited very reproducible static water contact angles of 64° and 58° (± 1º), respectively, which is in agreement with previous reports on similar monolayers. Indeed, water contact angles of EO_3-modified Si_xN_4 surfaces (64 ± 1º) are identical to those measured on EO_3 monolayers obtained with thiols on gold or silver,[22] but lower values were obtained for EO_3 monolayers obtained by reaction of alkenes with hydrogen-terminated silicon (58 ± 1º).[40,44] In general, substrates coated with EO_3 monolayers display water contact angle values smaller than 11-methoxyundecene thiol monolayers on gold surfaces (~ 84º),[24,62] suggesting that internal ether bonds of the ethylene glycol moieties are always partially exposed. EO_6 coatings on Si_xN_4 were even more hydrophilic, with a contact angle of 58 ± 1º, which is between the values of 66° and 49 ± 1º for EO_6 monolayers on gold[23] and silicon[44] surfaces, respectively. The hydrophilic character of modified surfaces correlates with the disorder within and the packing density of oligo-ethylene glycol monolayers, exposing polar internal C-O bonds to the outer environment. It can thus be concluded that EO_3 monolayers on Si_xN_4 are comparable to thiol monolayers on gold or silver, while EO_6 monolayers on Si_xN_4 are slightly less densely packed.

This difference in density and resulting thickness was confirmed by X-Ray reflectivity measurements, revealing thicknesses of 2.6 ± 0.2 nm for both types of monolayers, which would correspond to 95% and 70% of the length of extended EO_3 and EO_6 molecules, respectively. However, besides the 0.2 nm uncertainty associated with the reflectivity measurement, the initial roughness of bare amorphous Si_xN_4 surfaces must be considered: taking into account rms values of 0.45 ± 0.05 nm, these calculated thicknesses are only semi-quantitative. This uncertainty does not allow for a direct comparison with reported values for EO_3 and EO_6 monolayers on gold surfaces (2.0 ± 0.2 and 2.8 ± 0.2 nm,[24] respectively). Although the absolute values cannot be obtained, the deduced different packing densities imply different structuring of the layers, EO_3 molecules being more or less in an extended conformation, whereas EO_6 molecules are highly disordered. This result is consistent with water contact angle measurements, which indicated for EO_3 a packing density comparable to monolayers on gold, but a lower packing density for EO_6 monolayers. Such a decrease in

packing density with increasing chain length of oligoethylene glycols was also observed with the formation of thiol monolayers on gold surfaces.[23]

The C_{1s} regions of XPS data measured on EO_3 and EO_6 monolayers (Figure 3) display the two characteristic peaks of carbon from the hydrocarbon chains ($CH_{2/3}$ at 285 eV) and oxygen-bound carbon (C-O at 286.8 eV). After fitting the high-resolution spectra, the measured (CH_n)/(C-O) ratios of 1.3 (EO_3 coatings) and 0.77 (EO_6 coatings) match very well the theoretical stoichiometric values of 1.25 (10/8) and 0.71 (10/14), showing the intact attachment of the EO alkenes. Similar attachment experiments at higher temperature lead to cleavage of the EO moieties (data not shown), showing the necessity of this mild attachment.

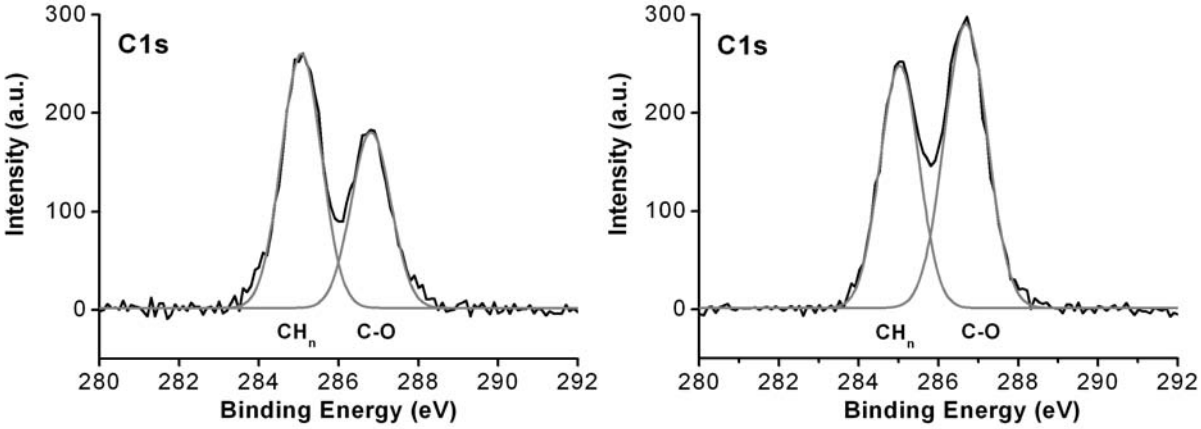

Figure 3. C_{1s} region of XPS data from Si_xN_4 ($x \approx 4$) surfaces coated with ethylene oxide-containing monolayers. Left: monolayer of $CH_3O(CH_2CH_2O)_3(CH_2)_{11}$ [EO_3]; right: monolayer of $CH_3O(CH_2CH_2O)_6(CH_2)_{11}$ [EO_6].

The AFM pictures of Figure 4 show a typical clean Si_xN_4 surface after oxidation (left), and two analogous surfaces coated with EO_3 (center) and EO_6 (right) monolayers. Images and profile traces appear identical before and after modification, still displaying the structure of the initial Si_xN_4 substrate. All surfaces had a similar roughness with an rms value of 0.45 ± 0.05 nm. From these characterizations (Water contact angle, XPS, AFM and X-ray reflectivity) it can be concluded that UV irradiation can reproducibly produce homogeneous EO_3 and EO_6 monolayers on silicon nitride surfaces. The obtained layers possess better features than the ones obtained on silicon, and EO_3 monolayers even seem comparable to similar monolayers on gold. However, the previously reported much higher stability[54] of these coatings on Si_xN_4 make them very appealing candidates for applications where long-term stability of surfaces is required.[54,55,60]

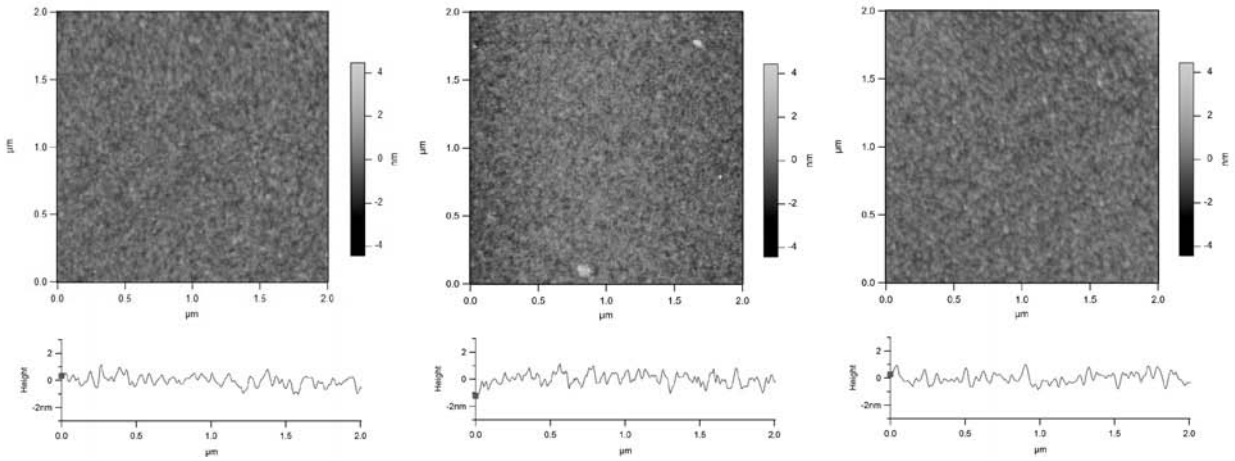

Figure 4. AFM pictures of oxidized (left), EO_3-coated (center), and EO_6-coated (right) Si_xN_4 surfaces and corresponding profile traces. Horizontal scale of pictures: 2 μm, height scale: 8.8 nm. Profile height scale: 6 nm.

Exposure of (modified) Si_xN_4 surfaces to protein

In contrast with all the *ex situ* techniques used to monitor protein adsorption onto surfaces (contact angle, AFM, ellipsometry), reflectometry allows *in situ* observation of protein adsorption without removing the surface from the protein-containing solution and without intermediate cleaning steps. Additionally, this allows one to distinguish between reversible and irreversible adsorption during the adsorption and desorption phases, respectively. One example of reflectometry data recorded *in-situ* during adsorption of fibrinogen onto oxidized and EO6-coated silicon nitride surfaces can be seen on Figure 5.

An overview of the reflectometry results is given in Figure 6. When submitted to protein solutions, the oxidized surfaces (silicon oxy-nitride on top of the Si_xN_4) showed a very reproducible maximum adsorbed amount of 1.25 ± 0.05 mg/m^2 of BSA, and 2.7 ± 0.05 mg/m^2 of fibrinogen after about 30 min. This adsorption is almost irreversible since an exposure to clean buffer cannot remove more than 20 % of BSA or 10 % of fibrinogen, and typically even less.

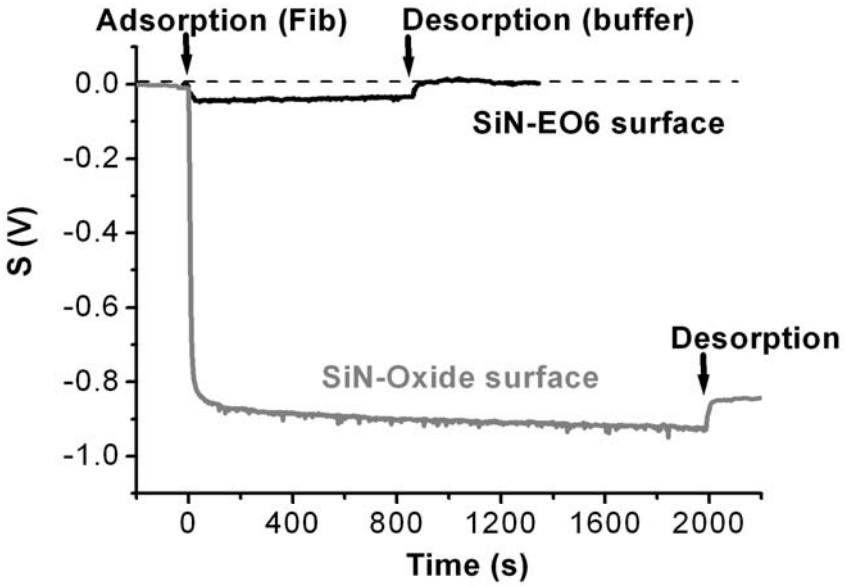

Figure 5. Example of raw reflectometry data: adsorption of fibrinogen from solution onto bare oxidized (gray) and EO_6-coated (black) silicon nitride substrates.

The surface coverage of the adsorbed proteins gives some information about the structure of the adsorbed layers: BSA is a globular protein (MW = 69 kDa) with dimensions 4 × 4 × 14 nm in solution,[63] whereas fibrinogen is a bigger protein (MW = 340 kDa) with dimensions of about 9 × 9 × 45 nm.[64] Considering these sizes, a monolayer of adsorbed BSA corresponds to a maximum coverage of 2 to 6.8 mg/m^2, depending on whether the protein is laying flat or standing on the surface. For fibrinogen, these maximum coverage values are 1.4 and 7 mg/m^2. From the reflectometry data, the amount of BSA irreversibly adsorbed onto bare, oxidized Si_xN_4 surfaces in Figure 6 (1 mg/m^2) would correspond to only 50% of a BSA monolayer laying flat on the surface. However, the measured adsorption of fibrinogen (2.5 mg/m^2) lies within the limits of the predictions, indicating a relatively dense adsorbed layer of this protein. Possibly, the ability of BSA to change its conformation and spread over a larger area can explain the lower adsorbed amounts observed in this experiment.[27,63,65] However, the different surface saturations could also be due to the different isoelectric points of the proteins (4.8 for BSA and 5.3 for fibrinogen[66]): at pH 6.75 – as used in these experiments – BSA is more charged than fibrinogen, and protein adsorption could thus be partially hindered by electrostatic repulsions. This difference in charge can also be the cause of the different adsorption rates of the two proteins: adsorption of BSA onto oxide surfaces was much slower than for fibrinogen, with adsorption saturation being reached after 20 and 3 min, respectively.

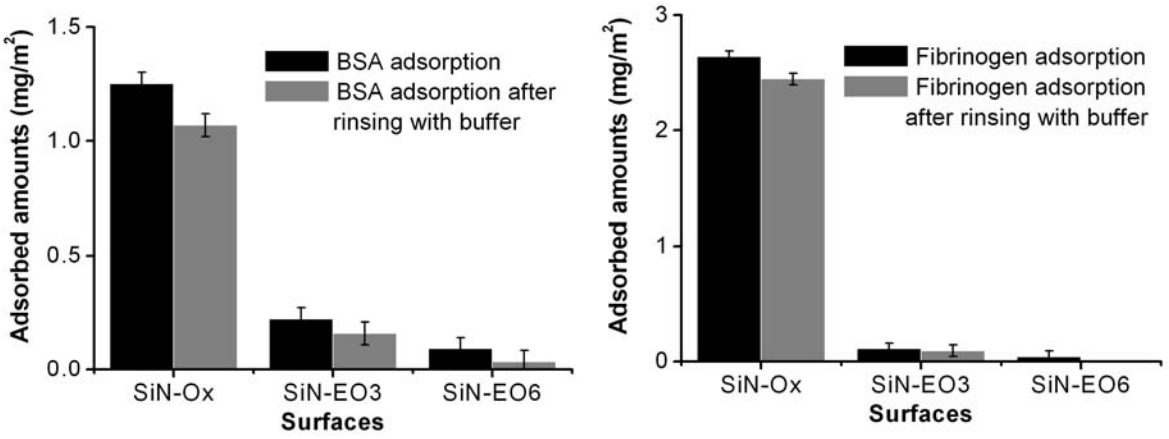

Figure 6. Adsorbed amounts of BSA (left) and fibrinogen (right) onto clean (SiN-Ox) and EO_3/EO_6-coated Si_xN_4 surfaces, after subsequent exposure to protein solution and to buffer without protein.

Silicon nitride surfaces coated with EO_3 or EO_6 monolayers reduced the adsorption of both proteins considerably, regardless of the exposure time. Indeed, after the initial signal change (in the first 5 min), no visible change in the signal was observed after up to 3 h. Compared to oxidized surfaces, BSA and fibrinogen adsorption was sometimes so reduced, that accurate quantification above the noise level of the experiment was not possible. For our calculations, the value of Q_f, used to calculate the adsorbed amounts of proteins, could only be used if the thickness of the adsorbed layer is more than ~2 nm (variation of Q_f < 5%). For thinner adsorbed layers, Q_f decreases and the associated uncertainty in the calculations increases significantly. The result of this is that values well below 0.3 mg/m^2, as found for both the EO_3 and EO_6 modified surfaces, are overestimated. In other words, the values in Figure 6 display a worst-case scenario: the actual amount of adsorbed protein is very likely even less than shown.

Only for BSA on EO_3, some adsorption can still be observed (residual signal of 15%) compared to adsorbed amounts on oxidized Si_xN_4 surfaces. Possibly, due to its smaller size and flexible structure, BSA may be able to penetrate defects in the monolayer, and interact with the underlying surface or the hydrophobic hydrocarbon chains. The longer ethylene glycol moiety of EO_6 seems to minimize this residual interaction, and provides essentially complete antifouling behavior. The better performance of EO_6 can also be noted for fibrinogen adsorption, bringing adsorbed amounts below the detection level of reflectometry.

Another noticeable point concerns the use of oxidized surfaces as reference surfaces for adsorption. Other studies have reported protein-repellent behavior by comparison with methyl-terminated surfaces, obtained by formation of alkyl monolayers on silicon[40] or gold surfaces.[24] Some of our preliminary measurements showed that such hydrophobic surfaces (water contact angles > 100º) induce more protein adsorption (+ 20% in average) with a lower reproducibility than found for oxidized surfaces (data not shown). Therefore, it is clear that oxidation of Si_xN_4 surfaces is a more reliable way to obtain reproducible reference surfaces.

Investigation of the wetting properties of surfaces also confirms the antifouling character of these monolayers. Figure 7 shows water contact angles before and after protein adsorption: the oxidized surfaces showed a clear change in the wettability, with contact angles values from < 10º initially to values of 39 ± 2º and 70 ± 5º after adsorption of BSA and fibrinogen, respectively. These latter values no longer reflect the surface properties of oxidized Si_xN_4, but those of the adsorbed layers of protein. The increased variation in the contact angles measured on different positions on the samples after adsorption also points to inhomogeneity of the obtained protein layers. Ethylene oxide-coated surfaces, however, retained their initial well-defined contact angle values of 64 ± 1º (EO_3) and 58 ± 1º (EO_6) after exposure to the protein solution during the reflectometry experiment. Since both the value and the standard deviation of the observed contact angles were not affected, this strongly confirmed that these EO_3 and EO_6-coated surfaces were not contaminated by protein adsorption.

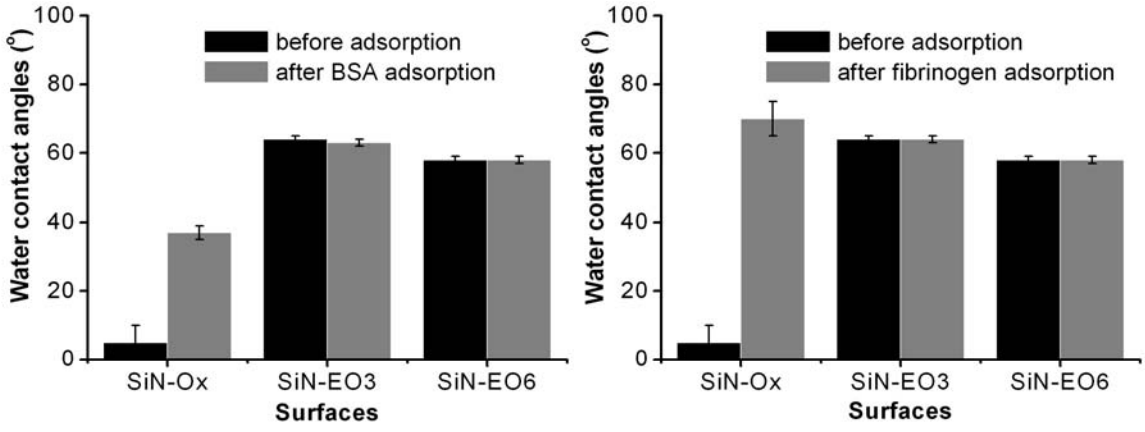

Figure 7. Static water contact angles values before and after adsorption of BSA (left) and fibrinogen (right) onto clean (SiN-Ox) and monolayer-coated (SiN-EO_3 and SiN-EO_6) Si_xN_4 surfaces.

After each reflectometry experiment (exposure to protein, and rinsing with buffer, followed by rinsing with MilliQ water and drying), surfaces were also studied with AFM to provide more information on surface fouling. Figure 8 and Figure 9 show pictures of oxidized and EO_n-coated Si_xN_4 surfaces after exposure to BSA (Figure 8) and fibrinogen (Figure 9). Whereas massive protein adsorption is clearly visible on the oxidized surfaces (Figure 8, left and Figure 9, left), exposure to BSA caused only small patches of contamination on the EO_n-coated sample (See Figure 4 for comparison with surfaces before protein adsorption). Exposure of EO_n-coated surfaces to fibrinogen caused almost no visible contamination.

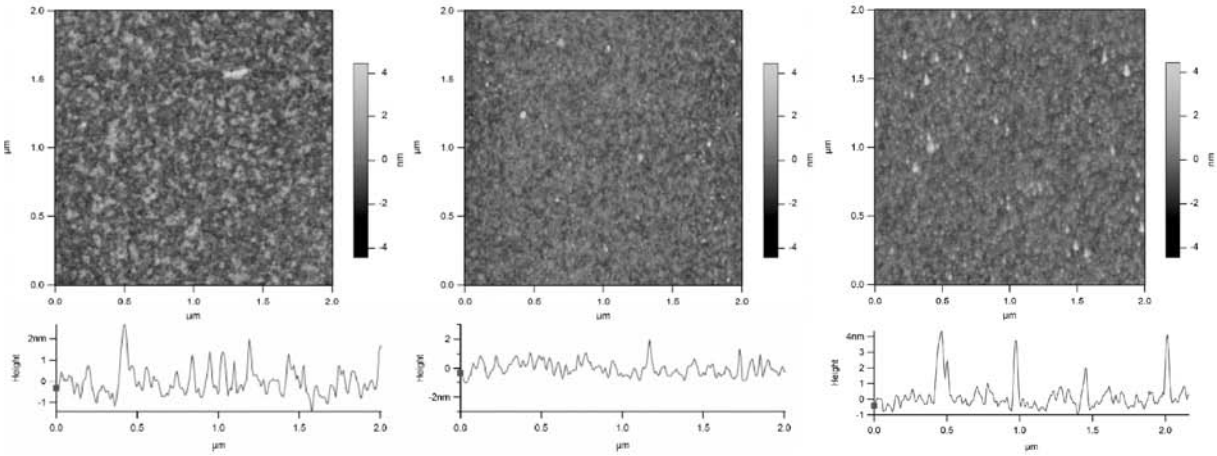

Figure 8. AFM pictures and height profiles of oxidized Si_xN_4 (left) and EO_3-coated Si_xN_4 (center), and EO_6-coated Si_xN_4 (right), after exposure to BSA.

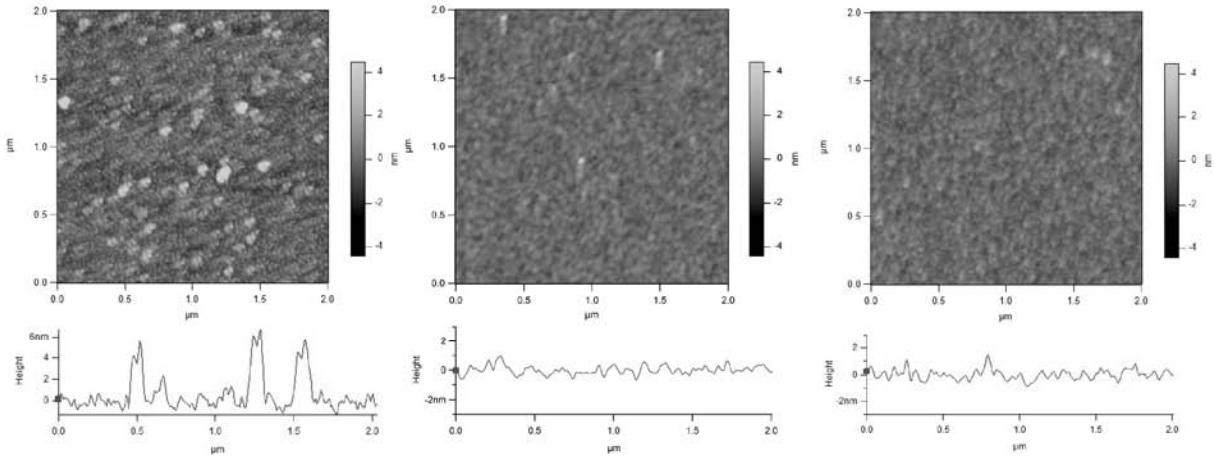

Figure 9. AFM pictures and height profiles of oxidized Si_xN_4 (left), EO_3-coated Si_xN_4 (center), and EO_6-coated Si_xN_4 (right) after exposure to fibrinogen.

A quantitative impression of the AFM pictures can be obtained from the roughness measurements before and after exposure of the surfaces to protein solutions (Table 2). For both proteins, the surface roughness of the reference oxidized Si_xN_4 surfaces clearly increased upon adsorption: the rms values of oxidized surfaces changed from 0.45 ± 0.05 nm in average to 0.81 ± 0.10 nm after adsorption of BSA or fibrinogen, while the AFM topology provides the impression of much more corrugated surfaces (Figure 9). With EO_3- and EO_6-modified surfaces, the change in the rms-values is very low (within the experimental error of the measurement), implying only little adsorption, if any.

Table 2. Rms roughness (in nm) measured by AFM on oxidized Si_xN_4 and on EO_n-coated Si_xN_4, before and after exposure to protein solution. (Values are given ± 0.05 nm)

Samples	Before adsorption	After BSA adsorption	Before adsorption	After FIB adsorption
Oxidized Si_xN_4	0.48	0.81	0.49	0.80
Si_xN_4-EO_3	0.49	0.57	0.40	0.37
Si_xN_4-EO_6	0.45	0.52	0.40	0.44

The water contact angle and roughness measurements were mainly used to confirm the results of the reflectometry experiments, and these two *ex-situ* techniques revealed a slightly less good behavior of EO_3 monolayers regarding BSA adsorption. Indeed, we observed a very small decrease in contact angle (~ 1°), and an increase in roughness (from 0.45 to 0.57 nm) of these surfaces upon exposure to BSA solutions. However, these variations are still within the experimental error associated with these measurements. Moreover, AFM pictures give only a local and qualitative impression of surface contamination or the lack thereof.

Only reflectometry could detect unambiguously and reproducibly the small variations in surface contamination on EO_3- and EO_6-coated Si_xN_4 on a macroscopic scale. The observed outstanding protein repellence of these layers, specifically of EO_6, was comparable to that obtained with similar EO-monolayers on gold and silicon oxide surfaces. However, the increased stability of the coatings on Si_xN_4 makes them much more suitable than either of these inorganic substrates (Au, SiO_x, Si, etc.) for applications where permanent surface properties are needed.

Conclusions

For the first time, well-defined monolayers of short oligoethylene glycols, $CH_3O(CH_2CH_2O)_3(CH_2)_{11}$ [EO_3] and $CH_3O(CH_2CH_2O)_6(CH_2)_{11}$ [EO_6] were successfully grafted onto silicon-enriched Si_xN_4 surfaces using a photochemical attachment[60] at room temperature. Such EO_n-modified Si_xN_4 surfaces displayed excellent protein-repelling behavior. EO_6 monolayers, especially, reduced the adsorption of BSA and fibrinogen to negligible amounts (below the detection limit of reflectometry). The proteins were not only repelled during the adsorption phase, but when small residual amounts were present, they could efficiently be washed away by buffer.

In addition, while the monolayers on Si_xN_4 display protein-repelling properties comparable to similar thiol monolayers on gold surfaces or silanes on oxide surfaces, we have shown that their stability in aqueous environments[60] and in a wide pH range provides surfaces with long term stability. The excellent antifouling behavior of these monolayers opens up a wide variety of possible applications of protein-repelling silicon nitride, e.g. in the use of reactor walls or lithographically prepared microsieves.

Acknowledgments.

The authors thank Graduate School VLAG and MicroNed (Project no. 6163510395) for financial support, and Prof. Remko Boom (Wageningen University) for stimulating discussions.

References

(1) Patil, L. S.; Pandey, R. K.; Bang, J. P.; Gaikwad, S. A.; Gautam, D. K. *Opt. Mater*. **2005,** *27*, 663-670.

(2) Bermudez, V. M.; Perkins, F. K. *Appl. Surf. Sci.* **2004,** *235*, 406-419.

(3) Antsiferov, V. N.; Gilev, V. G.; Karmanov, V. I. *Refract. Ind. Ceram.* **2003,** *44*, 108-114.

(4) Rathi, V. K.; Gupta, M.; Agnihotri, O. P. *Microelectron. J.* **1995,** *26*, 563.

(5) Kuiper, S.; van Wolferen, H.; van Rijn, G.; Nijdam, W.; Krijnen, G.; Elwenspoek, M. *J. Micromech. Microeng.* **2001,** *11*, 33-37.

(6) van Rijn, C. J. M. *Nano and Micro Engineered Membrane Technology*. Aquamarijn Research BV, The Netherlands: 2002.

(7) van Rijn, C. J. M.; Veldhuis, G. J.; Kuiper, S. *Nanotechnology* **1998,** *9*, 343-345.

(8) Girones, M.; Lammertink, R. G. H.; Wessling, M. *J. Membr. Sci.* **2006,** *273*, 68-76.

(9) Kuiper, S.; van Rijn, C.; Nijdam, W.; Raspe, O.; van Wolferen, H.; Krijnen, G.; Elwenspoek, M. *J. Membr. Sci.* **2002,** *196*, 159-170.

(10) Marshall, A. D.; Munro, P. A.; Tragardh, G. *Desalination* **1993,** *91*, 65-108.

(11) Vanloosdrecht, M. C. M.; Lyklema, J.; Norde, W.; Zehnder, A. J. B. *Microbiol. Rev.* **1990,** *54*, 75-87.

(12) Koehler, J. A.; Ulbricht, M.; Belfort, G. *Langmuir* **2000,** *16*, 10419-10427.

(13) Ulbricht, M.; Belfort, G. *J. Appl. Polymer Sci.* **1995,** *56*, 325-343.

(14) Ulbricht, M.; Belfort, G. *J. Membr. Sci.* **1996,** *111*, 193-215.

(15) Girones, M.; Borneman, Z.; Lammertink, R. G. H.; Wessling, M. *J. Membr. Sci.* **2005,** *259*, 55-64.

(16) Amirgoulova, E. V.; Groll, J.; Heyes, C. D.; Ameringer, T.; Rocker, C.; Moller, M.; Nienhaus, G. U. *Chemphyschem* **2004,** *5*, 552-555.

(17) Krishnan, S.; Ayothi, R.; Hexemer, A.; Finlay, J. A.; Sohn, K. E.; Perry, R.; Ober, C. K.; Kramer, E. J.; Callow, M. E.; Callow, J. A.; Fischer, D. A. *Langmuir* **2006,** *22*, 5075-5086.

(18) Cecchet, F.; De Meersman, B.; Demoustier-Champagne, S.; Nysten, B.; Jonas, A. M. *Langmuir* **2006,** *22*, 1173-1181.

(19) Bremmell, K. E.; Kingshott, P.; Ademovic, Z.; Winther-Jensen, B.; Griesser, H. J. *Langmuir* **2006,** *22*, 313-318.

(20) Bosker, W. T. E.; Iakovlev, P. A.; Norde, W.; Stuart, M. A. C. *J. Colloid Interf. Sci.* **2005,** *286*, 496-503.

(21) Lazos, D.; Franzka, S.; Ulbricht, M. *Langmuir* **2005,** *21*, 8774-8784.

(22) Harder, P.; Grunze, M.; Dahint, R.; Whitesides, G. M.; Laibinis, P. E. *J. Phys. Chem. B* **1998,** *102*, 426-436.

(23) Herrwerth, S.; Eck, W.; Reinhardt, S.; Grunze, M. *J. Am. Chem. Soc.* **2003,** *125*, 9359-9366.

(24) Palegrosdemange, C.; Simon, E. S.; Prime, K. L.; Whitesides, G. M. *J. Am. Chem. Soc.* **1991,** *113*, 12-20.

(25) Prime, K. L.; Whitesides, G. M. **1991,** *252*, 1164-1167.

(26) Prime, K. L.; Whitesides, G. M. **1993,** *115*, 10714-10721.

(27) Seigel, R. R.; Harder, P.; Dahint, R.; Grunze, M.; Josse, F.; Mrksich, M.; Whitesides, G. M. *Anal. Chem.* **1997,** *69*, 3321-3328.

(28) Unsworth, L. D.; Sheardown, H.; Brash, J. L. *Langmuir* **2005,** *21*, 1036-1041.

(29) Vanderah, D. J.; Pham, C. P.; Springer, S. K.; Silin, V.; Meuse, C. W. *Langmuir* **2000,** *16*, 6527-6532.

(30) Yam, C. M.; Deluge, M.; Tang, D.; Kumar, A.; Cai, C. Z. *J. Colloid Interf. Sci.* **2006,** *296*, 118-130.

(31) Norde, W.; Gage, D. *Langmuir* **2004,** *20*, 4162-4167.

(32) Chan, Y. H. M.; Schweiss, R.; Werner, C.; Grunze, M. *Langmuir* **2003,** *19*, 7380-7385.

(33) Heyes, C. D.; Kobitski, A. Y.; Amirgoulova, E. V.; Nienhaus, G. U. *J. Phys. Chem. B* **2004,** *108*, 13387-13394.

(34) Hoffmann, C.; Tovar, G. E. M. *J. Colloid Interf. Sci.* **2006,** *295*, 427-435.

(35) Lee, S. W.; Laibinis, P. E. *Biomaterials* **1998,** *19*, 1669-1675.

(36) Ma, H. W.; Li, D. J.; Sheng, X.; Zhao, B.; Chilkoti, A. *Langmuir* **2006,** *22*, 3751-3756.

(37) Roosjen, A.; Kaper, H. J.; van der Mei, H. C.; Norde, W.; Busscher, H. J. *Microbiology* **2003,** *149*, 3239-3246.

(38) Roosjen, A.; van der Mei, H. C.; Busscher, H. J.; Norde, W. *Langmuir* **2004,** *20*, 10949-10955.

(39) Schlapak, R.; Pammer, P.; Armitage, D.; Zhu, R.; Hinterdorfer, P.; Vaupel, M.; Fruhwirth, T.; Howorka, S. *Langmuir* **2006,** *22*, 277-285.

(40) Bocking, T.; Gal, M.; Gaus, K.; Gooding, J. J. *Aust. J. Chem.* **2005,** *58*, 660-663.

(41) Bocking, T.; Kilian, K. A.; Hanley, T.; Ilyas, S.; Gaus, K.; Gal, M.; Gooding, J. J. *Langmuir* **2005,** *21*, 10522-10529.

(42) Bocking, T.; Killan, K. A.; Gaus, K.; Gooding, J. J. *Langmuir* **2006,** *22*, 3494-3496.

(43) Yam, C. M.; Gu, J. H.; Li, S.; Cai, C. Z. *J. Colloid Interf. Sci.* **2005,** *285*, 711-718.

(44) Yam, C. M.; Lopez-Romero, J. M.; Gu, J. H.; Cai, C. Z. *Chem. Comm.* **2004**, 2510-2511.

(45) Ebner, A.; Wildling, L.; Kamruzzahan, A. S. M.; Rankl, C.; Wruss, J.; Hahn, C. D.; Holzl, M.; Zhu, R.; Kienberger, F.; Blaas, D.; Hinterdorfer, P.; Gruber, H. J. *Bioconjugate Chem.* **2007,** *18*, 1176-1184.

(46) Gabriel, S.; Jerome, C.; Jerome, R.; Fustin, C. A.; Pallandre, A.; Plain, J.; Jonas, A. M.; Duwez, A. S. *J. Am. Chem. Soc.* **2007,** *129*, 8410-+.

(47) Gu, C.; Ray, C.; Guo, S.; Akhremitchev, B. B. *J. Phys. Chem. C* **2007,** *111*, 12898-12905.

(48) Kamruzzahan, A. S. M.; Ebner, A.; Wildling, L.; Kienberger, F.; Riener, C. K.; Hahn, C. D.; Pollheimer, P. D.; Winklehner, P.; Holzl, M.; Lackner, B.; Schorkl, D. M.; Hinterdorfer, P.; Gruber, H. J. *Bioconjugate Chem.* **2006,** *17*, 1473-1481.

(49) Riener, C. K.; Kienberger, F.; Hahn, C. D.; Buchinger, G. M.; Egwim, I. O. C.; Haselgrubler, T.; Ebner, A.; Romanin, C.; Klampfl, C.; Lackner, B.; Prinz, H.; Blaas, D.; Hinterdorfer, P.; Gruber, H. J. *Anal. Chim. Acta* **2003,** *497*, 101-114.

(50) Wang, T.; Xu, J. J.; Qiu, F.; Zhang, H. D.; Yang, Y. L. *Polymer* **2007,** *48*, 6170-6179.

(51) Suo, Z. Y.; Arce, F. T.; Avci, R.; Thieltges, K.; Spangler, B. *Langmuir* **2006,** *22*, 3844-3850.

(52) Girones, M.; Bolhuis-Versteeg, L.; Lammertink, R.; Wessling, M. *J. Colloid Interf. Sci.* **2006,** *299*, 831-840.

(53) Cerruti, M.; Fissolo, S.; Carraro, C.; Ricciardi, C.; Majumdar, A.; Maboudian, R. *Langmuir* **2008**, ASAP article.

(54) Arafat, A.; Giesbers, M.; Rosso, M.; Sudhölter, E. J. R.; Schroën, K.; White, R. G.; Yang, L.; Linford, M. R.; Zuilhof, H. *Langmuir* **2007,** *23*, 6233-6244.

(55) Arafat, A.; Schroën, K.; de Smet, L. C. P. M.; Sudhölter, E. J. R.; Zuilhof, H. *J. Am. Chem. Soc.* **2004,** *126*, 8600-8601.

(56) Rosso, M.; Arafat, A.; Schroën, K.; Giesbers, M.; Roper, C. S.; Maboudian, R.; Zuilhof, H. *Langmuir* **2008,** *24*, 4007-4012.

(57) Sieval, A. B.; Linke, R.; Zuilhof, H.; Sudhölter, E. J. R. *Adv. Mater.* **2000,** *12*, 1457-1460.

(58) Scheres, L.; Arafat, A.; Zuilhof, H. *Langmuir* **2007,** *23*, 8343-8346.

(59) Sieval, A. B.; Vleeming, V.; Zuilhof, H.; Sudhölter, E. J. R. *Langmuir* **1999,** *15*, 8288-8291.

(60) Rosso, M.; Giesbers, M.; Arafat, A.; Schroën, K.; Zuilhof, H. *Langmuir* **2009,** *25*, 2172-2180.

(61) Dijt, J. C.; Stuart, M. A. C.; Fleer, G. J. *Adv. Colloid Interface Sci.* **1994,** *50*, 79-101.

(62) Laibinis, P. E.; Bain, C. D.; Nuzzo, R. G.; Whitesides, G. M. *J. Phys. Chem.* **1995,** *99*, 7663-7676.

(63) Su, T. J.; Lu, J. R.; Thomas, R. K.; Cui, Z. F.; Penfold, J. *J. Phys. Chem. B* **1998,** *102*, 8100-8108.

(64) Feng, W.; Zhu, S. P.; Ishihara, K.; Brash, J. L. *Langmuir* **2005,** *21*, 5980-5987.

(65) Ramsden, J. J. *Chem. Soc. Rev.* **1995,** *24*, 73-78.

(66) Liu, M. L.; Zhang, Y. Y.; Wang, M. L.; Deng, C. Y.; Xie, Q. J.; Yao, S. Z. *Polymer* **2006,** *47*, 3372-3381.

Chapter 8

Formation of Biorepellent Oligoethylene Glycol Monolayers on Silicon Nitride Microsieves

This chapter presents our initial work on the formation of covalent organic monolayers on microsieves (silicon nitride coated microfabricated membranes). Oligoethylene glycol monolayers were successfully formed on microsieves using a UV light technique. The sieve surfaces were characterized by X-ray photoelectron spectroscopy (XPS) and atomic force microscopy (AFM). Flux measurements, XPS and AFM were used to evaluate the coatings and their performance during filtration.

This chapter will be published as:
"Protein-Repellent Coatings on Silicon Nitride Microsieves", Rosso, M.; Schroën, K.; Boom, R.; Zuilhof, H. in preparation.

Introduction

Microsieves are a new type of micro-perforated filtration membranes, produced using photolithography to create membrane pores with a very well-defined size and shape.[1-3] The coating of these membranes consists of a layer of silicon-rich silicon nitride (Si_xN_4; x typically 3.5 - 5) - deposited by chemical vapor deposition (CVD). This material is used to reinforce the structure of the microsieves, initially created from more brittle silicon. Indeed, Si_xN_4 is often used as an insulating or passivating coating for microelectronics and microelectromechanical systems.[4-6]

Typical commercial microsieves can be obtained with pore diameters ranging from 0.45 to 8 µm, with an effective thickness of the filtration layer of about 1 µm (Figure 1). The very thin effective membrane layer of microsieves results in a high permeability, and allows very low transmembrane pressures (< 100 mbar[7]) compared to ceramics membranes (with pressures of typically 0.5 to 5 bar[8,9]). Moreover, the possibility to accurately design the pore size and shape, the porosity and the thickness of membranes gives a new freedom to optimize the filtration process.[10-13] Microsieves have been especially studied for food applications, such as the filtration of beer or the cold sterilization of milk.[2]

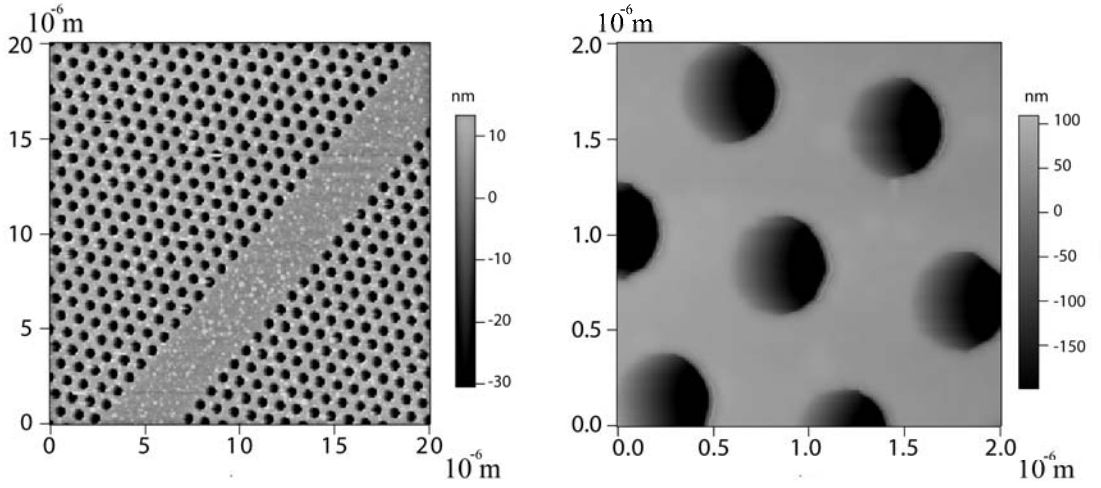

Figure 1. AFM picture of silicon nitride microsieves with 0.45 µm diameter. Two neighboring pore arrays (left: horizontal scale 20 µm) and details of the circular pores (right: horizontal scale 2 µm).

However, the surface contamination of microsieves seriously limits their application to purify food products, by causing a dramatic decrease in permeate flux during filtration.[14-16] This is a general problem encountered in microfiltration of biological solutions.[17,18]

Proteins or protein aggregates constitute the main source of biocontaminants for membrane surfaces during the filtration of biological solutions and liquid food products.[18-20] In turn, this protein layer favors the adsorption of other components, such as biological cells, and is therefore a primary target when aiming for biorepellent surfaces.

Some studies have shown that plasma treatment with air or oxygen, which is commonly used to clean and oxidize polymeric membranes, also yields highly hydrophilic surfaces[21,22]. The same approach can be used for Si_xN_4 microsieves.[23] Plasma treatment combines efficient oxidation with the convenience of dry treatments, and allows a non-destructive treatment of porous microstructures such as microsieves. The oxygen plasma, consisting mainly of free oxygen atoms,[24] activates the surfaces of oxidized silicon nitride by breaking surface siloxane bridges (Si-O-Si). The resulting silanol groups (Si-OH) make the surface completely hydrophilic (water contact angle ~ 0º). This dry process can be easily scaled up from the dimensions of experimental microsieves (5 x 5 mm) to the wafer-sized membranes required for industrial processes. However, the effects of the plasma treatment are only temporary, as the high surface energy of the obtained oxide surface promotes the adsorption of new contaminants from air or water. As a result, the treatment must then be repeated to recover a highly hydrophilic, wettable surface, which again only remains this way for a short period. It is clear that if a surface is hydrophilic, this is not enough to prevent surface contamination.

Recently, we have shown that it was possible to covalently attach an organic monolayer onto a silicon nitride[25,26] or silicon carbide[27] surface, using conditions close to those used for the thermal hydrosilylation of silicon surfaces.[28-30] Stable and good-quality monolayers were obtained with several simple alkenes, as well as esters, allowing further (bio-)chemical surface modifications. The layers were stable in aqueous solutions, which is essential for application on e.g. microsieves. We also demonstrated that this modification can be initiated by UV light at room temperature using less compound and a simpler experimental set-up.[31] This extends the method to monolayers formed with more labile and/or more expensive alkenes. In particular, we already used this UV modification to attach oligo-EO-terminated monolayers onto silicon-rich silicon nitride surfaces in a single step procedure (Chapter 7).[32] Methoxy-tri(ethylene oxide) undec-1-ene ($CH_3O(CH_2CH_2O)_3(CH_2)_9CH=CH_2$; EO_3), and methoxy-hexa(ethylene oxide) undec-1-ene ($CH_3O(CH_2CH_2O)_6(CH_2)_9CH=CH_2$; EO_6) were

synthesized and grafted onto etched silicon-rich silicon nitride (Si_xN_4) surfaces. These coatings could 'prevent' adsorption of bovine serum albumin (BSA) and fibrinogen from solution, which actually means that the signals were below the experimental detection limit, while considerable amounts of protein always adsorbed onto bare oxidized (plasma-treated) Si_xN_4 surfaces.

In this work, we apply the EO_6 coatings to silicon nitride to microsieves. The study includes amongst others cross-flow filtration experiments with BSA solutions and AFM study of the surface of the microsieves at different stages of the filtration.

Experimental Section

Materials

Bovine serum albumin (fraction V, min 96% lyophilized powder) was purchased from Sigma. Sodium phosphate dibasic (analytical grade, Acros), potassium dihydrogenophosphate (ACS grade, Merck), potassium chloride (pro analysis, Merck) and sodium chloride (puriss., Riedel-de-Haën) were used to prepare the PBS buffer. Milli-Q water was used to prepare all the aqueous solutions. The buffer solutions were always filtered before dissolving the BSA with 0.2 µm syringe filters (Sartorius, Goettingen, Germany). The synthesis of the oligoethylene glycol-functionalized alkenes (methoxy-hexa(ethylene oxide) undec-1-ene ($CH_3O(CH_2CH_2O)_6(CH_2)_9CH=CH_2$; EO_6), is described in Chapter 7.[32] The alkyl monolayers were formed on silicon-rich silicon nitride (Si_xN_4) microsieves, which were a generous gift from Aquamarijn Micro Filtration B.V., The Netherlands (pore diameter: 0.45 µm). The surface area of the sieves was 5.0 x 5.0 mm; the actual filtration area is around 50% of the total area.

Monolayer Formation

Si_xN_4 microsieves were first cleaned with acetone and milliQ water, followed by an air-based plasma treatment for 15 min. The resulting oxidized surfaces were etched with a 2.5% solution of HF for 2 min. The membranes were then rinsed with water and acetone, and put under vacuum for 5 min to dry the devices. Right after this step, they were placed with their upper side (filtration layer) against the curved wall of a fused silica flask. Prior to this, a drop of the neat to be grafted alkenes was placed on this curved wall and was argon-saturated for at least 30 min. The amount of alkene was just sufficient to wet the surface of the microsieves

and parts of the inner structure. After 30 more min with the etched microsieves and alkenes under an argon flow, the UV pen lamps (low pressure mercury vapor, wavelength 254 nm, double bore lamp, Jelight Company, Irvine, California) were placed 4 mm away from the sample surface and turned on for the desired time. At the end of the experiment, samples were removed and rinsed several times with ethyl acetate, water and acetone.

Surface Characterization

X-ray Photoelectron Spectroscopy (XPS)

The XPS analysis of surfaces was performed using a JPS-9200 Photoelectron Spectrometer (JEOL, Japan). The high-resolution spectra were obtained under UHV conditions using monochromatic Al K_α X-ray radiation at 12 kV and 25 mA, using an analyzer pass energy of 10 eV. High-resolution spectra were corrected with a linear background before fitting.

Atomic force microscopy (AFM)

Images were obtained with an MFP-3D AFM from Asylum Research (Santa Barbara, CA). Imaging was performed in AC mode in air using OMCL-AC240 silicon cantilevers (Olympus Corporation, Japan). The root mean square (RMS) roughness was calculated from the fluctuations of the surface height around the average height in the image. In this way the RMS value describes the topography of the surface. The RMS is the standard deviation, i.e. the square root of the variance, of the Z-values within the image, according to: RMS = $\sqrt{(\sum(Z_i)^2/n)}$.

Filtration experiments

The filtration experiments were carried out in a flat-plate module with a channel height of 0.7 mm. The transmembrane pressure was recorded with electronic sensors (Keller Druckmesstechnik, Winterthur, Switzerland), while the filtrate weight was measured using a balance (Sartorius CP4202S, Goettingen, Germany). A personal computer logged the pressure and weight. For cross-flow experiments, solutions of bovine serum albumin (BSA) were recirculated using a 5003U Watson & Marlow gear pump (Cornwall, England) at a flow rate of 100 $mL.min^{-1}$. A valve situated at the retentate tubing, downstream of the module was used to keep the transmembrane pressure at 50 mbar for all experiments, while the cross-flow velocity was kept at 0.05 $m.s^{-1}$.

Results and Discussion

The microsieves were characterized with XPS and AFM right after the UV-initiated surface modification with EO_6 molecules. The XPS survey spectrum of Figure 2 reveals the presence of the EO_6 monolayers, by the increased amount of carbon compared to bare etched silicon nitride surfaces. The presence of the oligomers is especially put in evidence by the high resolution C1s spectra, where the two main contributions of carbon atoms of the ***C***H_n (285.0 eV) and ***C***-O (286.7 eV) are visible. The ratio of these two contributions amounts to I (***C***-O) /I (***C***H_n) = 0.72, which is exactly the ratio expected from the stoechiometry of the initial compound, and totally matches our previous study of the same coatings on flat silicon nitride surfaces (Chapter 7). Another small contribution appears at higher binding energy (288 eV), which could correspond to carbon atoms having two bonds with oxygen. This signal was not observed when studying the coatings on plain surfaces (Chapter 7) and could be due to some oxidation occurring during the UV-irradiation.

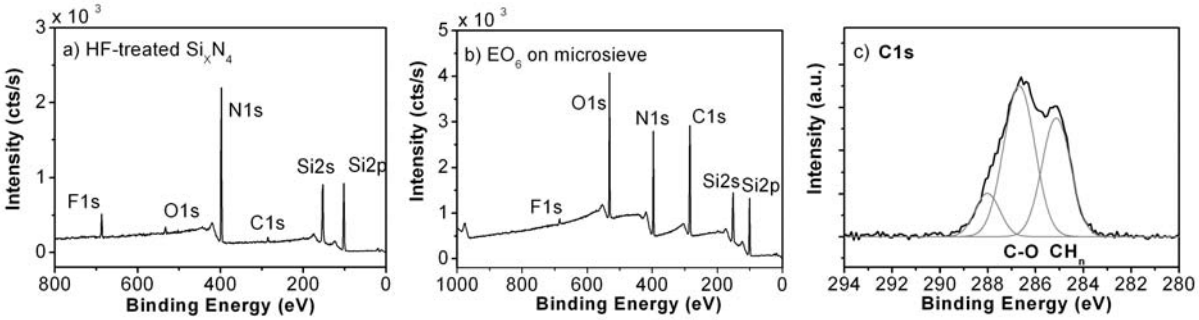

Figure 2. Survey XPS spectra measured on a) HF-treated silicon nitride and b) EO_6-coated silicon nitride microsieve and c) C_{1s} region of the high-resolution XPS measured on EO_6 coatings.

AFM pictures recorded for the area between the pores of the membranes (Figure 4), do not show any differences between plasma cleaned and EO6-coated microsieves. The surface roughness was also identical with a value of 2.2 ± 0.2 nm for the rms. The fact that both surfaces appear identical with AFM, confirms that monolayers of EO_6 successfully form homogeneous coatings on the microsieves; the UV-induced reaction did not cause any uncontrolled degradation or polymerization on the surfaces.

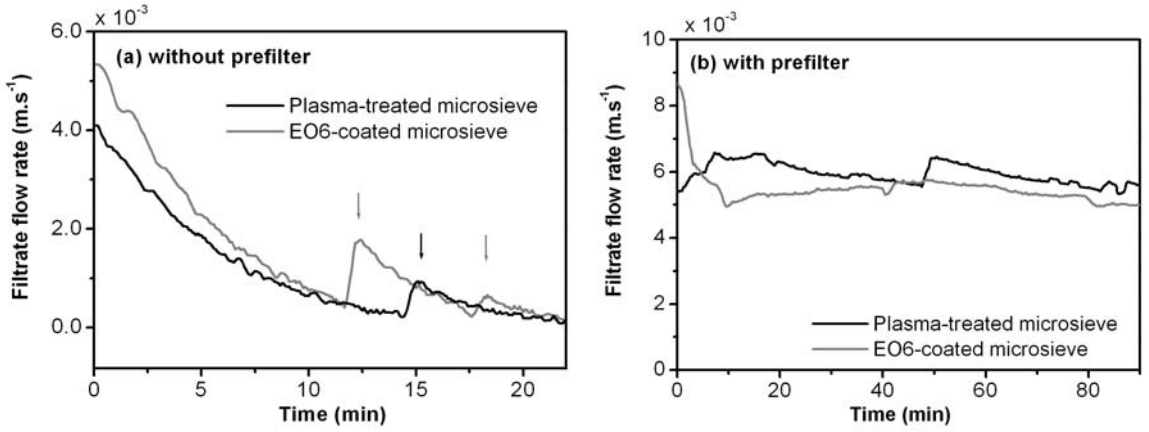

Figure 3. Flux measured during cross-flow filtration of 0.1 $g.L^{-1}$ BSA solution in PBS buffer, a) without prefilter and b) with a 0.2 μm prefilter. The vertical arrows indicate a short manual back-flush, applied by squeezing the outlet tubing.

The membranes were then tested during cross-flow filtration with 0.1 $g.L^{-1}$ solutions of bovine serum albumin (BSA) in phosphate buffer saline (PBS: pH 6.75, ionic strength 0.08 M). In these conditions, we did not observe adverse wetting effects, even though the EO_6 coating of flat Si_xN_4 surfaces yields static water contact angles of 56 ± 1 º (Chapter 7), compared to the extremely hydrophilic surface of plasma-treated surfaces (contact angle < 5 º). For the start-up of the filtration, no pre-wetting with e.g. ethanol was needed, as is the case for hydrophobic membranes.

Before installation of the pre-filter, the experiments did not show significant differences between plasma-treated and EO_6-coated membranes (Figure 3a). Both types of membranes were 'blocked' after about 15 min; a short back-flush would partially restore the flow (arrows in Figure 3a), but after two or three times, this action did not have any effect and the membranes were completely blocked. It is important to note that the same experiment carried out with milliQ water instead of BSA solutions gave exactly the same behavior, with the membranes being 'blocked' after 15 to 20 min, and that is rather surprising since regular membranes don't show this flux behavior.

As intriguing as this effect is, we decided to not investigate in depth, and go for a solution which is often used in membrane labs all over the world, the use of a pre-filter. When a 0.2 μm prefilter was applied, (Figure 3b) a value of 0.07 ± 0.01 $mL.s^{-1}$ was obtained for the flux, both for the plasma treated and EO-modified microsieve. Given the size of a single protein

molecule, it is not expected that even the presence of a monolayer of protein would result in any effect on the flux; therefore, closer observations of the surface were needed.

An AFM study of the surfaces was done to monitor the adsorption of single proteins on the surface of the microsieves (Figure 4): plasma-treated and EO_6-coated microsieves were analyzed after the filtration of 5, 50, and 100 mL of a 0.1 $g.L^{-1}$ BSA solution; the set-up did contain a pre-filter. Figure 4 (a and e) show the clean surfaces of plasma-treated and EO_6-coated microsieves, respectively. As mentioned previously, the roughness of both membranes is the same. The main corrugation visible on these pictures is due to the high grain size of these silicon nitride surfaces, resulting in round features with diameters between 100 and 300 nm. In our previous work on biorepellent Si_xN_4 surfaces (Chapter 7), these big features were not observed, and are due to the deposition conditions of the Si_xN_4 coatings. Smaller features in the background are also visible, which have a size close to horizontal resolution of the AFM (10 to 50 nm), and a height of about 1 nm. These small-sized grains were also observed on other smoother Si_xN_4 surfaces.

After the filtration of only 5 g of BSA solution (Figure 4b and f), the surface of plasma-treated microsieves clearly shows the appearance of surface contamination by proteins, in the form of 2 to 4 nm-high structures. In comparison, this contamination was hardly detectable on the EO_6-coated microsieves, which display at this stage good protein repellence.

After the filtration of 50 and 100 mL of protein solution, the initial features of the plasma-treated microsieve surfaces are barely recognizable, as protein aggregates accumulate on the surfaces. Even at this stage, the EO_6 coatings seem to prevent a massive adsorption of BSA on the Si_xN_4 surfaces, although Figure 4h reveals at least some surface contamination, observed via an increase in the number of round features with diameters of 50 to 100 nm.

This minor surface contamination (compared to the one observed with plasma-treated surfaces) could cause a loss in resolution of the AFM, by the adsorption of surface contaminants on the tip. Despite this observation, the surfaces of EO_6-coated microsieves mostly retained their initial features after the filtration experiments, thus displaying good biorepellent properties; therefore, it is also expected that the cleanability of these surfaces is much better.

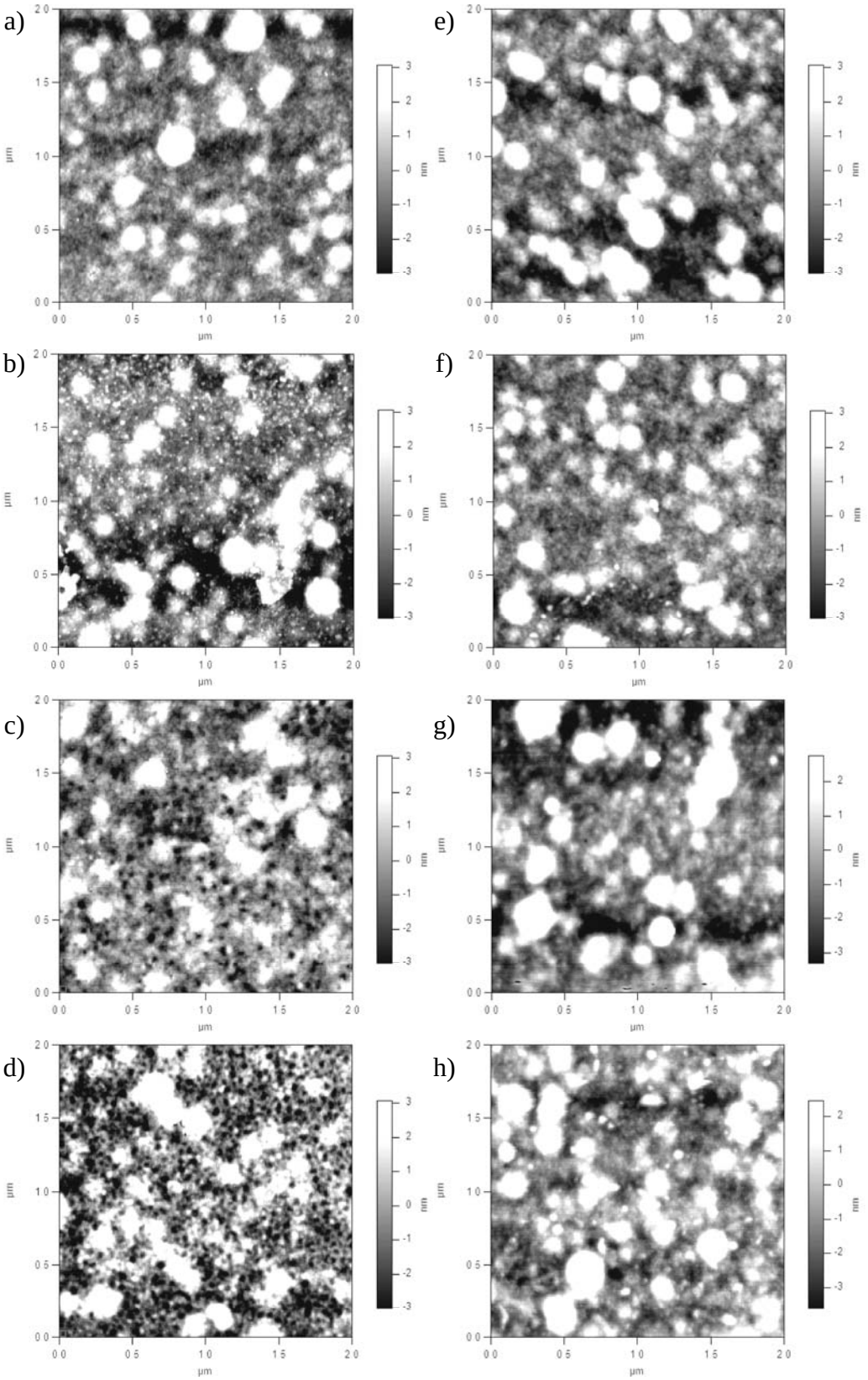

Figure 4. AFM pictures of plasma treated (left) and EO6-coated microsieves. a/e: clean surfaces, and after filtration of (b/f) 5 mL, (c/g) 50 mL and (d/h) 100 mL of BSA solution (0.1 $g.L^{-1}$). Horizontal scale: 2 µm, vertical scale: 6 nm.

Conclusions

EO_6 coatings applied via a UV technique, which were originally designed for flat surfaces, can successfully be applied to porous microsieves. The coatings do not influence the liquid flux, nor do they have any adverse wetting effects. An AFM study of the surfaces between the pores of the membranes after filtration clearly points to the superiority of the EO_6 coatings compared to plasma treatment, regarding protein repellence. The plasma treated microsieve (very hydrophilic) is heavily contaminated, and therewith, it is clear that the functionality of the EO groups is needed to effectively prevent protein adsorption.

Acknowledgments.

The authors thank Jos Sewalt and Dr. Gerben Brans for the assistance in the filtration experiments, and Graduate School VLAG and MicroNed (Project no. 6163510395) for financial support.

References

(1) van Rijn, C. J. M.; Nijdam, W.; Kulper, S.; Veldhuis, G. J.; van Wolferen, H.; Elwenspoek, M. *J. Micromech. Microeng.* **1999,** *9*, 170-172.

(2) van Rijn, C. J. M. *Nano and Micro Engineered Membrane Technology*. Aquamarijn Research BV, The Netherlands: 2002.

(3) Kuiper, S.; van Wolferen, H.; van Rijn, G.; Nijdam, W.; Krijnen, G.; Elwenspoek, M. *J. Micromech. Microeng.* **2001,** *11*, 33-37.

(4) Bermudez, V. M. *J. Electrochem. Soc.* **2005,** *152*, F31-F36.

(5) Bermudez, V. M. *Surf. Sci.* **2005,** *579*, 11-20.

(6) Patil, L. S.; Pandey, R. K.; Bang, J. P.; Gaikwad, S. A.; Gautam, D. K. *Opt. Mater.* **2005,** *27*, 663-670.

(7) Brans, G.; Kromkamp, J.; Pek, N.; Gielen, J.; Heck, J.; van Rijn, C. J. M.; Van der Sman, R. G. M.; Schroën, C. G. P. H.; Boom, R. M. *J. Membr. Sci.* **2006,** *278*, 344-348.

(8) Brans, G.; Schroën, C. G. P. H.; van der Sman, R. G. M.; Boom, R. M. *J. Membr. Sci.* **2004,** *243*, 263-272.

(9) Daufin, G.; Escudier, J. P.; Carrere, H.; Berot, S.; Fillaudeau, L.; Decloux, M. *Food Bioprod. Process.* **2001,** *79*, 89-102.

(10) Brans, G.; Van der Sman, R. G. M.; Schroën, C. G. P. H.; van der Padt, A.; Boom, R. M. *J. Membr. Sci.* **2006,** *278*, 239-250.

(11) Kuiper, S.; Brink, R.; Nijdam, W.; Krijnen, G. J. M.; Elwenspoek, M. C. *J. Membr. Sci.* **2002,** *196*, 149-157.

(12) Chandler, M.; Zydney, A. *J. Membr. Sci.* **2006,** *285*, 334-342.

(13) Kuiper, S.; van Rijn, C.; Nijdam, W.; Raspe, O.; van Wolferen, H.; Krijnen, G.; Elwenspoek, M. *J. Membr. Sci.* **2002,** *196*, 159-170.

(14) Mulder, M. *Basic Principles of Membrane Technology*. 2 ed.; Kluver Academic Publishers: Dordrecht, 1996; p 418.

(15) Girones, M.; Bolhuis-Versteeg, L.; Lammertink, R.; Wessling, M. *J. Colloid Interf. Sci.* **2006,** *299*, 831-840.

(16) Girones, M.; Lammertink, R. G. H.; Wessling, M. *J. Membr. Sci.* **2006,** *273*, 68-76.

(17) Belfort, G.; Davis, R. H.; Zydney, A. L. *J. Membr. Sci.* **1994,** *96*, 1-58.

(18) Palacio, L.; Ho, C. C.; Pradanos, P.; Hernandez, A.; Zydney, A. L. *J. Membr. Sci.* **2003,** *222*, 41-51.

(19) Bowen, W. R.; Calvo, J. I.; Hernandez, A. *J. Membr. Sci.* **1995,** *101*, 153.

(20) Ho, C. C.; Zydney, A. L. *J. Colloid Interf. Sci.* **2000,** *232*, 389-399.

(21) Ulbricht, M.; Belfort, G. *J. Appl. Polymer Sci.* **1995,** *56*, 325-343.

(22) Ulbricht, M.; Belfort, G. *J. Membr. Sci.* **1996,** *111*, 193-215.

(23) Girones, M.; Borneman, Z.; Lammertink, R. G. H.; Wessling, M. *J. Membr. Sci.* **2005,** *259*, 55-64.

(24) Dai, X. J.; Hamberger, S. M.; Bean, R. A. *Aust. J. Phys.* **1995,** *48*, 939-951.

(25) Arafat, A.; Giesbers, M.; Rosso, M.; Sudhölter, E. J. R.; Schroën, K.; White, R. G.; Yang, L.; Linford, M. R.; Zuilhof, H. *Langmuir* **2007,** *23*, 6233-6244.

(26) Arafat, A.; Schroën, K.; de Smet, L. C. P. M.; Sudhölter, E. J. R.; Zuilhof, H. *J. Am. Chem. Soc.* **2004,** *126*, 8600-8601.

(27) Rosso, M.; Arafat, A.; Schroën, K.; Giesbers, M.; Roper, C. S.; Maboudian, R.; Zuilhof, H. *Langmuir* **2008,** *24*, 4007-4012.

(28) Sieval, A. B.; Linke, R.; Zuilhof, H.; Sudhölter, E. J. R. *Adv. Mater.* **2000,** *12*, 1457-1460.

(29) Scheres, L.; Arafat, A.; Zuilhof, H. *Langmuir* **2007,** *23*, 8343-8346.

(30) Sieval, A. B.; Vleeming, V.; Zuilhof, H.; Sudhölter, E. J. R. *Langmuir* **1999,** *15*, 8288-8291.
(31) Rosso, M.; Giesbers, M.; Arafat, A.; Schroën, K.; Zuilhof, H. *Langmuir* **2009,** *25*, 2172-2180.
(32) Rosso, M.; de Jong, E.; Giesbers, M.; Fokkink, R. G.; Norde, W.; Schroën, K.; Zuilhof, H., submitted.

Chapter 9

Controlled Oxidation, Bio-functionalization, and Patterning of Alkyl Monolayers on Silicon and Si_xN_4 Surfaces using Plasma Treatment

A new method for the fast and reproducible functionalization of silicon and silicon nitride surfaces coated with covalently attached alkyl monolayers is presented. After formation of a methyl-terminated 1-hexadecyl monolayer on H-terminated Si(100) and Si(111) surfaces, short plasma treatments (1 to 3 s) are sufficient to create oxidized functionalities without damaging the underlying oxide-free silicon. The new functional groups can e.g. be derivatized using the reaction of surface aldehyde groups with primary amines to form imine bonds. In this way, plasma-treated monolayers on silicon or silicon nitride surfaces were successfully coated with nanoparticles, or proteins such as avidin. In addition, we demonstrate the possibility of patterning, using a soft contact mask during the plasma treatment, which yields micron-sized arrays. Using water contact angle measurements, ellipsometry, XPS, IRRAS, AFM and reflectometry, proof of principle is demonstrated of a yet unexplored way to form patterned alkyl monolayers on oxide-free silicon surfaces.

This chapter will be published as:
"Controlled Oxidation, Bio-functionalization, and Patterning of Alkyl Monolayers on Silicon and Silicon Nitride Surfaces using Plasma Treatment", Rosso, M.; Giesbers, M.; Schroën, K.; Zuilhof, H., in preparation.

Introduction

Plasma treatments of organic materials have been widely studied to prepare modified surfaces for organic membranes[1] or materials of biotechnological and biomedical interests.[2-4] Indeed, a short exposure of organic surfaces, usually polymers, to plasma can create directly new surface functionalities. The gas present in the plasma chamber determines the obtained functionalization:[5,6] oxygen or water plasma leads to the oxidation of surfaces, and to the formation of polar surface groups (-OH, C=O, O-C=O), whereas exposure to ammonia, for instance, will mainly yield surface amine groups ($-NH_2$). In most cases, these treatments produce surfaces with a higher biocompatibilty,[7-9] but another interesting application involves the subsequent functionalization of these surfaces with bio-active molecules for specific recognition and sensing.[10] While plasma treatments yield lower densities of surface functional groups than classical chemical reactions, this does not have to be a drawback given the size of the subsequently grafted moieties, whether they consist of biomolecules[2] (proteins, antibodies, DNA…) or polymer brushes.[11,12]

Beside the work carried out on polymer surfaces, several groups have also studied the effects of oxygen plasma,[13-15] as well as atomic oxygen[16,17] or ion beams[18,19] on organic thiol monolayers on gold. In comparison, very little has been done concerning the further functionalization of plasma-treated monolayers. Indeed, plasma treatment provides an easy and fast activation of chemically inert organic monolayers (e.g. methyl-terminated), with potential applications in bio-sensing. Recently, carbon dioxide[20] and oxygen[21] plasma treatments were used to functionalize alkylsilane monolayers on glass, and the latter work demonstrated the attachment of antibodies.

In this work, we extended the plasma functionalization to alkyl monolayers on oxide-free silicon, produced from the reaction of alkenes with hydrogen-terminated silicon surfaces and with HF-etched silicon-enriched silicon nitride ($Si_{3.9}N_4$). These high-quality alkyl monolayers, prepared by thermal or photochemical reaction of alkenes with hydrogen-terminated silicon surfaces,[22-33] have been studied for their high potential in sensing and nanotechnology applications,[34-36] due to the possibility to attach biomolecules onto these surfaces.[37-42] Importantly, these densely packed monolayers possess a much higher stability than thiol monolayers on gold or alkylsiloxane monolayers on oxide surfaces, because of the formation of strong Si-C bonds,[23,25,43] which makes them more robust in various applications.

Within the alkenes available for the formation of methyl-terminated alkyl monolayers, methyl-terminated, monofunctional alkenes are probably the most convenient to use: their purification is easy (distillation) and their grafting conditions are very flexible (liquid state, heat-resistant, UV-resistant > 250 nm). Once these stable monolayers are formed, a short plasma treatment (0.5 to 2 s) is able to form oxidized functionalities within the top few angstroms of the surface, while the underlying alkyl chains retain their initial packing and insulation properties of the inorganic substrate.

In addition, we show the easy formation of coatings of gold nanoparticles and functional proteins. In this latter case, the attachment of avidin was used, and the specific interaction with biotin-labeled BSA was monitored on the surface with reflectometry. Further, we demonstrate the feasibility of surface patterning, using a soft contact mask during the plasma oxidation. To our knowledge, this is the first attempt to functionalize alkyl monolayers on oxide-free silicon or silicon nitride using plasma. Besides the fundamental interest raised by the behavior of monolayers submitted to the plasma treatment, this technique provides a very fast (a few seconds) and reproducible grafting and dry patterning method for silicon surfaces.

Experimental Section

Materials

1-Hexadecene (99%) was purchased from Sigma-Aldrich and distilled twice under reduced pressure before use. m-(Trifluoromethyl)benzylamine (TFBA) (97%), cysteamine (2-aminoethanthiol), dimethyl sulfoxide (DMSO, spectrophotometric grade, 99.9%, dried over molecular sieves) and N-methyl-2-pyrrolidone (NMP, anhydrous, 99.5%) were purchased from Sigma-Aldrich and used as received for surface reactions. Citrate-terminated gold nanoparticles (AuNPs; diameter 15 nm) were purchased from Aurion BV, Wageningen, The Netherlands. Biotin hydrazide (98%), bovine serum albumin (BSA: fraction V, min 96% lyophilized powder), biotin-labeled BSA (lyophilized powder, 80%, extent of labeling: 8-16 mol biotin per mol BSA) and Avidin (recombinant protein from egg white, expressed in corn, ~ 12 units/mg protein) were purchased from Sigma.

Surface Modification

Monolayer formation onto Si(100) and Si(111) surfaces.

1-Hexadecyl-terminated silicon surfaces were obtained via a thermal modification in neat alkenes.[25] Silicon wafers of Si(100) ± 0.5º and Si(111) ± 0.5º, (both N-type Si, resistivity 1-5 Ω.cm; Siltronix, France) were first cleaned by sonication in acetone, followed by oxidation in air-based plasma for 5 min. Si(100) substrates were then H-terminated using etching in a 2.5% aqueous HF solution for 2 min, whereas Si(111) substrates were etched in a argon-saturated 40% aqueous solution of NH_4F for 15 min and subsequently rinsed with ultra-pure water. Right after etching, substrates were dried with an argon flow, and dipped into argon-saturated neat 1-hexadecene at 200 ºC to react for 4 h. After reaction, the modified substrates were rinsed thoroughly with petroleum ether and acetone and finally sonicated in acetone.

Monolayer formation onto Si_xN_4 surfaces.

Si-rich silicon nitride, (Si_xN_4: x ~ 3.9) deposited by CVD on Si(100) (thickness of 147 nm) was obtained from Lionix B.V., The Netherlands. 1-Hexadecyl-terminated silicon nitride substrates were obtained according to our previous work:[44] Si_xN_4 samples (with sizes of 1 × 1 cm for XPS or 4 × 0.75 cm for reflectometry) were cleaned by sonication in acetone, followed by oxidation in an air-based plasma for 15 min. The oxidized samples were then etched with a 2.5% aqueous HF solution for 2 min and dried in a nitrogen flow. They were then immediately dipped into argon-saturated neat alkenes in a fused silica flask. After 30 more min under argon flow, a UV pen lamp (254 nm, low pressure mercury vapor, double bore lamp from Jelight C^{ie}, California) was placed 4 mm above the Si_xN_4 surface and the sample was irradiated for 24 h. Afterwards, samples were removed and rinsed several times with petroleum ether and acetone, and sonicated in the same solvents.

Plasma oxidation and derivatization.

Monolayer-coated substrates were oxidized using a Harricks plasma cleaner/sterilizer (RF power 7.2 W), under a pressure of 5.10^{-2} mbar, with an air flow of about 25 l/h. After evacuation of the plasma chamber, the plasma was turned on for the desired time (0.5 to 3 s). The control of the position of the sample in the plasma chamber was important to obtain a reproducible degree of oxidation. Oxidized substrates were then directly used for subsequent treatments or analysis. *Amine attachment:* plasma-treated surfaces were dipped into 0.01 M solutions of TFBA in dry DMSO for 24 h. After reaction, samples were rinsed with DMSO

and acetone, sonicated in acetone and dried in a nitrogen flow. *Attachment of AuNPs:* plasma-treated surfaces were reacted with 10^{-2} M solutions of cysteamine in NMP for 24 h. The obtained thiol-terminated surfaces were then reacted with Au NPs in water for 2 h. After rinsing with water and acetone, samples were sonicated in acetone and dried. *Avidin attachment:* the plasma-oxidized surfaces were dipped for 24 h in a 10^{-2} M solution of biotin hydrazide in DMSO at room temperature for 24 h, followed by a 1 h incubation in 1 ml of a 1 mg/l solution of avidin in PBS buffer (pH 6.75). After attachment of avidin, the substrates were incubated in a 0.1 g/l solution of unlabeled BSA for 1 h, to passivate the remaining free area of the surface and thus avoid non-specific adsorption of protein during the reflectometry measurements.

Monolayer Characterization

Static Water Contact Angle

The wetting properties of modified surfaces were characterized by automated static water contact angle measurements performed with an Erma Contact Angle Meter G-1 (volume of the drop of demineralized water = 3.5 μl).

Ellipsometry

Thickness measurements were performed with a computer-controlled null ellipsometer (Sentech SE-400) using a He-Ne laser (λ = 632.8 nm) and an incident angle of 70°. The mode "polarizer + retarder, aperture, strict" was used. The layer thickness was determined using a three-layer model in the ellipsometry software from Sentech.

X-ray Photoelectron Spectroscopy (XPS)

The XPS analysis was performed using a JPS-9200 Photoelectron Spectrometer (JEOL, Japan). The high-resolution spectra were obtained under UHV conditions using monochromatic Al K_α X-ray radiation at 12 kV and 25 mA, with an analyzer pass energy of 10 eV. High-resolution spectra were corrected using a linear background subtraction before any peak deconvolution.

Fourier-transform infrared reflection absorption spectroscopy (FT-IRRAS)

Spectra were measured with a Bruker Tensor 27 FT-IR spectrometer, using a commercial variable-angle reflection unit (Auto Seagull, Harrick Scientific). A Harrick grid polarizer was installed in front of the detector, and was used to measure spectra with p-polarized (parallel)

radiation with respect to the plane of incidence at the sample surface. Single channel transmittance spectra were collected using a spectral resolution of 4 cm^{-1}, using 1024 scans in each measurement. The optimal angle for data collection was found to be 68º for all the surfaces studied. All the reported measurements were performed at this angle. Raw data files were divided by data recorded on a plasma-oxidized reference surface, to give the reported spectra.

X-ray photoelectron spectroscopy (XPS)

The XPS analysis was performed using a JPS-9200 Photoelectron Spectrometer (JEOL, Japan). The high-resolution spectra were obtained under UHV conditions using a monochromatic Al K_α X-ray radiation at 12 kV and 25 mA, using an analyzer pass energy of 10 eV and a take-off angle of 1º relative to the surface normal. All high-resolution spectra were corrected with a linear background before fitting. Binding energies were calibrated at 285.0 eV for the C_{1s} peak corresponding to carbon in alkyl chains. To facilitate the comparison between samples, XPS intensities measured on Si were normalized to the intensity of the Si_{2p} signal.

Atomic force microscopy (AFM)

Images were obtained with an MFP-3D AFM from Asylum Research (Santa Barbara, CA). Imaging was performed in AC mode in air using OMCL-AC240 silicon cantilevers (Olympus Corporation, Japan).

Reflectometry

The set-up used for reflectometry measurements has been described in Chapter 7. In short, a monochromatic light beam (He-Ne laser, λ = 632.8 nm) is linearly polarized and passes a 45 ° glass prism. This beam arrives at the interface with an angle of incidence of 66 º for the solvent/substrate interface. After reflection at the interface and refraction in the prism, the beam is split into its *p*- and *s*-polarized components relative to the plane of incidence by means of a beam splitter. Both components are separately detected by two photodiodes and the ratio between the intensity of the parallel and perpendicular components is the output signal *S* (*S* = *Ip*/*Is*). Combined with a stagnation point flow cell, the set-up allows the introduction of buffer or protein solutions, to study homogeneous adsorption on surfaces under diffusion-controlled conditions. Strips of Si_xN_4-coated silicon wafer (typical size of 4 × 0.75 cm) were coated with a monolayer on one end (about half of the sample length), while the other end was used to hold the strip in the measuring cell of the reflectometer. The BSA and biotin-labeled BSA (0.1 mg/L) were freshly prepared in PBS buffer (pH 6.75, ionic strength 0.08 M). All reflectometry experiments were performed at 23 ºC. Before measurements were made, surfaces were incubated 1 h in buffer to avoid artifacts due to initial surface wetting. After placing the samples in the reflectometer, the buffer solution was injected until the output signal was nearly constant: fluctuations of less than 0.001 V over 2 min were considered satisfactory. The adsorbed amounts of protein were calculated according to the method described Chapter 7.

Results and Discussion

Formation and plasma treatment of 1-hexadecyl monolayers on silicon

After 4 h of reaction in neat 1-hexadecene at 200 ºC, the silicon substrates were coated with a hydrophobic hexadecyl monolayer. Water contact angles of 109 ± 1º and 111 ± 1º were measured on Si(100) and Si(111) surfaces, respectively, in line with literature data.[45] No significant difference in layer thickness was measured with ellipsometry, giving monolayers on both surface orientations a thickness of 1.7 ± 0.1 nm.

When submitted to short plasma treatments, these hexadecyl monolayers on Si(100) and Si(111) surfaces showed similar behavior, when the reaction was monitored through water contact angle and monolayer thickness (See Figure 1): in the first 3 seconds of treatment, the

water contact angles decreased from ≥ 109º to 0º, indicating a complete surface coverage of polar oxidized species. Simultaneously, the monolayer thickness decreased from the initial 1.7 ± 0.1 nm down to about 1.3 ± 0.2 nm after 3 s. Shorter treatment times resulted in intermediate contact angles in a very reproducible way, indicating a progressive oxidation of surfaces. In particular, monolayers treated for 0.5 s (water contact angles: 89 ± 3º) were as thick as the initial 1-hexadecyl coatings (1.7 ± 0.1 nm), but less hydrophobic. At this stage, the oxidation of surfaces started, but no significant part of the monolayer was removed. After 1 s of treatment, the further decrease in contact angle (64 ± 3º) was accompanied by a small decrease in thickness of about 0.2 nm for both Si(100) and Si(111), indicating the oxidative fractionation of alkyl chains by the plasma. After 3 s of treatment, about a third of the monolayer thickness was removed.

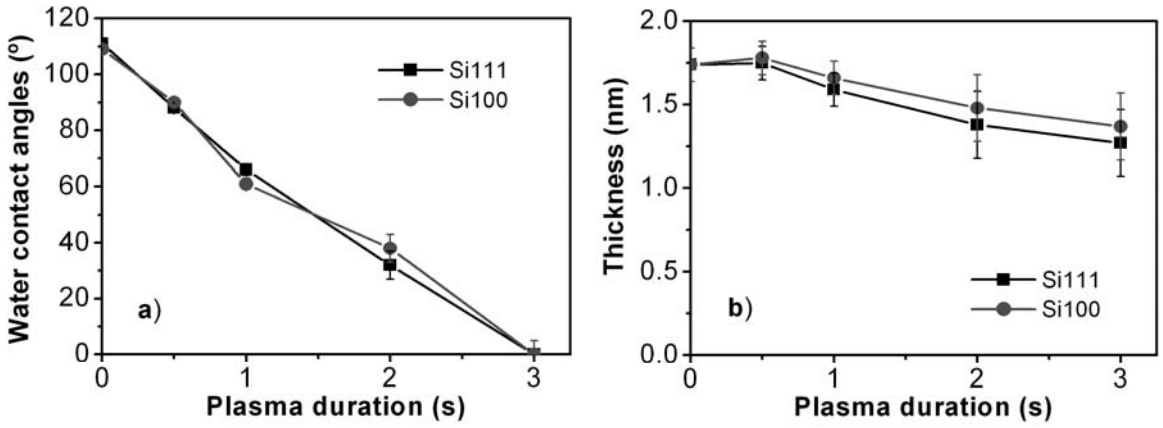

Figure 1. a) Water contact angles and b) ellipsometric thicknesses measured on hexadecyl-terminated Si(111) and Si(100) surfaces, before and after different times of plasma treatments.

The XPS analysis at the different stages of the plasma treatment gives more insight in the newly created surface functionalities. The C_{1s} region of the high-resolution XPS data measured at 0 to 3 s of plasma treatment reveals clearly the appearance of new oxygenated species on both Si(111) and Si(100) substrates (See Figure 2). The initial 1-hexadecyl monolayer showed a main peak at 285.0 eV, characteristic for alkyl chains (-CH_n-) and a small peak at 283.7 eV due to the terminal carbon bound to silicon (C-Si).[45]

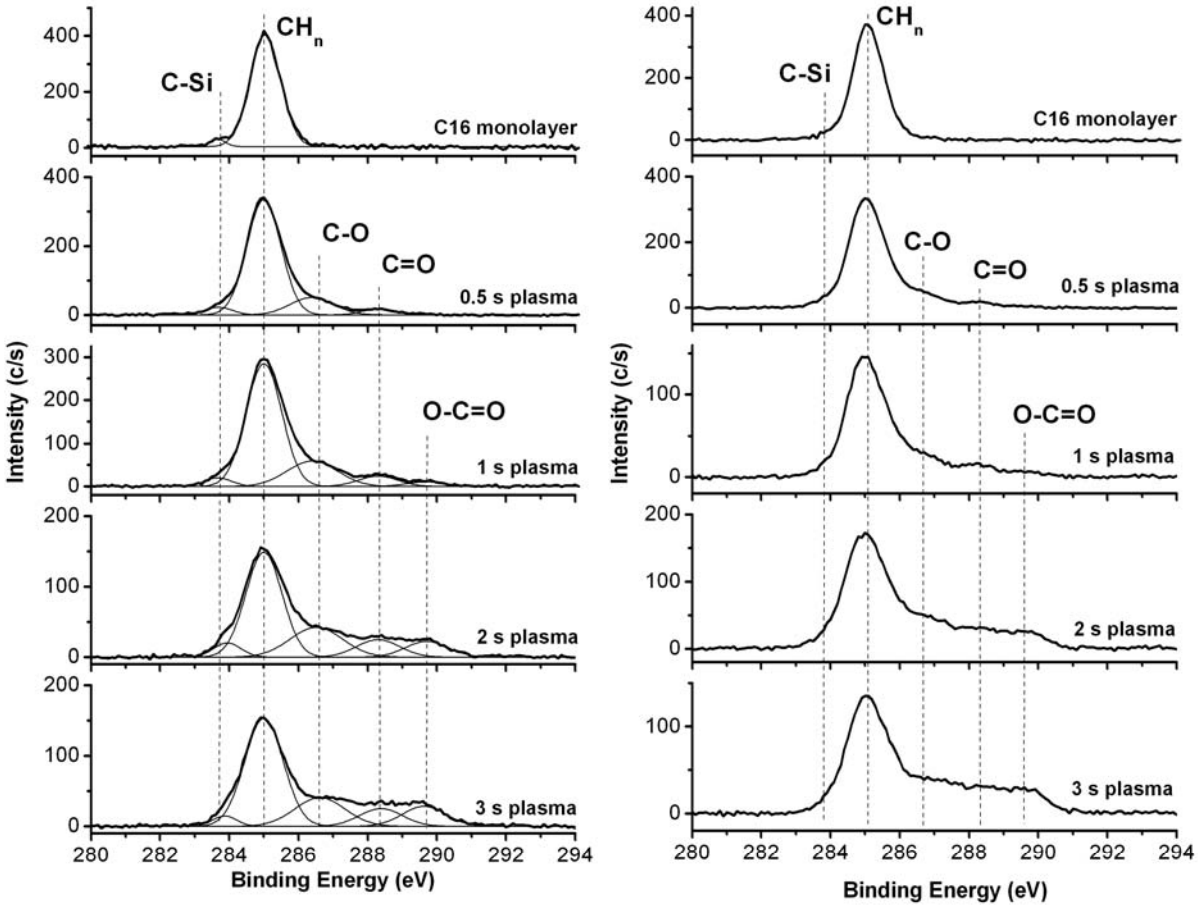

Figure 2. C_{1s} region of XPS data measured on plasma treated hexadecyl monolayers on Si(111) (left) and Si(100) (right) substrates after various reaction times. The data measured on Si(111) substrates is shown with the fitted contributions of the different carbon atoms.

After plasma treatment, a decrease in the intensity of the CH_n peak at 285.0 eV is associated with an increase in the intensity of peaks at higher binding energies. Interestingly, the total C_{1s} intensity did not decrease after 0.5 s of treatment, which implies that the top methyl groups are only partly oxidized and not yet removed. This confirms the conclusions already drawn from the ellipsometric measurements shown in Figure 1b. Despite the complexity of the plasma-induced oxidation reactions, which involve in particular the formation of highly reactive oxygen atoms,[46] the oxygen-bound carbons can be grouped under three main contributions at 286.6 eV (C-O), 288.3 eV (C=O) and 289.7 eV (O-C=O). Figure 3a gives an overview of the contributions of these different carbon species. Carbon atoms with a single bond to oxygen (C-O) seem the most favored throughout the whole treatment. After 1 s of oxidation, C=O bonds represent a significant part of the surface functionalities, most probably in the form of aldehyde groups that can react with primary amines to form imine bonds.[21] The

proportion of these C=O bonds on the surface did not increase much for plasma treatments longer than 1 s. This was confirmed by coupling these oxidized substrates with TFBA: samples treated for 1 s with plasma gave a maximum value of the normalized intensity of the F_{1s} peak measured on these samples at 689.0 eV (See Figure 3b). This maximum value, after correction for the different sensitivity factors of the C_{1s} and F_{1s} peaks, indicates that 35 to 40% of the C=O groups introduced after plasma treatment have reacted. The remaining part probably consists of aldehyde groups too hindered to react with the bulky TFBA molecules, or functionalities other than aldehydes that were also counted in the peak at 288.3 eV but with no or little reactivity towards amines under these conditions.

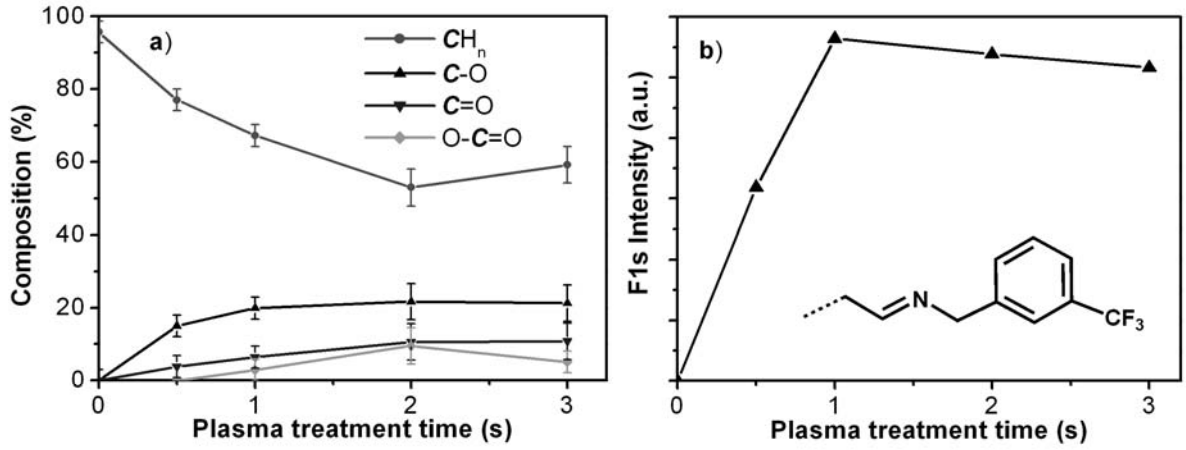

Figure 3. a) Relative proportions of the C_{1s} XPS signals at different times of plasma treatment (values for **C**-Si are omitted for clarity). b) Normalized F_{1s} intensity after coupling of oxidized surfaces with TFBA to form the fluorinated imine.

Unlike the C_{1s} region of XPS data, the Si_{2p} spectra measured on plasma-treated samples reveals an important difference between the Si(100) and Si(111) surfaces (See Figure 4): only for monolayers on Si(100) can we see the growth of a peak between 102.5 and 103.0 eV, corresponding to the formation of SiO_2 at the monolayer-substrate interface. After 3 s of treatment, this SiO_2 peak corresponds to 5% of the total Si_{2p} signal. In contrast to this behavior, the Si(111) substrate was not measurably affected by plasma treatment of monolayers. This difference in quality of the monolayers, already observed in their initial water contact angles (109 ± 1º and 111 ± 1º on Si(100) and Si(111) surfaces, respectively) can be explained by the different etching procedures of the two substrates. Indeed, unlike for Si(100), the buffered etching of Si(111) surfaces allows the formation of large atomically flat terraces, ensuring a better saturation of the surface after reaction with hexadecene.[45]

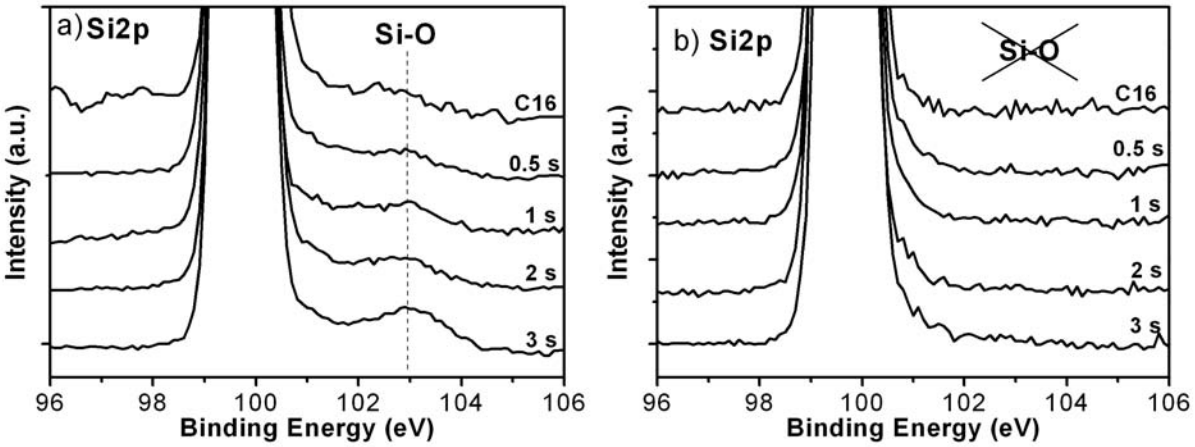

Figure 4. Si_{2p} region of the XPS data measured on 1-hexadecyl monolayers on a) Si(100) and b) Si(111) at different times of plasma treatment.

Plasma-treated samples were also characterized using IRRAS, where the observation of CH_n and C=O stretching vibrations corroborates the previous results. As can be seen in Figure 5 and Figure 6, the initial intensity of symmetric and antisymmetric CH_2 vibrations at 2851 and 2921 ± 1 cm^{-1}, respectively, gradually decreases upon increasing the duration of the plasma treatment. Meanwhile, the CH_3 vibration at 2965 cm^{-1} even disappears totally after 3 s of treatment, in line with complete loss of methyl-termination and formation of hydrophilic surfaces (water contact angle ~ 0º). The exact position of 2920 cm^{-1} and 2921 cm^{-1} for the symmetric CH_2 peaks on Si(111) and Si(100), respectively, implies a good packing density, since disordered monolayers can display values up to 2926 cm^{-1}.[47-49] It is remarkable that the plasma treatment does not influence the positions of both CH_2 peaks, even as their intensities decrease. This observation shows that the packing of the alkyl monolayers was not significantly affected by the plasma, even upon oxidation of the top surface. While the underlying alkyl chains remain unaffected by the plasma treatment, the growth of shoulders on the high-frequency side of the CH_2 peaks clearly reveals the appearance of a less dense layer in the upper part of the monolayer. Despite a low signal-to-noise ratio, IRRAS also allows us to monitor the growth of a wide peak centered at 1718 cm^{-1}, characteristic for C=O vibrations. This frequency is slightly lower than the typical value for aldehydes (~ 1728 cm^{-1}), but the large width of this peak indicates the presence of several carbonyl and carboxyl functionalities. Moreover, the exact position of this peak displayed some sample-to-sample variation, with values up to 1728 cm^{-1}.

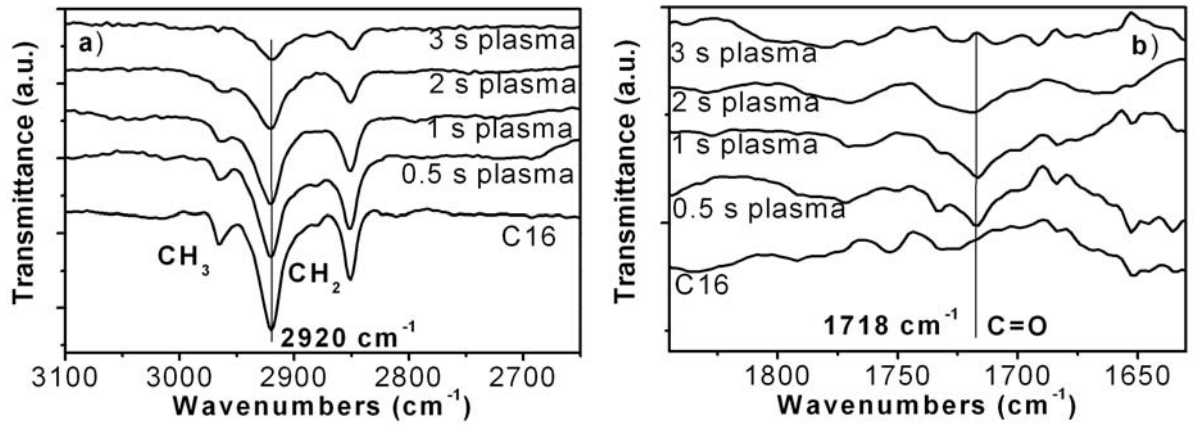

Figure 5. IRRAS data in the regions of a) CH_n and b) C=O stretching vibrations, measured on plasma-treated hexadecyl monolayers on Si(111) substrates, after different durations of plasma treatment.

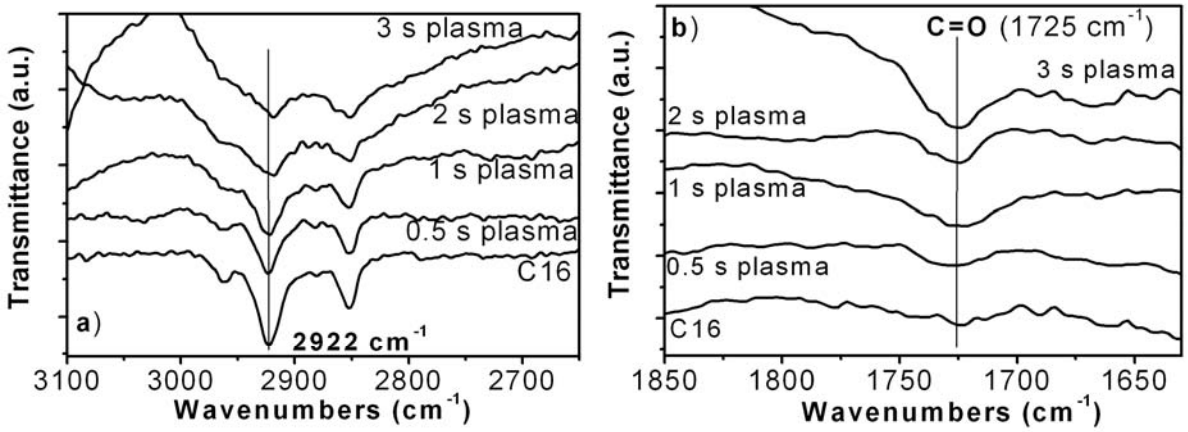

Figure 6. IRRAS data in the regions of a) CHn and b) C=O stretching vibrations, measured on plasma-treated hexadecyl monolayers on Si(100) substrates, after different durations of plasma treatment.

From ellipsometry, XPS and IRRAS measurements, it appears that the oxidation caused by the plasma treatment of coated Si(111) only affects the top of the monolayer, while its lower part retains its insulating properties. No sputtering or desorption of entire alkyl chains was observed, as it would lead to holes in the monolayers and subsequent oxidation of the substrate (See Figure 7).[16] Monolayers on Si(100) substrates displayed a less ideal behavior, probably due to the intrinsically lower quality of the etched surfaces, compared to the ones of Si(111).

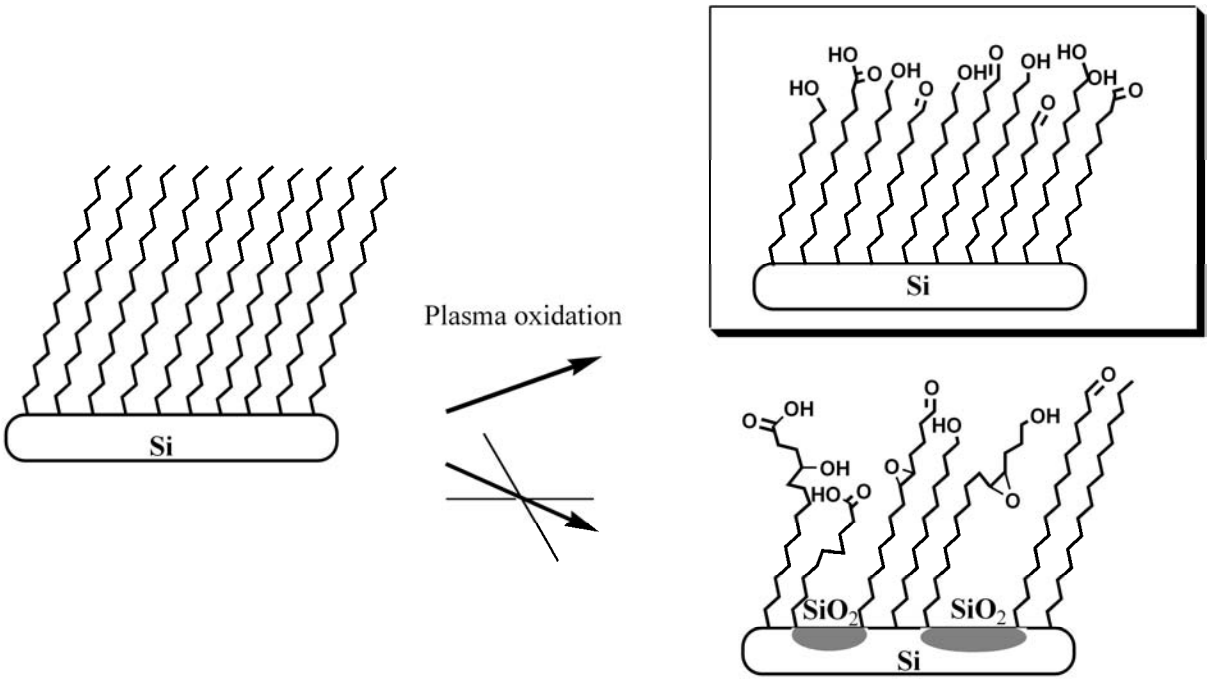

Figure 7. Surface reactions during plasma treatment of alkyl monolayers on silicon.

Attachment of Au NPs on plasma-treated monolayers and patterning.

For the attachment of gold nanoparticles (AuNPs), we only used Si(111) substrates, as these surfaces could completely withstand the plasma oxidation while allowing further functionalization. After plasma treatment of hexadecyl monolayers for 1 s, the resulting surface aldehydes were reacted with cysteamine (2-aminoethanethiol) to give substrates terminated with thiol functionalities. When samples were then placed in a solution of Au NPs, these would adsorb at the surface and remain attached due to the formation of Au-S bonds. After cleaning and sonication of the substrates in water, the dense coating of nanoparticles could be observed with AFM (See Figure 8b). The size of ~ 15 nm for individual Au NPs can be measured by the height-to-height distance on the AFM section, showing the presence of a single monolayer and the absence of aggregates. For comparison, Figure 8a shows the AFM picture of a monolayer-coated Si(111) surface before plasma treatment, which only displays the characteristic terraces of the underlying Si(111) surface.

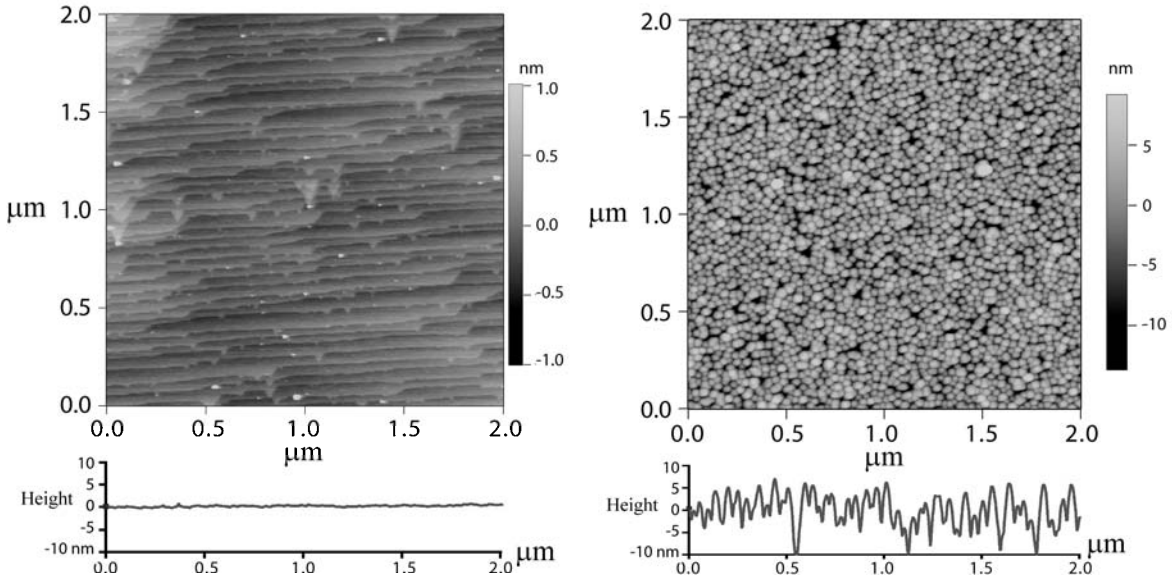

Figure 8. AFM pictures and sections measured on monolayer-coated silicon surfaces. Left: After exposure to cysteamine and gold nanoparticles without plasma treatment; right: after 1 s of air-based plasma followed by reaction with cysteamine and gold nanoparticles.

We subsequently used the grafting of Au NPs to demonstrate the possibility of surface patterning using plasma. Indeed, the combination of plasma treatments and classical photolithography techniques has already been proposed to carry out the fine patterning of surfaces[50,51] and the production of bio-arrays.[51] When a soft patterned PDMS mask was pressed to the monolayers during to the plasma treatment, the oxidation could be restricted to the unexposed area of the substrates. The result of such an experiment is presented in the AFM images in Figure 9, where the simple features of the stamp (straight line or angle) were perfectly reproduced after reaction with cysteamine and Au NPs. The non-exposed areas are comparable to Figure 8a, and retain their strong hydrophobic character, which proves the persistence of the intact hexadecyl monolayer. The boundary between the different areas displays some irregular features: at the edge of the PDMS stamps, an elevated line is visible, which was already observed in previous patterning experiments involving PDMS stamps on silicon surfaces.[52] In this case, the features might be due to some leaching of uncross-linked silicone polymer chains from the PDMS stamp. Since they were only found around, and not inside the areas that were covered by the stamps, we conclude that the plasma could oxidize these uncross-linked silicone polymers to yield these insoluble residues. The coverage of AuNPs does not show an abrupt transition, but a regular decrease over 0.5 µm as they

approach the boundary. This imperfection is probably due to limitations to the diffusion of the plasma at the edge of the stamp, during the short reaction time. Indeed, similar patterning experiments with micrometer-sized features, where the plasma can diffuse under the stamp, showed a small mean free path of the plasma (~ 1 μm). Nevertheless, the observed thin transition area (~ 0.5 μm) would allow the formation of complex patterns, using soft stamps with perforated micron-sized features, such as polymeric microsieves.[53]

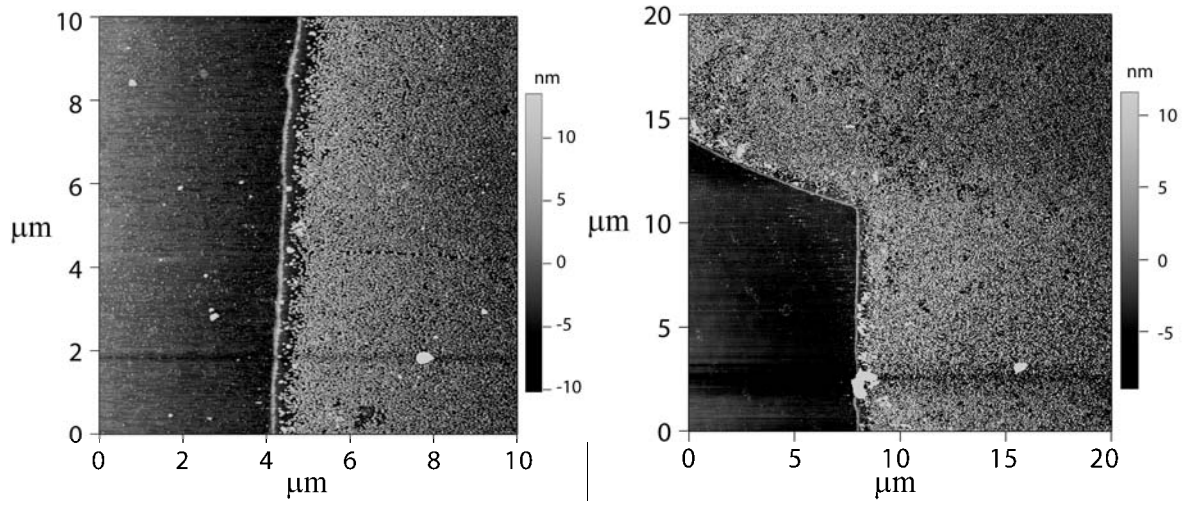

Figure 9. AFM images of monolayer-coated silicon surfaces patterned during plasma treatment, and reacted with cysteamine and AuNPs (horizontal range: left 10 μm, right 20 μm, vertical range left: 23 nm, right 20 nm).

Formation of biospecific surfaces.

To demonstrate the easy bio-functionalization of alkene-based monolayers using plasma oxidation, hexadecyl monolayers were prepared on silicon nitride,[48,49,54,55] using a hydrosilylation reaction similar to the one used for silicon. In particular we used a UV-mediated reaction of alkenes with etched silicon nitride surfaces,[55] and a plasma treatment as described above. The specific surface configuration (monolayer on silicon nitride deposited onto a silicon wafer) allows the use of reflectometry to monitor *in-situ* protein adsorption after attachment of specific biomolecules.[44]. For this purpose, plasma-treated hexadecyl monolayers were reacted with biotin hydrazide, and the resulting biotin-terminated substrate were incubated with avidin in PBS buffer, and then with BSA. As depicted in

Figure 10, avidin still has some of its 4 recognition sites available after a specific adsorption with the immobilized biotin.[56] The final saturation of free surface sites with BSA ensures that no protein will adsorb unspecifically during the reflectometry measurements.[21]

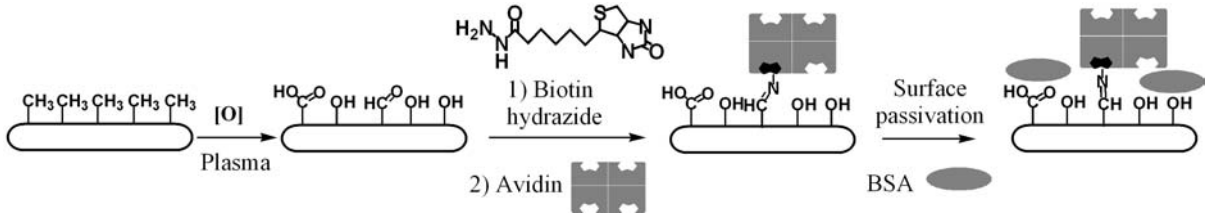

Figure 10. Formation of avidin-terminated surfaces, using plasma treatment, and subsequent reactions with biotin hydrazide and avidin, followed by passivation of the remaining areas with BSA.

The reflectometry measurements displayed in Figure 11a show the specific interaction of biotin-labeled BSA with avidin-functionalized silicon nitride surfaces: during the first phase of exposure to unlabeled BSA, no adsorption occurred, because all the areas available for non-specific adsorption have already been saturated, either by avidin attachment, or by the subsequent incubation with BSA. When biotin-labeled BSA is introduced in the cell, an adsorption of 0.5 mg/m^2 was measured, due to the specific avidin-biotin interaction. For comparison, reflectometry experiments were also carried out without the prior surface saturation with BSA (Figure 11b). In that case, a first slower non-specific adsorption of unlabeled BSA (~ 1 mg/m^2) is observed, followed by a fast adsorption of biotinylated BSA identical to that observed in the previous experiment. From these adsorbed amounts, we can deduce that the biotin-labeled BSA can still occupy roughly one third of the available surface: the total surface saturation (BSA and biotin-labeled BSA) of 1.5 mg/m^2 was comparable with the normal coverage of BSA on bare oxide surfaces.

The surface density of the functionalization obtained with the plasma treatment is an important issue if this method has to compete with classical chemical reactions. It is obvious that the simplicity, speed and effectiveness make this method highly competitive, specifically for use of binding of relatively big species, such as the proteins or nanoparticles presented in this work.

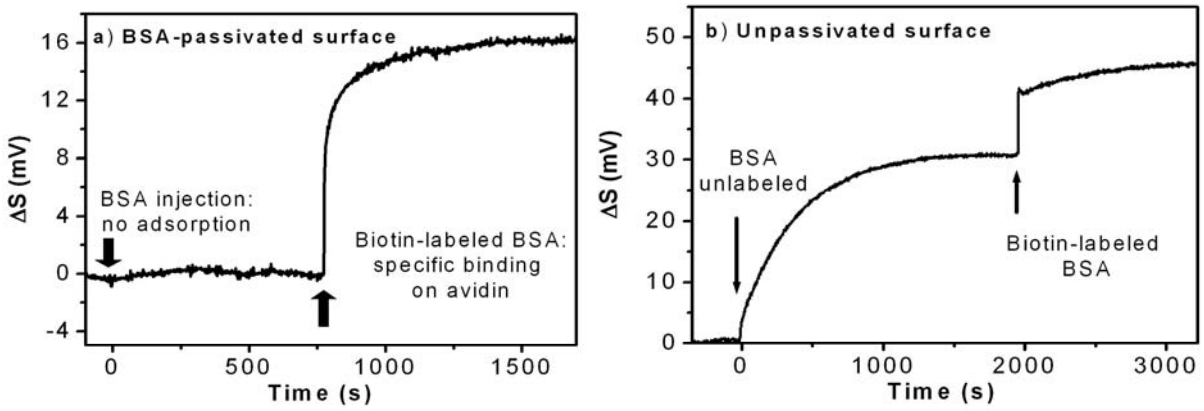

Figure 11. Reflectometry data obtained by subjecting avidin-coated silicon nitride surfaces to BSA and biotin-labeled BSA, a) with a passivation of the modified surfaces overnight in a BSA solution; b) without BSA passivation, directly after attachment of avidin.

Conclusions

The reported results show the possibility to use a simple and short (maximally 3 seconds) plasma treatment to functionalize methyl-terminated monolayers on silicon and silicon nitride surfaces in a fast and reproducible way. The quality of the monolayers and substrates was not affected by the activation of the top molecular layer of the coatings, as shown with IRRAS and XPS. The plasma treatment allows the ready attachment of functional proteins, as demonstrated by the avidin-biotin interaction. Grafting of gold nanoparticles and biomolecules can also easily be achieved, while the use of a patterned mask during the plasma treatment results in micron-sized arrays. This is a new technique for the spatially-controlled chemical and biochemical functionalization of silicon and silicon nitride surfaces, which can likely also be applied to organic monolayers that are covalently attached onto other surfaces. A similar method for the patterning of proteins on silicon surfaces was already described, using the AFM-induced electrooxidation of methyl-terminated oligoethylene oxide monolayers;[57] using plasma oxidation, larger areas of methyl-terminated monolayers could be patterned quickly and in mild conditions.

Acknowledgments

The authors thank Graduate School VLAG and MicroNed (Project no. 6163510395) for financial support, and Remko Fokkink (Wageningen University) for technical support.

References

(1) Durand, J.; Rouessac, V.; Roualdes, S. *Ann. Chim.-Sci. Mat.* **2007,** *32*, 141-158.

(2) Siow, K. S.; Britcher, L.; Kumar, S.; Griesser, H. J. *Plasma Process. Polym.* **2006,** *3*, 392-418.

(3) Denes, F. *Trends Polymer Sci.* **1997,** *5*, 23-31.

(4) Uyama, Y.; Kato, K.; Ikada, Y. *Adv. Polym. Sci.* **1998,** *137*, 1-39.

(5) Poncin-Epaillard, F.; Legeay, G. *J. Biomater. Sci. Polymer Ed.* **2003,** *14*, 1005-1028.

(6) Vandencasteele, N.; Merche, D.; Reniers, F. *Surf. Interface Anal.* **2006,** *38*, 526-530.

(7) Giroux, T. A.; Cooper, S. L. *J. Colloid Interf. Sci.* **1990,** *139*, 351-362.

(8) Ulbricht, M.; Belfort, G. *J. Membr. Sci.* **1996,** *111*, 193-215.

(9) Ulbricht, M.; Belfort, G. *J. Appl. Polymer Sci.* **1995,** *56*, 325-343.

(10) Steffen, H. J.; Schmidt, J.; Gonzalez-Elipe, A. *Surf. Interface Anal.* **2000,** *29*, 386-391.

(11) Kingshott, P.; Thissen, H.; Griesser, H. J. *Biomaterials* **2002,** *23*, 2043-2056.

(12) Kingshott, P.; McArthur, S.; Thissen, H.; Castner, D. G.; Griesser, H. J. *Biomaterials* **2002,** *23*, 4775-4785.

(13) Raacke, J.; Giza, M.; Grundmeier, G. *Surf. Coat. Technol.* **2005,** *200*, 280-283.

(14) Elms, F. M.; George, G. A. **1998,** *9*, 31-37.

(15) Dai, X. J.; Elms, F. M.; George, G. A. *J. Appl. Polymer Sci.* **2001,** *80*, 1461-1469.

(16) Wagner, A. J.; Wolfe, G. M.; Fairbrother, D. H. *J. Chem. Phys.* **2004,** *120*, 3799-3810.

(17) Torres, J.; Perry, C. C.; Bransfield, S. J.; Fairbrother, D. H. *J. Phys. Chem. B* **2002,** *106*, 6265-6272.

(18) Qin, X. D.; Tzvetkov, T.; Jacobs, D. C. *J. Phys. Chem. A* **2006,** *110*, 1408-1415.

(19) Qin, X.; Tzvetkov, T.; Jacobs, D. C. *Nucl. Instrum. Meth. Phys. Res. B* **2003,** *203*, 130-135.

(20) Delorme, N.; Bardeau, J. F.; Bulou, A.; Poncin-Epaillard, F. *Thin Solid Films* **2006,** *496*, 612-618.

(21) Xue, C. Y.; Yang, K. L. *Langmuir* **2007,** *23*, 5831-5835.

(22) Boukherroub, R.; Morin, S.; Bensebaa, F.; Wayner, D. D. M. *Langmuir* **1999,** *15*, 3831-3835.

(23) Buriak, J. M. *Chem. Rev.* **2002,** *102*, 1271-1308.

(24) Eves, B. J.; Sun, Q. Y.; Lopinski, G. P.; Zuilhof, H. *J. Am. Chem. Soc.* **2004,** *126*, 14318-14319.

(25) Linford, M. R.; Fenter, P.; Eisenberger, P. M.; Chidsey, C. E. D. *J. Am. Chem. Soc.* **1995,** *117*, 3145-3155.

(26) Shirahata, N.; Hozumi, A.; Yonezawa, T. *Chem. Rec.* **2005,** *5*, 145-159.

(27) Sieval, A. B.; Linke, R.; Zuilhof, H.; Sudhölter, E. J. R. *Adv. Mater.* **2000,** *12*, 1457-1460.

(28) Sieval, A. B.; Opitz, R.; Maas, H. P. A.; Schoeman, M. G.; Meijer, G.; Vergeldt, F. J.; Zuilhof, H.; Sudhölter, E. J. R. *Langmuir* **2000,** *16*, 10359-10368.

(29) Sun, Q.-Y.; de Smet, L. C. P. M.; van Lagen, B.; Giesbers, M.; Thune, P. C.; van Engelenburg, J.; de Wolf, F. A.; Zuilhof, H.; Sudhölter, E. J. R. *J. Am. Chem. Soc.* **2005,** *127*, 2514-2523.

(30) Sun, Q.-Y.; de Smet, L. C. P. M.; van Lagen, B.; Wright, A.; Zuilhof, H.; Sudhölter, E. J. R. *Angew. Chem., Int. Ed.* **2004,** *43*, 1352-1355.

(31) Wayner, D. D. M.; Wolkow, R. A. *J. Chem. Soc., Perkin Trans. 2* **2002**, 23-34.

(32) Boukherroub, R. *Curr. Opin. Solid State Mater. Sci.* **2005,** *9*, 66-72.

(33) Sieval, A. B.; Demirel, A. L.; Nissink, J. W. M.; Linford, M. R.; van der Maas, J. H.; de Jeu, W. H.; Zuilhof, H.; Sudhölter, E. J. R. *Langmuir* **1998,** *14*, 1759-1768.

(34) Lasseter, T. L.; Clare, B. H.; Abbott, N. L.; Hamers, R. J. *J. Am. Chem. Soc.* **2004,** *126*, 10220-10221.

(35) Aswal, D. K.; Lenfant, S.; Guerin, D.; Yakhmi, J. V.; Vuillaume, D. *Anal. Chim. Acta* **2006,** *568*, 84-108.

(36) Zhao, J. W.; Uosaki, K. *J. Phys. Chem. B* **2004,** *108*, 17129-17135.

(37) Letant, S. E.; Hart, B. R.; Van Buuren, A. W.; Terminello, L. J. *Nat. Mater.* **2003,** *2*, 391-396.

(38) Liao, W.; Wei, F.; Qian, M. X.; Zhao, X. S. *Sens. Actuators, B* **2004,** *101*, 361-367.

(39) Voicu, R.; Boukherroub, R.; Bartzoka, V.; Ward, T.; Wojtyk, J. T. C.; Wayner, D. D. M. *Langmuir* **2004,** *20*, 11713-11720.

(40) de Smet, L. C. P. M.; Stork, G. A.; Hurenkamp, G. H. F.; Sun, Q. Y.; Topal, H.; Vronen, P. J. E.; Sieval, A. B.; Wright, A.; Visser, G. M.; Zuilhof, H.; Sudhölter, E. J. R. *J. Am. Chem. Soc.* **2003,** *125*, 13916-13917.

(41) Lin, Z.; Strother, T.; Cai, W.; Cao, X. P.; Smith, L. M.; Hamers, R. J. *Langmuir* **2002,** *18*, 788-796.

(42) Strother, T.; Hamers, R. J.; Smith, L. M. *Nucleic Acids Res.* **2000,** *28*, 3535-3541.

(43) Bateman, J. E.; Eagling, R. D.; Worrall, D. R.; Horrocks, B. R.; Houlton, A. *Angew. Chem., Int. Ed.* **1998,** *37*, 2683-2685.

(44) Rosso, M.; de Jong, E.; Giesbers, M.; Fokkink, R. G.; Norde, W.; Schroën, K.; Zuilhof, H., submitted.

(45) Avila, A.; Montero, I.; Galan, L.; Ripalda, J. M.; Levy, R. **2001,** *89*, 212-216.

(46) Hijikata, Y.; Yaguchi, H.; Yoshikawa, M.; Yoshida, S. **2001,** *184*, 161-166.

(47) Guy, O. J.; Chen, L.; Pope, G.; Teng, K. S.; Maffeis, T.; Wilks, S. P.; Mawby, P. A.; Jenkins, T.; Brieva, A.; Hayton, D. J. **2006,** *527-529*, 1027-1030.

(48) Choyke, W. J.; Matsunami, H.; Pensl, G. *Silicon Carbide, Recent Major Advances*. Springer: Berlin, 2003.

(49) Muehlhoff, L.; Bozack, M. J.; Choyke, W. J.; Yates, J. T. **1986,** *60*, 2558-2563.

(50) Roccaforte, F.; La Via, F.; Raineri, V.; Musumeci, P.; Calcagno, L.; Condorelli, G. G. **2003,** *77*, 827-833.

(51) Starke, U. **1997,** *202*, 475-499.

(52) vanElsbergen, V.; Janzen, O.; Monch, W. **1997,** *B46*, 366-369.

(53) Lin, M. E.; Strite, S.; Agarwal, A.; Salvador, A.; Zhou, G. L.; Teraguchi, N.; Rockett, A.; Morkoc, H. **1993,** *62*, 702-704.

(54) Losurdo, M.; Giangregorio, M. M.; Capezzuto, P.; Bruno, G.; Brown, A. S.; Kim, T. H.; Yi, C. H. **2005,** *34*, 457-465.

(55) Bernhardt, J.; Schardt, J.; Starke, U.; Heinz, K. **1999,** *74*, 1084-1086.

(56) Sieber, N.; Seyller, T.; Graupner, R.; Ley, L.; Mikalo, R.; Hoffmann, P.; Batchelor, D. R.; Schmeisser, D. **2001,** *184*, 278-283.

(57) Sieval, A. B.; Demirel, A. L.; Nissink, J. W. M.; Linford, M. R.; van der Maas, J. H.; de Jeu, W. H.; Zuilhof, H.; Sudholter, E. J. R. **1998,** *14*, 1759-1768.

(58) Sun, Q.-Y.; de Smet, L. C. P. M.; van Lagen, B.; Giesbers, M.; Thune, P. C.; van Engelenburg, J.; de Wolf, F. A.; Zuilhof, H.; Sudhölter, E. J. R. **2005,** *127*, 2514-2523.

(59) Onclin, S.; Ravoo, B. J.; Reinhoudt, D. N. **2005,** *44*, 6282-6304.

(60) Arafat, A.; Schroën, K.; de Smet, L. C. P. M.; Sudhölter, E. J. R.; Zuilhof, H. **2004,** *126*, 8600-8601.

(61) Arafat, A.; Giesbers, M.; Rosso, M.; Sudhölter, E. J. R.; Schroën, K.; White, R. G.; Yang, L.; Linford, M. R.; Zuilhof, H. **2007,** *23*, 6233-6244.

(62) Mischki, T. K.; Donkers, R. L.; Eves, B. J.; Lopinski, G. P.; Wayner, D. D. M. **2006,** *22*, 8359-8365.

(63) Onneby, C.; Pantano, C. G. **1997,** *15*, 1597-1602.

(64) Soraru, G. D.; Modena, S.; Guadagnino, E.; Colombo, P.; Egan, J.; Pantano, C. **2002,** *85*, 1529-1536.

(65) Iler, R. K. *The Chemistry of Silica*. New York, 1979.

(66) Knickerbocker, T.; Strother, T.; Schwartz, M. P.; Russell, J. N.; Butler, J.; Smith, L. M.; Hamers, R. J. **2003,** *19*, 1938-1942.

(67) Bain, C. D.; Evall, J.; Whitesides, G. M. **1989,** *111*, 7155-7164.

(68) Faucheux, A.; Gouget-Laemmel, A. C.; de Villeneuve, C. H.; Boukherroub, R.; Ozanam, F.; Allongue, P.; Chazalviel, J. N. **2006,** *22*, 153-162.

(69) Asanuma, H.; Noguchi, H.; Uosaki, K.; Yu, H. Z. **2006,** *110*, 4892-4899.

(70) Strother, T.; Cai, W.; Zhao, X. S.; Hamers, R. J.; Smith, L. M. **2000,** *122*, 1205-1209.

Chapter 10

General Discussion

In this last chapter, some of the most striking effects that are described in the previous chapters are put into a wider perspective. In particular, the formation and stability of organic monolayers is discussed for the various methods that were applied. Further, the application of such layers is discussed in relation to biofunctionalization and biorepellence, and the chapter is concluded with an overview of the opportunities this provides for surface engineering.

Formation and stability of organic monolayers

We have succeeded in the formation of stable, covalently bound alkyl monolayers on silicon nitride and silicon carbide, two materials with interesting mechanical, chemical, optical and electrical properties. So far, the only reported way to bind molecules to the surface of these materials was to use the reaction of silanes with the poorly defined native oxide resulting from the oxidation of these materials.

The main advantage of the methods we describe in Chapter 4 to 6 is the clear increase in stability due to the direct functionalization of the etched materials: all of the native oxide is removed by etching, and the alkyl monolayers are attached via the strong predominant Si-C and C-O-C bonds resulting from the alkylation of Si_xN_4 and SiC, respectively. These intrinsically more robust materials can also contribute to the stability of monolayers, since they will be less sensitive to the presence of pinholes in the monolayers, compared to silicon or silicon oxide surfaces. The UV modification technique presented in this thesis also adds to the chemical resistance of the coatings: the possibility to form multilayers with controlled thicknesses seems to point to a radical mechanism that can be propagated through the monolayer. In this scenario, the presence of radicals within the monolayer can possibly cause cross-linking of the organic chains, which would explain the observed increase in stability. In this regard, but also considering its other advantages (small required amount of alkenes, reproducibility), the UV-induced reaction should be preferred to the thermal method, as long as the organic compounds have a low absorption at the wavelengths used.

The stability of the obtained alkyl monolayers with the UV-initiated attachment on Si_xN_4 and SiC can perhaps be increased even more. For example, the use of other reactive groups, such as terminal alkynes instead of alkenes could result in a stronger bond to the surface. This superior stability of alkynes over alkenes was indeed observed in the thermal monolayer formation on Si_xN_4 surfaces (Chapter 4) and previous studies on silicon also mention the possibility to form multiple bonds with the surfaces.[1] It is expected that the stability of UV-induced monolayers can also be improved by the inclusion of internal groups (alkenes, alkynes or others) in the middle of the linear alkyl chains, as long as the cross-linking and the formation of thin homogeneous coatings could be controlled.

The mechanism of the UV-induced reaction is open to various experimental challenges. The reaction apparently involves radicals, but the causes of the reaction initiation are still

unclear. Therefore, it might be interesting to study the formation of UV-induced monolayers on surfaces with different doping levels: in particular, SiC wafers can be obtained with different doping concentrations and the change in electronic band-gap caused by the doping could have some influence on the monolayer formation, if a mechanism involving radical-cation activation were involved, like in the case of silicon.[2]

Unlike silicon, SiC and Si_xN_4 are high-bandgap materials and a straightforward explanation based on energy differences can be difficult to justify: the electronic bandgaps of SiC (2.3 to 3.3 eV) and Si_xN_4 (2 to 4 eV) are very similar to the bond enthalpies of most bonds present at the surface of the etched materials. In other words, the optimal 254 nm-irradiation wavelength that we use, corresponding to an energy per photon of 4.9 eV could well cause both homolytic bond cleavages and bandgap excitations. The use of materials with more defined properties and/or different bandgaps could show a preference for one or another mechanism. If such well-defined SiC surface can be prepared and coated with monolayers, the different reactivities of the crystal faces could be studied; notably, the formation of monolayers on the most frequently encountered C-terminated (000-1) face and the Si-terminated (0001) face could be investigated.

Apart from these mechanistic studies, it would be highly interesting to know whether doping could reduce the irradiation times (number of photons) or the photon energy required for the formation of a monolayer. The possibility to use wavelength above 320 nm would also allow the direct attachment of sensitive biomolecules, as is possible on silicon using visible light.[3] In addition, a shorter irradiation time would also make surface patterning with light practically easier.

Another way to improve the monolayers formed on SiC surfaces would be to modify the etching method prior to the reaction: indeed, we present here a bench-top wet etching that can easily be applied in any laboratory, but these conditions do not allow the formation of oxygen-free surfaces on this material. Atomically flat hydrogen-terminated SiC surfaces, for example, might show reaction conditions more similar to the one observed on etched silicon surfaces, i.e. milder reaction conditions and higher packing density of the monolayer. All the combined benefits of a robust material, a well-defined surface and a dense monolayer would yield coatings with outstanding stabilities. Moreover, an atomically flat surface might favor the more efficient propagation of a radical chain reaction, and the coating procedure could be done in a shorter time, as is the case for silicon(111) surfaces. In contrast to this, the high density of defects found on hydroxyl-terminated surfaces can prevent this propagation of the

coating reaction. Such oxygen-free SiC surfaces could be prepared in high-vacuum conditions,[4-6] and reacted with alkenes or alkynes in the gas phase. This more controlled environment would also allow to scale-up the production of coated surfaces: with a proper engineering of the deposition process, batches of several wafers covered with the devices to modify could be prepared at the same time.

Biofunctional monolayers

The functionalization of both Si_xN_4 and SiC surfaces is clearly demonstrated in this thesis through the direct attachment of alkyl chains, esters, phtalimides and oligoethylene glycols. Additionally, the deprotection of phtalimides and esters can yield amines and carboxylic acids on the surfaces, which can be coupled with virtually any interesting compound via the chemistry of activated esters, etc.

Since UV-induced monolayer formation gives the best results (stability, coating density), the preparation of functional monolayers on SiC and Si_xN_4 can be achieved best using activated esters: 2,2,2-trifluoroethyl undecenoate, for example, can be coupled with amines in almost quantitative yield (> 80%), after a basic hydrolysis and the formation of an NHS (*N*-hydroxysuccinimide) ester. This reaction is probably mostly limited by steric hindrance at the surface. When the density of surface grafting can be lower, like for the attachment of big biomolecules (compared to the size of the alkene precursors), a surface activation with the controlled plasma oxidation described in chapter 9 offers a simple and fast alternative to produce bioactive surfaces, without the need of a chemical deprotection step.

However, amines can also react directly with the 2,2,2-trifluoroethyl ester[7] (in organic solvents), and preliminary solution studies with simple amines, such as 1,2-diaminoethane (neat or in DMSO; data not shown) indicated a the possibility for a quantitative surface conversion. This approach could be used to produce dense coatings of biologically relevant molecules on the surfaces in a fast and reproducible way: The reaction of biotin hydrazide in anhydrous DMSO or DMF with a trifluoroester-terminated monolayer would create a dense layer of biotin on the surface (Figure 1). Any further biofunctionalization could be done in aqueous solutions: the binding of streptavidin on the biotinylated surface and the final attachment of a biotinylated proteins (or any biomolecule of interest).

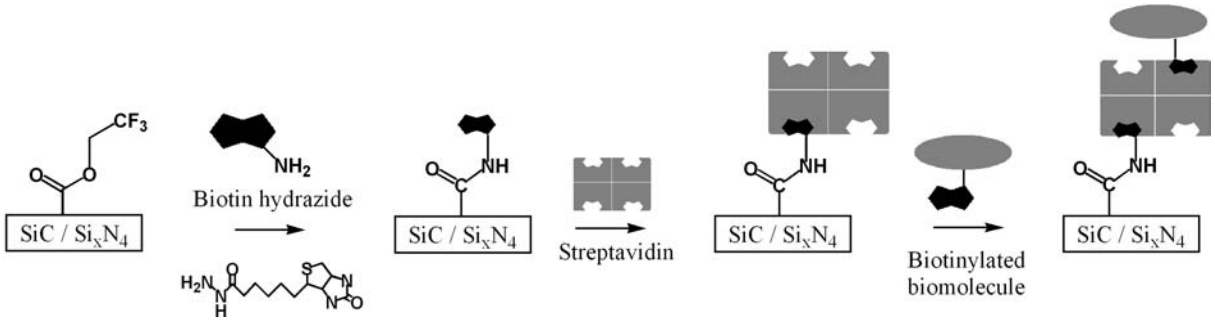

Figure 1. Reaction scheme for the biofunctionalization of SiC and Si_xN_4 surfaces coated via UV-induced monolayer formation with 2,2,2-trifluorethyl undecenoate. The use of the biotin-streptavidin interaction provides a flexible attachment platform.

In theory, many combinations of monolayer formation and chemical functionalization are possible. But the one described in Figure 1 currently seems the most promising: It combines the reproducibility of the trifluoroethyl ester-terminated monolayer with the fast and quantitative reaction with primary amines in anhydrous solvents to form stable amide bonds, and the flexibility offered by the widely used streptavidin-biotin system. Indeed, many biological molecules can be purchased with a biotin-tag nowadays, and can thus be used for the preparation of Si_xN_4 or SiC-based sensor systems.

If the modification of doped monocristalline SiC surfaces (*vide infra*) will become possible under milder conditions (e.g. temperatures < 60 ºC or irradiation wavelength > 320 nm), as should in theory be the case, the direct attachment of biomolecules can be envisaged, analogous to what is possible on silicon using visible light.[3]

Biorepellent monolayers

The protein repellence of EO_3 and EO_6 molecules demonstrated in Chapter 7 and Chapter 8 can provide a sensitive improvement in the filtration of biological and food-related solutions with microfabricated silicon nitride membranes or "microsieves".[8-10] In particular, the results shown in Chapter 8 are encouraging to further develop bioresistant microsieves with improved filtration performances, by combining surface modification with membrane actuation by back-pulsing. Such studies are currently ongoing in our and other laboratories. When considering industrial applications of biorepellent coatings, additional improvements in coating stability would still be valued: the use of terminal alkynes or extra internal functionalities (*vide infra*) could be used also for biorepellent coatings to allow inter-chain cross-linking, while retaining high grafting densities. Another improvement in stability could

be reached by using SiC instead of Si_xN_4 for the coating of microsieves, to give them more mechanical and chemical robustness. SiC has been much less used than Si_xN_4 in microfabrication, but more and more facilities nowadays offer the possibility to produce reproducible SiC surfaces by chemical vapor deposition (CVD).

Biorepellent coatings could also be used for sensing applications: protein microarrays, for example, require in practice the absence of non-specific protein adsorption. The passivation of unfunctionalized areas could be done, either by UV-induced monolayer formation, as described in Chapter 7 and 8, using a photolithography mask. This patterning could also be achieved by a selective activation of an already formed monolayer: If an ethylene glycol monolayer is exposed to a plasma with a properly perforated soft contact mask, such as suggested at the end of Chapter 9, and subsequently exposed to amine-functionalized bioactive compounds, then patterned biofunctional and biorepellent areas could be formed (Figure 2). This approach was already successful, for example, to create nanoarrays of proteins, using the electrooxidation of oligoethylene glycol monolayers on silicon surfaces with AFM.[11] However, the use of plasma with a contact mask as we describe here allows the functionalization of bigger areas in a single fast step.

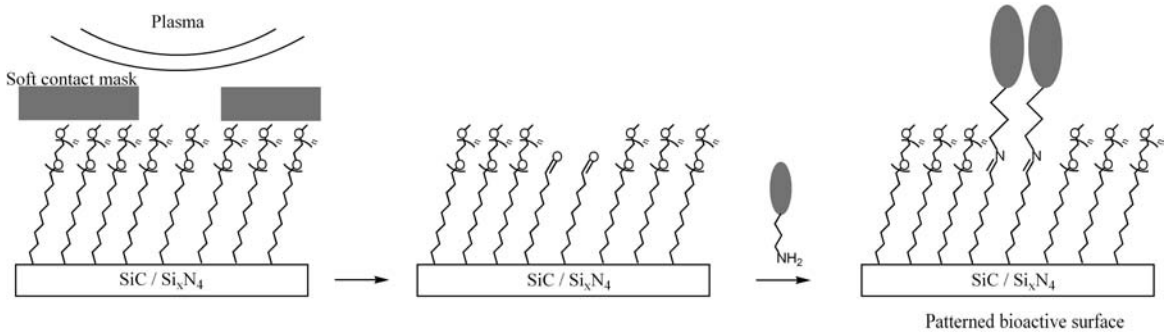

Figure 2. Opportunity for biospecific patterning of surfaces using plasma activation of protein-repellent oligomers monolayers.

Opportunities for surface engineering

Many sensing methods could be developed, using the combination of Si_xN_4 or SiC and covalent organic monolayers. During the course of this project, for example, we attempted the modification of silicon nitride microcantilevers with organic monolayers, in order to develop an online gas sensor based on the shift in resonance frequency of the cantilever upon specific binding of gas molecules. The complexity of the phenomena we observed did not allow us to

draw direct conclusions yet, but this concept, if carried out with due efforts, might yield an elegant combination of microfabrication and organic surface engineering.

Several other techniques already use, or could use, silicon nitride (waveguide refractometric or fluorescence sensor,[12] field-effect transistors) or silicon carbide surfaces (nanoelectromechanical systems or NEMS[13], MOSFET or impedance sensors[14,15]) and a complete list of the possible combinations is already too long to be given here. However, the formation of robust organic monolayers on the surfaces of materials with diverse properties such as silicon, silicon nitride, or silicon carbide bears the promise of challenging material design far beyond the limits that are currently in place.

Surface engineering is one of the best practical contributions that chemists can make to microfabrication, micro- and nanoelectromechanical systems, microfluidics, process engineering or biosensing, which were once the exclusive domains of physicists, engineers, or biochemists. Through the available chemistry and clear opportunities for other fields of research, the field of surface engineering will inevitably become more multi-disciplinary and create more potent devices than either of the disciplines could have produced individually, and allow us to face new challenges for science and society.

References

(1) Sieval, A. B.; Opitz, R.; Maas, H. P. A.; Schoeman, M. G.; Meijer, G.; Vergeldt, F. J.; Zuilhof, H.; Sudhölter, E. J. R. *Langmuir* **2000,** *16*, 10359-10368.

(2) Sun, Q.-Y.; de Smet, L. C. P. M.; van Lagen, B.; Giesbers, M.; Thune, P. C.; van Engelenburg, J.; de Wolf, F. A.; Zuilhof, H.; Sudhölter, E. J. R. *J. Am. Chem. Soc.* **2005,** *127*, 2514-2523.

(3) de Smet, L. C. P. M.; Stork, G. A.; Hurenkamp, G. H. F.; Sun, Q. Y.; Topal, H.; Vronen, P. J. E.; Sieval, A. B.; Wright, A.; Visser, G. M.; Zuilhof, H.; Sudhölter, E. J. R. *J. Am. Chem. Soc.* **2003,** *125*, 13916-13917.

(4) Bernhardt, J.; Schardt, J.; Starke, U.; Heinz, K. *Appl. Phys. Lett.* **1999,** *74*, 1084-1086.

(5) Sieber, N.; Seyller, T.; Graupner, R.; Ley, L.; Mikalo, R.; Hoffmann, P.; Batchelor, D. R.; Schmeisser, D. *Appl. Surf. Sci.* **2001,** *184*, 278-283.

(6) vanElsbergen, V.; Janzen, O.; Monch, W. *Mater. Sci. Eng.* **1997,** *B46*, 366-369.

(7) Latham, A. H.; Williams, M. E. *Langmuir* **2006,** *22*, 4319-4326.

(8) Tong, H. D.; Jansen, H. V.; Gadgil, V. J.; Bostan, C. G.; Berenschot, E.; van Rijn, C. J. M.; Elwenspoek, M. *Nano Lett.* **2004,** *4*, 283-287.
(9) van den Berg, A.; Wessling, M. *Nature* **2007,** *445*, 726-726.
(10) van Rijn, C. J. M.; Veldhuis, G. J.; Kuiper, S. *Nanotechnology* **1998,** *9*, 343-345.
(11) Gu, J. H.; Yam, C. M.; Li, S.; Cai, C. Z. *J. Am. Chem. Soc.* **2004,** *126*, 8098-8099.
(12) McDonagh, C.; Burke, C. S.; MacCraith, B. D. *Chem. Rev.* **2008,** *108*, 400-422.
(13) Yang, Y. T.; Callegari, C.; Feng, X. L.; Ekinci, K. L.; Roukes, M. L. *Nano Lett.* **2006,** *6*, 583-586.
(14) Stutzmann, M.; Garrido, J. A.; Eickhoff, M.; Brandt, M. S. *Phys. Stat. Sol. A* **2006,** *203*, 3424-3437.
(15) Yakimova, R.; Petoral, R. M.; Yazdi, G. R.; Vahlberg, C.; Spetz, A. L.; Uvdal, K. *J. Phys. D Appl. Phys.* **2007,** *40*, 6435-6442.

Summary

Silicon-rich silicon nitride (Si_xN_4, x > 3) is a robust insulating material widely used for the coating of microdevices: its high chemical and mechanical inertness make it a material of choice for the reinforcement of fragile microstructures (e.g. suspended microcantilevers, micro-fabricated membranes-"microsieves") or for the coating of the exposed surfaces of sensors (field-effect transistors, waveguide optical detectors). To a more limited extent, silicon carbide (SiC) can find similar applications, and this material also starts to be more and more applied in coating and sensor technologies.

In all these applications, control over the surface properties of inorganic materials is crucial, for example to avoid blockage of membranes during filtration, or to provide sensor surfaces with specific (bio-)recognition properties. In this thesis, a variety of methods is developed to obtain and study robust functional coatings on Si_xN_4 and SiC. These enable a whole new range of applications involving biocompatible and bio-specific surfaces, while retaining the bulk mechanical, structural, electrical or optical properties of the inorganic substrates.

Chapter 2 and 3 of the thesis give an overview of the great potential of covalent organic monolayers: Chapter 2 presents the formation of alkylthiol, alkylsilane and alkene monolayers, as well as a number of applications in biocompatible surfaces, micro- and nanopatterning of surfaces and sensing. The emphasis of this review chapter is put on the possible combinations of the bulk properties of inorganic materials (electrical, optical, structural) and the surface properties of organic monolayers (wettability, biospecificity, biorepellence). Chapter 3 is focused on biorepellent surfaces in the field of filtration with microfabricated membranes. Indeed, silicon nitride microsieves, despite their high permeability and structural homogeneity, are prone to pore blocking, when submitted to biological solutions. The chapter gives a review of the available surface modification techniques involving organic coatings that can minimize or even prevent this surface contamination. These coatings involve highly hydrophilic oligomers and polymers, which have been widely explored for organic surfaces. Covalent organic monolayers formed onto inorganic surfaces can extend the applications of these biorepellent coatings to microdevices like Si_xN_4 microsieves (as also discussed in Chapters 7 and 8)

Chapter 4 and 5 present the thermal functionalization with highly stable alkene-based organic monolayers of the surfaces of silicon-rich silicon nitride (Chapter 4) and silicon carbide (Chapter 5). This work was motivated by the substantial knowledge of similar

monolayer formation on silicon surfaces[1,2] and the initial success of simple functionalizations on silicon nitride.[3] The strong covalent attachment of the coating molecules with the substrates makes the obtained hybrid structures much more resistant to chemical degradation than other types of monolayers on these substrates. The reaction proceeds via attachment of the terminal double bond of alkenes with the surface groups (Si-H in the case of silicon nitride surfaces or –OH for silicon carbide surfaces). Besides methyl-terminated surfaces, functional coatings can be obtained by the use of bi-functionalized alkenes (Figure 1), also allowing further surface reactions and the attachment of bio-recognition elements, through covalent attachment of diverse chemical (carboxylic acid, amine) or biological (oligo-peptides, protein) moieties.

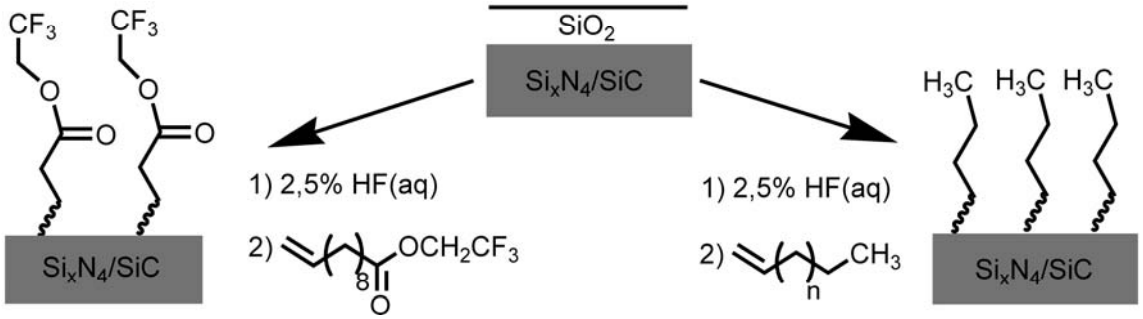

Figure 1. Modification of SiC and Si_xN_4 surfaces with alkyl monolayers

Chapter 6 describes a modification of this method, where UV irradiation is used instead of heat to initiate the modification of both silicon nitride and silicon carbide. For both materials, this method allows the grafting of heat-sensitive compounds, needs less starting material (using only a liquid film) and provides monolayers with higher quality (as e.g. indicated by grafting density and stability) and higher reproducibility. Here again the attachment of diverse functionalities is possible, via formation of activated esters. After hydrolysis and activation of such grafted ester, amines can be attached in high yield (> 80 %), as demonstrated using X-ray photoelectron spectroscopy (XPS). Besides the homogeneous modification of plain surfaces, this method also opens the way to surface patterning of silicon nitride and silicon carbide and the modification of mechanically sensitive microfabricated devices.

In Chapters 4 to 6, the chemical functionalizations are studied using X-ray photoelectron spectroscopy (XPS), infrared reflection absorption spectroscopy (IRRAS), atomic force microscopy (AFM), time-of-flight secondary ion mass spectrometry (ToF-SIMS) and static water contact angles. Si-C bonds are formed preferentially upon reaction of Si_xN_4 surfaces

with alkenes, similarly to what is reported for pure silicon surfaces, albeit that no measurement could totally exclude the presence of C-N bonds. The wet etching of SiC yields hydroxyl-terminated surfaces, and an IRRAS study reveals the attachment of alkenes via a Markovnikov-type addition (O-C bond formed on the second carbon of the double bond). The stability of these monolayers is reported in acidic and basic conditions, and it was shown that UV initiation yields even more stable monolayers, probably due to some cross-linking of the alkyl chains.

Chapter 7 explores the biorepellence of UV-initiated monolayers on silicon nitride surfaces Oligomers of ethylene glycols (3 or 6 units: methoxy-tri(ethylene oxide) undec-1-ene ($CH_3O(CH_2CH_2O)_3(CH_2)_9CH=CH_2$; EO_3, and methoxy-hexa(ethylene oxide) undec-1-ene ($CH_3O(CH_2CH_2O)_6(CH_2)_9CH=CH_2$; EO_6) are attached on the silicon nitride surfaces. The adsorption of two proteins, bovine serum albumin (BSA) and fibrinogen is used to test the biorepellence of the monolayers, in comparison with bare oxidized silicon nitride. Both proteins adsorb readily onto bare Si_xN_4 surfaces, with adsorbed amounts of 1.25 and 2.7 $mg.m^{-2}$ for BSA and fibrinogen, respectively, of which more than 80 % is irreversibly bound. In contrast to this, when oligomers are attached to the surface, this adsorption decreases to under the detection limit of the method used for this experiment (optical reflectometry). The *ex situ* study of surfaces with AFM and water contact angles also indicates that some of the monolayers completely prevent the adsorption of proteins.

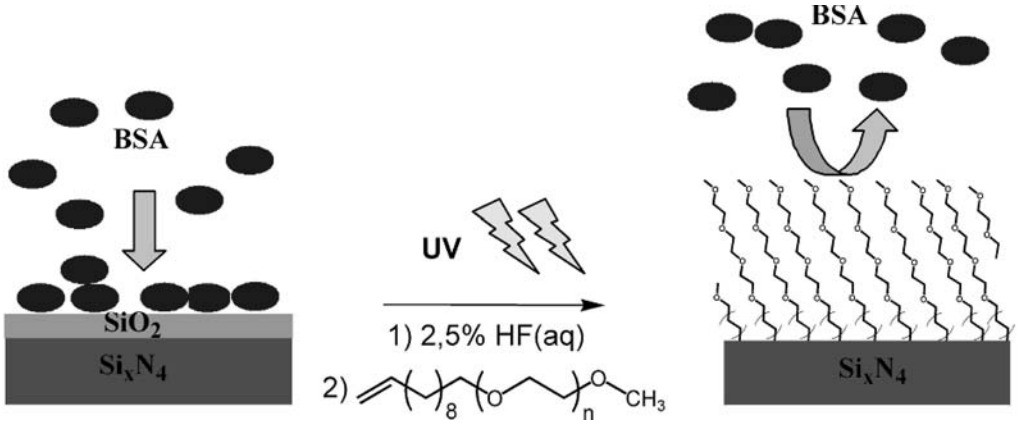

Figure 2. Biorepellent behavior of oligoethylene oxide coated Si_xN_4 surfaces

Chapter 8 describes the applications of the biorepellent coatings used in Chapter 7 (EO_6) to silicon nitride microsieves, in order to improve the filtration of biological solutions and liquid food products. The EO_6 coatings are successfully formed on microfabricated membranes with

pore diameters of 0.45 micrometer, using the UV-initiated monolayer formation described in Chapter 6. This work shows that these coatings could be applied without loss of permeability due to wettability or pore blocking. Moreover, AFM showed that these coatings significantly decrease the adsorption of proteins on the surface between the pores.

Chapter 9 describes an alternative functionalization technique for inorganic surfaces, namely the use of plasma oxidation of alkyl monolayers to reproducibly form aldehydes (among other oxidized species) onto surfaces. The method described here for silicon and silicon nitride surfaces, is developed for the functionalization of sensitive devices and substrates. The formation of methyl-terminated alkyl monolayers from linear terminal alkenes is one of the easiest to perform, since linear monofunctional alkenes are readily available, their purification is easy (distillation) and their grafting conditions are very flexible (liquid state, heat-resistant, UV-resistant > 250 nm). Once these stable monolayers are formed, a short plasma treatment (0.5 to 2 s) is able to form oxidized functionalities within the top few angstroms of the surface, while the underlying alkyl chains retain their initial packing and insulation properties of the inorganic substrate. The grafting of gold nanoparticles shows that micron-sized patterns can be formed using a soft contact mask to protect a limited area of the monolayer. Alternatively, the aldehydes can be used to attach biotin and avidin onto Si_xN_4 surfaces. The selective adsorption of biotinylated BSA onto the avidin-modified surfaces shows that the plasma treatment of methyl-terminated monolayers is a fast and efficient method to produce surfaces displaying high specific biochemical interactions.

In the chapter 10, some of the most striking effects that are described in the previous chapters are put into a wider perspective. Especially the formation and stability of monolayers is discussed, also in relation to biofunctionalization, biorepellence, and opportunities for surface engineering are proposed.

Samenvatting

Silicium-verrijkt silicium nitride (Si_xN_4, x > 3) is een robuust, isolerend materiaal dat veel wordt gebruikt voor het bedekken van functionele microstructuren. Vanwege zijn hoge chemische en mechanische inertheid wordt Si_xN_4 bij voorkeur gebruikt voor de versterking van fragiele microstructuren (bijvoorbeeld vrijhangende microcantilevers, of membranen die gefabriceerd zijn met behulp van microtechnologie “microzeven”) en voor het bedekken van onbeschermde sensoroppervlakken (veldeffecttransistoren, optische detectoren op basis van golfgeleiders). Silicium carbide (SiC) wordt minder wijdverbreid gebruikt, maar begint steeds meer zijn weg te vinden in de coating- en sensortechnologie.

Voor al deze toepassingen is de beheersing van de oppervlakte-eigenschappen van deze anorganische materialen cruciaal, bijvoorbeeld om verstopping van membranen te voorkomen tijdens filtratie of om sensoroppervlakken van specifieke (bio-) herkenningseigenschappen te voorzien. In dit proefschrift staan een aantal methoden beschreven die zijn ontwikkeld om robuuste en functionele coatings aan te kunnen brengen op Si_xN_4 en SiC. Deze coatings zullen tot een heel nieuw bereik aan toepassingen leiden, waarin de oppervlakken biocompatibel en biospecifiek zijn, terwijl de mechanische, structurele, elektrische en/of optische bulkeigenschappen van het anorganische materiaal behouden blijven.

Hoofdstuk 2 en 3 van dit proefschrift geven een overzicht van de vele mogelijkheden voor covalente organische monolagen: hoofdstuk 2 behandelt de vorming van alkylthiol, alkylsilaan en alkeen monolagen, evenals een aantal toepassingen op het gebied van biocompatibele oppervlakken, het aanbrengen van micro- en nanopatronen, en detectie. De nadruk van dit overzicht ligt op de mogelijke combinaties van de bulkeigenschappen van anorganische materialen (elektrische, optische, structurele) met de oppervlakte-eigenschappen van organische monolagen (bevochtiging, biospecificiteit, bio-afstotendheid). Hoofdstuk 3 richt zich op eiwitafstotende oppervlakken voor het specifieke gebied van filtratie met microzeven. Ondanks hun hoge permeabiliteit en structurele homogeniteit zijn silicium nitride microzeven vatbaar voor porieverstopping wanneer ze aan biologische oplossingen worden blootgesteld. Het hoofdstuk geeft een overzicht van de beschikbare coatingtechnieken die oppervlaktebesmetting kunnen verminderen en in sommige gevallen zelfs voorkomen. Deze technieken zijn gebaseerd op het enten van oligomeren en polymeren en zijn uitgebreid onderzocht voor organische membranen. Covalente organische monolagen, zoals die hier gepresenteerd worden, maken het mogelijk om ook anorganische materialen, zoals gebruikt

voor microzeven, te voorzien van een goede coating (zoals ook besproken wordt in hoofdstukken 7 en 8).

Hoofdstukken 4 en 5 behandelen de thermische functionalisatie van stabiele alkeen-gebaseerde organische monolagen op Si_xN_4 (hoofdstuk 4) en SiC (hoofdstuk 5). Dit werk komt voort uit substantiële kennis over de vorming van soortgelijke monolagen op zuivere silicium oppervlakken en het initiële succes van simpele functionalisering van silicium nitride. De sterke covalente binding tussen het substraatoppervlak en de coatingmoleculen maken de verkregen hybride structuren veel beter bestand tegen chemische degradatie dan vergelijkbare monolagen. De reactie verloopt via de koppeling van de eindstandige dubbele binding van alkenen aan de oppervlaktegroepen (Si-H in het geval van Si_xN_4 en –OH in het geval van SiC oppervlakken). Naast methyl-getermineerde oppervlakken kunnen functionele coatings verkregen worden door het gebruik van bi-functionele alkenen welke verdere oppervlaktereacties mogelijk maken en de koppeling van bioherkenningselementen, door covalente binding van diverse chemische (carboxylzuren, amines) of biologische groepen (oligo-peptides, eiwitten) toestaan.

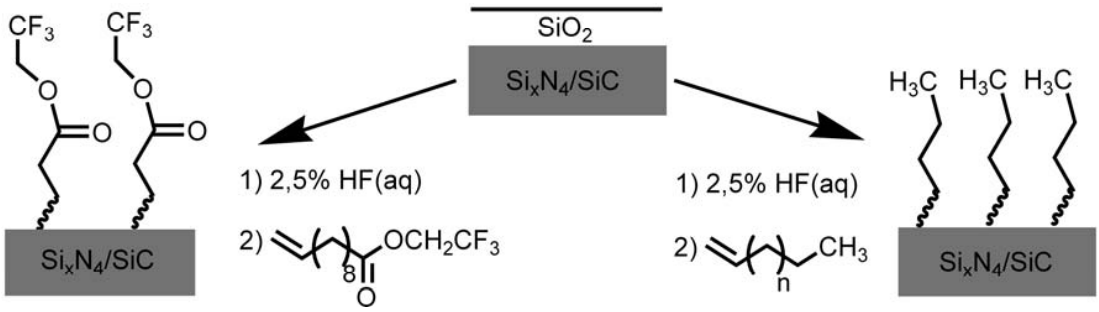

Figure 1. Vorming van alkeen-gebaseerde monolagen op SiC and Si_xN_4 oppervlakken.

Hoofdstuk 6 beschrijft een variant van deze methode, waarin ultraviolet licht wordt gebruikt in plaats van warmte om zowel Si_xN_4 als SiC te modificeren. Voor beide materialen geldt dat de koppeling van hittegevoelige verbindingen mogelijk is, minder uitgangsmateriaal vereist is (slechts een vloeistoffilm wordt gebruikt) en dat beter reproduceerbare monolagen van een hogere kwaliteit worden verkregen (op basis van pakkingsdichtheid en stabiliteit). Ook hier is de koppeling van verschillende functionaliteiten mogelijk via de vorming van geactiveerde esters. Uit Röntgen fotoelectronspectroscopie (XPS) blijkt dat na hydrolyse en activering van een gekoppeld ester, de vervolgreactie met een simpel amine met een hoge omzettingsgraad

(> 80%) verloopt. Naast de homogene modificatie van vlakke oppervlakken geeft deze methode ook mogelijkheden tot het aanbrengen van patronen op Si_xN_4 en SiC.

In hoofdstukken 4 tot 6, wordt de chemische functionalisatie bestudeerd met XPS, infrarood absorptie spectroscopie (IRRAS), atoomkrachtmicroscopie (AFM) en statische randhoek meting. Op het Si_xN_4 oppervlak worden bij een reactie met alkenen bij voorkeur Si-C bindingen gevormd, zoals dat ook verwacht wordt voor pure Silicium oppervlakken, al kan niet helemaal uitgesloten worden dat ook C-N bindingen gevormd worden. Het nat etsen van SiC geen hydroxyl-getermineerde oppervlakken, en IRRAS analyse geeft aan dat de binding via een Markovnikov-achtige additie verloopt (O-C binding wordt gevormd op het tweede C atoom van de dubbele binding. De stabiliteit van deze monolagen is onderzocht voor zure en basische condities, en we konden laten zien dat bij UV initiatie de lagen nog stabieler zijn, wat hoogst waarschijnlijk wordt veroorzaakt door crossslinking van de alkyl ketens.

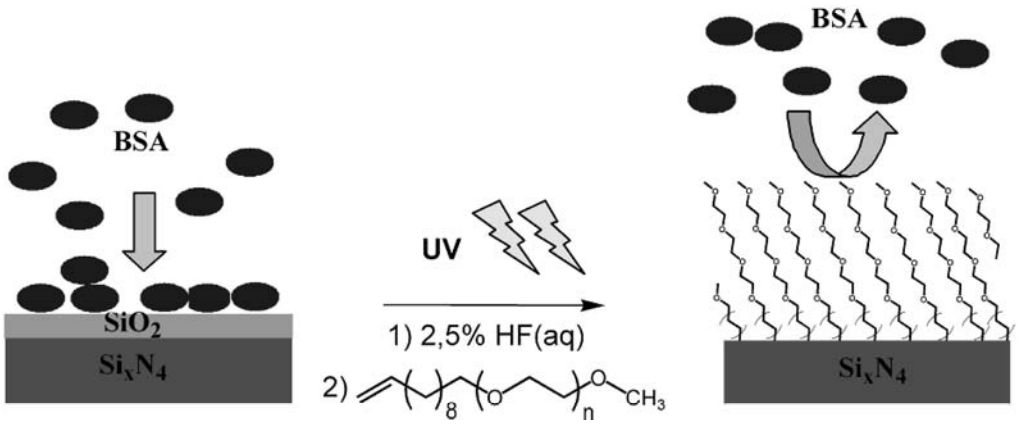

Figure 2. Bio-afstotende ethyleenglycol monolagen op Si_xN_4 oppervlakken.

In hoofdstuk 7 wordt de bio-afstotendheid van fotochemisch (UV) gevormde monolagen op Si_xN_4 oppervlakken onderzocht. Oligomeren van ethyleenglycol (drie of zes eenheden; methoxy-tri(ethyleenoxide) undec-1-een ($(CH_3O(CH_2CH_2O)_3(CH_2)_9CH=CH_2$; EO_3 en methoxy-hexa(ethyleen oxide) undec-1-een ($CH_3O(CH_2CH_2O)_6(CH_2)_9CH=CH_2$; EO_6) zijn vastgezet op Si_xN_4 oppervlakken, waarna de adsorptie van twee eiwitten, runderserumalbumine (BSA) en fibrinogeen is gebruikt om de bio-afstotendheid van de monolagen te testen ten opzichte van kaal, geoxideerd Si_xN_4. Beide eiwitten adsorberen gemakkelijk op de onbehandelde oppervlakken (1,25 en 2,7 $mg.m^{-2}$ voor BSA en fibrinogeen), waarvan 80% irreversibel gebonden wordt. In tegenstelling tot dit, wordt door de aanwezigheid van ethyleenglycol oligomeren de adsorptie tot beneden de detectielimiet

van de gebruikte analysemethode (reflectometrie) verlaagd. Verdere bestudering van de oppervlakken met AFM en statische randhoek meting duidt er eveneens op dat een aantal van deze monolagen de adsorptie van eiwitten volledig verhindert.

Hoofdstuk 8 beschrijft de toepassing van de bio-afstotende coatings (zoals gebruikt in hoofdstuk 7) op silicium nitride microzeven, met het doel de filtratie van biologische oplossingen en vloeibare voedingsproducten te verbeteren. De EO_6 coatings zijn met succes aangebracht op microgefabriceerde membranen met een poriediameter van 0.45 μm, door middel van de fotochemische (UV) monolaagvorming beschreven in hoofdstuk 6. Er is aangetoond dat de lagen kunnen worden aangebracht zonder verlies aan permeabiliteit, door verschillen in bevochting of porieblokkering. Verder laat AFM zien dat deze coating de adsorptie van eiwitten op het oppervlak tussen de poriën significant vermindert.

In hoofdstuk 9 wordt een alternatieve functionaliseringstechniek voor anorganische oppervlakken beschreven, namelijk het gebruik van plasma-oxidatie van alkyl monolagen om op een reproduceerbare wijze aldehyden aan het oppervlak te vormen (tussen andere geoxideerde groepen). Deze methode, hier beschreven voor silicium en Si_xN_4, is speciaal ontwikkeld voor het functionaliseren van gevoelige structuren met gevoelige substraten. De vorming van methyl-getermineerde alkyl monolagen is relatief makkelijk uit te voeren, omdat lineaire monofunctionele alkenen beschikbaar zijn, hun zuivering simpel is (door middel van destillatie) en hun eigenschappen (vloeistof, hittebestendig, UV-resistent > 250 nm) flexibele koppelingscondities toelaten. Wanneer deze stabiele monolaag gevormd is, is een korte behandeling (0,5 tot 2 s) genoeg om geoxideerde functionaliteiten in de toplaag (bovenste Angströms) te vormen, terwijl de onderliggende monolaag zijn oorspronkelijke pakkingdichtheid en isolatie-eigenschappen behoudt. En patroon van gouden nanodeeltjes op microschaal kan ook worden aangebracht door specifieke blootstelling van het oppervlak. Een andere mogelijkheid is de aldehyden te gebruiken om biotine en avidine aan Si_xN_4 oppervlakken te koppelen. De selectieve adsorptie van biotinileerd BSA op avidine-gemodificeerde oppervlakken laat zien dat de plasmabehandeling van methyl-getermineerde monolagen een snelle en efficiënte methode is om oppervlakken met een hoge specifieke biochemische interactie te maken.

Ten slotte worden in hoofdstuk 10 sommige van de meest opvallende resultaten uit de eerdere hoofdstukken beschreven en worden ze in een breder kader geplaatst. De vorming en stabiliteit van monolagen wordt besproken, vooral in relatie tot biofunctionalisatie en bio-afstotendheid, en mogelijkheden voor oppervlakte engineering worden voorgesteld.

About the Author

Michel Rosso was born in Cannes (France) on the 15th of August 1978. After finishing his high school education (lycée Bristol, Cannes), he entered the University of Nice in 1996, where he started his studies in physical sciences and received in 2000 a 4th year degree (maîtrise) in organic chemistry with distinction, as first of his promotion.

Instead of embarking on a PhD program directly, he chose to enter the ENSCM (National higher school of chemistry of Montpellier) where he developed a special interest for chemical and bioprocess engineering. In 2003, he graduated from the ENSCM and the University Montpellier II as an engineer with these two specializations.

Before that, he had spent three traineeships, at Henkel France (Châlons-en-Champagne, France: safety & environment management on a production plant), at Agrotechnology & Food (Wageningen: enzymatic transesterification of sugars for the production of natural polymers, Dr. C. Boeriu) and in the laboratory of process engineering of Maribor University (Maribor, Slovenia: critical fluid extraction for the preparation of enzymatic sol-gel membranes, Prof. Ž. Knez).

Michel started his PhD project at Wageningen university in 2004, to work on the research presented in this thesis. In 2008, he received a young scientist award from the European Material Research Society for the research he presented at the EMRS spring meeting in Strasbourg.

Since December 2008, he has left the green countryside of Gelderland, and has been working as a post-doctoral researcher at DelftChemTech and Multi-Scale Physics (TUDelft) on the development of microfluidics biosensors.

Publication list

Covalent biofunctionalization of silicon nitride surfaces, Arafat, A.; Giesbers, M.; Rosso, M.; Sudhölter, E. J. R.; Schroën, K.; White, R. G.; Yang, L.; Linford, M. R.; Zuilhof, H. *Langmuir* **2007,** *23*, 6233-6244.

Protein-repellent silicon and germanium surfaces. Schroën, K.; Rosso, M.; Zuilhof, H. European patent n. 07113632.9-2203, **2007**.

Covalent attachment of organic monolayers to silicon carbide surfaces, Rosso, M.; Arafat, A.; Schroën, K.; Giesbers, M.; Roper, C. S.; Maboudian, R.; Zuilhof, H. *Langmuir* **2008,** *24*, 4007-4012.

Covalently Attached Organic Monolayers on SiC and Si_xN_4 Surfaces: Formation Using UV Light at Room Temperature, Rosso, M.; Giesbers, M.; Arafat, A.; Schroën, K.; Zuilhof, H. *Langmuir* **2009,** *25*, 2172-2180.

Biorepellent Organic Coatings for Improved Microsieve Filtration, Rosso, M.; Schroën, K.; Zuilhof, H., in *New Membranes and Advanced Materials for Wastewater Treatment*, ACS books **2009**, in press.

Protein-Repellent Silicon Nitride Surfaces: UV-Induced Formation of Oligoethylene Glycol Monolayers, Rosso, M.; de Jong, E.; Giesbers, M.; Fokkink, R. G.; Norde, W.; Schroën, K.; Zuilhof, H., submitted.

Controlled Oxidation, Bio-functionalization, and Patterning of Alkyl Monolayers on Silicon and Silicon Nitride Surfaces using Plasma Treatment, Rosso, M.; Giesbers, M.; Schroën, K.; Zuilhof, H., in preparation.

Covalent Organic Monolayers for Bionanotechnology, Rosso, M.; Schroën, K.; Zuilhof, H., in preparation.

Protein-Repellent Coatings on Silicon Nitride Microsieves, Rosso, M.; Schroën, K.; Boom, R.; Zuilhof, H. in preparation.

Use of in-situ NMR to Monitor the Lipase-Catalyzed Formation of Sugar-Containing Hydrogel Precursors. Rosso, M.; Boeriu, C. G. *Sci. Tech. Bull.-Chem. Food Sci. Eng., University "A. Vlaicu" Arad, Romania*, **2007**, *12*, 69-73

Training and Supervision Plan

Graduate School VLAG	Year	ECTS
Discipline specific activities		
Courses		
Bio-Nano Technology, VLAG	2005	1.0
Surface Analysis Course EPFL, Lausanne, Switzerland	2006	1.3
Photophysics, Photochemistry and Photobiology, VU Amsterdam	2007	1.0
Meetings		
European Conference on SiC & Related Materials, Newcastle	2006	1.0
Spring Meeting of the European Material Research Society, Strasbourg	2008	1.0
10th International Conference on Inorganic Membranes, Tokyo, Japan	2008	1.0
Wageningen Symposium of Organic Chemistry, Wageningen University	2006/8	0.6
Wageningen Bionanotechnology Symposium, 88th Dies Natalis	2006	0.3
Annual NWO Conference, Lunteren	2004-8	2.5
Annual NanoNed Conference	2004-8	4.0
MicroNed-MinacNed meeting, Wageningen University	2007	0.6
PhD study trip, Organized by Laboratory of Organic Chemistry, USA	2005	2.0
PhD study trip, Organized by Laboratory of Organic Chemistry, Sweden	2007	2.0
General courses		
PhD Scientific Writing, Centa, Wageningen	2008	1.7
Organizing and supervising MSc thesis project, Wageningen	2007	0.7
Optionals		
Preparation PhD research proposal		6.0
Literature study (Laboratory of Organic Chemistry)	2004	2.0
Group meetings (Laboratory of Organic Chemistry), Wageningen	2004-8	3.0
Colloquia (Laboratory of Organic Chemistry), Wageningen	2004-8	3.0
Group meetings (Laboratory of Food Process Engineering), Wageningen	2004-8	3.0
Total		**37.7**

Acknowledgments

During the past four years in Wageningen, I met many people, which contributed directly or indirectly to the realization of this PhD thesis. I wish to thank them in these following lines.

The writing of this book was first made possible through the joint efforts of my supervisors: Dr. Karin Schroën, Prof. Han Zuilhof and Prof. Remko Boom. Indeed, the flexible collaboration between the two departments of Organic Chemistry and Food & Bioprocess Engineering has offered me a lot of freedom to fulfill my scientific and personal wishes.

Karin, working with you was a pleasure; your door was always open for advice and discussions despite a busy schedule. Your ability to see and make good use of the good sides of students while always taking care of stressful details probably has a lot to do with the relaxed atmosphere in the group.

Han, you were always a challenging and ambitious supervisor, and I appreciate the trust and support that I felt in these four years. I am also grateful for learning a lot about the other part of a scientist's job, which is not only about working in the lab or writing articles.

Remko, although we only had a few discussions, I wish to thank you for your openness and interest, and for the dynamic way you run the department, and also especially for making it possible to present my work in two international conferences in my last year.

I also wish to thank Prof. Ernst Sudhölter for hiring me in Wageningen before his departure to Delft University. Ernst, I especially appreciate your constant optimism and the kind attention you show to people working for you. It was also a pleasure to travel with you for our two PhD trips of the laboratory of organic chemistry to San Francisco and Sweden. After your departure from Wageningen, it was a difficult decision not to include you as my thesis promotor, and I am happy that you accepted to be part of my thesis committee.

I also have to thank Dr. Carmen Boeriu from A&F in Wageningen, for being such a dedicated supervisor, during my first internship in Wageningen in 2002, and who actually inspired me to work as a researcher in the Netherlands.

Other people have contributed to this thesis, through collaborations, discussions and technical assistance. I wish to thank Prof. Roya Maboudian and Christopher Roper from Berkeley University, California, for our fruitful collaboration on silicon carbide. In the same way, I should thank Prof. Matthew Linford and Li Yang from Brigham Young University, Utah, for their help with ToF-SIMS analysis. I also wish to thank Richard White from Thermo Electron Co. for XPS analysis and his assistance during our visit to the Thermo facilities in East Grinstead, U.K. I also thank Prof. Herre v.d. Zandt, Dr. Emile v.d. Drift and Gijs Babaei Gavan, from Delft University, for our interesting collaboration on microcantilevers. Within our MicroNed work package, I wish to thank Prof. Lina Sarro from Delft University, and of course Prof. Cees van Rijn from Aquamarijn B.V. (and from Wageningen University) for supplying us with microsieves, and for his stimulating way to lead our work discussions within MicroNed.

In Wageningen, I wish to thank Prof. Willem Norde (Physical Chemistry and Colloid Science) for his help and expertise on protein adsorption. In the same department, my thanks also go to Remko Fokkink, who assisted not only me, but a lot of people from our group, with ellipsometry, reflectometry, light scattering and many other technical issues with an constant dedication and availability. From Process Engineering in Wageningen, I wish to thank especially Jos Sewalt and Dr. Gerben Brans, for their great technical help in the lab, as well as the other people I shortly met there, including Francisco (for the music in the lab), Salomon, Hassan, Thanawit, Joyce and Martin.

In these 4 years, I spent most of my time in the Surface group of the laboratory of organic chemistry, where we developed more than superficial relations: first of all I thank Dr. Ahmed Arafat, for modifying the first silicon nitride surfaces, thereby being a direct cause of my displacement from Cannes to Wageningen, but also for the close friendship we developed in the time he stayed there. Ahmed, I enjoyed a lot our collaboration, and I wish you all the best, as well as to your family, and I hope you will find happiness as a (sometimes too) dedicated scientist.

Menglong, from the beginning, your pleasant character and your love of teaching almost convinced me to learn Chinese from you. Tireless in the lab work and in discussion, and gifted with the ability to find appropriate animal names for each of us everyday, you were for sure not a boring roommate. I hope you enjoyed as I did our work together. Now a confirmed movie star and a dad, I hope to see you someday, maybe in China.

Louis, as my first collaborator in the lab, you apparently showed me well how to work with surfaces, since this thesis is now written. Our work in Delft will hopefully be as fruitful as this one. Kishore, thanks for all the good times, cooking and travelling, and a friendship that, I hope, you'll bring with you to India. Best wishes for your growing family. Luc and Jurjen, thanks for the fun in the lab and outside, for table football and dinners, and especially for hunting parties. Ruud, thanks for being such a strict Dutch teacher with me. Ed, it was nice working with you. Although your thesis work did not go as smooth as we expected, it helped a lot to set up successful experiments after you left, and we will very soon have this work published. Is it this, or a inspiring snowy (!) conference in Germany, that made you decide for a PhD?

I thank of course all the other people in the lab, and especially Marcel ("is someone using the XPS today?"), Teris, whose very good nature I put a bit to the test, Ai Nguyen and Jos Paulusse for continuing the protein adsorption studies, and also Geb, Elbert, Frank, Ronald, Erik, Elly, Aleida, Maurice, Frans, Maarten, Anne-Marie, Aliaksei, Cees, Remko, Ganesan, Suzanne, Agnes, Bin, Giedrus, Feng, Melle, Kim, Murali, TuHa, Nagesh, Willem, Jerome, Loes, Gregor, Cindy, Evan, Alessandro, Bart, Tin and Rokus.

Also a big thank to Ioan and Maud, for your friendship and for being witnesses of our special wedding in Denmark.

Anouk and Rosalie, thanks for the fun, friendship and for being my paranymphs on the big day. I also thank all the friends from Wageningen and around: Peter Paul, Janneke, Zoran & Marita, Olja & Hans, Mirjana & Mladjan, Gavrilo & Djurdja, Tiago & Sonia, Vesna and Arun.

Finally, I wish to thank all my family, and especially my parents and my sisters, whose love and support has made me what I am now. I also thank my Serbian family, and in particular Snežana and Minja, for all the good times we shared until now, and all my friends in France and elsewhere.

Finally, Milena, although I did not suspect it when we first met, you turned out to be the perfect combination of strength and fun to get along well with me. I am happy that our two travelling lives met and joined in such a small office, to make each of my days more colorful.

Michel Rosso